Enzymatic synthesis of DHA-lysophosphatidylcholine and evaluation of its effect on the MDA-MB-231 human breast cancer cell line

Dalal Mohamad Ali

THESE DE DOCTORAT DE

LE MANS UNIVERSITE

ECOLE DOCTORALE N° 598
Sciences de la Mer et du Littoral
Spécialité : « Biochimie, Biologie Moléculaire et Cellulaire »

Par
Dalal Mohamad Ali

Enzymatic synthesis of DHA-lysophosphatidylcholine and evaluation of its effect on the MDA-MB-231 human breast cancer cell line

Thèse présentée et soutenue à Laval, le 22 février 2022
Unité de recherche : BiOSSE, Biologie des Organismes, Stress, Santé, Environnement
Thèse N°: 2022LEMA1003

Rapporteurs avant soutenance :

Catherine Humeau	Professeur, Université de Lorraine
Vincent Rioux	Professeur, Institut Agro-campus Rennes-Angers

Composition du Jury :

Président	
Benoît Schoefs	Professeur, Le Mans Université
Examinateurs	
Yolande Perrin	Professeur, Université Technologique de Compiègne
Laurent Picot	Maitre de conférence -HDR, Université de la Rochelle
Directeur de thèse	
Lionel Ulmann	Maitre de conférence -HDR, Le Mans Université
Co-encadrants de thèse	
Gaelle Pencreac'h	Maitre de conférence, Le Mans Université
Laurent Poisson	Maitre de conférence, Le Mans Université
Invité	
Kevin Hogeveen	Chargé de projet, ANSES, Laboratoire de Fougères

ACKNOWLEDGEMENTS

The process of acquiring PhD has been a long and stressful journey and would not have been possible without the help of some wonderful people along the way. Thank you to everyone who has supported me during my graduate studies and who has been there to hold my hand during the scary parts.

I would first like to acknowledge "**Collectivités Locales Mayennaises**" for the financial support and research funding.

I would like to thank Prof. **Catherine Humeau** and Prof. **Vincent Rioux** for accepting the role of reporters as well as Prof. **Yolande Perrin**, Prof. **Benoit Schoefs**, Dr. **Laurent Picot** as reviewers in the evaluation of this work.

I thank my former thesis director Prof. **Françoise Ergan**, and my new director Dr. **Lionel Ulmann**, for having accepted to supervise my thesis, for their availability and the exchanges we had together during the thesis follow-up.

I express my most sincere thanks to Dr. **Gaëlle Pencreac'h**, my co-supervisor, without whom this thesis could not have been completed. I thank you for your scientific and experimental rigor, for all the advice you gave me and for your human qualities. I thank you for your encouragement throughout the thesis. You always made yourself available and you took a close interest in my work. For all this, I am grateful.

I am grateful to **Laurent Poisson**, my second co-supervisor, for his time, corrections and exchanges in the realization of my thesis.

I would like also to express my gratitude to Dr. **Kevin Hogeveen** (guest member in my thesis jury), for carrying out the immunolabelling experiments and for the exchange we had on the cell experiments. Also, for Prof. **Roberto Fernandez Lafuente** for being generous and donating some biocatalysts and Prof. **Arnaud Martel** for the NMR experiments and help with the analysis of the spectra.

I express my sincere gratitude to Dr. **Latifa Chebil** and Prof. **Roberto Fernandez Lafuente** for accepting to evaluate this work every year and the interesting exchanges we had together during the thesis follow-up. Especially Dr. **Latifa Chebil** for supporting me since my master.

I do not forget to warmly thank Prof. **Mohamed Ghoul**, to whom I am grateful and honored to know him. I thank him for supporting me since my Master's degree for the help that he proposed and provided me

to process my experimental design. I would therefore like to show him my attachment and respect. I will always be grateful to you.

To the interns of Master 2, **Tiphaine Le Gal de Kerangal**, **Thibaut Bourdain** and **Diala Damen** who helped me to advance in this work, thank you.

I would like to thank Dr. **Sophie Ledru**, for her kind welcome and help in my teachings. I thank all the **teachers-researchers of the BIOSSE laboratory** and the biological engineering - **GB department** of the IUT Laval, for their kindness.

Also, I would like to acknowledge **Rose-Marie Leroux** for having trained me to perform the cell culture and for having done the cell experiments with me, and especially for her distinguished support and the adorable coffee outings that she organized.

I thank **Martine Come** for carrying out some experiments when in need. And the **technical and administrative service** of the department, **Isabelle Martin** and **Jean-Luc Hoarau**, and all other staff members.

I would like to thank the **IT and administrative departments** for making my work life easier, especially **François Lelièvre** for being present when needed and solving problems as quickly as possible and **Thierry Amiard** and **Yvon Jehanno** for their warm welcoming, kindness and help.

I thank **Carine** for the warm discussions and the coffee breaks we had.

I would like to thank all the **post-doctoral and doctoral students** with whom I had a great time, it has been a pleasure to share these moments with you.

Last but not least, a very heartfelt thanks to my **family** for their extensive support and continuous encouragement at all stages of my life. Thank you for navigating both the heaviness and beauty of the world with me. For believing in me. For providing me with all I ever needed, and so much more than that. For helping me live my dreams out in the world, even if it hurt you to have me so far away.

Mom, **Dad** thank you for letting me be proud to have you as a parent. Thank you for letting me feel surrounded by a family despite the distance and thank you for supporting my incessant calls every day without complaining one day and with pleasure. I love you.

Acknowledgements

For my **friends** in France and in Lebanon for their friendship and their unlimited encouragement. **Aurélie** thank you for your true friendship and your lovely supportive messages. A heartfelt thanks to the true friends that I earned in my expatriation **Sarah**, **Omar**, **Elio**, **Julie**, **Christelle**, **Inéss and Ibtissam**. **Sarah** and **Inéss** thank you for being by my side despite the distance. To my beloved friends in Lebanon especially **Danati, Hibzz, le 3ebs** and **Zaino** thank you very much for including such a large number of fond memories and fulfilling moments in my life.

Special thanks to Dr Abbas Samaha "**le 3ebs"**. There are no words that can express my gratitude for having such and amazing friend like you. You were always there to support and care for me when I need it most. You go above and beyond, and even though I know you have your problems to deal with sometimes.

I dedicate this thesis to my **grandfather Mahdi and my grandmother Zainab**. Who were an incredible people, dedicated and there for everyone. I will always keep good memories of you, your jokes, the evenings spent by your side, your kindness, your generosity and your great soul. These memories became treasure since you left us. I wish RIP means return if possible. Miss you so much jeddo lhajj & teta zanouba!

To my beloved **Lebanon**, you will rise again despite it all!

Table of contents

List of figures

List of tables

Abbreviation list

A
AG: Acylglycerol
ALA: α-linolenic acid
a_w: Water activity

B
BBD: Box-Behnken design
BQ: Biocatalyst quantity

C
CALB: Lipase B from *Candida antarctica*
CALB-IB 150: Lipase B from *Candida antarctica* immobilized on Immobead 150
CCD: Composite central design

D
DAG: Diacylglycerol
DAG-DHA: Didocosahexaenoin
DHA: Docosahexaenoic acid
DOE: Design of experiment
E
EPA: Eicosapentaenoic acid: EPA

F
FA: Fatty acid

G
GPC: Glycerophosphocholine

H
HDL: High-density lipoprotein cholesterol
HPLC: High performance liquid chromatography

L
LBC: Lipase from *Burkholderia cepacia* immobilized on diatomite
LDH: Lactate dehydrogenase
LDL: Low-density lipoprotein cholesterol
LPA: Lysophosphatidic acid
LPC: Lysophosphatidylcholine
LPC-CLA: Lysophosphatidylcholine rich in conjugated linoleic acid
LPC-DHA: Lysophosphatidylcholine rich in DHA
LPE: Lysophosphatidylethanolamine
LPI: Lysophosphatidylinositol
LPG: Lysophosphatidylglycerol
LPL: Lysophospholipid
LPL-DHA: DHA rich lysophospholipids

LPS: Lysophosphatidylserine

M
MAG: Monoacylglycerol
MAG-DHA: Monodocosahexaenoin
MR: Molar ratio
MUFA: Monounsaturated fatty acid

N
N 435: Novozym 435®

P
PUFA: Polyunsaturated fatty acid
PG: Phosphatidylglycerol
PC: Phosphatidylcholine
PS: Phosphatidylserine
PI: Phosphatidylinositol
PE: Phosphatidylethanolamine
PLA2: Phospholipase A2
PL: Phospholipid
PL-DHA: DHA rich phospholipids
P_{atm}: Atmospheric pressure

R
RSM: Response surface method

T
T: Temperature
TAG: Triacylglycerol
TAG-DHA: Tridocosahexaenoin
TLC: Thin layer chromatography
TL-IB 150: Lipase from *Thermomyces lanuginosus* immobilized on Immobead 150
TL-IM: Lipozyme TL-IM®

INTRODUCTION

Introduction

Docosahexaenoic acid (DHA, C22:6 ω–3) is a polyunsaturated fatty acid (PUFA) of the omega-3 family, essential for the development and the physiology of the human body. *In vivo*, DHA is synthesized in low amounts in human metabolism, insufficient to ensure its functions and it is therefore necessary to compensate this lack with a dietary intake. However, the assimilation of DHA in its free form remains low. It is therefore interesting to associate it with a lipidic carrier to promote its absorption and protect it from oxidation. The incorporation of DHA in a carrier such as lysophospholipid (LPL) has proven to be effective. It has been shown that DHA carried by a LPL is more stable toward oxidation and better absorbed than other forms such as free, ethyl ester or triglyceride. For example, DHA was transported by a lysophosphatidylcholine (LPC), without oxidation, to the brain across the blood-brain barrier. Also, this combination showed anti-inflammatory effects and improvement of capacities such as learning. Moreover, numerous studies have shown the potential of DHA in inhibiting and reducing various cancer risks. This inhibitory effect was enhanced when DHA was carried by different lipidic carriers such as monoacylglycerol (MAG) or phospholipid (PL).

Structured LPLs, containing desired fatty acids, can be synthesized by chemical and enzymatic routes. The enzymatic route is more advantageous than the chemical route and allows working under non-drastic conditions. The main advantage of biocatalysts over chemical catalysts is their substrate specificity. Lipases and phospholipases are used to obtain LPLs enriched with the desired fatty acid either from a natural source or from a synthetic substrate. Immobilized lipases, which are thermostable and reusable, are preferred over those in free form.

In our laboratory the production of structured LPL using immobilized lipases is investigated. A first study consisted in producing LPL-DHA by hydrolysis of PL naturally rich in DHA extracted from the microalga *Isochrysis galbana*. The feasibility of this approach has been demonstrated by Marie Devos (Devos *et al*. 2006). However, this approach is not industrially favored because of the expensive cost to obtain large quantity of microalgae. For this reason, a synthesis approach is currently being developed in the laboratory to synthesize these valuable LPLs, which is the esterification of DHA on a glycerophosphorylated skeleton (GPC), by an enzymatic reaction using a lipase in a free solvent medium.

The general goal of this PhD work was to optimize the esterification synthesis of LPC-DHA using mild conditions (no toxic solvents) to allow production in view of a potential industrial scale production of this compound as food supplement or for therapeutic purposes. The esterification reaction was optimized

according to the response surface methodology (RSM). Various factors influence the reaction such as the applied pressure, molar ratio, biocatalyst quantity and the temperature. First, preliminary experiments were realized to select the most important factors influencing the reaction. And then, RSM was applied to identify the optimal values of the influencing factors that give higher conversion yield and LPC-DHA quantity.

The second objective of this work was to evaluate the effect of LPC-DHA on breast cancer cells (MDA-MB-231) to demonstrate if the LPC carrier of DHA enhances its inhibitory effect. For this purpose, different DHA lipid carriers of DHA were selected to evaluate their effect on these cells and to compare them with the LPC carrier. Then, the mechanisms of cell death exerted by the molecules presenting a protective effect have been studied.

This PhD report is organized around four chapters. The first chapter untitled **Literature Review** consists of a bibliographic synthesis focusing on 4 themes. The first one reviews the structure and main roles of lipids. The second theme covers the health benefits of DHA, its bioavailability and the physiological interest of lipids enriched with DHA. The third theme summarizes the previous studies about the cancer preventive effect of DHA and lipids enriched with DHA as well as a general presentation of the main cell death mechanisms. Finally, the fourth theme focuses on the enzymatic synthesis of LPLs. Here, an overview on the used enzymes to catalyze this synthesis was introduced and the different reactions carried out to synthesize such molecules are cited. Moreover, the parameters that can influence these reactions such as the temperature, the biocatalyst quantity, and the undesirable reactions that can occur during these reactions such as the migration of the acyl group are discussed. Then a summary of the published studies that aim to synthesize structured LPCs through direct esterification is presented. This chapter will be completed with the presentation of experimental designs and their interest in the optimization of reaction conditions.

The second chapter, **Material and Methods** presents the various materials and experimental protocols and techniques used to achieve the thesis objectives.

Chapter three, untitled **Results and discussion** consists of two parts. The first part is devoted to the optimization of the synthesis parameters for LPC-DHA synthesis by the response surface methodology (RSM) approach. It presents also the effect of LPC-DHA on the selected lipase, the purification of LPC-DHA and its structural characterization by NMR. The second part is devoted to the effect of LPC-DHA and other lipid carriers of DHA on MDA-MB-231 viability. This part presents the cell viability tests and cell death

mechanisms and mode of action involved in cell death caused by the molecules exhibiting an inhibitory effect.

The last chapter untitled **Conclusion and Perspectives** summarizes the main results and the proposed perspectives for further development.

Literature review

Chapter 1 : Literature review

I. Lipid overview

Lipids are a chemical heterogenous group of substances including fatty acids (FA) and their derivatives (acylglycerols, phospholipids, sterols, etc..).

According to their structure, lipids can be classified into simple and complex lipids. The simple lipids include FAs, acylglycerols, sterols and ether acylglycerols, while complex lipids include phospholipids, glycolipids and sphingolipids.

A. Simple lipids

1. Fatty acids

Fatty acids (FAs) serve as a base for almost all lipid structures. They consist of a hydrocarbon chain of 4 to 36 carbon atoms, attached to a carboxyl group (COO^-), as illustrated in figure 1.

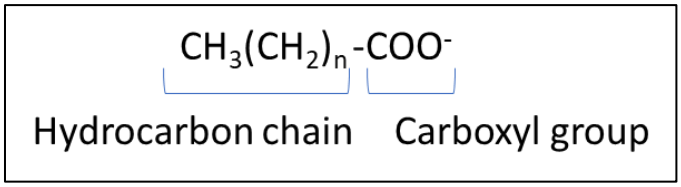

FIGURE 1: EXAMPLE OF A FATTY ACID CHEMICAL STRUCTURE

The biochemical nomenclature of FAs is concerned with the number of carbons and the number of double bonds and it can be presented in the following forms:

$$X : Y\ n\text{-}Z \text{ or } X : Y\ \omega\text{-}Z$$

With,

X: number of carbon atoms

Y: number of double bonds

Z: position of the first double bond from the methyl end $-CH_3$

For example, C22:6 ω-3, namely docosahexaenoic acid, is a FA that belongs to the ω-3 family, composed of 22 carbons and containing 6 double bonds.

FAs could be classified based on their degree of unsaturation. If the carbon-carbon bonds are all single, the FA is saturated (figure 2). If any of the bonds is double, the FA is monounsaturated (MUFA) (figure 3).

There can be more than one double bond in an unsaturated FA. In this case, FAs are polyunsaturated FAs (PUFAs) (figure 4).

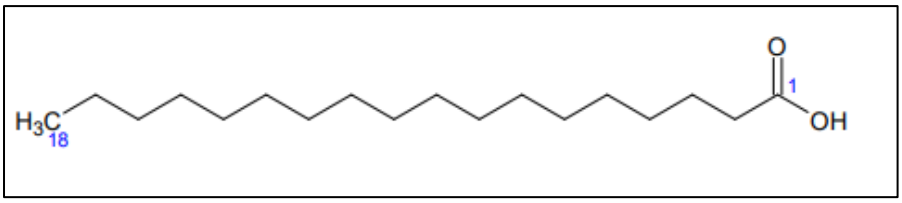

FIGURE 2: STEARIC ACID (C18:0) CHEMICAL STRUCTURE

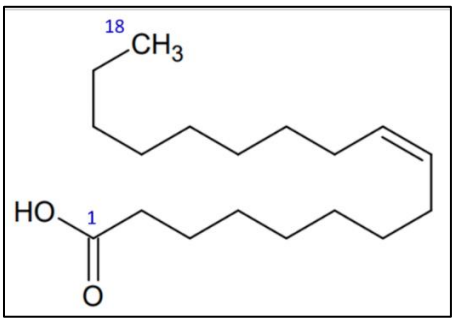

FIGURE 3: OLEIC ACID (C18:1 ω -9) CHEMICAL STRUCTURE

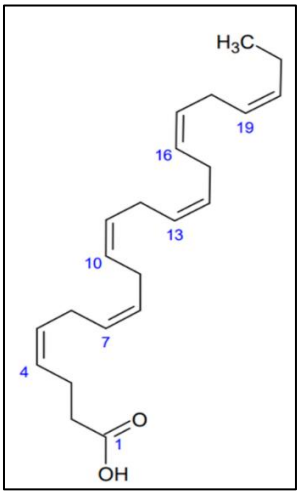

FIGURE 4: DOCOSAHEXAENOIC ACID (C22:6 ω -3) CHEMICAL STRUCTURE

The existence of a double bond leads to the formation of two possible configurations *cis* (or Z) and *trans* (or E), that can be taken by the two alkyl chains adjacent to the double bonded carbons. *Cis* configuration means that the 2 adjacent alkyl chains (R and R^1 in figure 5) on both sides of the double bond are oriented in the same direction. In the case of *trans* configuration, they lie on opposite sides as it can be seen in figure 5 where the 2 adjacent R and R^1 surround the double bond.

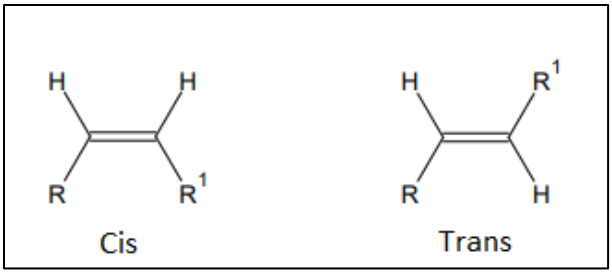

FIGURE 5: CIS AND TRANS CONFIGURATION

(R and R^1 =alkyl chains)

Cis configuration is mainly present in biological unsaturated FAs. Small amounts of *trans* FAs are naturally present in some foods, such as dairy products and meat (Sommerfeld 1983). They are also found in breast milk, in concentrations directly related to the mother's dietary intake of *trans* fats (Chappell *et al.* 1985).

FAs with *trans* configuration make the membrane less fluid and raise the melting point of the fats of which they are part (Valenzuela and Morgado 1999). Therefore they exhibit a solid texture at room temperature, which is a property required by the food industry, especially for the preparation of margarines (Silva *et al.* 2021).

Trans fats are known to increase low-density lipoprotein cholesterol (LDL) and decrease high-density lipoprotein cholesterol (HDL), thereby increasing the risk of cardiovascular disease (Islam *et al.* 2019).

FAs can also be classified according to the body's ability to produce them or not. There are the non-essential FAs which play a vital role and can be synthesized by the body, and there are the essential FAs that cannot be synthesized by the body and need to be provided by food intake because the body requires them for good health (Clissold and Thickitt 1994).

Linoleic acid (C18:2 ω-6) and α-linolenic acid (C18:3 ω-3), are essential FAs, and are the precursors of the long chain PUFAs (LC-PUFA) of the omega 6 (ω-6) and omega 3 (ω-3) families, respectively. The ω-3 family includes for example α-linolenic acid (ALA), eicosapentaenoic acid (EPA) and docosahexaenoic acid (DHA). The ω-6 family includes for example linoleic acid (LA) and arachidonic acid (ARA).

2. Acylglycerols

Acylglycerols (AGs) are the predominant constituents of commercially important oils and fats. They are esters made up of one, two or three residues of FAs and glycerol.

The glycerol is made up of three hydroxyl functional groups that can be esterified with one, two or three FAs. This esterification gives a monoacylglycerol (MAG), a diacylglycerol (DAG) and a triacylglycerol (TAG), respectively (figure 6).

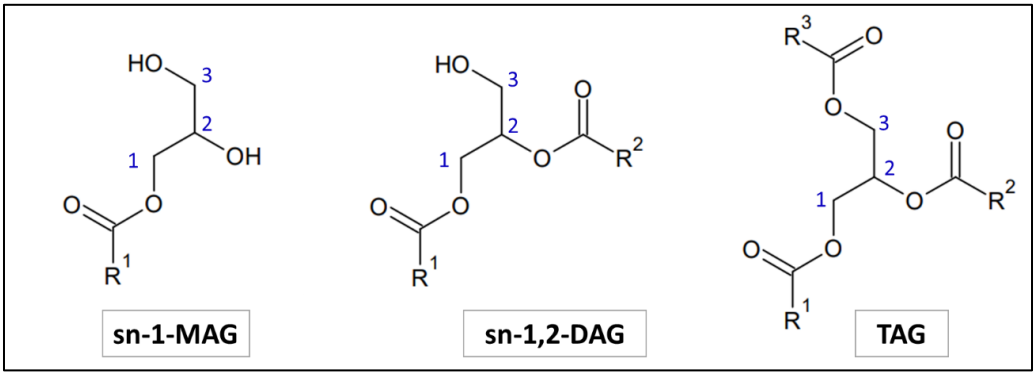

FIGURE 6: *SN*-1-MONOACYLGLYCEROL, *SN*-1,2-DIACYLGLYCEROL AND TRIACYLGLYCEROL CHEMICAL STRUCTURES

(R^1, R^2 and R^3 =alkyl chains)

These structures vary in that the FA alkyl groups can differ in carbon number, degree of unsaturation and configuration of the double bonds. In addition, these FA alkyl groups may be esterified on the 1st, 2nd or 3rd hydroxyl group of the glycerol leading to the stereospecific numbering *sn*-1, -2 or -3 nomenclature.

B. Complex lipids

1. Phospholipids

Phospholipids (PLs) consist of a glycerol skeleton associated with two FAs (named hydrophobic tails), and a hydrophilic head consisting of a phosphate group linked to a simple organic molecule such as glycerol, choline, serine, inositol or ethanolamine (Da Costa and Ito 2003) (figure 7). The corresponding PLs are phosphatidylglycerol (PG), phosphatidylcholine (PC), phosphatidylserine (PS), phosphatidylinositol (PI) or phosphatidylethanolamine (PE).

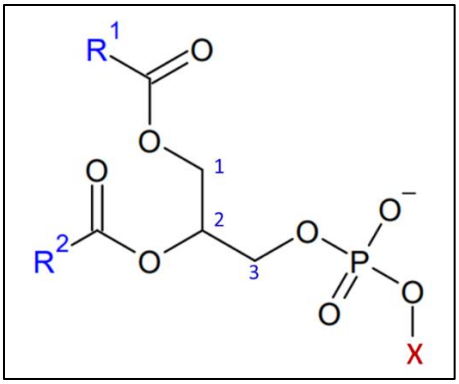

FIGURE 7: PHOSPHOLIPID CHEMICAL STRUCTURE

(R^1 and R^2 = alkyl chains; X= organic molecule)

PLs are therefore different from each other depending on the nature of the FAs and the nature of the organic molecule linked to the phosphate group.

PLs are essential components of biological membranes. They provide structural assurance of membrane integrity. They play a role in the fluidity of membranes as well as in their permeability to some molecules or ions (Béréziat *et al.* 1988). The FA chain length and unsaturation (Van Meer *et al.* 2008), the size of the phosphate head group (Cullis and De Kruijff 1979) and its hydration status (Crowe *et al.* 1987) have been shown to alter membrane fluidity.

Besides the structural role of PLs, some more specific functions are attributed to them. They are involved in various cellular processes such as signaling, cell proliferation, metabolism or modulation of enzyme activities (Rosen *et al.* 1992; Zeisel 1993; Wang *et al.* 2006; Lykidis 2007).

In addition, PLs play an essential role in the food and pharmaceutical industries due to their emulsifying properties. Indeed, due to their amphiphilic character, PLs have the ability to decrease surface tension by adsorbing at interfaces in water/oil emulsions (Van Meer *et al.* 2008). They are used in the composition of margarines, chocolates, pastries and dairy products. Their amphipathic character and their aggregation properties are the subject of extensive biomedical research such as emulsion in pharmaceutical (Okuro *et al*. 2019), preparation of liposomes for cosmetics and drug delivery (Bozzuto and Molinari 2015; Breitsamer and Winter 2019).

2. Lysophospholipids

Lysophospholipids (LPLs) possess the same structure as PLs but lack one acyl chain. There are two isomers of LPLs depending on the position of the acyl chain: *sn*-1-LPLs maintain the acyl chain in position 1, while the *sn*-2-LPLs are acylated at position 2 (figure 8).

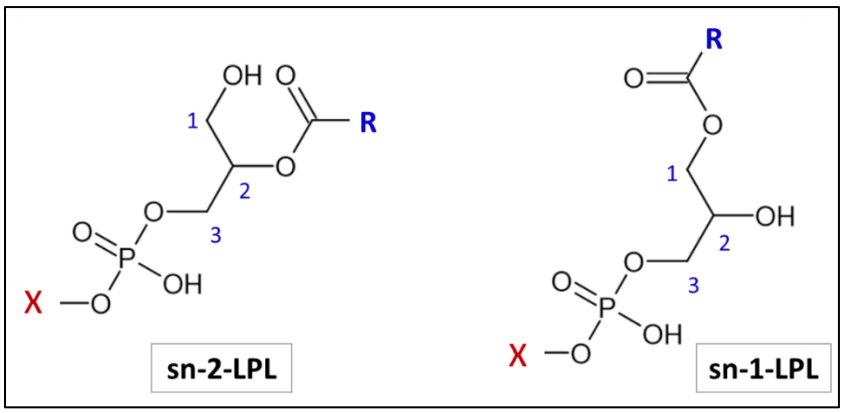

FIGURE 8: LYSOPHOSPHOLIPIDS CHEMICAL STRUCTURE

(R=alkyl chain, X= organic molecule)

There are different molecular species of LPLs: lysophosphatidic acid (LPA), lysophosphatidylglycerol (LPG), lysophosphatidylserine (LPS), lysophosphatidylethanolamine (LPE), lysophosphatidylcholine (LPC), lysophosphatidylinositol (LPI) and lysophosphatidylglycerol (LPG).

These LPLs possess properties similar to those of PLs. However, unlike PLs, LPLs are only found in small amounts in biological cell membranes (Birgbauer and Chun 2006).

The presence of LPLs and their receptors in various tissues and cell types, show their involvement in several physiological processes. Indeed, they are involved in normal and pathogenic biological processes, such as carcinogenesis (LPC, LPA, LPS), neurological disorder (LPC), immunity (LPC), cardiovascular system (LPC, LPI, LPG), inflammation (LPC, LPA, LPS) or regulation of metabolic pathologies as recently reviewed by Tan *et al.* (2020).

They are useful emulsifying and solubilizing agents and synthetic intermediates for the preparation of PLs for applications in cosmetics, food, pharmaceutical drugs and agrochemicals (Schneider 2001).

LPLs physiological roles are highly dependent on their biochemical structure. The structural diversity of LPLs results in their interactions with a variety of biomolecular targets. Both, the FA and the hydrophilic

head group, define the specific chemical structure of LPLs molecules and thereby affect their biological activities. For example, Kim *et al.* (2007) have shown that the cytotoxic effect in leukemia cancer was most prominent with LPC than with LPA, LPS, LPE and LPG. Also, in the context of studying how endocytosis is affected by different exogenously added LPLs, Ailte *et al.* (2017) have demonstrated that the use of LPLs with large head groups strongly inhibits endocytosis in various cell lines, while LPLs with small head groups do not. Moreover Kim *et al.* (2007) demonstrated that palmitoyl-LPC (LPC-C16:0) was the most toxic in leukemia among various LPC tested with different chain length and unsaturation degree.

II. DHA

DHA (all cis 4, 7, 10, 13, 16, 19- docosahexaenoic acid, 22:6) (C22:6 ω-3) is a PUFA that belongs to the ω-3 family. It has a structure that gives unique physical and functional features.

DHA availability is regulated by many *in vivo* factors. Several studies have investigated the influence of the type and esterified form of DHA on AGs, PLs and LPLs on its bioavailability and health benefits. It was shown that the difference in lipid structure in which DHA is delivered influence its bioavailability.

In the following paragraphs, an overview of DHA's interests, sources and metabolism will be discussed as well as the bioavailability of DHA and its effects when integrated into lipids.

A. Overview

DHA has been of interest for the scientific world since the work of Dyerberg *et al.* (1978), which highlighted the prevention of cardiovascular diseases (CVD) in Eskimos by the contribution of DHA in the diet.

Since that time, a large number of experimental works have been conducted to study the role of ω-3 PUFAs, and specifically DHA, in the prevention of CVD as reviewed by Innes and Calder (2020) and Elagizi *et al.* (2021). They provided evidence regarding the potential of DHA on modulating cardiovascular risk factors such as lowering blood pressure, triglyceride content, platelet aggregation, reducing resting heart rate and increasing HDL level (AbuMweis *et al.* 2018; Hidayat *et al.* 2018; Mason *et al.* 2020).

Besides the benefit of DHA on the cardiovascular health, previous studies in the 1960s and 1970s demonstrated a functional role of DHA in eyes and brain health, since DHA was found to be abundant in both synaptic (Cotman *et al*. 1969) and retinal membranes (Benolken *et al.* 1973; Anderson *et al.* 1974). So the effect of DHA was intensively investigated and a significant number of reviews are now available such as Lauritzen *et al.* (2016); Echeverría *et al.* (2017); Lacombe *et al.* (2018); Mallick *et al.* (2019).

DHA has also been identified as a neuroprotective agent against cerebral aging, neurodegenerative diseases and cerebrovascular diseases. DHA-derived mediators such as neuroprotectins, resolvins, and maresins produced in the brain, play important roles in protection against ischaemia, injury and inflammation (Bazinet and Layé 2014). For example, DHA allows the prevention of neurodegenerative pathologies such as Alzheimer's disease. It protects the neurons by limiting the release of pro-inflammatory signals and by promoting the antioxidant activity (Heras-Sandoval *et al.* 2016).

Regarding the neuroprotective effects of DHA supplementation, possible mechanisms have been proposed: DHA maintains the integrity and function of the neuronal membranes, reduces neuronal death and preserves neuronal signaling pathways (Echeverría *et al.* 2017).

It is also well known that DHA is essential for the sight of the developing fetus and infant, as epidemiological studies have shown the role of DHA, and other ω-3 PUFAs, on the maternal health during pregnancy and child health (Carlson *et al.* 2013, Mun *et al.* 2019). Moreover, supplementation of DHA in children has been proven to be effective in improving cognition and memory (Chouinard-Watkins *et al.* 2017; Wilczynska and Modrzewski 2019).

Along with the benefits of DHA for brain development and function, studies have demonstrated that DHA is an important structural component for retinal photoreceptors. Fluidity of membrane mediated by DHA improves the process of rhodopsin activation in visual signaling (Stillwell and Wassall 2003). Hence, DHA supplementation during pregnancy has contributed to the maturation of the visual system (Judge *et al.* 2007).

Over the past decade it has been shown that DHA is able to reduce the risk of cancer. These findings are supported by several clinical studies as previously reviewed by Shahidi and Ambigaipalan (2018), but more clinical trials are needed to find out the effective doses and formulas of DHA for specific cancer pathologies. The role of DHA in preventing cancer will be more developed in the upcoming paragraphs.

Besides, DHA effect on diabetes have been described by some authors, revealing some controversies in the obtained results. Indeed, for instance, Wang *et al.* (2003) have reported that ω-3 PUFA supplementation provides beneficial effects against type 2 diabetes, although, Djoussé *et al.* (2011) showed the opposite effect. Recently, Cadario *et al.* (2019) reported that ω-3 PUFAs with a vitamin D co-supplementation diet display benefits for children with type 1 diabetes. Therefore, further investigations are necessary to determine whether ω-3 PUFAs positively influence diabetes or not.

DHA is either provided by the diet or synthesized by the conversion of α-linolenic acid (ALA) (C18:3 ω-3) to eicosapentaenoic acid (EPA) (C20:5 ω-3), which is subsequently metabolized into DHA. The metabolic pathway that synthesizes DHA, involves a series of desaturation (insertion of double bonds) and elongation (addition of 2 carbon atoms) steps (figure 9).

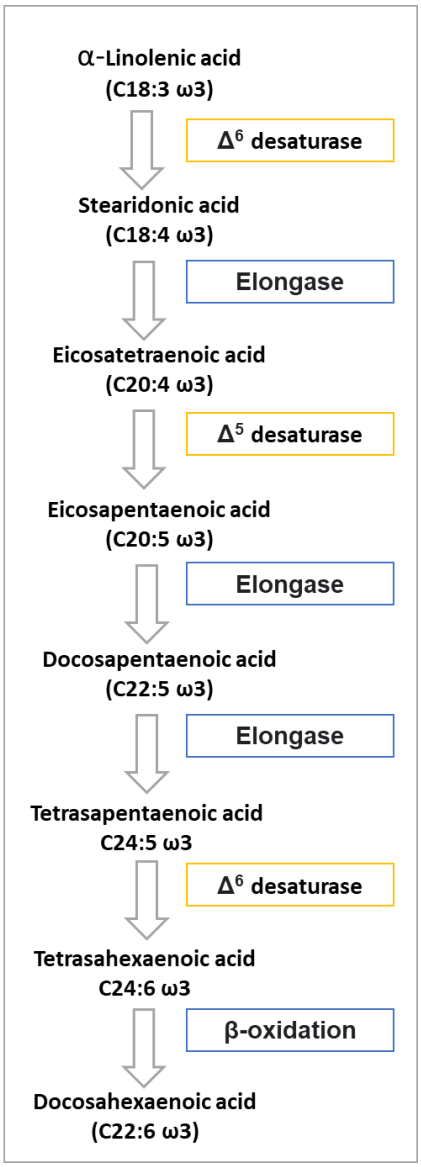

FIGURE 9: THE METABOLIC PATHWAY OF CONVERSION OF α-LINOLENIC ACID TO DHA IN MAMMALS

The conversion yield of ALA to EPA is very limited, on the order of 5-8%, and less than 0.5% of ALA is converted to DHA (Plourde and Cunnane 2007). This could be due to several causes. Among them, is that the desaturases which are necessary for the synthesis of DHA, are also involved in the desaturation of ω-6 PUFAs. So, a competition exists between the conversion of ω-3 and ω-6 PUFAs and the conversion yield

of ALA is low because in industrialized countries, the diet provides more linoleic acid than ALA (Calder 2016).

A number of other factors have been shown to regulate this pathway. These include the availability of ALA and various oligo-elements, including zinc and iron, as the enzymes involved in the pathway need them as cofactors (Calder 2016).

Therefore, it is recommended to consume DHA directly from foods or dietary supplements (Burdge and Calder 2005). There are not many sources containing DHA. Marine sources are the main sources of human DHA intake, among which is found an initial source which are microalgae. Microalgae contain high levels of ω-3 PUFAs (ALA, EPA and DHA) which vary according to the species as well as the culture conditions. DHA is also found in high amounts in fatty fishes such as salmon and herring (table 1).

TABLE 1: MARINE SOURCES RICH IN DHA

Source	Species	DHA (g/100g portion)
Microalgae	*Schizochytrium sp.* (*)	40
	Crypthecodinium cohnii (*)	40
Fish	Shad	1.32
	Herring	1.18
	Salmon	1.10
	Chinook salmon	0.94
Mollusks	Mussels	0.51
	Pacific oysters	0.50
Shellfish	Shrimp	0.20
	Alaskan crab	0.20

(Data from the U.S. Department of Agriculture, release 28 (2015) - (*): Ryan *et al.* 2009)

DHA is also present at low concentrations in beef, lamb, pork and poultry meat, dairy products and eggs. The content of DHA in these products varies according to the composition of the diet and the digestive system of the animal. It has been demonstrated that feeding animals with a diet rich in ALA can increase the contents of DHA in animal derived products (Moghadasian 2008; Lee *et al*. 2019).

Significant efforts have been made to produce many products fortified in ω-3 PUFAs, such as DHA, like infant milk, sausages, juices, *etc*. Despite significant achievements in this field, there are some limitations

regarding the quality, availability and consumer acceptability of these fortified food products. As a consequence of these limitations, the current research are focused on the production of transgenic plants and animals capable of efficiently converting ω-6 to ω-3 PUFAs (Shanab *et al.* 2018).

B. DHA bioavailability

To exert the health benefits that exhibit DHA, its bioavailability should be taken in consideration for the efficacy of DHA supplements, which depends on many factors. Bioavailability is the extent in which a nutrient can be absorbed and transported to the systemic circulation or the site of the physiological activity.

So far, many studies were interested in studying the lipid formulations needed to improve the bioavailability of DHA. To our knowledge three reviews have been published on the bioavailability of DHA. Schuchardt and Hahn (2013) and Ghasemifard *et al.* (2014) have focused on the used analytical and methodological approaches to perform these studies. Recently a review by Li *et al.* (2021a) focused on the different factors that alter the bioavailability of DHA.

According to Li *et al.* (2021a) numerous factors were found to influence the DHA bioavailability, such as the chemical forms and stereospecific (*sn*) position of DHA, the food composition in which DHA bioavailability was higher in high fat diet than low fat diet, food excipients and human hormones and health state.

DHA chemical form differs according to the dietary supplement source. The most common source of DHA supplementation are fish and algal oils. In fish oils, DHA is mainly present in TAG form (primarily esterified on the *sn*-2 position), and to a less extent in free form. DHA is also naturally present in PL form in krill and algal oils (almost always in the *sn*-2 position). Other commercial dietary lipids with high DHA content are present in food in the form of MAG, DAG and ethyl ester (Destaillats *et al.* 2018; Li *et al.* 2021a).

It was shown that the bioavailability in ethyl ester form is lower than that in TAG form and that free DHA has the highest bioavailability (Beckermann *et al*. 1990). These findings could be attributed to the fact that TAGs and ethyl esters need to be hydrolyzed into free DHA before their incorporation into chylomicrons, which are lipoprotein particles that transport dietary lipids from intestines to other locations in the body. Moreover, ethyl esters are 50 times more resistant to the hydrolysis by pancreatic lipase than TAGs (Grimsgaard *et al.* 1998).

The different AG forms bioavailability was investigated by Banno *et al.* (2002). The lymphatic absorption of DHA was significantly higher in the order MAG-DHA > DAG-DHA (didocosahexaenoin) > TAG-DHA (tridocosahexaenoin). Destaillats *et al.* (2018) have also showed that DHA was better absorbed when provided as MAGs than as TAGs. These findings were supported by Cruz-Hernandez *et al.* (2016), who demonstrated that MAGs did not require to be hydrolyzed by the pancreatic lipase to be absorbed.

Many studies have focused on the importance of FAs esterified on the *sn*-2 position of TAG. Christensen and Høy (1997) have shown that the absorption of DHA was enhanced when the DHA is esterified at the *sn*-2 position of the TAG. This was attributed to the fact that the lipases from the gastrointestinal tract are *sn*-1,3 regioselective (Jensen *et al.* 1983). Moreover, it has been shown that *sn*-2 MAG enhanced absorption and accretion of DHA to tissues (Cruz-Hernandez *et al.* 2012, 2016), as DHA are absorbed by the intestine as *sn*-2 MAG (Straarup and Høy 2000).

Regarding the PL form, it was reported that DHA is better absorbed by the body when provided in the form of PLs rather than in free or TAG forms (Cook *et al.* 2016, Destaillats *et al.* 2018). The higher DHA bioavailability from PL than from TAG is still not fully understood. However, this could be attributed to the fact that PL protect the DHA from oxidation, since it is particularly sensitive to oxidation due to DHA numerous unsaturations. Lyberg *et al*. (2005) studied the oxidation of free DHA and DHA incorporated into PC, PE and TAG, and found that DHA was protected against hydroperoxide formation when it was incorporated in either PC or PE. No explanation for these results was given.

However, Köhler *et al.* (2015) showed that there was no significant difference in the DHA level of red blood cell membrane between the TAG and PL forms. This contradiction could be attributed to the different doses, duration of treatment, the variations in krill oil compositions (19%-81% of PL) and the various forms of PL (PS, PE or PC).

Recently there is a particular interest towards the LPC-DHA, since it has been found to be more potent at enriching brain and eye in DHA compared to free DHA, PC-DHA (*sn*-1,2) or TAG-DHA (*sn*-1,2,3) (Sugasini *et al.* 2019; Sugasini *et al.* 2020). Indeed, the blood-brain and blood-retinal barriers have a specific transporter (Mfsd2a) that does not transport TAG or free DHA, but instead, requires a LPC form of DHA (Wong and Silver 2020).

Few informations are available about the influence of DHA positional distribution in PL on its bioavailability. According to Sugasini *et al*. (2020), *sn*-1 PC-DHA is preferred to increase brain DHA, as FA at the *sn*-2 position of PC would be released and *sn*-1 DHA would be retained as LPC.

Regarding LPC form, both *sn*-1 and *sn*-2 LPC-DHA increased DHA content in brain (Sugasini *et al.* 2020). However, Hung *et al.* (2011a) reported that the metabolic effects of *sn*-1 LPC-DHA are different from those of *sn*-2 LPC-DHA. The s*n*-2 isomer was reported to be more efficient in reducing inflammation in mice compared to *sn*-1 isomer, and this has been attributed to the more effective absorption of *sn*-2 LPC-DHA in lymph by Sugasini *et al.* (2017).

These studies support the fact that bioavailability of DHA depend on the DHA carrying lipidic form, its position on it as well as the studied organ. Thus, this should be considered when studying a physiological role.

C. Effects of DHA lipid forms

In the following paragraphs the effects of DHA when esterified on different lipid (AGs, PLs and LPLs) will be presented.

Acylglycerols rich in DHA

MAGs containing a ω-3 PUFA have been shown to have various beneficial effects on health. We will be interested only in the beneficial roles of MAG-DHA in the upcoming paragraphs. Figure 10 illustrates the *sn*-1 MAG-DHA structure.

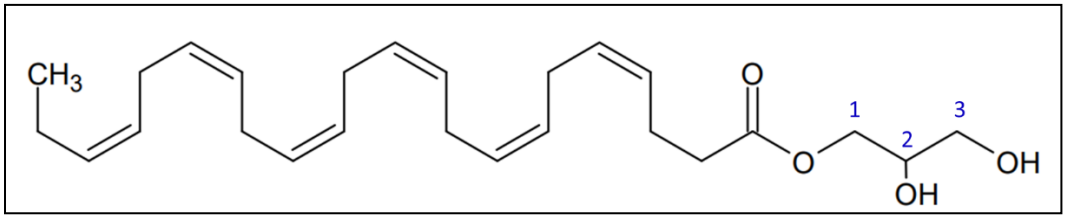

FIGURE 10: 1-MONODOCOSAHEXAENOIN STRUCTURE

Morin *et al.* (2012) have demonstrated that MAG-DHA can be used as an efficient treatment for pulmonary arterial hypertension disease. Moreover, it could serve as a precursor to generate a variety of PUFA-derived mediators, such as resolvins, that are known to mediate antiproliferation and anti-inflammation via specific receptors (Khaddaj-Mallat *et al.* 2016; Park *et al.* 2021). Moreover, MAG-DHA exhibits an interesting antiproliferative effect that will be discussed in the following sections.

As well, MAG-DHA may provide an interesting approach for the prevention of hypertension and cardiovascular disease. Rats supplemented with *sn*-1 MAG-DHA revealed an increase in DHA levels correlated with the production of DHA metabolites in aortic tissues. These metabolites resulted in a

decrease in total cholesterol level, prevented aortic wall thickness increase and reduced pro-inflammatory levels such as interleukines-6 (Morin *et al.* 2015).

Regarding DAG-DHA and TAG-DHA, to our knowledge, there are few publications that address the vectors role of these forms on the physiological effects of DHA.

In 2013, contrary to TAG-EPA, TAG-DHA was reported to confer neuroprotection after hypoxic-ischemic injury, a type of brain dysfunction, in a neonatal mice. The mechanism of this neuroprotection remained unclear (Williams *et al.* 2013). In more recent studies, Mayurasakorn *et al.* (2016) found that administration of TAG-DHA after hypoxic-ischemic injury resulted in significant accumulation of DHA and DHA derived bioactive metabolites in the brain. These metabolites which are protectins (anti-inflammatory and neuroprotective metabolites) and D-series resolvins (promoting restoration of normal cellular function after injury) confer neuroprotection. Uptake of DHA into the brain when esterified on a TAG was interesting to investigate as it was reported to be very low (Sugasini *et al*. 2017). Recently, Kollareth *et al.* (2020) have demonstrated that TAG-DHA administration increased DHA contents in plasma LPC and non-esterified FAs. These findings suggest that the transfer of DHA through plasma lipid pools plays an essential role in DHA brain transport.

Regarding DAG-DHA, Madani *et al.* (2004) showed that DHA esterified on the *sn*-2 of DAG activates the MAP kinase in cultured leukemia cells.

Phospholipids and lysophospholipids rich in DHA

DHA rich phospholipids (PL-DHA) and lysophospholipids (LPL-DHA) have received considerable attention in recent decades due to their various health benefits. Particularly, there are several reviews underlying the health benefits of PL-DHA (Zhang *et al.* 2019a; Zhang *et al.* 2020a; Ahmmed *et al.* 2020). Yet, LPL-DHA health benefits are lately starting to be increasingly investigated. *Sn*-1,2 PL-DHA and *sn*-1 LPL-DHA chemical structures are given in figure 11 and 12, respectively.

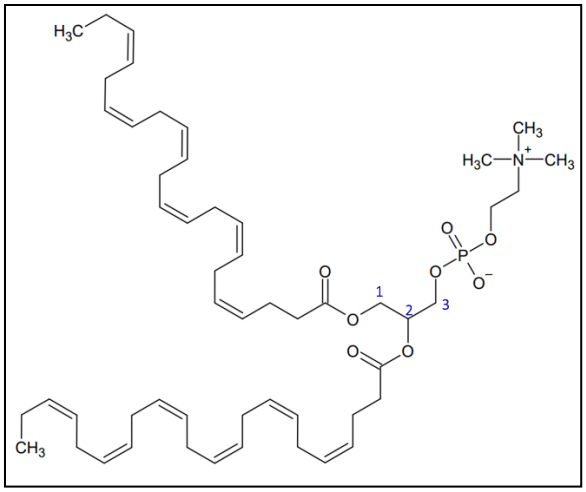

FIGURE 11: *sn*-1,2 DHA-PHOSPHATIDYLCHOLINE CHEMICAL STRUCTURE

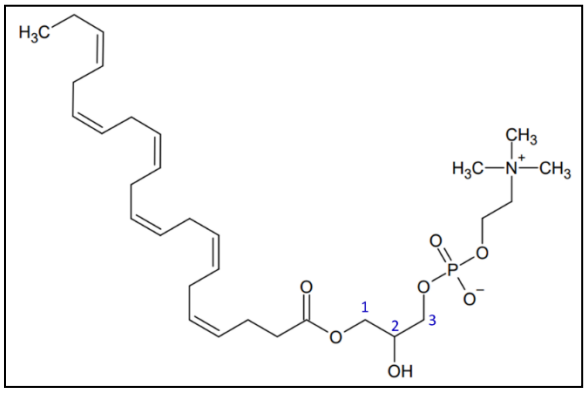

FIGURE 12: *sn*-1- DHA-LYSOPHOSPHATIDYLCHOLINE CHEMICAL STRUCTURE

Besides the bioavailability advantage, many effects have been attributed to PL-DHA and LPL-DHA, starting with the effect of these two molecules on the brain. In animal experiments, PL-DHA have shown a range of beneficial effects including improvement of brain function, memory and cognition in mice by decreasing β-amyloid peptide concentration, which is a peptide that causes Alzheimer's disease (Zhou *et al.* 2018). However, PS-DHA exhibited better improvement compared to PC-DHA and PE-DHA, indicating an advantage of PS over PC and PE (Wang *et al.* 2018).

The effect of LPC-DHA on the brain has been the most studied since the brain shows the particularity of absorbing DHA in the form of LPC as previously described. For this reason, it was shown that LPC-DHA helps in the treatment of depression and also in the treatment of neuroinflammatory diseases (Yalagala *et al.* 2019), improves brain function (Sugasini *et al.* 2017) and improves memory and learning abilities (Valenzuela Bonomo *et al.* 2010).

A recent study showed the potential role of LPC-DHA in the delivery of DHA through basal plasma membrane mediated by Mfsd2a to the fetus (Ferchaud-Roucher *et al*. 2019). These findings suggest that LPC-DHA is critical to support fetal growth, in particular for the fetal brain development.

Along with brain health benefits, PLs-DHA exhibit other health benefits against cardiovascular disease by reducing cholesterol and improving lipid metabolism in mice (Zhang *et al.* 2019a). Regarding LPC-DHA, animal experiments showed that it exhibits a hypolipidemic effect. A diet rich in LPC-DHA reduced LDL cholesterol level. Conversely, it increased HDL cholesterol in female mice, which promotes good cardiovascular health (Osborn and Akoh 2002). Hosomi *et al.* (2019) showed that LPC-DHA intake reduced TAG concentration in the serum and liver of rats.

Moreover, PLs-DHA exhibit benefits against kidney and liver diseases. Dietary supplements of PC-DHA were found to be functional against nephrotoxicity (Shi *et al.* 2018). They present a promising supplement for the relief of renal dysfunction (Zhang *et al.* 2021). Earlier, LPC-DHA was shown to activate the metabolism detoxification of the liver and restore the gastrointestinal mucosa, thus improving its functioning (Hosokawa *et al.* 1998).

In addition, LPC-DHA exhibits anti-inflammatory activity in mice by inhibiting pro-inflammatory cytokine formation in response to lipopolysaccharides, in contrast to free DHA which does not exhibit an anti-inflammatory effect (Huang *et al*. 2010, Jin *et al.* 2012).

Overall, these studies indicate that PL-DHA and LPL-DHA are effective not only in brain health but also for general health. Yet, most of the studies have been conducted on animal models.

III. DHA and cancer

Epidemiological studies have established a link between high consumption of fatty fish and a reduction in the risk of breast, prostate and colorectal cancers (Berquin *et al.* 2008; Gerber 2012). And this was linked to the fact that fatty fishes were highly rich in ω-3 PUFAs.

In this thesis, one of the objectives was to study the effect of lipids carrying DHA on breast cancer cell viability and to identify the mechanisms that trigger cell death by these molecules.

Thus, an overview on the cell death mechanisms and a summary on the effect of DHA on cancer cells viability will be addressed below.

A. Cell death mechanisms

Cell death plays an important role in eliminating damaged cells and maintaining the homeostasis of the organism.

1. Apoptosis

Apoptosis, or programmed cell death, is a normal, intrinsically programmed cellular mechanism by which cells destruct themselves in response to an internal or external signal.

Apoptosis is characterized at the cellular level by invagination of plasma membranes, chromatin condensation and DNA fragmentation. Apoptotic bodies, which correspond to fragments of the cell, appear and can be phagocytosed (figure 13) (Majno and Joris 1995).

Apoptosis occurs in a caspase-dependent manner. Caspases define a class of proteases. Mammalian caspases are present in inactive form and are categorized into two groups: a group made of enzymes involved in the regulation of inflammation and a group that plays a pivotal role in the regulation of cell apoptosis. After stimulation, a cell undergoes an organized degradation of cell organelles by activation of caspases. Caspases implicated in apoptosis can be split into two main groups, the initiating caspases (caspases 8, 9 and 10) and the downstream effector caspases (caspases 2, 3, 6 and 7) (Thornberry 1998).

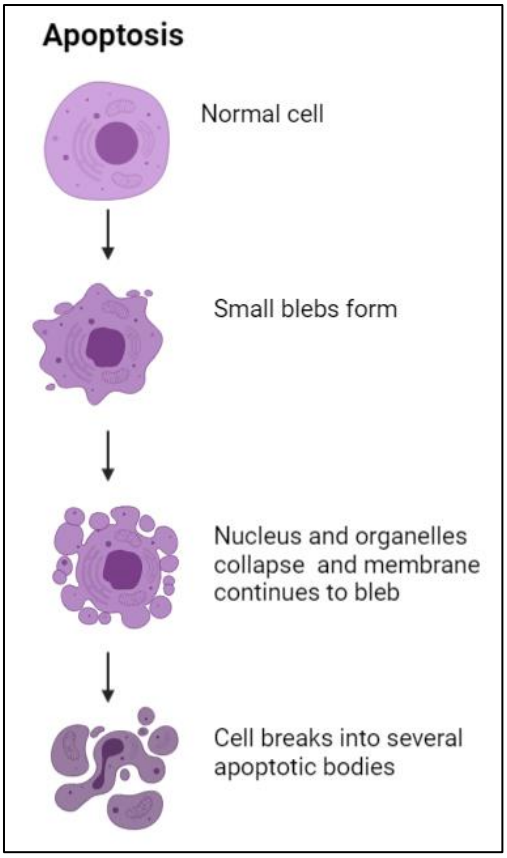

FIGURE 13: SCHEME REPRESENTING APOPTOSIS PROCESS

(Adapted from **PANAWALA** 2017)

2. Necrosis

Necrosis is the abnormal and unscheduled death of a cell or tissue (Majno and Joris 1995). It is therefore opposed to apoptosis. A number of external factors, like toxins, infection and physical injuries, stimulate necrosis, resulting in morphological alterations, such as cell plasma membrane rupture, cytoplasmic swelling and consequent loss of intracellular organelles (Yan *et al.* 2020).

The Figure 14 illustrates necrosis processes.

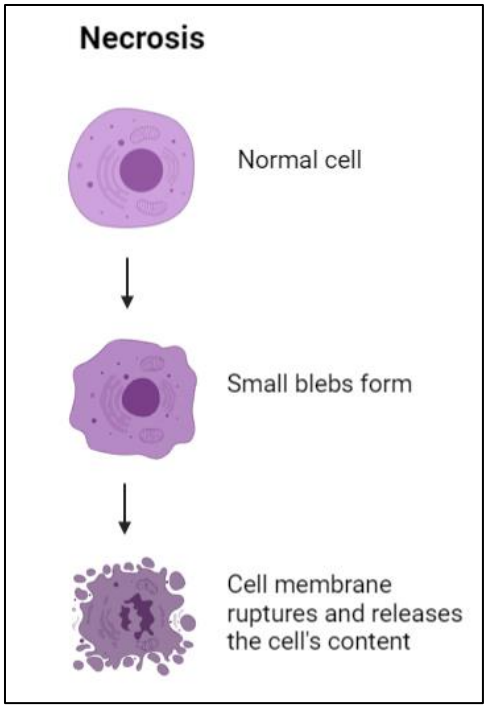

FIGURE 14: SCHEME REPRESENTING NECROSIS PROCESS

(Adapted from **PANAWALA** 2017)

3. Autophagy

Autophagy is a cellular mechanism that consists in the partial degradation of cell cytoplasm using its own lysosomes. Autophagy is activated during cellular stress as a protective response. It is involved at different levels, whether in the repair of cellular elements, in the immune response or in cell death (Mortimore *et al.* 1996).

There are 3 forms of autophagy, among which the macro-autophagy is found. Macro-autophagy is known to deliver cytoplasmic components to the lysosome *via* the intermediary of a large intracellular vesicle, namely autophagosome, that fuses with the lysosome to form an autolysosome (figure 15) (Mizushima and Komatsu 2011).

Macro-autophagy is considered as the main type of autophagy, and it has been studied most extensively than the other forms of autophagy (micro-autophagy and chaperone-mediated autophagy). Therefore, in this work the macro-autophagy will be simply referred as "autophagy."

It is characterized by the appearance of large intracellular vesicles (autophagosome), enlarged organelles, plasma membrane blebbing and depletion of cytoplasmic organelles in the absence of chromatin condensation (Liu and Levine 2015).

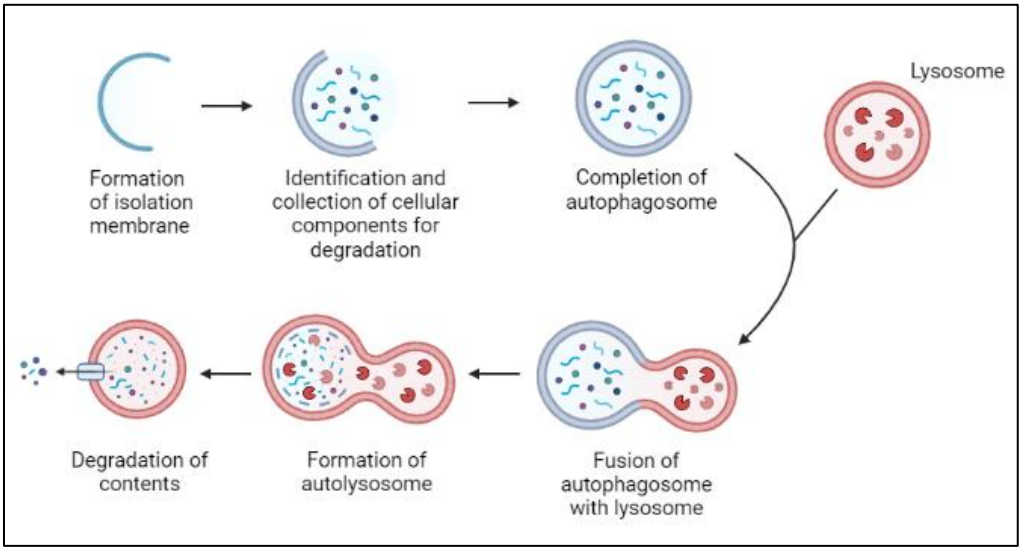

FIGURE 15: SCHEME REPRESENTING MACRO-AUTOPHAGY PROCESS

(adapted from MITCHELL 2012)

B. Protective effect of DHA

Numerous studies suggest that ω-3 PUFAs have anticancer effects, while ω-6 PUFAs promote cancer (Berquin *et al.* 2007, Shahidi and Ambigaipalan 2018). Therefore, the preventive potential role of ω-3 PUFAs became a subject of deep interest and debate. So, numerous studies have been performed either *in vivo* or *in vitro* to demonstrate the protective effect of ω-3 PUFAs against cancer risk as reviewed by Berquin *et al.* (2008), Newell *et al.* (2017) and Brown *et al.* (2020). Some of these studies are listed in Table 2 (page 41).

Among the various ω-3 PUFAs, DHA showed higher effectiveness in decreasing cancer cell viability compared to others, such as EPA and ALA.

1. Clinical and preclinical studies

Numerous clinical studies have been conducted and have shown a link between high intake of ω-3 PUFAs, such as DHA, and risk reduction of colorectal and breast cancer in patients (Cockbain *et al.* 2012; Fabian *et al.* 2015; Troesch *et al.* 2020). In these clinical studies, the dose, the duration of the treatment, and the effect of the supplementation on the expression of proteins involved in cell death mechanisms as well as

the side effects, have been reported. It should be pointed out that most of these studies showed that the supplementation did not show any side effects in the patients. There was just a dislike about the smell of the supplements, when the supplementation was done with fish oils. All these reviews highlighted the need for further clinical studies to optimize supplement dosage, duration and to better determine the mechanisms of action.

Several preclinical studies, performed in mice and rats, have also attempted to investigate the link between ω-3 PUFAs (DHA and EPA) supplementation and cancer prevention (Carroll and Braden 1984). The results supported the protective effect of ω-3 PUFAs. Results reported from preclinical studies showed that DHA causes tumor growth decreases and protects against cancer progression stages by reducing metastasis (Rahman *et al.* 2013; Bilyk *et al.* 2021) (Table 2).

Table 2 lists some of the preclinical studies that demonstrated the effect of DHA on breast cancer cells in rodents. The table indicates the type of cancer, the tested concentrations and the observed results.

2. *In vitro* studies

Simultaneously, many studies have investigated the protective effect of DHA *in vitro* on different cultured cancer cell lines. Table 2 lists some of these studies.

TABLE 2: *IN VITRO* AND *IN VIVO* PRECLINICAL STUDIES OF DHA SUPPLEMENTATION FOR THE TREATMENT OF CANCER

Reference	Cancer model	Cancer cell line	Tested concentrations	Results	Mode of action
(Rizzo *et al*. 2021)	Breast	MDA-MB-231, MCF7	50, 100 and 200 µM	Different sensitivity of MDA-MB-231 and MCF7 to DHA. MDA-MB-231: [DHA]>200 µM viability significantly reduced. MCF7: no effects are revealed with DHA.	Apoptosis
(Bilyk *et al.* 2021)	Ovarian	ES2, SKOV3, A2780cp (*in vitro* and *in vivo* on mice)	* 10 - 320 µM *3.9 % DHA (w/w of 20% fat)	↓ cancer cell growth ↑ apoptosis ↑ necrosis *ES2: $IC_{50}(DHA)_{72h}$= 30 µM *A2780cp: $IC_{50}(DHA)_{72h}$= 229 µM *SKOV3: was resistant to DHA	Apoptosis, Necrosis
(Blanckaert *et al.* 2010; Chénais *et al.* 2020)	Breast	MDA-MB-231	100 µM	Upregulate pro-apoptic and anti-invasive genes expression.	Apoptosis, Anti-invasive
(Sharma *et al.* 2020)	Breast	MDA-MB-231, MCF7	80 µM	↓ microcalcification (by blocking the osteoblast-like potential of breast cancer cells)	Apoptosis, Inhibited calcification
(Javadian *et al*. 2020)	Breast	MDA-MB-231	100 µM	↓ metastasis (DHA and DHA-Taxol combination)	/
(Tamarindo and Góes 2020)	Prostate	PNT1A, 22rv1, PC3 (GRL1435)	10, 20, 50 and 100 µM	↓ cancer cell growth (by 27% for PNT1A, 26% for 22rv1 and by 34% for PC3 lines)	Cell cycle arrest (G_2/M), Oxidative stress, Lipid deregulation
(Kim *et al.* 2018)	Brain	D54MG, U87MG, U251MG	10, 20, 30, 40, 50 and 60 µM	*D54MG: $IC_{50}(DHA)_{24h}$= 45 µM *U87MG: $IC_{50}(DHA)_{24h}$= 40 µM *U251MG: $IC_{50}(DHA)_{24h}$= 50 µM	Apoptosis, Autophagy
(Yin *et al.* 2017)	Lung	A549	6.25, 12.5, 25, 50, 75, 100 µM	↓ cancer cell growth (by 40% (100 µM)) ↓ invasion ↓ metastasis	Apoptosis, Oxidative damage
(Kim *et al.* 2015)	Lung	Human NSCLC, A549, H1299	10, 30 and 60 µM	Induce apoptosis and autophagy through p53, AMPK, mTOR signaling (30 µM).	Apoptosis, Autophagy
(Rahman *et al*. 2013)	Breast	MDA-MB-231 (*in vitro*), MDA-231 Luc (*in vitro* and *in vivo* on mice)	50 and 100 µM (DHA and EPA)	↓ cancer cell growth ↓ invasion 100 µM DHA > 100 µM EPA	/
(Yamagami *et al.* 2009)	Leukemia	KG1A	100 and 150 µM	↑ apoptosis ↑ DNA fragmentation	Apoptosis, Cell cycle arrest (G_1)
(Mandal *et al.* 2010)	Breast	MDA-MB-231 (*in vivo* on mice)	150 µM DHA	↓ autograft tumor growth ↓ metastasis	/

↓: decrease, ↑: increase

In vitro studies provided further evidence on the mechanism of action on cancer cells where apoptosis was the most related mechanism to cancer cell death induced by DHA. The apoptotic pathways triggered by DHA are reviewed by D'Eliseo and Velotti (2016). More recently, a transcriptomic analysis revealed an upregulation in endoplasmic reticulum stress response, explaining the apoptotic effect of DHA. Genes related to invasion and migration were also impacted (Chénais *et al.* 2020).

Besides the apoptotic effect, many studies discussed the effect of DHA treatment on cancer cell cycle (Newell *et al.* 2017). For example, Tamarindo and Góes (2020), showed that DHA leads to cell cycle arrest in the three studied prostate cancer cell lines.

Some studies were carried out over a range of concentrations allowing the determination of the IC_{50}, while others only study a specific concentration (table 2).

Regarding dose and sensitivity, dose-response relationships were different from a cell line to another, indicating a variety of sensitivity of different cancer cell lines to the same tested molecule. Bilyk *et al.* (2021) showed the different sensitivity of three different ovarian cancer cell lines to DHA. An IC_{50} of 30 µM and 229 µM were obtained for ES2 and SKOV3 cell lines, respectively. The A2780cp cell line was resistant to DHA as no inhibition of growth was observed. A difference in sensitivity to DHA in three different brain cancer cell lines was also observed by Kim *et al.* (2018).

Moreover, a difference in dose response relationship was observed with the same cancer cell line. A concentration of 100 µM of DHA was found to significantly decrease MDA-MB-231 cell viability (Rahman *et al.* 2013; Chénais *et al.* 2020) although Rizzo *et al.* (2021) showed that a DHA concentration over 200 µM was needed to obtain a similar effect. This difference could be due to the different adopted culture conditions in these studies.

DHA was also thought to be more potent than EPA in inhibiting the proliferation and invasion of breast cancer cells. It showed greater cytotoxicity than EPA towards MDA-MB-231 and MCF-7 cells (Ewaschuk *et al*. 2012, Rahman *et al*. 2013).

In liver, clinical and preclinical results have shown contradictory results. Shan *et al.* (2021) showed that DHA prevents the development of liver fibrosis in mice by inhibiting the activation of hepatic stellate cells involved in liver fibrosis. In contrast, a chinese clinical study showed that dietary intake of DHA increased liver cancer risks (Ji *et al*. 2021). Further investigations on the direct effect of DHA on different hepatic cells by *in vitro* culture experiments should be conducted to resolve these contradictions.

3. DHA as adjuvant in cancer therapy

Besides its anticancer properties against various cancer types, DHA has been shown to be useful as an adjuvant in cancer therapy. It was found to increase the chemotherapy drugs transport across the cell membrane and therefore improve their efficiency and reduce therapy associated side effects (Siddiqui *et al.* 2011; Corsetto *et al.* 2012; D'Eliseo and Velotti *2016;* Morland *et al.* 2016). For example, *in vitro* studies demonstrated that DHA was able to enhance the therapeutic effects of doxorubicin, a drug used to treat breast cancer (Ewaschuk *et al.* 2012, Newell *et al*. 2020). A clinical study showed that the activity of gemcitabine, a chemotherapy drug used to treat pancreatic cancer, was also improved when injected in combination with DHA (Arshad *et al.* 2017).

4. DHA carried on lipids protective effect

In recent years, authors have been interested in studying the anticancer effects of lipids carrying ω-3 PUFAs since they were more effective than their free form. Some of these studies are listed in Table 3.

TABLE 3: TABLE ILLUSTRATING ARTICLES THAT INVESTIGATE THE EFFECT OF DHA LINKED WITH LIPID CARRIERS ON CANCER

Reference	Molecule	Cancer model	Cancer cell line	Tested concentrations	Results	Mode of action
(Liu *et al.* 2021)	PC-DHA PC-EPA	Lung	LLC (*in vivo* xenografts in mice)	300 µM 200 mg/kg of mice body weight	↓ transplanted tumor growth ↓ metastasis ↑apoptosis	Apoptosis
(Zhang *et al*. 2020b)	MAG-DHA	Breast	SKBR3(*in vitro*) E0771 (*in vitro* and *in vivo* xenografts in mice)	20, 40, 60 and 80 µM	↑apoptosis ↑autophagy *SKBR3: IC_{50} (MAG-DHA)72h= 20 µM *E0771: IC_{50} (MAG-DHA)72h= 16 µM	Apoptosis Autophagy
(González-Fernández *et al*. 2019)	MAG-DHA MAG-ARA	Colon	HT-29	50, 100, 150, 250, 300, 500 and 600 µM	MAG-DHA > MAG-ARA *IC_{50} (MAG-DHA)48h= 135 µM *IC_{50} (MAG-ARA)48h= 236 µM	Apoptosis (MAG-DHA) Necrosis (MAG-ARA)
(Morin *et al.* 2013)	MAG-DHA	Colon	HCT116	0.1, 0.3, 1, 3, and 10 µM	*IC_{50} (MAG-DHA)48h= 2.31 µM	Apoptosis
(Tsushima *et al.* 2012)	PC and LPC-DHA	Angiogenesis	HUVEC	10, 25, 50 and 100 µM	LPC-DHA > PC-DHA *100 µM exhibited the most effective suppression on angiogenesis.	/
(Hossain *et al.* 2008)	PC-DHA and DHA PC-EPA and EPA	Colon	HT-29 Caco-2 DLD-1	*150 µM free PUFA *100 µM PC-PUFA	PC-DHA and PC-EPA > DHA and EPA Level of sensitivity against n-3 PUFAs of the cells tested was as follows: HT-29 > Caco-2 > DLD-1	Apoptosis
(Hossain *et al.* 2006)	PC-DHA PS-DHA	Colon	Caco-2 CCD-18Co	100 µM	↓ cell viability ↑ apoptosis	Apoptosis

↓: decrease, ↑: increase

Hossain *et al.* (2008) extracted PLs from starfish and demonstrated that free DHA and EPA inhibitory effect, on various colon cancer cell lines growth, was enhanced when they were carried with PC. PC-DHA triggered cell apoptosis as proved by the increase of caspase-3 activity. Similarly, PS-DHA was found to reduce cell viability and to induce apoptosis in colon cancer (Hossain *et al.* 2006).

Recently, a preclinical study on mice conducted by Liu *et al.* (2021) showed that both PC-DHA and PC-EPA inhibited transplanted lung tumor growth and metastasis. This protective effect was reached by the activation of the nuclear peroxisome proliferator-activated receptor γ (PPARγ), which, once activated, promotes apoptosis and inhibits cell migration and invasion.

No IC_{50} was calculated in these studies for PL carrying a DHA, as fixed concentration, that vary between 50 µM and 300 µM, were tested (table 3).

MAG-DHA was the most studied molecular form of DHA. Two studies have been conducted on different cell lines of colorectal cancer and one on breast cancer cells (table 3). In these studies, the MAG-DHA was more effective than the free form. The cell death mechanism triggered by MAG-DHA was mainly related to apoptosis in the mentioned studies. Different concentrations of MAG-DHA, varying between 0.1 µM and 600 µM, were tested in these studies. The obtained IC_{50} indicated different sensitivities of cancer cell lines to MAG-DHA. Obtained IC_{50} are listed in table 3 (Morin *et al.* 2013, González-Fernández *et al.* 2019, Zhang *et al.* 2020b).

Antiangiogenic therapeutics are well established strategies for cancer suppression. To our knowledge, no study has been conducted on the anti-cancer effects of LPC-DHA neither on any LPC containing ω-3 PUFAs. However, one article studied the anti-angiogenic activity of LPC-DHA and showed stronger antiangiogenic effect of LPC-DHA than that obtained with PC-DHA on the human umbilical vein endothelial cell line (HUVEC) (Tsushima *et al.* 2012). The anti-angiogenic effect of LPC-DHA and its underlying mechanisms remain elusive as no investigations have been conducted to elucidate this effect.

In this work, we aimed to evaluate and compare how different forms of DHA, free or linked to various lipids, affect breast cancer cells. Thus, focusing on the studies that investigated the effect of DHA on breast cancer, we found that MDA-MB-231 are the most studied cell lines. MDA-MB-231 are triple negative breast cancer cells (TNBC), refers to the fact that the cancer cells don't have estrogen or progesterone receptors and also don't make any or too much of the protein called human epidermal growth factor receptor 2, which means they do not respond to hormonal therapy (Badve *et al*. 2011). In general, if cancer is dependent of estrogen, progesterone or HER2 (human epidermal growth factor), therapists can use

hormone treatment or other drugs against the cancer cells. But in the case of TNBC, the lack of hormone receptors has rendered cells insensitive to hormonal therapy medicines, such as Tamoxifen, which is widely used in breast cancer chemoprevention (Osborne 1998; Radmacher and Simon 2000). That is why this type of breast cancer is more aggressive and has higher death and recurrence rates than other breast cancer types in the first years of treatment (Dent *et al*. 2007, Liedtke *et al*. 2008).

Regarding the dose-response, it can be observed that there is a difference in the concentrations that exhibit a significant decrease in cell viability. For example, Rizzo *et al.* (2021) showed that a concentration higher than 200 µM was required to observe a significant reduction in MDA-MB-231 viability, while studies in our laboratory conducted by Blanckaert *et al.* (2010) and Chénais *et al.* (2020) reported that 100 µM of DHA significantly decreased cell viability. This may be due to the variations in culture conditions between the studies.

Overall, there is evidence in the literature that DHA can be used in a variety of ways for the treatment of cancers. It also highlights that lipid carrying DHA have potential as functional factors in cancer treatment. Additional studies are required, especially for LPC-DHA which, to our knowledge, has not been studied until now, and for cancers that are not yet well studied like brain and liver. Also, *in vivo* experiments are needed to confirm the positive effect of PL-DHA and MAG-DHA on cancer and elucidate their mechanism of action.

IV. Synthesis of lysophospholipids

Considerable interest has been received for LPL-DHA as they are known to promote the biological effects of DHA. Numerous studies have synthesized LPL-DHA through chemical or enzymatic synthesis, in order to supply the increasing demand. In this work, we aimed to synthesize LPC-DHA through an enzymatic pathway. So, in the following sections the different routes found in literature to synthesize LPLs as well as an overview on the used enzymes in this field will be mentioned.

A. Overview

Several chemical routes have been developed to synthesize LPLs. These routes have been reviewed by D'Arrigo and Servi (2010). Only few chemical synthetic pathways have been developed for large-scale preparation of LPLs because they are generally carried out under anhydrous conditions at high pressures and temperatures and require several steps to achieve the desired product.

Considering the specific synthesis of LPL-DHA, only a single chemical route has been described for the production of *sn*-2 LPL-DHA starting from ether-PLs, which are PLs exhibiting an ether bound instead of the ester bound at the *sn*-1 position (Hung *et al.* 2011a). In this study, alkaline and acidic hydrolysis steps were used to synthesize the *sn*-2 LPC-DHA from lecithin extracted from beef heart (this lecithin was a mixture of small amount of ether-PCs and an important amount of PCs) as illustrated in figure 16 (Tokumura *et al.* 2002).

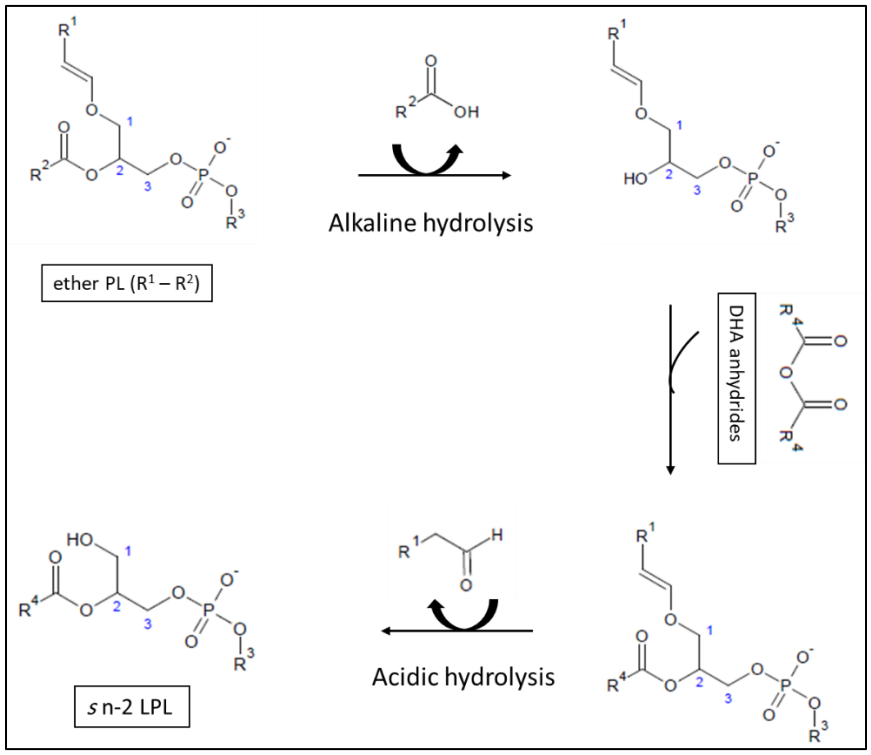

FIGURE 16: SCHEME ILLUSTRATING THE MAIN STEPS OF *SN*-2-LPL-DHA CHEMICAL SYNTHESIS FROM ETHER-PLS

(R^1 – R^2: alkyl chains, R^4 : DHA chain, R^3 : organic molecule) adapted from (Tokumura *et al*. 2002)

Besides chemical methods, LPLs can be synthesized using lipolytic enzymes, namely lipases and phospholipases. Comparing to chemical synthesis routes, the enzymatic synthesis has several advantages:

1- Low generation of by-products and consequently an easy purification procedure due to the selectivity and specificity of the enzyme catalysis.
2- Mild reaction conditions: low temperature, low amount of chemical reagents which are often deleterious and toxic.

B. Enzymes catalyzing synthesis of lysophospholipids

Enzymatic synthesis of LPLs can be performed using different enzymes and substrates. The type of enzyme used depends on the type of the used substrate.

The enzymes that catalyze the synthesis of esters in living organisms are acyl transferases. They allow the incorporation of an acyl group (most often from an activated substrate: an acyl-CoA) on an alcohol function. However, the use of coenzyme A derivatives is avoided in industrial processes, mainly because of their high cost. Nevertheless, some researchers have succeeded in recycling this coenzyme but with low yields (Nakajima *et al*. 2000).

However, there are enzymes that catalyze the hydrolysis and synthesis of ester bonds without coenzymes. Phospholipases and lipases form a large category of these enzymes.

1. Phospholipases

PLs represent a precursor for LPLs synthesis. As already described, they have two hydrophobic tails derived from FAs and a hydrophilic head containing a phosphate group, joined by a glycerol molecule. The phospholipases are the enzymes that selectively catalyze the transformation of PLs. These enzymes hydrolyze PLs into FAs and other lipophilic molecular species, such as LPLs and DAGs.

Phospholipases are classified into three main groups according to the type of bond cleaved (figure 17):

1- Phospholipases A_1 and A_2 (PLAs): catalyze the hydrolysis of one of the two carboxylic ester bonds in PLs either at the *sn*-1 or *sn*-2 position, respectively.
2- Phospholipases B (PLBs): catalyze the hydrolysis of the two carboxylic ester bonds in PLs either at the *sn*-1 or *sn*-2 position.
3- Phospholipases C (PLCs): catalyze the hydrolysis of the phosphate ester bond at the glycerol end of the phosphate group giving phosphoalcohol and DAG.
4- Phospholipases D (PLDs): catalyze the hydrolysis of the phosphate ester bond at the alcohol end giving alcohol moieties and phosphatidic acid.

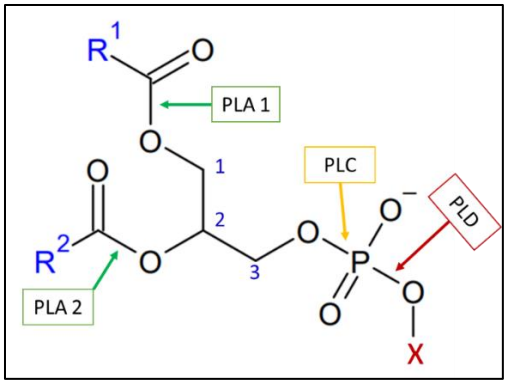

FIGURE 17: PHOSPHOLIPASE SITES OF ACTION ON PHOSPHOLIPIDS

(R^1 and R^2 =alkyl chains; X= organic molecule)

The Figure 18 gives an example of the PLs hydrolysis by PLA_1 to produce a *sn*2-LPL.

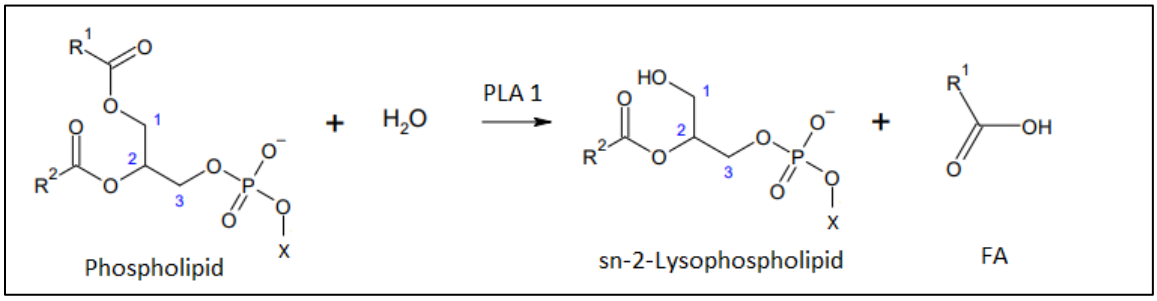

FIGURE 18: PHOSPHOLIPID HYDROLYSIS REACTION CATALYZED BY PHOSPHOLIPASES TO SYNTHESIS A LYSOPHOSPHOLIPID

(R^1 and R^2 =alkyl chains; X= organic molecule)

2. Lipases

In addition to phospholipases, another type of enzymes exists for the synthesis of LPLs. Lipases are enzymes with broad substrate specificity. Lipases are of great interest due to their selectivity, their stability in organic solvents and their ability to catalyze reactions without addition of expensive cofactors. Furthermore, they are easily produced, active at ambient temperature and are more commercially available (Casas-Godoy *et al.* 2012).

Lipases are carboxylic ester hydrolases. TAGs are the preferred substrates of these enzymes. Their hydrolysis led to DAG, MAG, glycerol and free FAs. Because of this action on TAGs, lipases have been classified in the international classification under the systematic name of TAG acylhydrolases (EC 3.1.1.3).

Lipases are water soluble due to their protein nature but they can act on lipids, which are insoluble in water, at the interface between oil and water and catalyze esterification, transesterification in addition to their hydrolytic activity on TAGs.

a) Lipase sources

Lipases are ubiquitous in nature. They are found in all types of organisms: plants, mammals and microorganisms.

Plant lipases

Lipases are widely distributed in the plants although they are mainly found in the seeds where TAGs are stored in intracellular structures called oleosomes (oil bodies) (Beisson *et al.* 2001). Under the action of lipases, TAGs are hydrolyzed into FAs whose role is to provide energy for the germination of the seed and the development of the young plant (Adlercreutz *et al.* 1997).

Mammalian lipases

Lipids are an essential and valuable source of energy for mammals. They are involved in the control of digestion, absorption and reconstitution of fats.

Mammalian lipases can be classified into three groups. The first group consists of lipases involved in digestion, such as lingual, pharyngeal, gastric and pancreatic lipases. The second group corresponds to lipases present in the brain, muscles, arteries, kidneys, spleen, tongue, liver and adipose tissue. The third group corresponds to the lipases produced by the milk-producing glands (Baba *et al*. 1991).

The most studied mammalian lipases are those related to fat digestion and absorption. These are gastric lipase, pancreatic lipase, lipoprotein lipase and hepatic lipase (Warden *et al*. 1993).

Microorganism lipases

Microbial lipases are the most industrially used due to their stability. They originate from bacteria, yeasts and filamentous fungi (Stead 1986).

The advantages of these lipases are that they have relatively simple manufacturing processes compared to mammalian lipases and have greater stability towards temperature, detergents and proteolytic enzymes. These features have allowed the development of numerous applications for microbial lipases that have resulted in many commercial products (Chandra *et al*. 2020).

Among these lipases, the lipase B from the yeast *Candida antarctica* (CALB) is widely used in research and industrial fields. It is among the most stable commercialized lipases (Anderson *et al.* 1998; Stauch *et al*. 2015).

b) Lipase-catalyzed reactions

Depending on the operating conditions, lipases can catalyze two types of reactions: hydrolysis and synthesis. Lipases naturally catalyze the hydrolysis of the ester bonds of TAGs into glycerol and FAs. Besides their hydrolytic activity they catalyze a large variety of synthesis reactions in a medium with low water activity (a_w) such as molten medium (solvent free medium) or organic solvents (Jala *et al*. 2012).

1. Hydrolysis reaction

In aqueous medium, lipases catalyze hydrolysis of ester bonds (figure 19). This reaction takes place at the interface between the hydrophobic substrate and the aqueous medium.

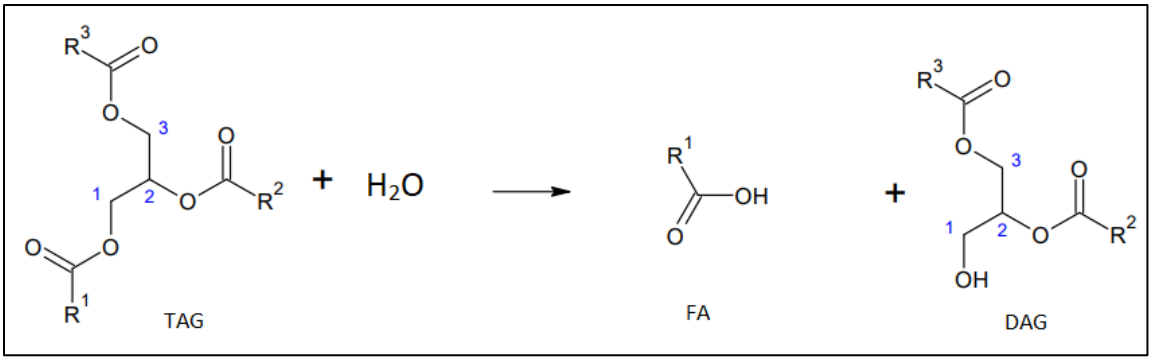

FIGURE 19: HYDROLYSIS OF TAG CATALYZED BY LIPASES

2. Synthesis reactions

Lipases catalyze a wide range of synthesis reactions.

a) Esterification

Ester synthesis catalyzed by lipases is the reverse reaction of the hydrolysis (figure 20).

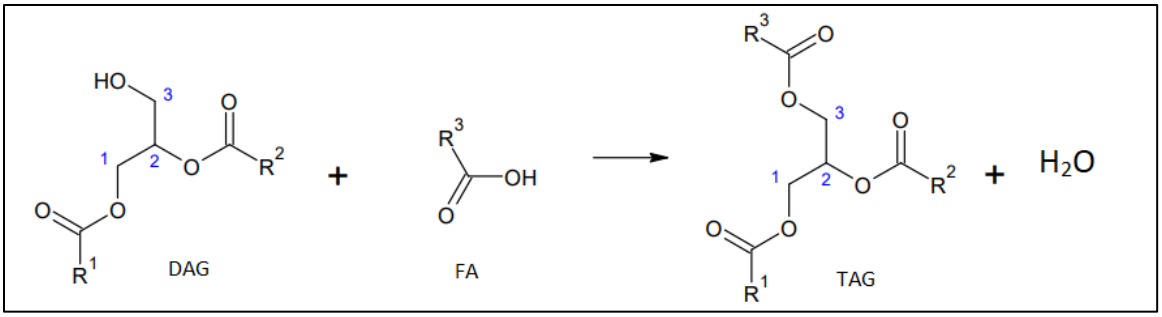

FIGURE 20: ESTERIFICATION REACTION CATALYZED BY LIPASES

b) Transesterification

Transesterification is an acyl transfer between an ester and an acyl acceptor (ester, alcohol or acid). It is divided into three reactions: interesterification, alcoholysis and acidolysis.

i. Interesterification

Interesterification allows the synthesis of esters from two esters, by the exchange of an acyl group (figure 21).

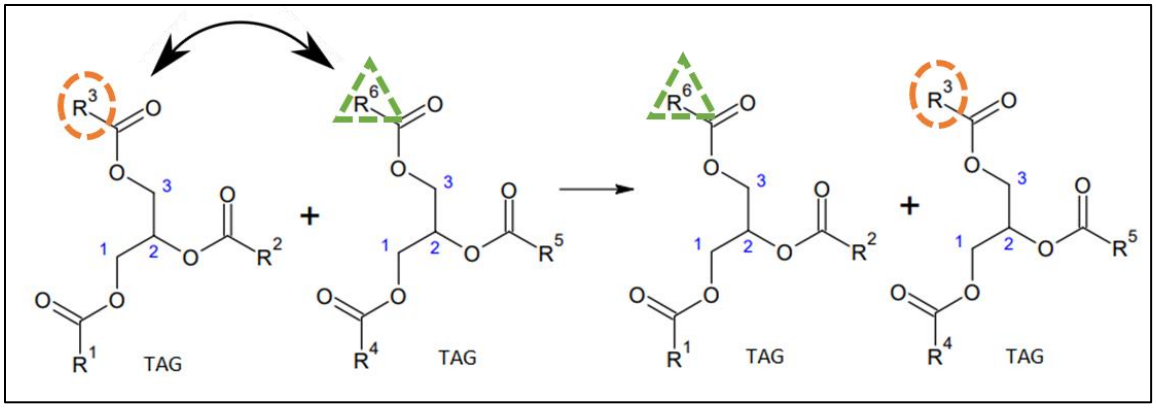

FIGURE 21: INTERESTERIFICATION REACTION CATALYZED BY LIPASES

ii. Alcoholysis

Alcoholysis is the synthesis of esters from an ester and an alcohol (figure 22).

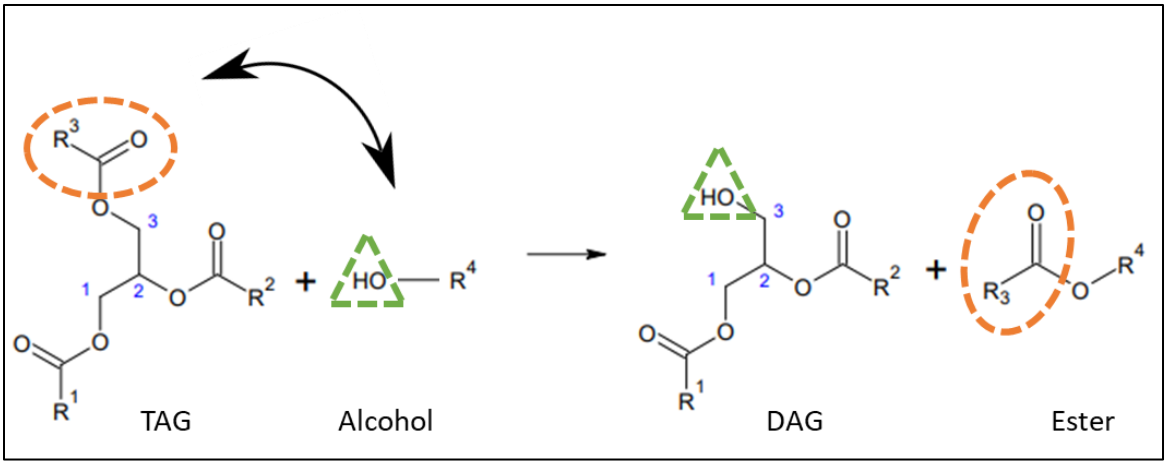

FIGURE 22: ALCOHOLYSIS REACTION CATALYZED BY LIPASES

iii. Acidolysis:

Acidolysis is the synthesis of ester from an ester and a FA (figure 23).

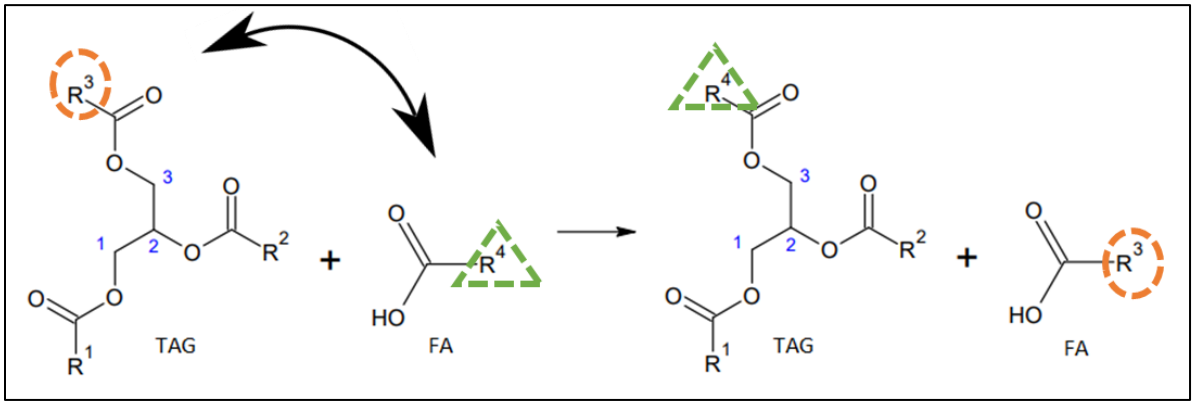

FIGURE 23: ACIDOLYSIS REACTION CATALYZED BY LIPASES

c) Lipase structure

The first lipase structures obtained were those of *Rhizomucor miehei* lipase and human pancreatic lipase. Referred to as α/β-type hydrolases, all lipases with a known structure have a common structural base composed of a central β-sheet formed of mainly parallel strands, connected to each other by α-helices (figure 24) (Jaeger *et al.* 1999).

The active site of lipases is composed of a catalytic triad. The catalytic triad is composed of a nucleophile (serine residue activated by a hydrogen bond) in relay with a histidine and an aspartate or glutamate.

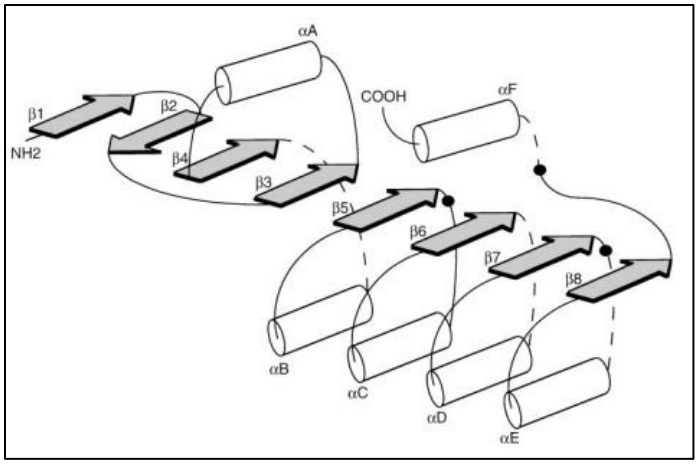

FIGURE 24: SCHEME OF α / β FOLDING

(α Helices are indicated by cylinders, and β strands are indicated by shaded arrows. The position of the active-site residues is shown by a solid circle) (From Jaeger *et al.* 1999)

Some lipases have an amphiphilic peptide flap called a "lid" covering the active site. The hydrophobic side of this flap is oriented towards the inside of the active site. When the flap covers the active site, there is no catalytic activity and this situation is called the inactive or closed form of lipases (figure 25).

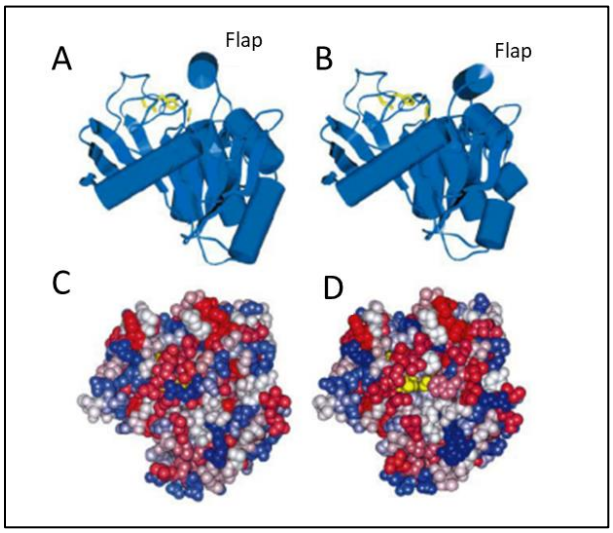

FIGURE 25: *MUCOR MIEHEI* LIPASE STRUCTURE

(A, C: closed form, B, D: open form. Active site: presented in yellow in A and B (side view). C and D: top view. Colors indicate decreasing polarity (dark blue, light blue, white, light red and dark red) (From Schmid and Verger 1998)

Crystallographic studies have shown that the transition from the inactive (or closed) to the active (or open) form is accompanied by a movement of the flap exposing its hydrophobic face towards the outside of the

active site and creating a surface supposed to interact with the lipid/water interface. This phenomenon is called interfacial activation (Verger and De Haas 1976; Ericsson *et al.* 2008).

However, some lipases do not have a flap at the entrance of the active site, such as CALB. The active site of CALB is indeed accessible through a thin tunnel whose sides are hydrophobic (Uppenberg *et al.* 1994).

d) Catalytic mechanism of lipases

Since 1960, the mechanism of action of lipases has been studied intensively. The two-substrate enzymatic mechanism, called ping pong bi bi mechanism, is often used to describe the catalytic activity of lipases.

The mechanism of catalytic action of lipases involves the catalytic triad located within the active site (Cygler *et al*. 1994). Once the acylating agent (acid or ester) is adsorbed on the catalytic site, the particular arrangement of the 3 residues forming the triad allows, in a first step (figure 26-1), the transfer of a proton between aspartic acid, histidine and serine, leading to the nucleophilic attack of the serine hydroxyl group on the carbonyl of the substrate to form the first tetrahedral intermediate called acyl-enzyme with release of the alcohol.

In a second step (figure 26-2), this acyl-enzyme intermediate undergoes a nucleophilic attack which can be exerted by a water molecule (hydrolysis reaction) or by an alcohol molecule (synthesis reaction) to form the second tetrahedral intermediate. Finally, there is the formation of the second product of the reaction (acid or ester) with regeneration of the native enzyme (figure 26-3).

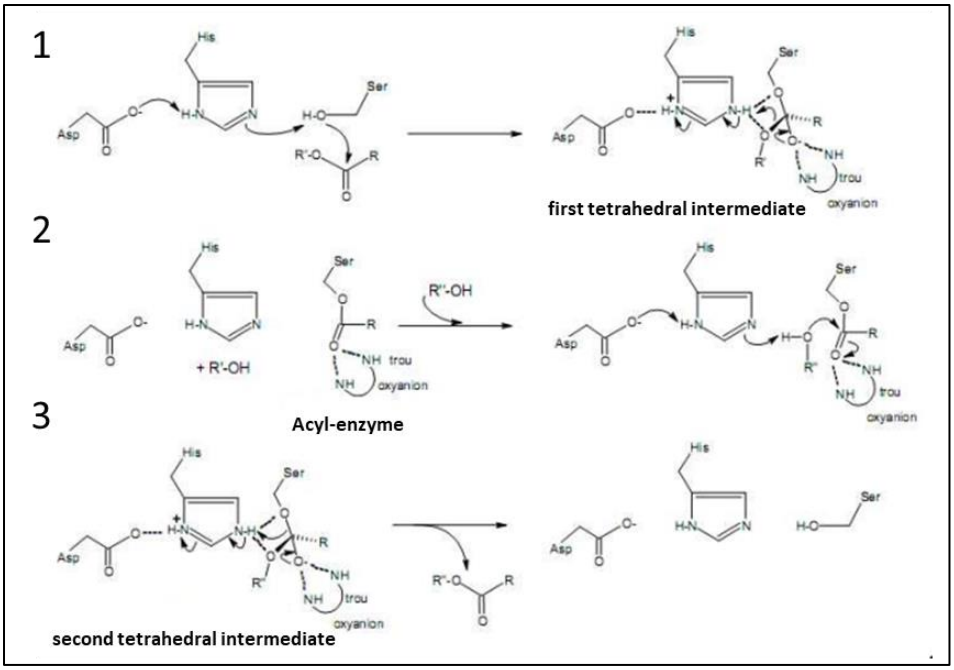

FIGURE 26: CATALYTIC MECHANISM OF LIPASES: INTERVENTION OF THE TRIAD (SER, HIS AND ASP)

From (Belafriekh 2017)

e) Lipase specificity

Lipases are able to catalyze several reactions and can also act more or less efficiently on different substrates.

The literature distinguishes 4 types of selectivity: substrate selectivity, typoselectivity, regioselectivity, and stereoselectivity (Jensen *et al.* 1983).

Substrate selectivity:

The substrate selectivity of an enzyme is defined as the preference of this enzyme for a particular substrate. For lipases, TAGs are the natural and preferred substrates, however, many of them accept a large variety of substrates and efficiently catalyze their hydrolysis or synthesis, such as PLs, DAGs, MAGs, glycolipids or other esters. Indeed, lipases are well known for their broad substrate selectivity.

Typoselectivity:

Typoselectivity or specificity with respect to a given type of FA, refers to the ability of lipases to be selective towards a particular FA. This FA will therefore be preferentially released during hydrolysis reaction compared to the others.

Regioselectivity:

Regioselectivity or position specificity, represents the ability of lipases to hydrolyze preferentially the primary esters (in external positions *sn*-1 or *sn*-3) or secondary esters (in internal position *sn*-2) of TAGs.

Stereoselectivity:

Stereoselective lipases are selective towards one or more stereoisomers.

f) Lipase immobilization

Enzymes offer a distinctive advantage due to their specificity, biodegradability and limitation of by-product formation. However, the enzyme must be stable to be a viable industrial catalyst. The lack of stability of enzymes often limits their practical application in biotechnological processes.

A possible approach for stabilizing enzymes is their immobilization on a suitable support. From an industrial point of view, immobilized biocatalysts show increased stability, changes in enzymatic activity and recovery possibilities (Balcão *et al.* 1996). These changes depend on the type of support and the method of immobilization. The following paragraph reviews the different immobilization techniques.

Physical adsorption: This technique consists in fixing the enzyme on the surface of an adsorbent mineral support (silica, aluminum, etc.) or organic support (activated carbon, etc.) through hydrogen bonds or weak interactions such as van der Waals forces. This method is the most economical and simplest method of enzyme immobilization (Trevan 1988).

Immobilization by covalent bonding: This technique was developed in order to obtain very strong bonds between enzyme and support. It is achieved through irreversible and covalent bonds between the functional groups of the enzyme and the reactive groups of the support (Trevan 1988). Different supports such as silica, adsorbent resin, carboxymethylcellulose have been used for this technique.

This technique offers several advantages since covalent bond provides enzymatic stability and high attachment of the lipase to the support, ensuring rigidity of its structure. This rigidity can keep the enzyme structure unaffected by denaturing agents such as heat, extreme pH, organic solvents. However, covalent binding may alter the active site of the enzyme, causing its partial inactivation.

Immobilization by inclusion: The concept of inclusion is to retain the enzyme trapped in the matrix of a polymer or in a microcapsule. This matrix retains the enzyme but allows the substrate and the product to pass through it (Pollak *et al*. 1980). Several polymers, including alginate, chitosan, polyacrylamide gel and

starch gel, are used in inclusion immobilization. The process is very simple and versatile, but the risks of leakage are not negligible if the mesh size of the network is large (Sheldon and Pelt 2013).

Cross-linking: It is an irreversible method that consists on the formation of intermolecular cross-links between enzyme molecules (linking enzymes together by their end groups) through covalent bonds. It is performed using a multifunctional reagent that acts as a linker (crosslinker) to link the enzyme molecules into three-dimensional cross-linked aggregates. Aggregates are thus formed and are called "cross-linking enzyme aggregates" (Govardhan 1999).

Crosslinkers are molecules that contain two or more reactive ends capable of chemically attaching to the primary amines groups of an enzyme.

This technique offers several advantages since the enzyme concentration in the catalyst is high, the enzyme is well protected and finally the cost of production is expected to be low due to the lack of support. The figure 27 illustrates the above-mentioned immobilization techniques.

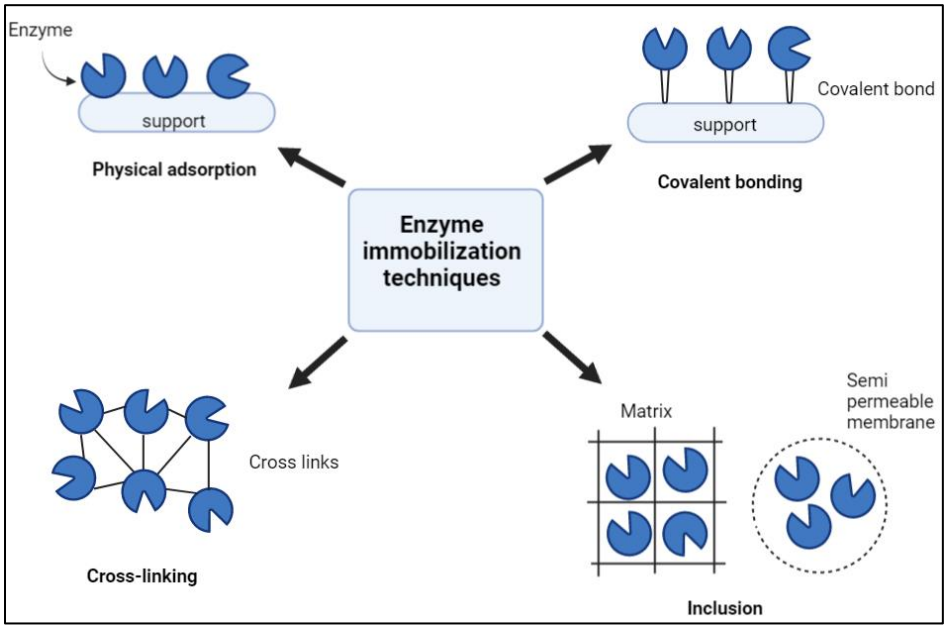

FIGURE 27: METHODS OF ENZYME IMMOBILIZATION

(Adapted from Nguyen and Kim 2017)

g) Industrial applications of lipases

Lipases are an important group of biotechnologically relevant enzymes and they are widely used in food, biomedical applications and biotechnology industries.

Lipases are ranked third in the global ranking of commercial enzymes, after the proteases and carbohydrases. The lipases from microorganisms, being resistant to industrial temperatures and pH, are the most used (Jaeger and Eggert 2002).

Some industrial applications of lipases are reported in the following table 4.

TABLE 4: INDUSTRIAL APPLICATIONS OF LIPASES

Industrial field	Application	References
Food	Synthesis of structured lipids	Jolly (2015); Sá *et al.* (2017); Sharma and Sharma (2018); Chandra *et al*. (2020)
	Synthesis of emulsifiers	
	Synthesis of aromatic esters	
	Synthesis of cheese and enhance their flavor	
Textile	Removal of size lubricants	Hasan *et al.* (2006)
	Modification of synthetic fibers	
Cosmetics and perfumery	Synthesis of aroma	Sharma and Kanwar (2014); Gupta *et al.* (2015)
	Synthesis of surfactants	
	Synthesis of additives used in cosmetics and sunscreens	
Oleochemical	Synthesis of ester	El-Gawad (2014); Chandra *et al.* (2020)
	Hydrolysis of fats	
Detergent	Hydrolysis of fats (oil removal)	Niyonzima and More (2015); Holland *et al.* (2020)
Paper	Removal of hydrophobic components found in wood	Karl-Erich Jaeger and Reetz (1998); Chandra *et al*. (2020)
Environmental	Biodegradation of plastic	Chandra *et al.* (2020)
	Synthesis of biodiesel	
	Treatment of wastewater	
Medical and pharmaceuticals	Synthesis of pharmaceutical components	Chandra *et al.* (2020)
	Synthesis of enantiopure compounds	
	Cancer treatment	
	Digestive aide	
	Diagnostic tool	

C. Enzymatic synthesis of lysophospholipids

In this thesis, the synthesis of docosahexaenoyl lysophosphatidylcholine (LPC-DHA) is considered. Therefore in the following sections, the different routes of LPLs, especially LPLs-DHA, synthesis will be reported.

In general, there are several routes to synthesize LPLs: hydrolysis, alcoholysis, transesterification and esterification. Many studies have focused on the enzymatic synthesis of LPLs as reviewed by Casas-Godoy *et al.* 2012 and Mnasri *et al.* 2017a, however, among them few studies aimed to the synthesis of LPLs-DHA.

The most commonly described pathway is the enzyme-catalyzed partial hydrolysis of PLs rich in DHA. Various natural sources of PL-DHA have been used, such as fish organs, microalgae, squid skin or egg yolk obtained from fish oil-fed hens (Devos *et al.* 2006; Gendaszewska-Darmach and Drzazga 2014).

For example, the lipase from *Rhizomucor miehei* has been used to catalyze the hydrolysis of PLs-DHA extracted from squid skin (Ono *et al.* 1997; Tsushima *et al.* 2012) or from egg yolk (Ono *et al.* 1997; Hosokawa *et al.* 1998). In our laboratory, LPC-DHA has been obtained by hydrolysis of PLs naturally rich in DHA from the marine microalgae *Isochrysis galbana* using lipases from *Mucor miehei* and from *Thermomyces lanuginosus* (Devos *et al.* 2006).

Phospholipases were also used at both laboratory and industrial scale for PL transformation reactions (Ulbrich-Hofmann 2000). Most often, PLA_2 is the enzyme used for this purpose. In the frame of studying the biological effects of LPC-DHA, many authors have obtained LPC-DHA by hydrolysis of commercially available pure PC-DHA using a PLA_2 (Huang *et al.* 2010, Hung *et al.* 2011b, Jin *et al.* 2012). PLA_2 has been also used to produce *sn*-1 LPA-DHA through hydrolysis of PC from beef heart (Tokumura *et al.* 2002). However, this process suffers from various drawbacks, including requirement for cofactors (Ca^{2+}), and the poor activity of PLA_2 in organic solvents (Sarney *et al.* 1994).

The disadvantages of these hydrolysis reactions is that the extraction of PLs from animal organs like bovine brain requires not only the use of large amounts of organic solvents, but can also transmit infectious diseases (Gendaszewska-Darmach and Drzazga 2014). Harmful solvents such as chloroform, hexane, acetone and ethanol are used to precipitate PLs from other lipids (Lee *et al.* 2012). High cost of some natural sources of PLs such as microalgae extracts is also disadvantageous.

Enzymatic alcoholysis of PLs was also applied to synthesize LPLs. The used alcohol can be methanol, ethanol or glycerol (Sarney *et al.* 1994; Adlercreutz 2013; Yang *et al.* 2015). For example, Adlercreutz and Wehtje (2001) synthesized *sn*-2 LPC-C16:0 by ethanolysis of PC-C16:0 from egg catalyzed by the lipase from *Rhizopus arrhizus* . As for hydrolysis reactions, the disadvantage of these reactions is the use of organic solvents such as methanol and ethanol as well as the high cost of natural sources of PLs.

LPLs were also produced with the esterification and transesterification reaction *via* acylation of glycerophosphoryl moiety with an acyl donor: FAs and FA esters, respectively (figure 28).

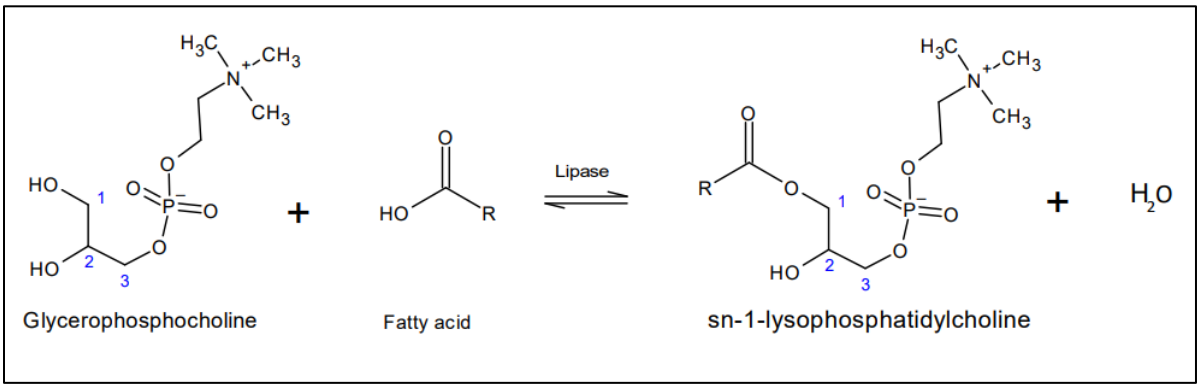

FIGURE 28: REACTION SCHEME OF 1,3-REGIOSELECTIVE LIPASE-CATALYZED ESTERIFICATION OF GLYCEROPHOSPHOCHOLINE WITH FREE FATTY ACID

These reactions proceeded very slowly or did not proceed in the presence of various organic solvents due to the insolubility of the glycerophosphoryl moiety (Han and Rhee 1995; Kim and Kim 2000). Therefore, reactions have been further performed in a solvent-free medium in which the free FAs or FA esters form the liquid phase.

Lipases have been used to synthesize LPA and LPC through esterification of one of the hydroxyl groups of glycerophosphatidic acid (GPA) (Virto *et al.* 1999) and glycerophosphocholine (GPC) (Wang *et al.* 2020b). Also, lipases catalyzed the transesterification reaction between glycerophosphocholine (GPC) and lauric acid vinyl esters (Virto and Adlercreutz 2000).

There are a few works published on the enzymatic synthesis of LPC through esterification between GPC and a FA, from 1998 until now. Nevertheless, to our knowledge, there are only two published articles (Liu *et al.* 2017 and Wang *et al.* 2020a), among these articles, on the production of LPC with ω-3 PUFAs.

These reactions have the advantageous of being environmentally friendly since they are realized in a solvent free medium which is a green promising process to synthesize LPL. Moreover, synthesizing LPLs

from inexpensive products such as GPC compared to natural PLs is economically important from an industrial point of view. However, the disadvantages of these reactions compared to the hydrolysis and alcoholysis reactions is first the high viscosity of the medium and secondly the insolubility of the glycerophosphoryl moiety in the FA.

D. Implementation of LPL enzymatic synthesis

The synthesis reactions of LPLs are governed by several parameters which are: water activity, reaction temperature, molar ratio of the substrates, biocatalyst quantity, nature of the reaction medium and acyl migration. These key parameters have to be considered in order to perform the reaction with satisfactory kinetics and yields.

1. Water

Water acts on the polarity of the catalytic site of the enzyme, on its flexibility and on the thermodynamic balance of the reaction**.**

Most lipases need a minimal hydration level allowing its interfacial activation. The a_w of the reaction medium allows the enzyme to have the functional mobility necessary for an optimal catalytic activity. Conversely, a low a_w would imply a rigidification of the enzyme leading to a lower activity (Klibanov 2001).

Moreover, the water formed during the ester synthesis reaction and initial a_w are a critical factor in determining whether the reaction equilibrium will progress to hydrolysis or ester synthesis. Indeed, an excess of water would shift the reaction equilibrium towards hydrolysis (Farnet *et al*. 2013).

In order to control formed water and a_w, several methods have been reported in the literature, such as the use of saturated salt solutions before the reaction to equilibrate the enzymes to a well-defined a_w, or their introduction into the reaction medium to remove the produced water during the reaction (Rosu *et al.* 1998, Virto *et al.* 1999). Other techniques are also reported such as blowing nitrogen gas (Rosu *et al*. 1999), adding molecular sieves (Blasi *et al*. 2008), and evaporating at reduced pressure (Rosu *et al*. 1998) to remove the water formed during the reaction.

Depending on the studied reaction, the enzyme source and the immobilization support, the a_w for maximal lipase activity is different (Petersson *et al.* 2007). Regarding lipase-catalyzed synthesis of LPLs, Han and Rhee (1998) have shown that the optimal a_w depends on the polar head of the glycerophosphoryl backbone. They have also shown that the optimal a_w depends on the hydrophilicity of the reaction substrates and products, the more hydrophilic they are, the higher the optimal a_w value is.

Kim and Kim (2000), established the relationship between the a_w of the RM-IM Lipozyme and the amount of dimethylformamide (DMF) used as organic co-solvent in LPL synthesis through direct esterification reaction of FA with GPC. When a_w is low, the enzyme cannot have its conformation to trigger its activity. On the other hand, an excess of water shifts the thermodynamic equilibrium in the direction of hydrolysis. According to these authors, the best conditions to have an efficient enzymatic activity is a a_w between 0.3 and 0.6 with 5 to 10% (volume/total weight of the substrates) of DMF as organic co-solvent.

2. Reaction temperature

Temperature normally affects lipase activity (Herbst *et al.* 2012). A very low temperature leads to an absence or a slow reaction. Nevertheless, high reaction temperatures deactivate the enzyme because of protein denaturation.

Many authors investigated the effect of temperature on lipase-catalyzed esterification reactions. The optimal temperature differs from a study to another depending on the lipase and the substrates used.

Recently, the effect of temperature on the synthesis of LPC-PUFA by lipase-catalyzed direct esterification of GPC and PUFAs was presented by Wang *et al.* (2020a). The range of temperature tested was from 50 to 70°C. The results demonstrated that the conversion yield increased from 58 to 65% when the temperature increased from 50°C to 55°C. However, when the temperature increased to 70°C the conversion yield decreased to 29% because of the denaturation of the lipase (immobilized MAS1 lipase from marine *Streptomyces sp.* strain W007).

3. Molar ratio

Among the variables affecting the yield of lipase-catalyzed synthesis reactions, the molar ratio between the substrates, which is the ratio of the molar concentration of the two substrates in the reaction medium, is essential to consider.

Synthesis of LPLs by esterification is a stoichiometric reaction. However, by the law of mass action, a large excess of FAs can favor the reaction in the direction of the formation of product. In a lipase-catalyzed esterification reaction, the first step consists in the fixation of the FA to the active site for the formation of the intermediate acyl-enzyme complex. Thus, adding an excess of FAs would favor the first step of the lipase catalytic mechanism to take place (Herries 1985, Kontogianni *et al*. 2003).

In studies aiming to synthesize LPL by direct esterification reaction between GPC and a FA in a solvent free medium, the substrate molar ratios vary between 20 and 50.

4. Biocatalyst quantity

The biocatalyst quantity used is important to consider because it allows the increase of the initial rate and thus the synthesis reaction will be occurred quickly. Nevertheless, for economic reasons, reducing the biocatalyst quantity is important due to the high cost of biocatalysts.

The used amount of immobilized lipase, named biocatalyst, is in the range of 10 to 20% of the total mass of the substrates.

Liu *et al.* (2017) reported that during Lipozym TL-IM catalyzed esterification of GPC with PUFAs mixture, the extent of PUFAs incorporation was enhanced by increasing the amount of enzyme in the reaction. However, when the enzyme amount was greater than 15% (by weight of substrates), there was no significant increase in the esterification yield. This could be due to the fact that too much swelling of the immobilized lipase would take up too much space in the reaction media as it was reported with Novozym® 435 (Kobata *et al.* 2002).

5. Reaction medium

The use of an organic solvent could be required to promote the solubility of substrates and their diffusion in the medium.

Lipase-catalyzed LPL synthesis has been studied extensively in systems using organic solvents. Yet, if such a process is destined to be used in the food industry, it is preferred to develop solvent-free systems. Indeed, organic solvents are expensive, toxic and flammable and their use implies higher investment costs to meet safety requirements.

Thus, enzymatic catalysis in a solvent free medium has received considerable attention in recent years, and it is used as an efficient approach to the synthesis of natural products, pharmaceuticals and food ingredients (Foresti *et al*. 2007, Feltes *et al*. 2012).

The lipase-catalyzed synthesis in a solvent free medium has several advantages compared to that in organic solvent medium (Dossat *et al.* 2002; Malipeddi *et al.* 2011; Casas-Godoy *et al.* 2012):

1- No need for solvent removal.
2- Avoid the use of toxic organic solvents.

However, the implementation of reactions in a solvent free medium has various drawbacks which are the high viscosity of the medium as well as the low solubility of the substrates (Sousa *et al.* 2021). For example,

LPL synthesis in a solvent free medium is based on the replacement of organic solvents by an excess of acyl donor (FA). The latter acts as both a solvent and a substrate. Long chain FAs are known for being viscous liquids. Regarding biocatalyst performance, the viscosity of the reaction medium can affect reagent diffusion to the active site of the enzyme (Uribe and Sampedro 2003). Therefore, the development of a process for lipase-catalyzed synthesis in a solvent free medium is of great interest, but with a great challenge.

6. Acyl migration

Acyl migration is the spontaneous, non-enzymatic, intramolecular transfer of an acyl group from one position to the adjacent position (Xu 2000). It provides thermodynamic stability within the molecule.

Acyl migration can occur either from the *sn*-2 to the *sn*-1 position (figure 29) or from the *sn*-1 to the *sn*-2 position. The *sn*-1-acyl compounds are thermodynamically more stable than the *sn*-2-acyl ones, which makes the acyl migration from *sn*-2 to *sn*-1 position at higher extent (Xu 2000).

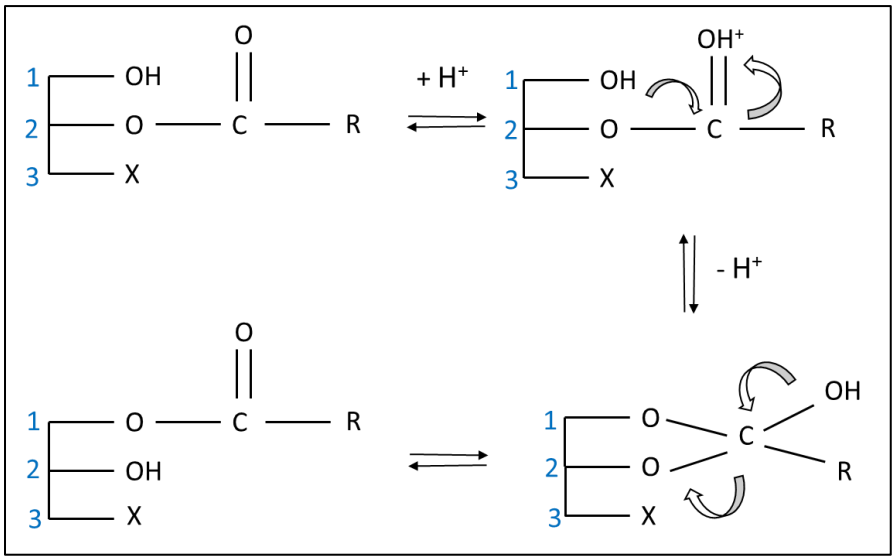

FIGURE 29: MECHANISM OF ACYL MIGRATION BETWEEN *sn*-2-LPL AND *sn*-1-LPL

(From Vikbjerg 2006)

This migration might lead to proportions of undesirable final product when preparing LPLs. Thus, it is important to be aware of this acyl migration phenomenon and it should be suppressed as much as possible.

There are several parameters that influence the acyl migration rate:

1- Reaction temperature: acyl migration could be reduced by lowering the reaction temperature to 30°C, while respecting the lipase activity (Poisson *et al.* 2009; Li *et al.* 2010; Zhou *et al.* 2021).
2- Water activity: there is a global consensus that acyl migration decreases when the reaction mixture a_w increases (Xu *et al.* 1998; Li *et al*. 2010; Peng *et al.* 2020).
3- Polarity of solvents: in general, increasing solvent polarity would result in decreasing acyl migration rate (Kapoor and Gupta 2012; Wang *et al.* 2020b).

Recently, Sugasini and Subbaiah (2017) showed that the rate of acyl migration from the *sn*-2 to the *sn*-1 in LPCs species depends on the FA nature. They compared the rate of acyl migration of LPC-DHA with three other LPC species, namely: LPC-C16:0, LPC-C18:1 and LPC-C20:4. Results showed that *sn*-2 LPC-DHA is far more stable than *sn*-2 LPC-C16:0. The acyl migration in *sn*-2 LPC-C18:1 and *sn*-2 LPC-C20:4 fell between the two extremes, which indicated a specific stability for LPCs containing DHA.

E. Enzymatic esterification synthesis of LPC

In the following section the studies that aimed to synthesis LPC by esterification will be reported, since as mentioned above, in the context of this work, we were interested in the synthesis of LPC-DHA through esterification.

Studies concerning esterification of GPC with FA are listed in table 5 (page 68). In this table, the obtained yields and the chosen parameters are reported, such as biocatalyst type and quantity, substrate ratio (GPC/FA), vacuum condition, reaction temperature, with or without addition of a solvent and a_w control.

According to table 5, it can be seen that lipases, and more specifically immobilized lipases, provide suitable catalysts for such reactions. Hong *et al.* (2011) compared various catalysts for the esterification of conjugated linoleic acid with GPC, namely: two free phospholipases, PLA1 and PLA2, and three immobilized lipases, which are Novozym® 435, Lipozym TL-IM®, Lipozym RM-IM®. It was shown that the free phospholipases are less effective (GPC conversion less than 10%) than the immobilized lipases.

Most of the studied biocatalysts are commercially available and widely known, and they are versatile for the synthesis of LPCs. However, in a couple of studies (Li *et al.* 2018, Wang *et al*. 2020a) non-marketed biocatalysts were prepared from newly characterized lipases. The prepared biocatalysts were shown to be more efficient than Novozym® 435 for synthesizing ω-3 PUFAs-LPC.

For the implementation of these reactions, assays were first carried out by mixing the substrates and the biocatalyst in various universal organic solvents such as, hexane and isooctane, for lipase-catalyzed

synthesis reactions (Kim and Kim 2000). It was shown that LPC was not produced at all due to the insolubility of GPC in these solvents.

GPC is a highly polar molecule soluble in water and lower alcohols, almost insoluble in organic solvents and slightly soluble in FAs. Lower alcohols cannot be used because they constitute a competitive hydroxyl donor for the esterification and consequently fatty alcohols could be formed. For this reason, experiments were performed in solvent free systems in which the free FAs constitute the liquid phase. However, solubilization of GPC under these conditions remained incomplete. Since GPC is slightly soluble in FAs, reactions usually occur while some solid GPC particles remained in suspension in the melted FA, and GPC slowly get solubilize as the reaction proceeds (Kim and Kim 2000). Also, in the context of synthesizing LPA, Virto *et al.* (1999) reported that GPA formed a separated gel phase or get dispersed in the media depending on the used FA.

The lipase-catalyzed GPC esterification is a water-producing reaction. Water can shift the reaction equilibrium towards hydrolysis; thus, water presents a crucial parameter that should be controlled in esterification reactions.

In GPC esterification studies, the amount of water was controlled during the reaction either by performing the reaction under low pressure or using salt hydrate pairs (Han and Rhee 1998) or adding a convenient co-solvent such as dimethylformamide (Kim and Kim 2000).

A high vacuum (1 and 10 mmHg) was typically used to remove the water formed from the reaction mixture. To our knowledge, Hong *et al*. (2011) are the only ones who compared different pressure values and clearly showed a positive effect of lowering the pressure. An increase of the yield from 5% to 70% was observed with the increase of vacuum from 760 mmHg to 1 mmHg, respectively. Other studies decided to work under vacuum without giving the reason for choosing to work under vacuum and as reported in table 5 not all studies indicated the applied vacuum value. However, in our laboratory, in the frame of synthesizing LPC-C18:1 ω-9 by lipase-catalyzed esterification of GPC with oleic acid in a solvent free medium, Mnasri *et al.* (2017b) showed that the removal of water produced while the reaction proceeds was not necessary to reach high yields. They showed that the complete solubilization of GPC was the main parameter to shift the reaction toward synthesis.

High yields have been claimed in these previously published studies as listed in table 5, except for Han and Rhee (1998) in which they obtained a conversion yield of GPC equal to 36%.

TABLE 5: TABLE ILLUSTRATING ARTICLES ON DIRECT ESTERIFICATION BETWEEN GPC AND FREE FATTY ACID IN A SOLVENT FREE MEDIUM IN ORDER TO SYNTHESIZE LPC

Reference	**Biocatalyst**	**Fatty acids**	**a_w control**	**T (°C)**	**Biocatalyst quantity** (% of total weight of the substrates)	**Molar ratio** (FA /GPC)	**Yield** (% of initial GPC consumed)
(Wang *et al*. 2020a)	Immobilized MAS1 lipase (from marine *Streptomyces sp. strain* W007)	Mixture of ω-3 PUFAs (DHA, EPA and DPA)	vacuum	55	20%	20:1	93% (37% EPA/ 7% DPA/ 45% DHA) after 24h
(Li *et al.* 2018)	Immobilized mutant lipase (MAS1-H108A)	Mixture of FA rich in CLA (C16:0, C18:0, C18:1n9, C18:2n6, 9c,11t-CLA, 10t,12c-CLA and others FA)	vacuum (1.5 mmHg)	55	12%	40:1	89 % after 48 h
(Mnasri *et al*. 2017b)	Lipozyme RM IM (from *Rhizomucor miehei*)	Pure oleic acid	No	50	10%	20:1	75 % after 24 h
(Liu *et al.* 2017)	Lipozyme TL IM (from *Thermomyces lanuginosus*)	Mixture of ω-3 PUFAs (DHA, EPA and DPA)	vacuum (10 mmHg)	45	15%	20:1	72% of LPC-DHA after 64h
(Hong *et al.* 2011)	Novozym 435 (from *Candida antarctica*)	Pure CLA	vacuum (1 mmHg)	40	10%	50:1	70 % after 48h
(Kim and Kim 2000)	Lipozyme IM (from *Mucor miehei*)	Mixture of FA (C12:0, C14:0 and C16:0)	dimethylformamide 7.5% (vol/wt)	60 (C12:0) 65 (C14:0) 70 (C16:0)	10%	10:1	90% after 24 h
(Kim and Kim 1998)	Lipozyme IM (from *Mucor miehei*)	Mixture of FA (caprylic acid, capric acid, lauric acid, myristic acid, palmitic acid and stearic acid)	No	70	13%	10:1.5	88% in 24h
(Han and Rhee 1998)	Lipozyme IM (from *Mucor miehei*)	Capric acid	salt hydrate pairs	50	5%	10:1.5	36% LPC (45% LPA and 23% LPE) after 60 h

F. Design of experiment

In order to optimize the esterification reaction and determine the optimal values of the factors that allow to have a high yield and amount of LPC-DHA a design of experiment (DOE) was implemented.

1. Overview

In order to optimize a response influenced by many factors, two methodologies can be used: one factor at a time (OFAT) method or DOE method.

OFAT is a method consisting on testing factors one at a time instead of multiple factors simultaneously.

DOE are mathematical designs that aim to describe the variation of a response under conditions that are hypothesized to influence it. They can be used to organize the experiments for scientific research or industrial studies.

They are applied when looking for the relation between a response of experiment (y) and factors (x). The response of an experiment can reasonably be assumed to depend on the experimental conditions (studied factors). This implies that the result can be described as a function based on the experimental variables (Lundstedt *et al*. 1998).

$$y = f(x_1, x_2, ..., x_k)$$

This function is approximated by a polynomial function that gives a representation of the relationship between the experimental variables and the responses in a limited experimental domain. It shows the change in a response produced by the change of one or more factors.

Each factor can be represented by a graduated and oriented axis (Figure 30). The value given to a factor to perform an experiment is called “a level”. When studying the influence of a factor, its variations is generally limited between two limits. Each factor is represented by 3 values: the low level (-1) representing the lowest value, the high level (+1) representing the highest value and the central level (0) representing the average value between the lowest and highest value.

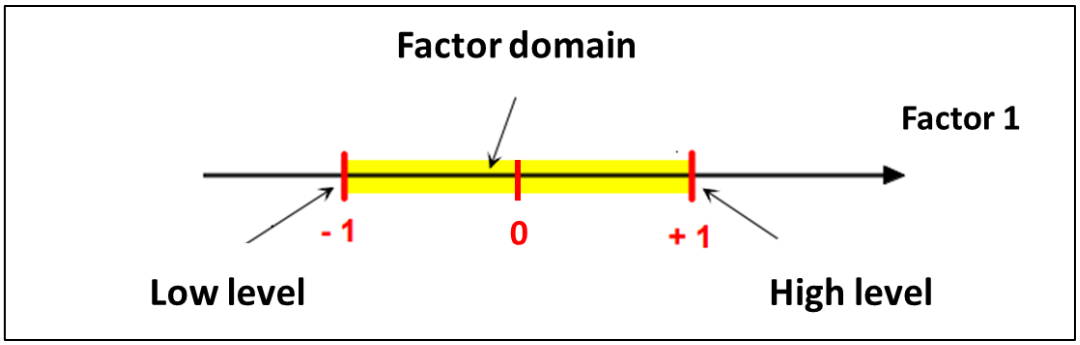

FIGURE 30: GRAPHICAL REPRESENTATION OF THE RANGE OF VARIATION OF A FACTOR

It is preferable to carry out a DOE rather than to study each factor in turn. OFAT requires more runs, cannot estimate interactions between factors and can miss optimal settings. While DOE require fewer runs and are more effective in finding the best optimal values to optimize the response as it predicts answers as a function of many factors and their combined effect.

2. Types of the design of experiment

There are four main families of DOE: screening designs, modeling designs or response surfaces designs and mixing designs (Pfleeger 1995):

a) Screening: The objective of this DOE is to determine which factors have the most important impact on the response. No specific relationship between the variations of the factors and the response is established.
b) Response surface method (RSM): when the aim is to optimize the response by taking into consideration the relation between factors and even quadratic effects (an interaction term where a factor interacts with itself).
c) Mixture design: mixture designs are particular designs adapted to the study of dependent factors. They are mainly used to study the influence of the proportions of the constituents of a product on a given response.

3. Methodology to implement a design of experiment

In order to carry out a DOE, the following steps must be conducted (Kirk 2002):

a) Specify the problem and define the response(s): identify the problem (e.g. insufficient performance, a tune-up to be done…) and quantify the objective to be achieved by defining one or more answers.
b) Select parameters: preliminary experiments should be performed to determine which experimental factors have a significant influence on the response. For these experiments, the factors should be held at a fixed level included in the experimental design.

c) Select a DOE: once the list of variables to be studied is completed, a DOE is chosen among several types of plans that exist (Box *et al.* 1978).

d) Carry out the experiments of the experience matrix: the experiment matrix is a table representing all the trial to be performed. It includes the number of experiments to be run and the levels assigned to each factor in each experiment. For instance, table 6 illustrates an experiment matrix of a Box-Behnken design with three factors.

TABLE 6: EXPERIMENT MATRIX OF A 3 FACTOR BOX-BEHNKEN EXPERIMENTAL DESIGN

Experiment number	Factor 1	Factor 2	Factor 3
1	1	1	0
2	1	-1	0
3	-1	1	0
4	-1	-1	0
5	1	0	1
6	1	0	-1
7	-1	0	1
8	-1	0	-1
9	0	1	1
10	0	1	-1
11	0	-1	1
12	0	-1	-1
13	0	0	0
14	0	0	0
15	0	0	0

e) Analyze the results: allows to visualize the influence of the parameters and their interactions on the response, aims at distinguishing, in the global variations of the response, the percentage due to the real influence of the parameters from the percentage due to experimental variation.

f) Validate the model: it consists in carrying out additional experiments within the study domain, and comparing the measured values with those calculated from the model. The model is validated if the differences between the measured values and calculated values are not statistically significant.

4. Application of the design of experiment

DOE have been employed to optimize various bioengineering processes as reviewed by Gündoğdu *et al.* (2016). Enzymatic synthesis of compounds such as lipids are also optimized by DOE. However, to our knowledge DOE was not applied to optimize the synthesis of LPL.

As it is known, each enzymatic reaction is affected by different factors. Optimizing these factors in order to maximize the yield using a DOE is important to find out the relationship between the response and the factors. In the literature it can be found numerous studies applying DOE.

Table 7 summarizes some studies using DOE to optimize lipase-catalyzed syntheses of lipids. It lists the type of used DOE, the optimized reaction (type, synthesized product, used lipase) and the studied factors.

TABLE 7: APPLICATION OF DOE IN LIPASE-CATALYZED SYNTHESIS OF LIPIDS TO OPTIMIZE THE YIELD

References	DOE	Reaction	Synthesized product	Biocatalyst	Studied factors
(Hvidsten and Marchetti 2021)	Box-Behnken (RSM)	Est	Biodiesel	Novozym® 435	BQ, Rt
(Li *et al.* 2021b)	Box-Behnken (RSM)	Est	Biodiesel	Liquid lipase from *Aspergillus oryzae*	T, BQ, Rt, MR
(Naranjo *et al.* 2021)	Central composite (RSM)	Acidolysis	TAG-DHA	Lipozyme ® RM-IM Lipozyme ® TL IM	T, BQ, Rt, MR
(Pando *et al.* 2021)	Central composite (RSM)	Est	TAG-DHA TAG-EPA	Lipozyme ® TL IM	MR, T, Pressure, Rt
(Rychlicka *et al.* 2020)	Box-Behnken (RSM)	Inter-Est	PLs	Novozym® 435	MR, Rt, BQ
(Bakir *et al.* 2018)	Central composite (RSM)	Est	Structured lipid of hazelnut oil rich of CLAs	Lipozyme ® TL-IM	MR, T, Rt
(Manan *et al.* 2018)	Box-Behnken (RSM)	Est	Eugenyl benzoate	Lipozyme ® RM-IM	Rt, T, MR, BQ
(Lux *et al.* 2014)	Plackett–Burman (screening)	Est	1-palmitoyl-2-oleoyl-sn-glycero-3-phosphocholine	PLA_2	T°C, [LPC], glycerol/MeOH (v/v)

RSM: response surface methodology, Est: esterification, Inter-Est: interesterification, MR: molar ratio, Rt: reaction time, T: temperature, BQ: biocatalyst quantity, []: concentration, CLA: conjugated linoleic acids

Most of these studies have been centered on the identification and optimization of the conditions of a particular lipase-catalyzed reaction using a small number of experiments that provide a large amount of information. The choice of the type of DOE in these studies depended on the number of the factors in the process and the objective which is maximizing the yield.

Plackett–Burman (PB) design has been employed by Lux *et al.* (2014) for its potential in screening factors that make the greatest impact on a reaction. However, few studies used a screening design, since some authors do not recommend the use of screening design because a reduction in the number of experiments affects the design resolution and causes important information to be lost (Pereira *et al*. 2021).

RSM, especially Box-Behnken (BBD) and composite central (CCD) designs are widely used in lipase-catalyzed reactions to optimize the yield but the reason for this choice has often not been specified. However, some studies justified the use of RSM because it is more accurate than the other designs by reducing the number of experimental runs, furnishing many informative datasets, allowing to understand the interactive impact of factors on the yield (Gündoğdu *et al*. 2016). A recent critical review has addressed this choice to the fact that in most of the literature studies, the Minitab software was used to conduct the RSM designs and data analysis. Since CCD and BBD are the two designs provided in Minitab, this may explain why these two are frequently used (Chong *et al.* 2021). However, nowadays there are more softwares that enlarge the choice of the DOE such as: Modde, Stagraphics, Statistica, etc.

Comparing these most used RSM models, BBD usually allows fewer runs than CCD as it requires three levels to each factor, while CCD requires five levels. Moreover, unlike CCD, BBD does not include experiments in which all factors are at their extreme levels, which could cause problem in some cases. In the cases of missing data or mismeasure responses the accuracy of the BBD becomes critical while CCD is more robust, as it studies many levels it is insensitive to missing data.

Despite all, RSM designs have shown a satisfactory ability in predicting the concrete properties, as most studies reported high statistical confidence and significance of the predicted models (Chong *et al.* 2021). For instance, a recent review highlighted the interest of RSM in optimizing the bioethanol production. The obtained models have contributed to enhancing bioethanol production as reviewed by Pereira *et al.* (2021).

Regarding the repetition of the experimental runs, a difference has been found in the literature where some experiments have been carried out in triplicate (Hvidsten and Marchetti 2021; Li *et al.* 2021b; Manan *et al.* 2018), or duplicate (Delgado Naranjo *et al.* 2021). Other authors did not replicate their runs without any discussion. Normally, the DOE are implemented to decrease number of experiments and replicates but in biological studies this may be difficult since the responses can display relatively high standard deviations. From our point of view, if the response is shown to be repeatable enough it would be obvious not to carry out the triplicates, but this depends from a study to another.

Besides, Pereira *et al.* (2021) underlined in their review that not all authors correctly followed the statistical procedure to obtain the reduced mathematical model (without the non-significant coefficients) to predict their response. For example, Rychlicka *et al.* (2020) included the non-significant coefficients in the models and generated response surfaces by using these models. Also, other authors did not experimentally validate the optimum conditions (Lux *et al.* 2014; Bakir *et al.* 2018).

So, it can be seen that DOE is a good tool to optimize reactions but it is necessary to specify the objective, to choose the appropriate DOE and to correctly follow and respect the statistical procedure to validate the model.

Materials and Methods

Chapter 2 : Material and Methods

I. Enzymatic synthesis of docosahexaenoyl lysophosphatidylcholine

A. Materials

1. Biocatalysts

The biocatalysts used in this experimental work and their suppliers are listed in table 8.

TABLE 8: LIST OF STUDIED BIOCATALYSTS

Biocatalyst	Supplier
Novozym 435®	Strem Chemicals (Bischheim, France)
CALB immobilized on Immobead 150	Sigma Aldrich (Saint-Quentin-Fallavier, France)
Lipozyme ® TL IM	Strem Chemicals (Bischheim, France)
Thermomyces lanuginosus immobilized on Immobead 150	Sigma Aldrich (Saint-Quentin-Fallavier, France)
Lipase from *Burkholderia cepacia* immobilized on diatomite	Sigma Aldrich (Saint-Quentin-Fallavier, France)

2. Reagents and solvents

The reagents used in this experimental work and their suppliers are listed in table 9.

TABLE 9: LIST OF USED REAGENTS AND SOLVENTS IN THE ENZYMATIC SYNTHESIS

	Name	Supplier	Purity
Reagents	Docosahexaenoic acid	Larodan (Solna, Sweden)	>99%
	1-Docosahexaenoyl-*sn*-glycero-3-phosphocholine (LPC-DHA)	Toronto Research Chemicals (Toronto, Canada)	90%
	Ammonium acetate Sesamol	Sigma-Aldrich (Saint-Quentin-Fallavier, France)	>99.9% >98%
	Glycerophosphocholine	Bachem (Bubendorf, Switzerland)	>99%
Solvents	Acetonitrile Methanol	Fisher Scientific (Illkirch, France)	>99.9%

B. Method

1. Enzymatic synthesis of docosahexaenoyl lysophosphatidylcholine by esterification of *sn*-3-glycerophosphocholine with docosahexaenoic acid

To achieve this reaction, several steps are necessary. First of all, the reaction mixture has to be prepared. For that GPC and sesamol (a natural antioxidant) are mixed with DHA in a beaker. GPC and sesamol are first weighed and introduced into the beaker and then DHA is added using a micropipette.

The mixture is then maintained at a defined temperature while stirring, using a digital hotplate stirrer, for 30 min until a homogeneous dispersion of GPC in DHA is obtained.

The amount of GPC and DHA varies according to the molar ratio studied during the experiment while keeping a reaction volume of 1 mL. Regarding the sesamol, the added quantity should be always equivalent to a fixed concentration of 8.4 mM. This concentration was taken from Fhaner *et al.* (2016), in which this concentration of sesamol provided antioxidant protection of marine ω-3 PUFAs. The same concentration was used by the PhD student Florence Hubert in our laboratory who verified that this concentration can protect DHA against oxidation.

One of the difficulties of this work is to solubilize the GPC in the DHA, since GPC is a polar molecule that is poorly soluble in DHA. Trials were performed to solubilize GPC in DHA by heating the mixture at high temperature (70°C) for 3 hours. However, the GPC was never totally dissolved in DHA and a fine dispersion of GPC in DHA was formed, that is relatively homogeneous when the mixture is stirred.

Once the reaction mixture is prepared, 1 mL of this mixture is introduced into a 50 mL plastic tube (conical bottom) or a 10 mL glass Pyrex tube (flat bottom), according to the reactor used, followed by the addition of the quantity of biocatalyst defined according to the desired experiment. Each experiment is carried in triplicate.

After addition of the biocatalyst, the reaction is carried out either in a Thermomixer® (Eppendorf, Hamburg, Germany) in Falcon tubes under atmospheric pressure, or in a temperature-controlled reactor (Multivapor P-12 equipped with a V-700 pump (Büchi, Rungis, France)) in glass Pyrex tubes under reduced pressure (20 mbar), at a stirring speed of 1000 rpm.

The reaction is then carried out over 30 hours. The synthesis of LPC-DHA is followed by sampling 5 µL of the reaction mixture at regular times. The samples are stored at -25°C in 0.5 mL Eppendorf tubes before analysis by high performance liquid chromatography (HPLC).

For HPLC analysis, the samples must be diluted in methanol and centrifuged as explained below.

Due to the high viscosity of the reaction medium, the sample volume is not accurate enough. Therefore, each sample is weighed and diluted in methanol with a dilution factor ranging from 4 to 64. The choice of these dilution factors will be discussed below (section B, 5). The methanol diluent volume is calculated basing on the measured mass of each sample according to the following formula:

$$V_{MeOH}\ (\mu L) = \frac{sample\ mass}{0.943\ (DHA\ density)} * (dilution\ factor\ -1)$$

In order to eliminate micro-particles which could clog the needle, the tubes or the column of the HPLC apparatus, diluted samples are centrifuged, at 10 000 rpm for 10 min, before HPLC analysis. The supernatants are then transferred into vials for HPLC analysis. The Figure 31 illustrates the steps to be followed during the reaction.

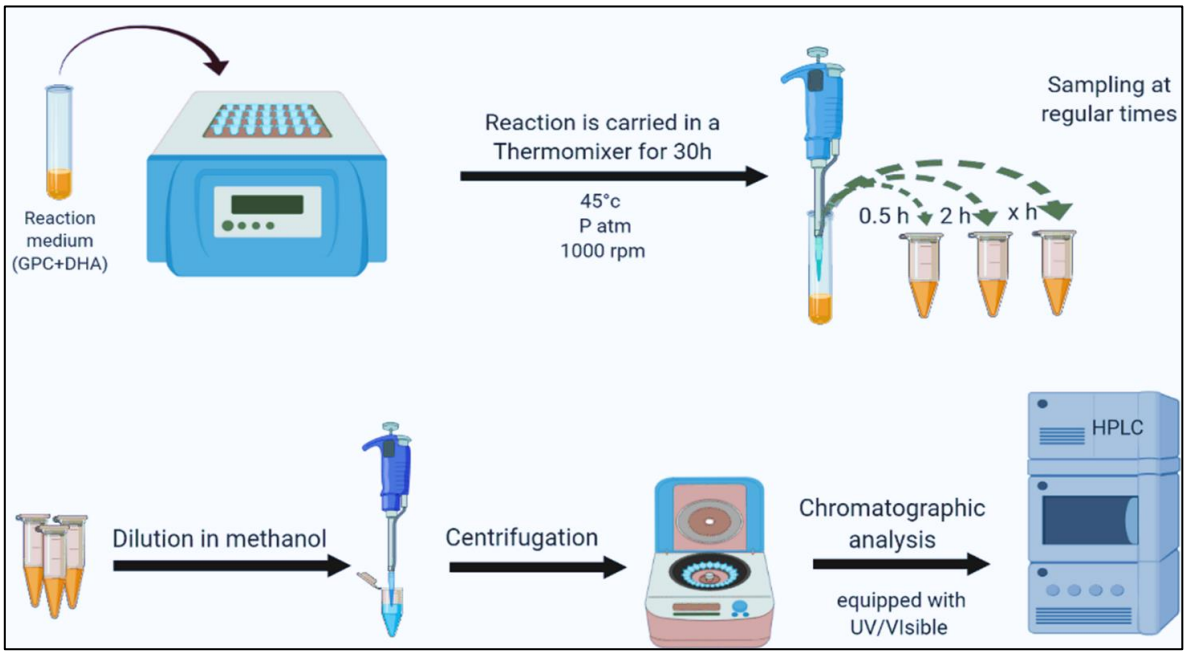

FIGURE 31: A SCHEMATIC FIGURE ILLUSTRATING THE SYNTHESIS STEPS FOLLOWED

2. Monitoring of the esterification reaction and HPLC analysis

Qualitative and quantitative analyses of the remaining substrates and synthesized product in the reaction mixtures were carried out using an HPLC system from Agilent Technologies model 1260 Infinity (Les Ulis, France), equipped with an in-line solvent degasser, a quaternary pump, an automatic injector and a UV/Visible spectrophotometric detector. The software used to control and process the data is Chemstation 32 (Agilent Technologies).

The column used is a Kinetex HILIC column (Phenomenex, Sartrouville, France) (4.6 mm x 50 mm, 2.6 µm). The mobile phase flow rate is set at 1 mL/min and the volume of injection at 3 µL. The mobile phase is composed of methanol, acetonitrile, ultra-pure water and a 100 mM ammonium acetate

solution. Several tests were carried out in order to optimize the elution gradient. The optimized elution gradient used is described in Table 10.

TABLE 10: ELUTION GRADIENT FOR HPLC ANALYSIS

Time (min)	Methanol (%)	Acetonitrile (%)	Water (%)	Ammonium acetate (100 mM, pH = 5.8) (%)	Flow rate (mL/min)
0	48	40	7	5	1
2.5	48	40	7	5	1
3.5	63	17	15	5	1
8	63	17	15	5	1

The wavelength of the UV detector is set at 205 nm, which allows the detection of molecules containing one or more double bonds.

3. Obtained chromatograms

Enzymatic kinetics are followed between 0 hours and 30 hours of synthesis.

Figure 32 below shows the chromatograms of the reaction medium at the beginning of the synthesis (t=0 hours) (figure 32 A), after 5 hours of reaction (figure 32 B) and at the end of the synthesis (t=30 hours) (figure 32 C).

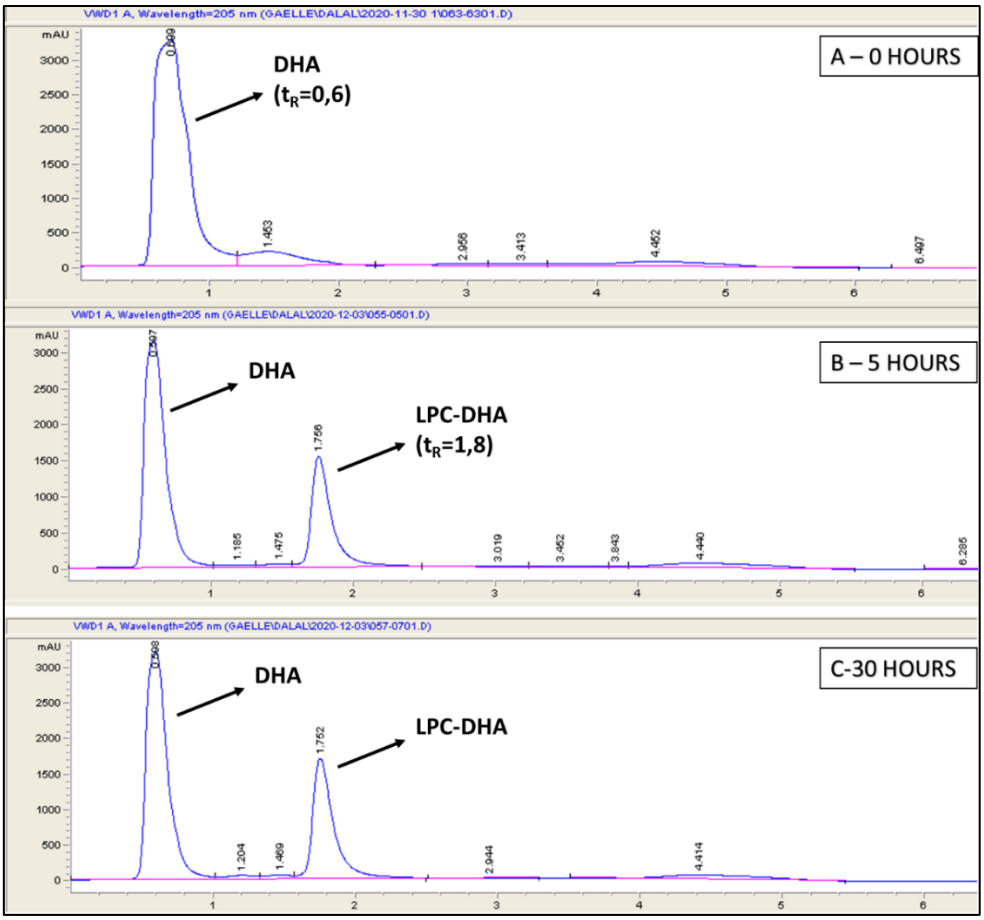

FIGURE 32: HPLC CHROMATOGRAMS OF ESTERIFICATION SAMPLE AT THE INITIAL REACTION TIME (A) AND AFTER 5 HOURS (B) AND 30 HOURS (C) OF SYNTHESIS

On these chromatograms, it is possible to see the appearance over time of the product of the synthesis, LPC-DHA. GPC disappearance could not be followed because of the instability of detection. Regarding the other substrate, DHA, it is present in great excess in the reaction medium and consequently, its consumption during the reaction is not visible.

The chromatograms obtained allow to determine the area of the peaks corresponding to LPC-DHA. This area is then used to calculate the concentration of LPC-DHA, *via* a calibration curve.

4. Calibration Range

An initial concentrated solution of LPC-DHA was prepared in methanol, followed by a serial dilution with methanol to obtain solutions with different concentrations of LPC-DHA. Calibration points were prepared in triplicate, and then analyzed by HPLC, in order to draw the curve representing the area of the peaks as a function of the concentration (figure 33).

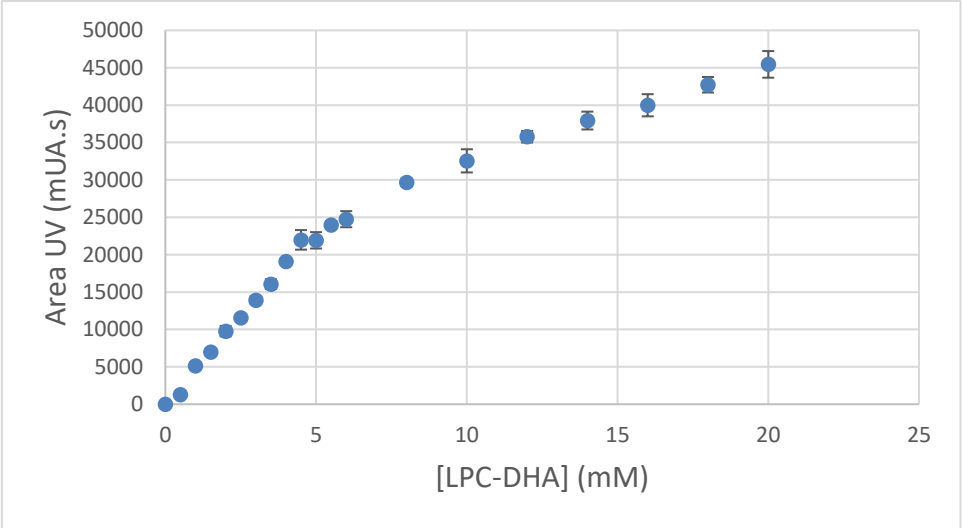

FIGURE 33: PEAK AREA OF LPC-DHA IN FUNCTION OF LPC-DHA CONCENTRATION

The curve obtained shows good linearity until a concentration of LPC-DHA of 4.5 mM. Above this concentration, the linearity is lost.

Thus, only the linear part of the curve can be used to determine the LPC-DHA concentration in each sample.

A trendline is drawn on the linear part of the curve between 0 and 4.5 mM (figure 34). Above 4.5 mM dilution is required. Therefore, the equation used for quantitation of LPC-DHA is:

$$\text{Area (mUA.s)} = 4849.2\ [\text{LPC-DHA (mM)}] - 334.6$$

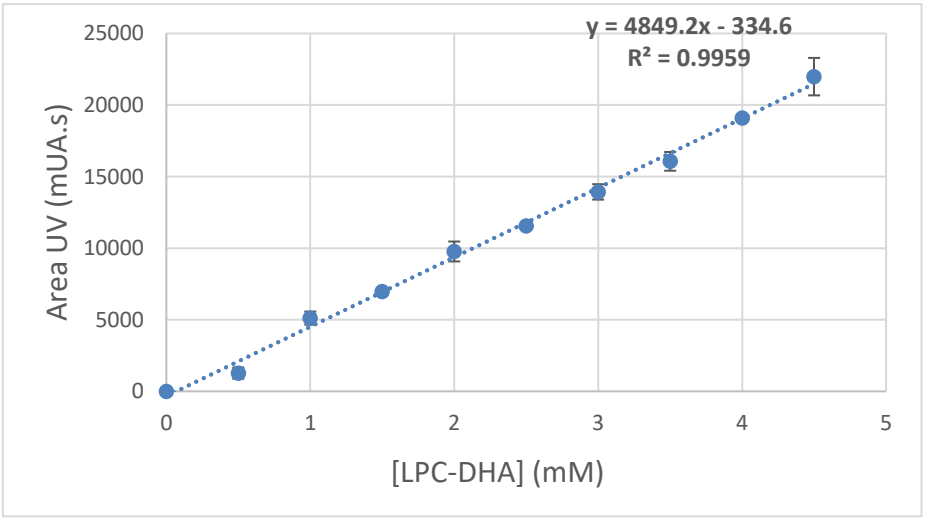

FIGURE 34: CALIBRATION CURVE FOR LPC-DHA QUANTIFICATION BY HPLC

5. Sample dilutions

One or more dilutions were performed for each sample in order to determine which one allows to obtain a peak area lower than 22000 mUA.s. Thus, dilution factors 4, 8, 20, 32, 64 were tested according to the cases (table 11).

TABLE 11: TESTED DILUTION FACTORS ACCORDING TO THE REACTION TIME

Time (hours)	Tested dilution factor	
Before adding biocatalyst	1/4	
0		
0.5	1/8	
1	1/20	1/32
1.5		
2	1/32	1/64
2.5		
3		
5		
7		
24		
27		
30		

Areas of the LPC-DHA peaks for each diluted sample are listed in table 12. Each column colors refers to the dilution factor mentioned in table 11.

TABLE 12: AREAS OF LPC-DHA PEAKS FOR EACH SAMPLE COLLECTED AT DIFFERENT REACTION TIME

Time (h)	LPC-DHA average peak area (mUA.s)		Relative standard deviation (%) of LPC-DHA average peak area	
Before adding biocatalyst	0		0	
0	0		0	
0.5	22156.5		12.22	
1	14965.7	9435.8	9.6	3.3
1.5	16549.6	10992.5	3.6	3.2
2	12541.6	6111.5	4.2	5.3
2.5	12923.2	6940.5	11.3	3.9
3	14319.8	7128.7	2.8	2.6
5	15126.4	7967.3	7.4	10.3
7	15860.4	8436.1	7.2	8.2
24	16264.9	9305.7	3.0	6.9
27	16552.3	8957.0	5.6	7.3
30	16056.5	8939.1	8.4	14.2

The obtained results show that from 0.5 h, a dilution higher than 1/8 is necessary to remain within the linearity boundary of the calibration curve. Indeed, at 0.5 h of synthesis, an average area of 22156.5 mUA.s (± 12,2%) is obtained with 1/8 dilution and this value is higher than 22000 mUA.s (tables 11 and 12).

At 1 h and 1.5 h, a 1/20 dilution gives an average area of 14965.7 mUA.s (± 9,6%) and 16549.6 (± 3,6%) mUA.s, respectively (tables 11 and 12). This is therefore adequate to obtain an area of less than 22000 mUA.s and thus allow quantification. However, a 1/32 dilution further decreases the concentration of LPC-DHA without reducing repeatability (tables 11 and 12). This allows a safety margin up to the maximum area value to anticipate a potential increase in LPC-DHA synthesis when variations in experimental conditions are later tested.

The 1/32 dilution allows good repeatability of LPC-DHA quantification until the end of the kinetics, since the relative standard deviations for this dilution do not exceed 11.2% (tables 11 and 12). However, a 1/64 dilution could be performed if the concentration of LPC-DHA would exceed 144 mM, which is equivalent to 4.5 mM in the 1/32 diluted sample, in some conditions.

In conclusion, the 1/32 dilution allows to decrease the peak area sufficiently to determine the LPC-DHA concentration. A larger dilution such as 1/64 would further decrease the peak area, but this would result in a larger error.

Figure 35 shows the detected chromatograms for diluted and undiluted samples.

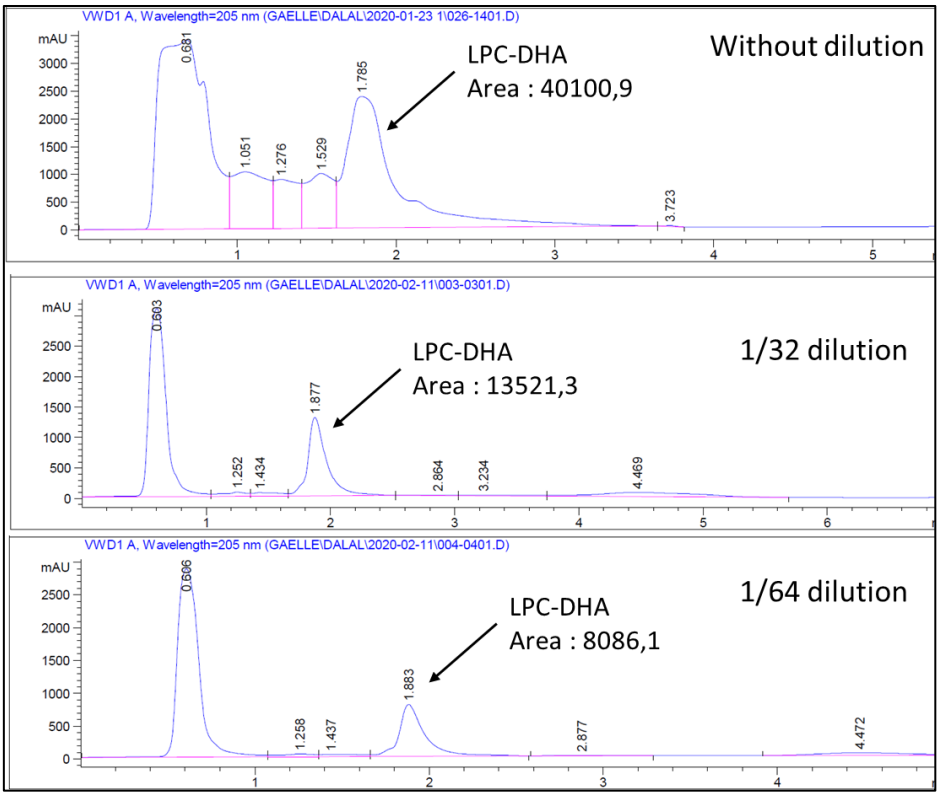

FIGURE 35: CHROMATOGRAMS OF ESTERIFICATION SAMPLE WITH AND WITHOUT DILUTION OF SYNTHESIS SAMPLES DETECTED BY HPLC

6. Result exploitation

Once the samples are appropriately analyzed by HPLC, a kinetic is plotted for each experiment (concentration as a function of time), and different parameters can be exploited. In this work the initial rate as well as the conversion yield of GPC will be exploited. These parameters are calculated according to the following formulas:

a) Initial rate

Theoretically the initial rate, Vi, of an enzymatic reaction is the instantaneous rate of the reaction product formation, determined at time t=0 and is equal to the slope of the tangent line of the kinetics at t=0. In this work, an estimated initial rate, called $V_{0.5}$ is explored. It is calculated by using the value of the LPC-DHA concentration in the reaction medium after 30 min of reaction, which is the time at which we collect the first sample.

$$\text{Rate after 30 min of reaction (mM/min)} = \frac{[LPC{-}DHA]\ (mM)}{time\ (\text{min})} = \frac{[LPC{-}DHA]\ (mM)}{30\ (\text{min})}$$

With:

[LPC-DHA]: Obtained concentration of synthesized LPC-DHA after 30 min of the reaction

b) Conversion yield of GPC

Y_{GPC} (%) = $\frac{[LPC-DHA]}{[GPC]i}$ x 100

With:

Y_{GPC}: GPC conversion yield

[LPC-DHA]: Concentration of synthesized LPC-DHA

$[GPC]_i$: GPC initial concentration

7. Purification of LPC-DHA by column chromatography

The LPC-DHA obtained must be purified from the reaction mixture in order to structurally characterize it and study its effect on breast cancer cells. The characterization was done in Institute of Molecules and Materials of Le Mans (IMMM- UMR CNRS 6283) by Pr. Arnaud Martel.

The separation of LPC-DHA from the reaction mixture was carried out on a column chromatography containing silica as a stationary phase. First dichloromethane was added to the column in order to eliminate the excess of DHA. Then a mixture of dichloromethane, methanol, and water (77:20:3, v/v/v) was used as the mobile phase to elute compounds.

The eluate is dispatched in different tubes and each fraction was analyzed by thin-layer chromatography plate using the same mobile phase, in order to identify the tubes containing the LPC-DHA. The tubes containing LPC-DHA were collected and the solvent was evaporated on a rotary evaporator. The obtained precipitates were then mixed with deuterated chloroform ($CDCl_3$) and analyzed by NMR.

8. Experimental design

In order to optimize the different parameters influencing the synthesis of LPC-DHA, an experimental design is implemented. The modeling of DOE is performed using a software, named MODDE® (SigmaPlus, Labège, France, v.10). This software provides the calculation of the regression coefficients of the response and allows the optimization of the corresponding factors.

The responses chosen to be studied are:

1- [LPC-DHA]: Synthesized concentration of LPC-DHA (mM)
2- Y_{GPC}: Conversion yield of GPC (%)

Concerning the choice of the factors, we were based on preliminary experiments that we have carried out. Based on these experiments, 3 factors were chosen to carry out the design. Table 13 represents the factors studied and their level of variation for each factor.

TABLE 13: STUDIED FACTORS AND THEIR LEVEL OF VARIATION

Factors	Low level (-1)		Central point (0)		High level (+1)	
	Coded value	Real value	Coded value	Real value	Coded value	Real value
Biocatalyst amount (%)	-1	5	0	10	+1	15
Molar ratio (DHA/GPC)	-1	4	0	11	+1	18
Temperature (°C)	-1	26	0	43	+1	60

In this study, the Box-Behnken design was applied. The three-factor Box-Behnken experiment matrix to be carried in this study, consisting of fifteen trials including 3 points at the center, is represented in the following table 14.

TABLE 14: BOX-BEHNKEN EXPERIMENT MATRIX TO BE CARRIED IN THIS STUDY

Experiment number	Run order	Molar Ratio	Biocatalyst quantity	Temperature
1	1	4	5	43
2	2	18	5	43
3	3	4	15	43
4	7	18	15	43
5	8	4	10	26
6	11	18	10	26
7	12	4	10	60
8	14	18	10	60
9	9	11	5	26
10	10	11	15	26
11	15	11	5	60
12	4	11	15	60
13	13	11	10	43
14	5	11	10	43
15	6	11	10	43

II. *In vitro* studies of LPC-DHA effect on the viability of MDA-MB-231 cells

A. Material

1. Cell line

MDA-MB-231 cell line is an epithelial breast adenocarcinoma cancer cell line of a 51-year-old woman. It comes from the ATCC (American Type Culture Collection; reference HTB-26) (figure 36).

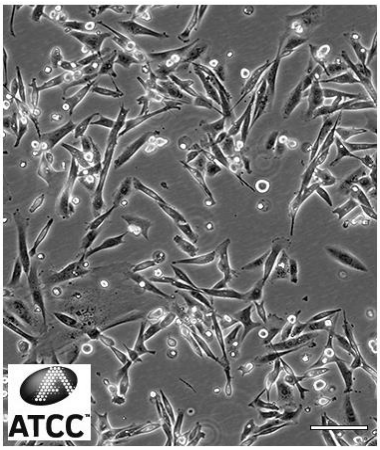

FIGURE 36: MDA-MB-231 CELL LINE

(Figure from ATCC)

2. Reagents and solvents

TABLE 15: LIST OF USED REAGENTS AND SOLVENTS IN THE IN THE BREAST CANCER EFFECT STUDIES PART

Reagent and solvents	Name	Supplier
For cell culture	MEM eagle	Dutscher (Bernolsheim, France)
	MEM non-essential amino acid solution	
	Fetal bovine serum (FBS) (PAN Biotech)	
	Penicillin-Streptomycin L-Glutamine	
Tested molecules	Docosahexaenoic acid	Larodan (Solna, Sweden)
	1-octanoyl-2-hydroxy-*sn*-glycero-3-phosphocholine (LPC-C8:0)	
	1-myristoyl-2-hydroxy-*sn*-glycero-3-phosphocholine (LPC-C14:0)	
	1-stearoyl-2-hydroxy-*sn*-glycero-3-phosphocholine (LPC-C18:0)	
	1-oleoyl-2-hydroxy-*sn*-glycero-3-phosphocholine (LPC-C18:1)	
	1-linoleoyl-2-hydroxy-*sn*-glycero-3-phosphocholine (LPC-C18:2)	
	1-behenoyl-2-hydroxy-*sn*-glycero-3-phosphocholine (LPC-C22:0)	
	Didocosahexaenoyl-*sn*-glycero-3-phosphocholine (PC-DHA)	
	1-Monodocosahexaenoin	
	Didocosahexaenoïn	
	Tridocosahexaenoïn 95%	
	1-docosahexaenoyl-*sn*-glycero-3-phosphocholine 90% (LPC-DHA)	Toronto Research Chemicals (Toronto, Canada)
	Glycerophosphocholine	Bachem (Bubendorf, Switzerland)
Other	Neutral red solution	Sigma-Aldrich (Saint-Quentin-Fallavier, France)
	LDH Kit	
	16% Formaldehyde solution methanol free	Thermo Fisher Scientific (waltham, USA)
	Ethanol	Fisher Scientific (Illkirch, France)

B. Methods

Maintenance, treatments, and cell experiments were performed under aseptic conditions in a laminar flow hood, and cells were incubated at 37°C under 5% CO_2 atmosphere.

1. Collagen microplate coating

Collagen is the predominant mammalian protein found in the body and is a major constituent of the extracellular matrix (ECM). Proteins of the extracellular matrix such as collagen provide a framework for the adhesion and growth of certain cell types *in vivo*, and may also be used for the attachment of cells to plate surfaces *in vitro*. Collagen microplate coating protocol comes from ANSES laboratory (Fougères, France).

In order to coat the 96 well microplates, a collagen solution is prepared with a final concentration of 60 µg/mL (450 µL of 4 mg/mL collagen solution is added to 30 mL of ultra-pure water). 50 µL of this solution is dropped in each well of the plate in order to have 3 µg/well of collagen. The plates are left closed under aseptic conditions in a laminar flow hood for two hours. Then the collagen solution is removed with a multichannel pipette, without touching the bottom of the wells. After emptying the wells, the plates are left to dry for 3 hours with the plate cover open. After drying, the plates are ready to be seeded with cells, and can be stored before use in a refrigerator in an airtight box to avoid moisture.

2. Cell freezing, thawing and culture

A cell suspension of 1 500 000 cells/mL is made in 1.5 mL growth medium (Complete medium containing 10% final FBS and 16% (v/v) dimethyl sulfoxide (DMSO). The suspension is placed in 2 mL cryotubes which are frozen at -80°C.

The thawing should be done quickly, by placing the cryotube in a water bath at 37°C. Once thawed, the cell suspension is transferred to a Falcon tube containing 10 mL of MEM (Minimal Essential Medium) with 10% FBS, and centrifuged at 7000 rpm for 10 min to eliminate the remaining DMSO by removing the supernatant. The cells are then transferred in a T-25 flask containing 7 mL of growth medium (MEM) supplemented with 10% FBS, 1% L-glutamine (200 mM solution) and 0.4% penicillin-streptomycin mixture (10,000 units/mL of penicillin and 10 mg of streptomycin /mL in 100 mL)), and incubated at 37°C and 5% CO_2 atmosphere.

Once cells reach confluence, cells are passed and 1 500 000 cells/mL are transferred in a T-75 flask containing 12 mL growth medium, and incubated at 37°C and 5% CO_2 atmosphere.

3. Cell maintenance

To maintain a stable cell culture, cell passages should be carried out. Cell passage involves transferring a small number of cells into a new vessel when they are confluent, to ensure the renewal of the nutrients brought to the cells and to maintain their growth activity. The cells can be cultured for longer if they are separated regularly, as this avoids the cell death associated with high cell density.

In general, confluence refers to the percentage of the surface of a culture flask that is covered by adherent cells. In our conditions, confluence is when 90% of the surface of the flask is covered by cells which refers to a cell density around 11 000 000 cells/mL. The volume to be transferred into a new T-75 flask is approximately between 0.6 and 0.8 mL.

Before trypsinization, the culture medium should be aspirated from the flask and rinsed 2 times with fresh growth medium without FBS. Two mL of trypsin are then added to the culture flask covering the entire cell mat. Cells are then incubated for 3 min at 37°C and 5% CO_2 atmosphere. After incubation, cell suspension in trypsin is transferred to a new falcon tube containing 2 mL of growth medium. This step allows the inhibition of trypsin activity by the FBS. The suspended cells are then counted using a Malassez hemocytometer, and 1 500 000 cells/mL are seeded in a new flask.

4. Microplate seeding

A cell suspension of 50 000 cells/mL is prepared to seed 200µL that contain 10 000 cells in each well of the microplates. The microplates are then incubated in the incubator at 37°C and 5% CO_2 atmosphere for 24 hours to obtain an adherent cell mat in each well.

5. Treatment of cells with products of interest

MDA-MB-231 cells at a concentration of 50 000 cells/mL were seeded into 96 well microplates containing 200 µL growth medium per well. The plates were preincubated without any treatment for 24 hours.

After 24 hours, 10 mM solution of each tested molecule is prepared in ethanol. These solutions are then diluted in growth medium in order to obtain the desired concentrations (between 6.25 and 200 µM), and final concentration of ethanol was maintained to 2%. Each tested concentration is plated in triplicate wells with cultured cells and incubated for 24 hours.

The 96 well microplate, allows to test, in triplicate, three molecules. Controls must be placed in each microplate in order to avoid the edge effect and to verify the growth of the cells without products, without and with ethanol. Figure 38 shows the microplate filling model that was adopted in this work.

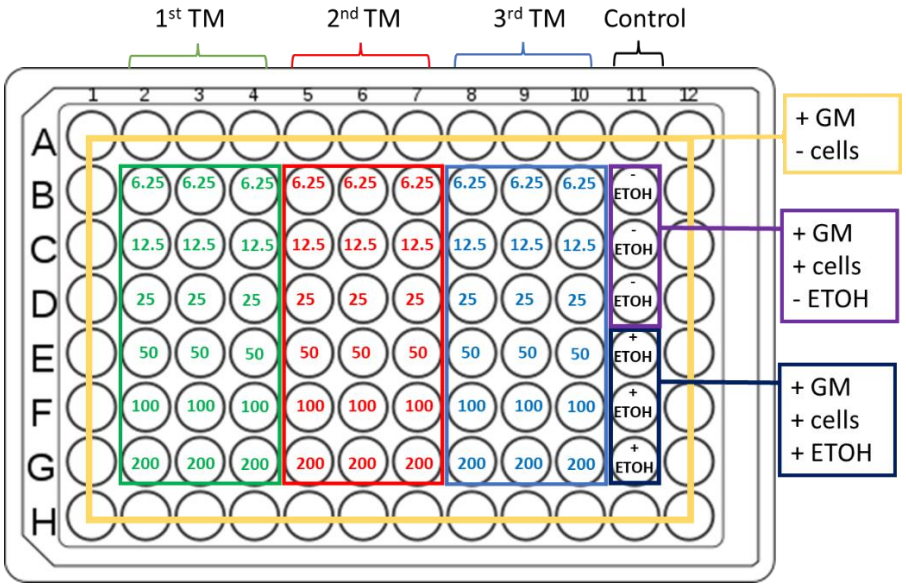

FIGURE 37: EXAMPLE OF 96 WELL MICROPLATE FILLING

(TM: tested molecule, -: without, +: with, GM: growth medium, ETOH: ethanol)

6. Cell viability study using the neutral red test

The neutral red (NR) test assesses the cytotoxicity of molecules based on the viability of the cells tested. NR is a dye that allows the lysosomes of cells to be stained only when they are viable because its integration into lysosomes requires active transport.

To evaluate living cells after treatment following exposure to reagents, the microplates are incubated for 2 hours with 100 µL of medium containing neutral red in each well (0.4% neutral red solution diluted to 1/100). Cells were then washed with 100 µL of a solubilization solution (1 volume of acetic acid in 99 volumes of ethanol 50%) followed by gentle shaking for 20 min so that NR get extracted from the cells and formed a homogeneous solution. Absorbance of wells is measured at 540 nm using a microplates reader spectrophotometer system (Epoch 2 from Biotek).

Cell viability (in %) is determined using the following formula:

$$\text{Viability} = \frac{AA\ (condition\ X) - AA\ (control)}{AA\ (control\ sample) - AA\ (control)} \text{ X } 100$$

With:

AA (condition X): the average of the absorbance of treated cells.

AA (control sample): the average of the absorbance of the untreated cells (with ethanol).

AA (control): the average of the absorbance of the external wells without cells.

IC_{50} were calculated using Excel® software. A scatter plot was created and the Y-axis scale was set to logarithmic. Then an exponential trendline was added and from the obtained equation, x, which refers to the concentration, is calculated for 50% of cell mortality.

7. Cell death mechanism and mode of action investigation

In order to investigate the mechanisms and mode of actions involved in cell death caused by LPC-DHA, MAG-DHA, PC-DHA and DHA on MDA-MB-231 breast cancer cells, immunolabelling's and commercial assay kit have been used

a) Evaluation of cell necrosis

Necrosis induced by reagents was assessed by lactate dehydrogenase (LDH) leakage into the culture medium. LDH is a stable cytoplasmic enzyme present in most cells. During cell cytoplasmic membrane damage, LDH is released from cells into the cell culture supernatant. LDH presence in the extracellular medium reflects a defect of membrane permeability, this permeability results in necrosis and/or cell lysis and indicates cell death.

The activity of LDH in the medium was determined using the commercially available kit "Cytotoxicity Detection Kit Plus (LDH) from the company Roche, and supplied by Sigma Aldrich.

The LDH presence in the medium participates in a coupled reaction that converts yellow tetrazolium salt into a red formazan product. The coupled reaction is based on the conversion of lactate to pyruvate, in the presence of LDH with parallel reduction of NAD^+ into NADH (figure 39).

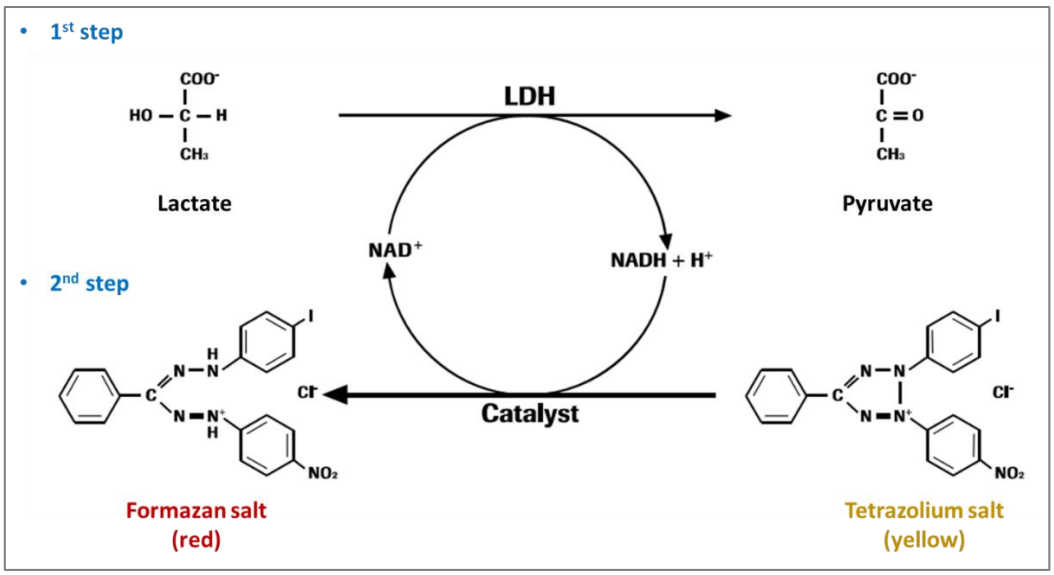

FIGURE 38: LDH ASSAY CHEMICAL REACTION

Cells were seeded in 96-well microplates at 10 000 cells/well for a 24 hours treatment. After treatment, the culture medium is transferred in a new microplate and diluted in order to fit in the calibration

range of the LDH absorbance. Then 100 µL of the reaction solution (mixture of catalyst and dye solution) were added to the diluted media. The plates were incubated 30 min in the dark, and then 50 µL of a stop solution were added. After shaking, the absorbances of the collected medium were read at 490 nm and 600 nm using a microplate reader spectrophotometer system (Epoch 2 from Biotek).

The percentage of LDH release was determined by dividing the subtracted absorbance ($A_{490} – A_{690}$) of the cultured medium by the absorbance of the high control wells (cells treated with lysis solution), and then multiplying the fraction by 100.

b) Immunolabelling

Immunolabelling's were carried out by Dr. Kevin HOGEVEEN (Toxicology Unit, ANSES, Fougères).

After a 24 hours treatment, cells were fixed 10 min with 4% formaldehyde in PBS and permeabilized with 0.2% Triton X-100. Plates were then incubated in blocking solution (PBS with 1% BSA and 0.05% Tween-20) for 60 min before addition of primary antibodies. All antibodies were prepared in blocking solution. The following primary and secondary antibodies were purchased from Abcam (Cambridge, UK): mouse monoclonal anti γH2AX ser139 (ab26350), rabbit polyclonal anti active Caspase-3 (ab13847), rabbit polyclonal anti HO-1 (ab13243), rabbit polyclonal anti LC3B (ab51520), mouse monoclonal anti ATM phospho serine 1981), goat anti-mouse IgG H&L AlexaFluor 647 (ab150115), goat anti-rabbit IgG H&L AlexaFluor 488 (ab150077). The rabbit polyclonal anti SOD2 antibody was provided by Thermo (PA5-30604). Primary antibodies were incubated overnight at 4°C.

After washing with PBS + 0.05% Tween-20, secondary antibodies (1/2000) were incubated for 45 min at room temperature. Nuclei were stained with DAPI (1 µg/ml in PBS) for 5 min for automated cell identification by high content analysis.

Plates were scanned with an ArrayScan VTI HCS Reader (Thermo Scientific, Waltham, USA) and analyzed using the Target Activation module of the BioApplication software. For each well, 10 fields (10× magnification) were scanned and analyzed for immunofluorescence quantification. Cytotoxicity was determined by cell counts from DAPI staining and was expressed as percentage of cells compared to control cells. All other markers were expressed as fold increase compared to control cells.Three independent experiments were performed.

Figure 39 summarizes all the steps performed to evaluate the effect of a studied molecule on the viability of the MDA-MB-231 cells.

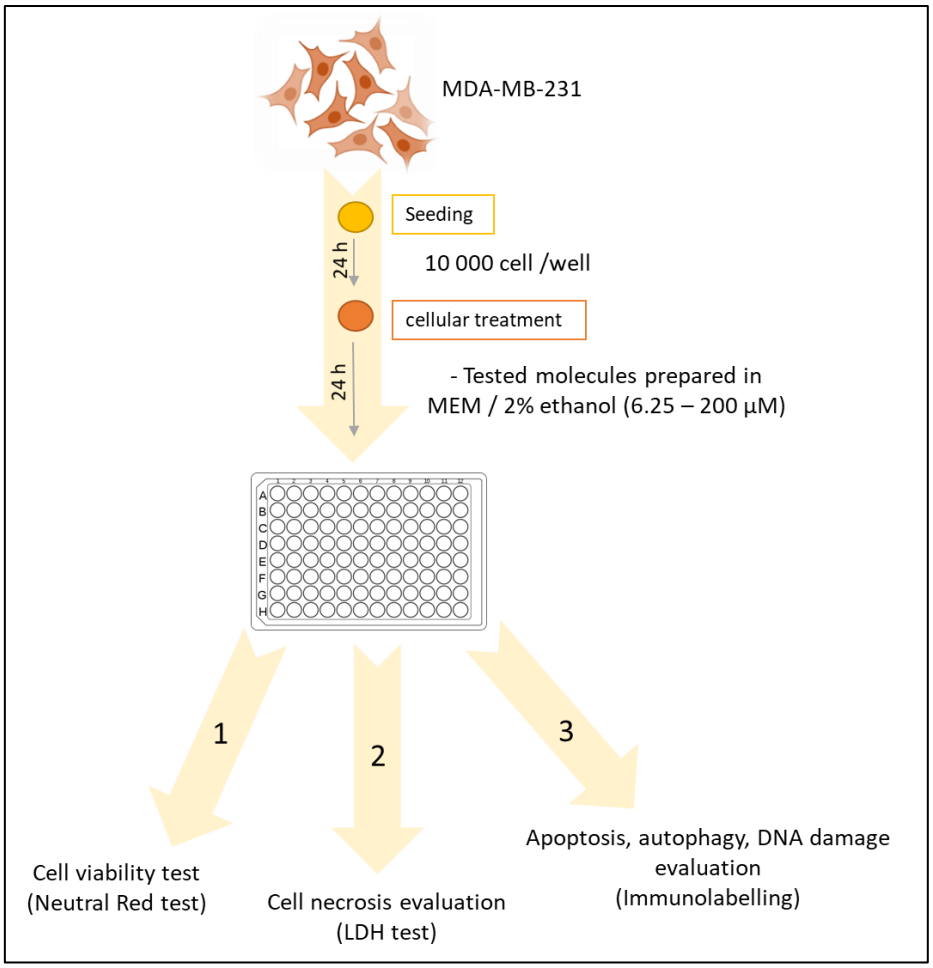

FIGURE 39: SCHEMATIC ILLUSTRATING THE CELLULAR EXPERIMENTAL PROTOCOL

III. Statistical analysis

All experiments are performed in triplicate whether in enzymology or in cell culture experiments. The statistical significance of difference between the values obtained for the studied parameters in enzymology was analyzed using T-test analysis, the level of p-value < 0.05 was considered significant. Data from cell experimental analyses are presented as mean values ± standard deviation (SD) (triplicate). After the analysis of variance, the mean values were compared using Fisher's least significant difference post hoc test (LSD). All statistical analyses were performed with Statgraphics Plus 5.1 (Manugistics Inc., Rockville, MD, USA).

Results and discussion

Chapter 3 : Results and Discussion

I. Enzymatic synthesis of DHA-rich lysophosphatidylcholine

The overall objective of this thesis is to contribute to the implementation and optimization of the enzymatic esterification of GPC with DHA, in order to synthesize LPC-DHA, using lipases and under environmentally friendly reaction conditions.

It should be noted that LPC-DHA was not commercially available until 2018, when it was furnished by the Toronto Research Chemicals company, and that in the studies considering its biological effects, the authors prepared the *sn*-1 isomer by phospholipase A2-catalyzed hydrolysis of PC-DHA followed by purification with preparative thin layer chromatography (TLC) (Hung *et al*. 2011b). So, during the first year of this thesis, in 2018, LPC-DHA became commercially available. At first, 10 mg of LPC-DHA were sold for 280 €. This price has risen each year until it reached 920 € in October 2021. This price evolution proves that demand exceed production capacity and therefore it is still interesting to develop new synthesis methods.

In BioSSE laboratory (formerly MMS laboratory) several works have been carried out on the lipase-catalyzed synthesis of structured lysophospholipids and phospholipids rich in particular FAs. Recently the synthesis of PC-C8:0-DHA was envisaged in the framework of the PhD work of Florence Hubert (Hubert 2018). However, the major product obtained under the conditions applied was LPC-DHA. Therefore, to initiate the present work on the synthesis of LPC-DHA, the initial working conditions (temperature, pressure, molar ratio and biocatalyst quantity) were those used by Florence Hubert.

A. Biocatalyst screening

In order to verify the feasibility of the reaction before carrying out a design of experiments, the ability of some biocatalysts to catalyze the esterification reaction was evaluated. For this, synthesis reactions have been implemented with five commercial immobilized lipases: Novozym 435® (N 435), Lipozyme TL-IM® (TL-IM), lipase from *Thermomyces lanuginosus* immobilized on Immobead 150 (TL-IB 150), lipase B from *Candida antarctica* immobilized on Immobead 150 (CALB-IB 150) and lipase from *Burkholderia cepacia* immobilized on diatomite (LBC). These lipases were chosen as they are known for their promising abilities in biotechnology in the synthesis reactions of different molecules.

The reactions were performed for 30 hours, under atmospheric pressure (P_{atm}), at a temperature (T) of 45°C and a substrate molar ratio (MR) of 18:1 (DHA:GPC). The amount of each biocatalyst (BQ) is 15% of the total mass of the substrate. The progress of the reaction was monitored by measuring LPC-

DHA and PC-DHA by HPLC (figure 40), and the conversion yield of the GPC was calculated at 30 hours of reaction (figure 41).

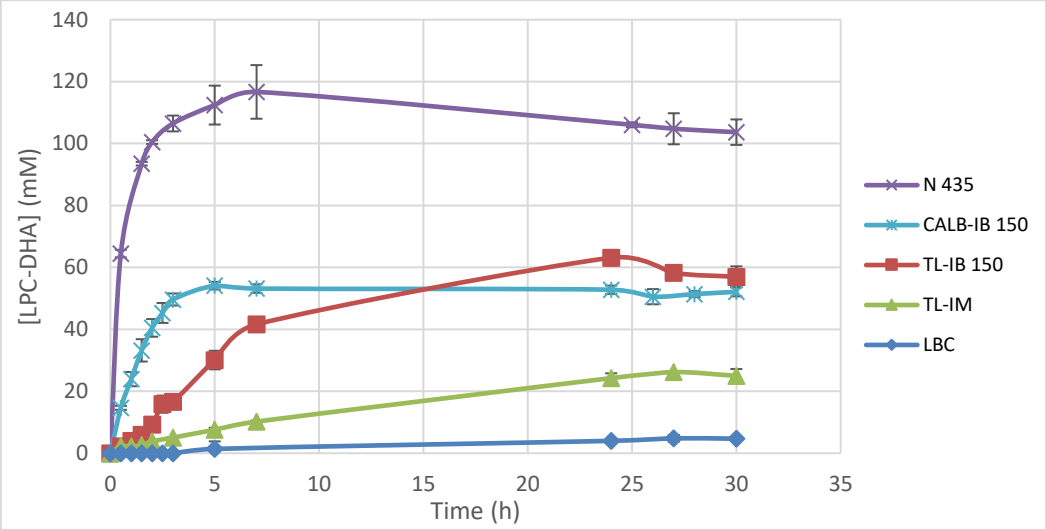

FIGURE 40: ESTERIFICATION KINETICS BETWEEN GPC AND DHA WITH VARIOUS IMMOBILIZED LIPASES

Esterification reactions were carried under the following reaction conditions: biocatalyst quantity (15%), molar ratio (18), temperature (45°C) and under atmospheric pressure. Data points are shown as mean ± SD of triplicate.

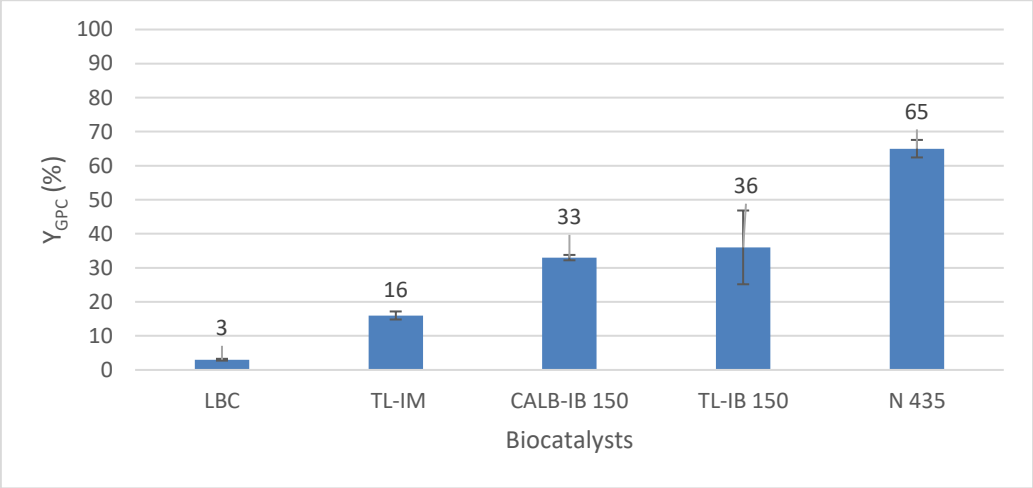

FIGURE 41: GPC CONVERSION YIELD AFTER 30 HOURS OF REACTION WITH VARIOUS IMMOBILIZED LIPASES

According to figure 40, LBC and TL-IM lipases gave very low syntheses of LPC-DHA (5 mM and 25 mM respectively at 30 hours of reaction), corresponding to GPC conversion yields (Y_{GPC}) of 3% and 16% (figure 41). TL-IB 150 and CALB-IB 150 lipases gave higher concentrations of LPC-DHA: 57 mM (Y_{GPC} =36%) and 52 mM (Y_{GPC} =33%), respectively. N 435 lipase was the most efficient biocatalyst with a LPC-DHA concentration of 104 mM at 30 hours of reaction, corresponding to a Y_{GPC} of 65%.

This conversion yield of 65% remains lower than those reported in the literature, where Y_{GPC} varies between 70% and 90%, as already mentioned in the bibliographic study (Chapter 1 (section IV, E) table 5).

Most of the published studies on this subject start the optimization by performing screening of 2 to 5 lipases, in order to select the most efficient one. Among the lipases studied, authors always studied N 435, TL-IM and RM-IM (from *Rhizomucor miehei*) lipases, and no one studied the use of these lipases immobilized in a covalent way on Immobead 150. In this study, no result is presented with RM-IM lipase, because it was already studied and it did not work well.

In the present study we found that N 435 was more effective for the synthesis of LPC-DHA than TL-IM lipase. This result has been also observed by Hong *et al.* (2011) for the synthesis of LPC rich in conjugated linoleic acid. In their study, they found that N 435 is the most efficient of the 5 biocatalysts tested in which among them there is the TL-IM lipase. On the contrary, Liu *et al.* (2017) reported that TL-IM is more efficient than N 435, for the esterification of GPC with a mixture of various ω-3 PUFAs. The difference in these results is certainly due to the difference of the studied FA and the reaction conditions.

Furthermore, when comparing the TL-IM lipase to the same lipase immobilized on a different support, namely Immobead 150 (TL-IB 150), it is observed that TL-IB 150 led about a twice higher synthesis of LPC-DHA (57 mM for TL-IB 150 and 25 mM for TL-IM). On the contrary, with CALB, the synthesis of LPC-DHA decreased when CALB was immobilized on Immobead 150 (32.6% for CALB-IB 150 and 64.8% for N 435). The difference in the obtained yields after 30 hours is due to the fact that the reaction did not reach the equilibrium yet.

It can be seen that with N 435 and CALB-IB 150 the highest yields were obtained after 5 hours and beyond that a plateau was observed. Different equilibrium was reached with these 2 biocatalysts, which is not in accordance with the theory.

In order to compare the behavior of the various lipases at the beginning of the reaction, the rate of LPC-DHA synthesis over the first half hour (called $V_{0.5h}$) was calculated (figure 42).

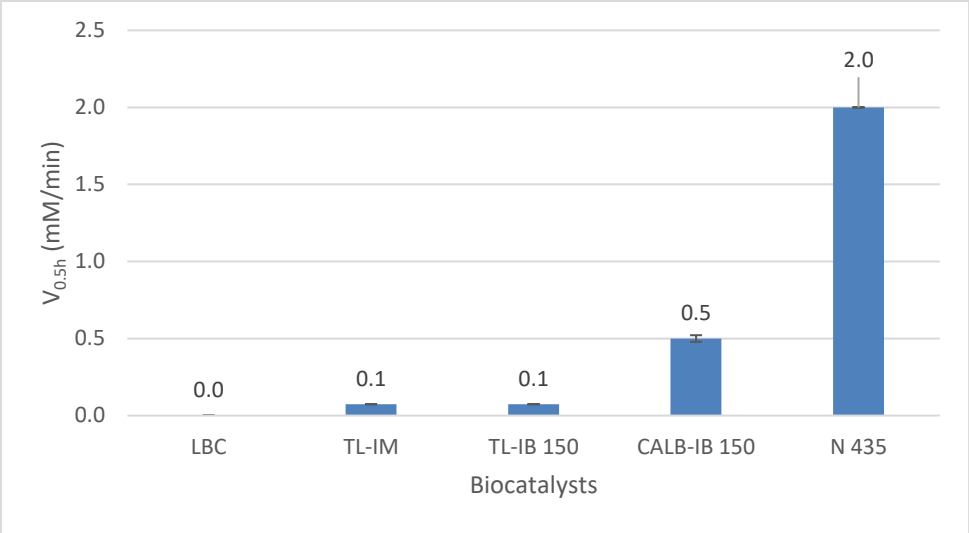

FIGURE 42: INITIAL REACTION RATES CALCULATED AFTER 0.5 HOURS OF REACTION CATALYZED BY DIFFERENT IMMOBILIZED LIPASES

We found that N 435 has a $V_{0.5h}$ (2 mM/min) approximately 30 times higher than that of TL-IM (0.07 mM/min), and 4 times higher than that of CALB-IB 150 (0.5 mM/min) (figure 42). The observed difference could be due to the fact that even if the same mass of each biocatalyst is used, this does not necessarily mean that the amount of enzymatic activity is the same. Indeed, the amount of activity per unit of mass can vary considerably from one biocatalyst to another. Also, we cannot forget that each lipase has a different reaction and substrate specificity.

Based on these results the N 435 was reserved for further experiments.

B. Novozym® 435 reuse

A major property of immobilized enzymes is the ability to be reused, which constitute an important economic aspect for industrial applications. Surprisingly, none of the published studies on the synthesis of LPC by direct esterification (Chapter 1 (section IV, E) table 5) have investigated the possibility of reusing the biocatalyst.

However, enzyme leaching from N 435 support is a known issue that should not be ignored. Indeed, previous studies have shown that in the presence of detergent-like compounds, the lipase adsorbed on the N 435 support may be released in the reaction medium (Rueda *et al*. 2015, Ortiz *et al.* 2019). This phenomenon is due to the fact that in N 435 ,the lipase is not covalently bound to the carrier, but physically adsorbed (Saunders and Brask 2021).

Therefore, to check if N 435 could be reused, the medium was withdrawn after 30 hours of a first reaction, carried out in the same conditions as above, and replaced by a fresh one (second use). The results are shown in figure 43.

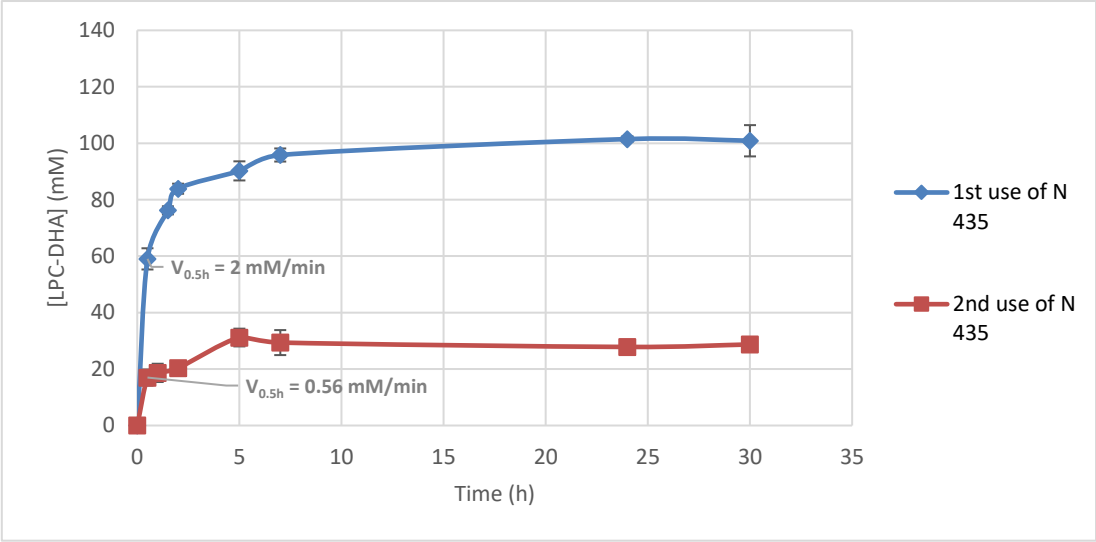

FIGURE 43: ESTERIFICATION KINETICS BETWEEN GPC AND DHA DURING FIRST AND SECOND USE (WITHOUT WASHING) OF N 435

Esterification reactions were carried under the following reaction conditions: biocatalyst quantity (15%), molar ratio (18), temperature (45°C) and under atmospheric pressure. Data points are shown as mean ± SD of triplicate.

According to figure 43, the concentration of synthesized LPC-DHA (59 mM) and the $V_{0.5h}$ (2 mM/min), reached after 0.5 hours of the first use of N 435, were 3.5 times higher than that obtained after the second use of biocatalyst (17 mM and 0.56 mM/min). This indicated that N 435 efficiency drastically decreased after the first use.

Lysophospholipids being known to have detergent-like properties, it can be suggested that as the concentration of LPC-DHA increases, it would desorb the lipase, thus preventing its reuse.

Furthermore, during our experiment it was noted that the N 435 beads took on a dark yellow color associated with the synthesized LPC-DHA. Thus, it can be suggested that LPC-DHA could bind to the support and limits the access of substrates to the active site of the enzyme.

Therefore, N 435 was collected after a first use, washed with n-hexane and dried at 40°C, and reused. After washing the beads, it was noticed that the beads recover their white color and that the hexane becomes yellow. A control experiment was carried out in order to check if the hexane has any inhibitory effect on N 435. For this, fresh N 435 beads were pre-washed with hexane and dried at 40°C before use.

The results are presented in figure 44. They showed that there was no difference between the reaction performed with (control) or without pre-wash with hexane of the biocatalyst (first use), indicating that hexane can be used for N 435 wash.

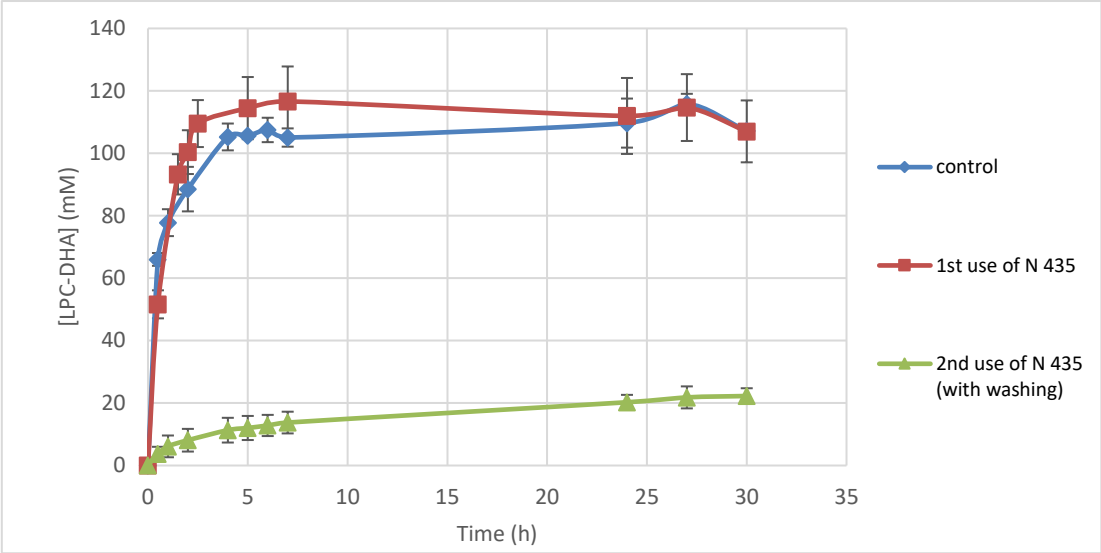

FIGURE 44: ESTERIFICATION KINETICS BETWEEN GPC AND DHA DURING FIRST AND SECOND USE (WITH WASHING) OF N 435

Esterification reactions were carried under the following reaction conditions: biocatalyst quantity (15%), molar ratio (18), temperature (45°C) and under atmospheric pressure. Data points are shown as mean ± SD of triplicate.

However, it appears that washing the N 435 with hexane in order to remove LPC-DHA possibly adsorbed to the support, does not improve its performance for a second use. Indeed, the LPC-DHA concentration obtained after 30 hours of reaction is as low as when the beads have not been washed between the two uses (figure 44 and 45).

The great reduction in the concentration of synthesized LPC-DHA indicated that even by washing the beads, N 435 reuse is still inconvenient. Two hypotheses can be suggested. The first hypothesis is that LPC-DHA caused the desorption of the enzyme due to its detergent-like property. The second hypothesis is that LPC-DHA or DHA inhibits the access of substrates to the active site by congestion in the microenvironment of the enzyme. Indeed, even if the beads were observed to recover their color when washed by hexane, it cannot be sure that the LPC-DHA and DHA attached to the microenvironment of the enzyme were totally washed.

C. Novozym® 435 and Purolite® CALB surface modification

Many authors have addressed the desorption problem of N 435. One of the most evident solutions is to cross-link the enzymes in order to prevent their desorption and improve the stability of N 435 (Ortiz *et al.* 2019).

To test this solution, in our case, cross linked modified N 435 with polyethyleneimine (PEI) and/or glutaraldehyde (GA) were kindly donated by Pr. Roberto Fernandez-Lafuente, (Institute of Catalysis and Petrochemistry (ICP-CSIC), Madrid, Spain). In addition, Purolite® CALB, native or with cross-linking

treatments, was also furnished. Purolite® CALB is a commercial biocatalyst in which CALB is immobilized by adsorption on a Lifetech™ ECR resin. This biocatalyst was proposed to be tested by Pr. Roberto Fernandez-Lafuente since one of its key features is the resistance to the leaching issues. All the donated biocatalysts were prepared by the PhD student Diego Carballares Navarro at the ICP-CSIC.

As already mentioned in the bibliographic study (Chapter 1 (section IV, B, 2, f)), to cross-link an enzyme, a linker such as GA or PEI, is used. GA is a linker that can be used to create intra or intermolecular covalent links. In addition, it produces a slight hydrophobization of the enzyme surface. Barbosa *et al*. (2012) proved that treatment of free CALB with GA was an effective way to improve activity and stability, as it resulted in a 5 – 6 times lower level of leaching in the presence of the detergent Triton X-100.

Alternatively, researchers physically cross-link the enzymes using ionic polymers such as PEI. PEI is an ionic polymer that generates a highly hydrophilic shell around the enzymes. Free CALB stability was greatly improved in different conditions (presence of detergents, in organic solvents or during thermal inactivation) after cross linking with PEI (Fernandez-Lopez *et al.* 2018).

Also, a combination of PEI and GA cross-linking has also proved to be efficient (Zaak *et al.* 2017).

These cross-linking solutions have been also used to reduce CALB leaching from N 435 support for the reaction of camelina oil alcoholysis (Verdasco-Martín *et al*. 2016).

In this work, the three modifications, *i.e.* with either GA, PEI or both, of N 435 and Purolite® CALB have been tested for the esterification of GPC and DHA in the same conditions as above (MR: 18 - T: 45°C - BQ: 15%) (figures 45 and 46).

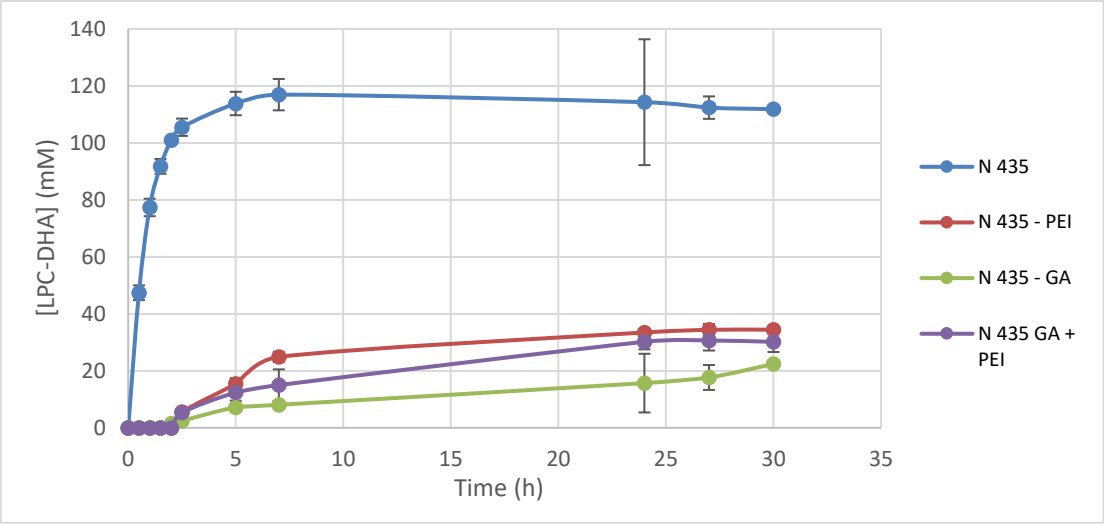

FIGURE 45: ESTERIFICATION KINETICS BETWEEN GPC AND DHA WITH DIFFERENT N 435 IMMOBILIZATION TREATMENTS

Esterification reactions were carried under the following reaction conditions: biocatalyst quantity (15%), molar ratio (18), temperature (45°C) and under atmospheric pressure. Data points are shown as mean ± SD of triplicate.

It appears that the changes in the N 435 support produced by the GA and PEI treatments have been negative. Indeed, these treatments lead to much lower LPC-DHA concentration after 30 hours of reaction (between 30 and 35 mM) (figure 46).

It can be suggested that treatment with PEI has produced a hydrophilic microenvironment that may not be positive for products as hydrophobic as the LPC-DHA. Moreover, regarding GA treatment, the covalent bonds created by GA may have limited the access of substrates to the active site of the enzyme.

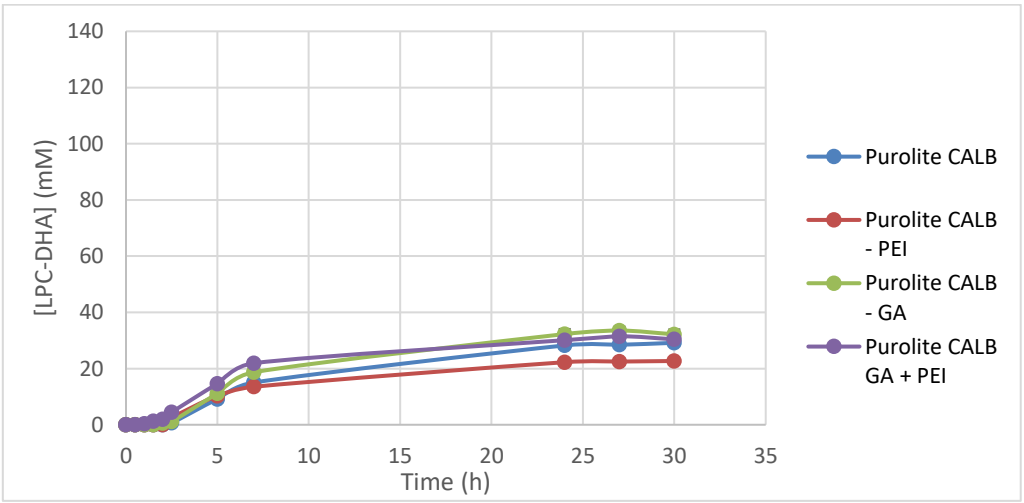

FIGURE 46: ESTERIFICATION KINETICS BETWEEN GPC AND DHA WITH DIFFERENT PUROLITE CALB® IMMOBILIZATION TREATMENTS

Esterification reactions were carried under the following reaction conditions: biocatalyst quantity (15%), molar ratio (18), temperature (45°C) and under atmospheric pressure. Data points are shown as mean ± SD of triplicate.

Regarding Purolite CALB® the concentration of synthesized LPC-DHA after 30 hours of reaction remained constant around 30 mM with and without treatments (figure 46). This showed that native and modified Purolite CALB® were not suitable for catalyzing this reaction.

Thus, the most efficient biocatalyst during this direct esterification process was the commercial preparation N 435, which allows to reach a conversion yield of GPC of 65%.

N 435 is one of the most commercially available stable and active preparations that have permitted many studies to be performed. Ortiz *et al.* (2019) review some examples of successful use of this biocatalyst in chemistry in food technology and in biodiesel production.

D. Optimization of LPC-DHA synthesis through Response Surface Methodology

This part of the study will focus on optimizing the production of LPC-DHA, by determining optimal levels of esterification reaction factors. The RSM, in accordance with the Box-Behnken matrix (BB), is applied to optimize the synthesis of LPC-DHA, by enzymatic esterification of GPC with DHA.

Classically in the optimization of enzymatic reactions the optimized response is the conversion yield of the substrates. In this study we aimed in addition to the Y_{GPC}, to investigate the productivity which means the concentration of synthesized LPC-DHA.

Before implementing the RSM, preliminary experiments were carried out in order to select the factors that had a significant effect on the responses.

1. Selection of factors influencing the responses

The factors examined in this study are: i) vacuum application, ii) the biocatalyst quantity (BQ), iii) the ratio of the molar concentration of the substrates called the molar ratio (MR) and iv) the temperature (T).

a) Vacuum

As mentioned in the bibliographic study (Chapter 1 (section IV, D,1), the water produced during the esterification reaction may favor the reverse reaction, *i.e.* the hydrolysis, reducing the synthesis of LPC-DHA.

Conducting the reaction under low pressure is an effective approach used to evaporate the produced water. Therefore, vacuum has been applied to investigate its effect on the synthesis.

In figure 47, kinetics of the reaction carried out with and without vacuum (20 mbar and atmospheric pressure (P_{atm}), respectively) are shown. The other reaction conditions were as follows: MR: 18 - T: 45°C - BQ: 15%.

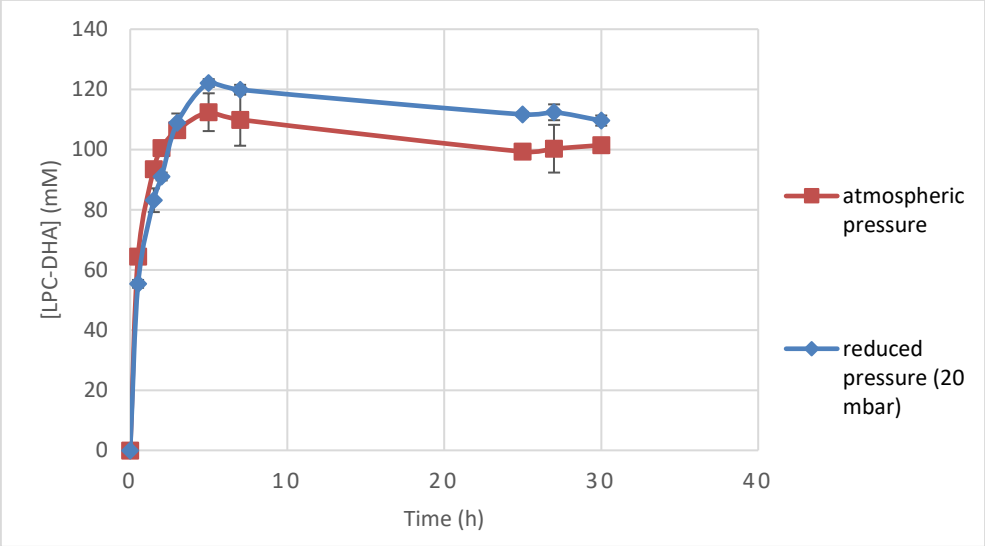

FIGURE 47: ESTERIFICATION KINETICS BETWEEN GPC AND DHA UNDER REDUCED AND ATMOSPHERIC PRESSURE

Esterification reactions were catalyzed by Novozym 435 and carried under the following reaction conditions: biocatalyst quantity (15%), molar ratio (18), temperature (45°C). Data points are shown as mean ± SD of triplicate. Statistical significance was determined using T- test analysis.

There is a slight significant difference between the concentrations of LPC-DHA for both reactions, 110 mM (Y_{GPC}= 69%) when applying vacuum (20 mbar) and 101 mM (Y_{GPC}= 63%) under atmospheric pressure (figure 47). These values are statistically different but it is not worthwhile to apply a vacuum which requires the use of special equipment, for a gain of 6% of Y_{GPC}.

In the literature, all published synthesis of LPC by direct esterification applied vacuum, except a previous study from our laboratory on the synthesis of oleoyl-LPC (Mnasri *et al.* 2017b), in which it was shown that the removal of produced water was not necessary when achieving a complete solubilization of GPC. Among the published studies, only Hong *et al.* (2011) investigated the effect of vacuum on the esterification of GPC and conjugated linoleic acid (CLA). These authors showed that a pressure as low as 1.4 mbar was needed to improve Y_{GPC} from 5% at P_{atm} up to 70%. In our conditions, a Y_{GPC} of 63% at P_{atm} was obtained while using the same biocatalyst as Hong *et al*. (2011) which is the N 435. Remarkably, in the rest of published studies authors applied vacuum without studying and comparing their reaction without vacuum.

Therefore, we may suggest that the Y_{GPC} could be improved if the reaction is performed at a pressure lower than 20 mbar, but this is not possible in our laboratory. At the same time, carrying out the

reaction under P_{atm} is advantageous from the point of view of ease of implementation. Thus, P_{atm} will be used for further studies.

b) Biocatalyst amount

The effect of the biocatalyst quantity (BQ) on the reaction yield was investigated using four different BQs: 5, 10, 15 and 20% (quantity of biocatalyst in relation to the total mass of the substrates). Esterification reactions were carried out with the following conditions: MR: 18 - T: 45°C - P_{atm}.

The BQ of 20% makes the reaction mixture very viscous due to the large volume occupied by the biocatalyst particles in the reaction mixture. Thus, the stirring of the particles became insufficient, even at the high stirring speed of 1000 rpm used throughout this study. This is why the kinetics with a BQ of 20% are not presented in the figure 48 below.

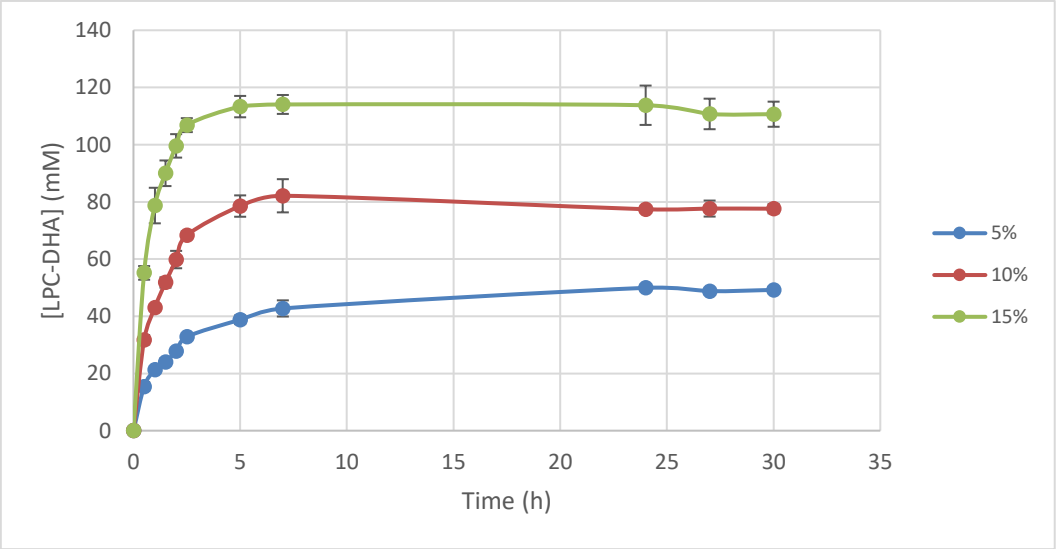

FIGURE 48: ESTERIFICATION KINETICS BETWEEN GPC AND DHA WITH DIFFERENT QUANTITIES OF NOVOZYM 435

Esterification reactions were catalyzed by Novozym 435 and carried under the following reaction conditions: biocatalyst quantity (5%, 10% and 15%), molar ratio (18), temperature (45°C) and under atmospheric pressure. Data points are shown as mean ± SD of triplicate. Statistical significance was determined using T- test analysis.

From these results, the reaction rates over the first half-hour ($V_{0.5h}$) were calculated for each BQ (figure 49). As expected, $V_{0.5h}$ increases proportionally to the BQ. This means that under the conditions used, the reaction rate at the beginning of the reaction is not limited by the concentration of the substrates and that the stirring of the reaction mixture is sufficient to ensure mass transfer of the substrates to the microenvironment of the enzyme.

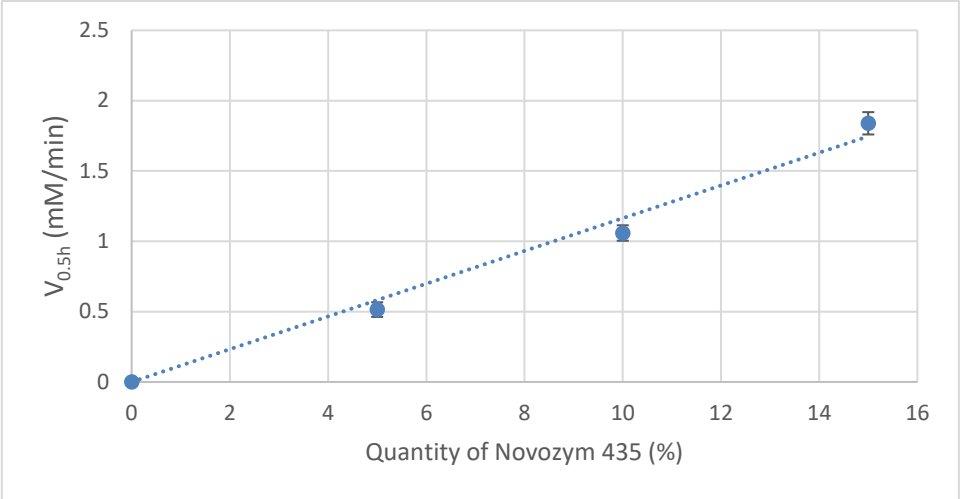

FIGURE 49: INITIAL REACTION RATES CALCULATED AFTER 0.5 HOURS OF REACTION WITH DIFFERENT QUANTITIES OF NOVOZYM 435

In figure 48, it can also be seen that the concentration of LPC-DHA at the equilibrium increased with the increase of BQ (49 mM (Y_{GPC}= 31%), 77 mM (Y_{GPC}= 48%) and 111 mM (Y_{GPC}= 69%) for BQ of 5, 10 et 15%, respectively) and that the equilibrium is reached at almost the same reaction time, close to 5-7 hours, irrespective to the BQ. However, in the theory the equilibrium is not modified by the biocatalyst quantity but it is reached at shorter reaction times the higher the BQ is.

In the literature, the biocatalyst quantity is very often one of the parameters studied to improve the yield of lipase-catalyzed reactions. However, most of the time, the complete kinetics is not performed and the reaction time is fixed, for example at 12 or 24 h. Thus, the yields given are not necessarily the one obtained at the equilibrium of the reaction and an increase of the yield with BQ reflects the increase of the reaction rate. Regarding the synthesis of LPC by direct esterification in conditions close to ours, only the study of Li *et al.* (2018) on the synthesis of LPC-CLA using an immobilized mutant lipase (MAS1-H108A) prepared by their own, showed the complete kinetics. They did not observe the same phenomenon as we did, since the kinetics in their case all reach the same equilibrium regardless the BQ.

The phenomenon observed in our case indicates that the reaction stopped after approximatively 7 hours of reaction time, preventing the equilibrium from being reached. This may be related to the inability to reuse the N435 described above and may be explained by inactivation of the enzyme by LPC-DHA or congestion of the microenvironment preventing contact between the enzyme and the substrate.

c) Substrate molar ratio

Several kinetics were carried out by varying the ratio of the molar concentrations of the two substrates, DHA over GPC, between 1 and 27. These molar ratios (MR) correspond to initial concentrations of GPC in the reaction medium ([GPC]i) ranging from 105 mM to 2871.2 mM. To vary the MR, the molar amount of GPC was varied while the molar amount of DHA was maintained constant. The reactions were carried out with the following conditions: BQ : 15% - T : 45°C - P_{atm}.

When working with a low MR, *i.e.*, MR = 1, 2 or 4, which means high [GPC]i, the viscosity of the reaction mixture became very important and consequently sampling the medium for analysis became difficult. Therefore, as can be seen in figure 50, no kinetics are shown for the MR = 1. Moreover, for the MR = 2, not all samples could be collected.

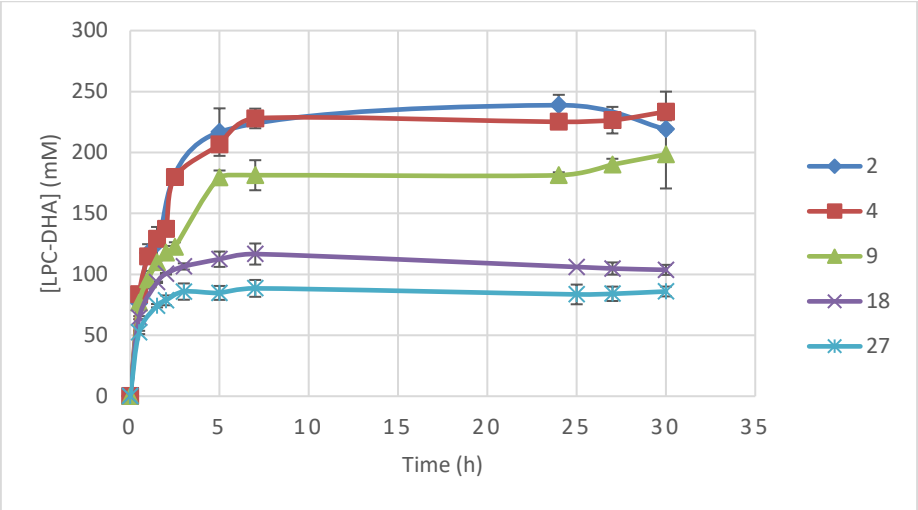

FIGURE 50: ESTERIFICATION KINETICS BETWEEN GPC AND DHA FOR VARIOUS MOLAR RATIOS

Esterification reactions were catalyzed by Novozym 435 and carried under the following reaction conditions: biocatalyst quantity (15%), molar ratio (2-4-9-18-27), temperature (45°C) and under atmospheric pressure. Data points are shown as mean ± SD of triplicate.

The reaction rates over the first half-hour ($V_{0.5h}$) were calculated for each [GPC]i (figure 51).

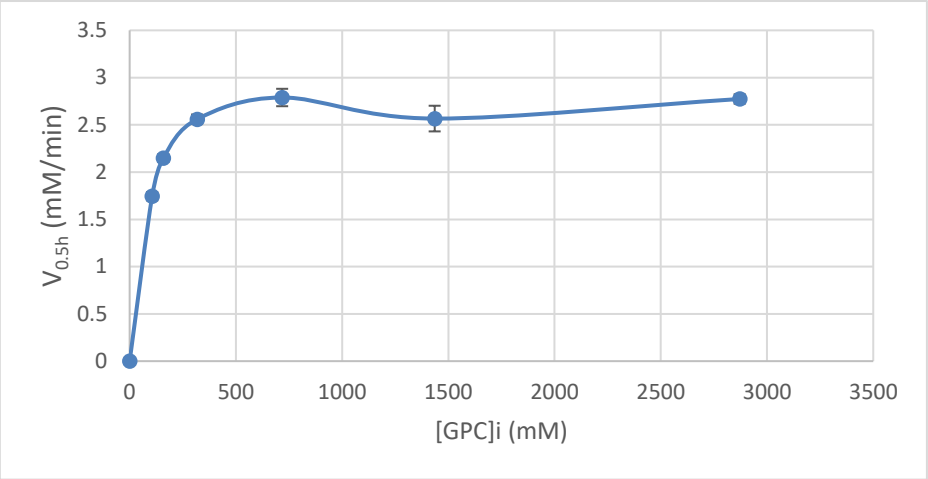

FIGURE 51: INITIAL REACTION RATES CALCULATED AFTER 0.5 HOURS OF REACTION WITH DIFFERENT VARIOUS GPC CONCENTRATIONS

According to figure 51, it can be seen that the $V_{0.5h}$ stop increasing from a [GPC]i of 720 mM corresponding to a MR of 4, thus, it seems that the biocatalyst is saturated with MRs lower than 4.

The values of Y_{GPC} and [LPC-DHA] after 30 hours of reaction obtained with the various MR tested, are compiled in the figure 52 below.

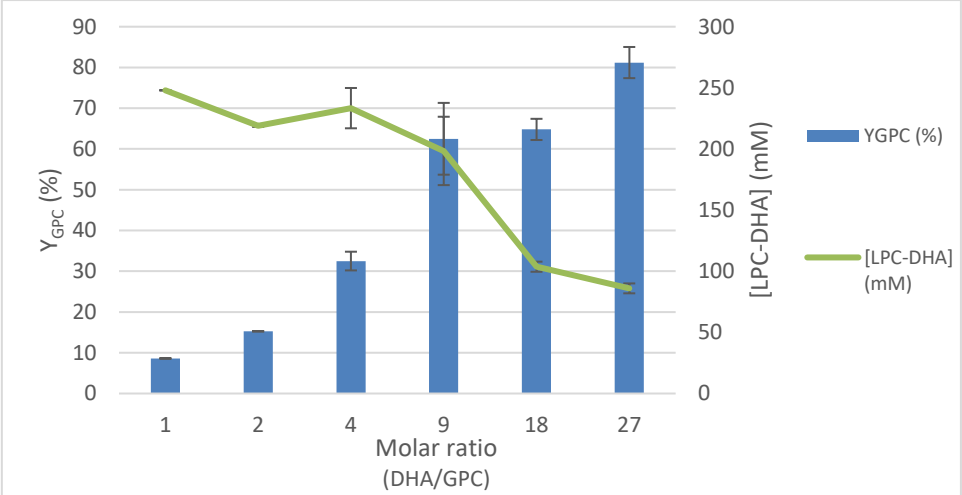

FIGURE 52: EFFECT OF THE MOLAR RATIO OF SUBSTRATES ON LPC-DHA CONCENTRATION AND Y_{GPC} AFTER 30 HOURS OF REACTION

The highest Y_{GPC} was of 81.2%, and was obtained with a MR = 27. The concentration of LPC-DHA increases from 86 mM to 200 mM with decreasing MR from 27 to 9 (figure 52). However, for MRs smaller than 9 (higher [GPC]i), the LPC-DHA concentration remains constant (figure 52).

With MR = 27, the yield was improved, up to 81%, while the [LPC-DHA] did not improve and remained constant to the one obtained with MR = 18 (figure 52). Thus, we will not be interested in MR = 27, as with MR = 18 the same [LPC-DHA] have been obtained while consuming less DHA.

At low MR (high [GPC]i) a low Y_{GPC} was obtained with a high [LPC-DHA]. The reaction equilibrium is moved to the product side with an increasing [GPC]i, which improves acyl incorporation. Simultaneously, the overall Y_{GPC} decreased which may be due to the decrease of the hydrophobicity of the reaction medium, since the quantity of DHA remains constant and it is the amount of GPC, which is a polar molecule, that increases. This hypothesis could be supported by the fact that lipase activation is enhanced in a hydrophobic environment (Peters *et al.* 1997). In addition, N 435 has been shown to display low substrate conversion (esterification activity) in polar media (Li *et al.* 2006). Moreover, considering the hygroscopic character of the GPC, it can be proposed that GPC strip the essential water layer of the enzyme and thereby inactivate the enzyme. It could be also thought that GPC provides water as long as it is not dried before. But this hypothesis is already eliminated as long as we tried to realize the synthesis with dried reaction mixture and biocatalyst and it has been demonstrated that the drying has decreased the synthesis.

Furthermore, as already mentioned in the Material and Methods section, it was difficult to solubilize the GPC at a MR = 18, and at MRs corresponding to a high [GPC]i the solubilization became even more complicated and a significant amount of GPC was not solubilized in DHA. Thus, it can be suggested that access of substrates to the active site of the enzyme may be limited.

In the literature, the studies dealing with the direct esterification reaction between GPC and a FA in a solvent free medium, use MRs which vary from 20 to 50. The choice of these MRs was based on experiments that investigated the effect of MR on Y_{GPC}. The results from these studies are in accordance with ours as an increase in Y_{GPC} was also observed with increasing MR. However none of these studies went down to low MRs, except Liu *et al.* (2017) who studied the effect of MR = 2 and 4 on the synthesis of LPC-PUFAs, and Mnasri *et al.* (2017b) who studied the effect of a MR = 5 on the synthesis of LPC-C18:1 ω-9. Low Y_{GPC} were obtained, 25% for MR 2 and 40% for MR = 4 and 5.

No publication addressing the synthesis of LPC by direct esterification, has announced the obtained LPC concentration under their conditions. So, to be able to compare our results with those of the literature, the LPC concentrations have been calculated, using the data available in the articles, when reported.

In the literature, the highest LPC concentration, which is approximately 142 mM, is obtained by Wang *et al.* (2020) that aimed to synthesize LPC-PUFAs. This value was reached using 20% of an immobilized

MAS1 lipase (from marine *Streptomyces sp. strain* W007), a MR of 20, under vacuum and at 55°C (Wang *et al.* 2020a). Comparing these results with ours, the productivity has not been doubled, but it has been increased with more favorable conditions. Indeed, we achieved a [LPC-DHA] of 200 mM, with 15% N 435, MR of 9, without applying vacuum and at 45°C.

Thus, for the implementation of the design of experiment MRs between 4 and 18 will be chosen.

d) Temperature

The influence of reaction temperature (T), on the esterification of GPC with DHA was examined between 25 and 60°C. Esterification reactions were carried out with the following conditions: BQ: 15% - MR: 18 - P_{atm}.

It should be noted that temperature did not enhance the solubilization of GPC in the mixture.

In figure 53, kinetics of the reaction carried out under different temperature are shown.

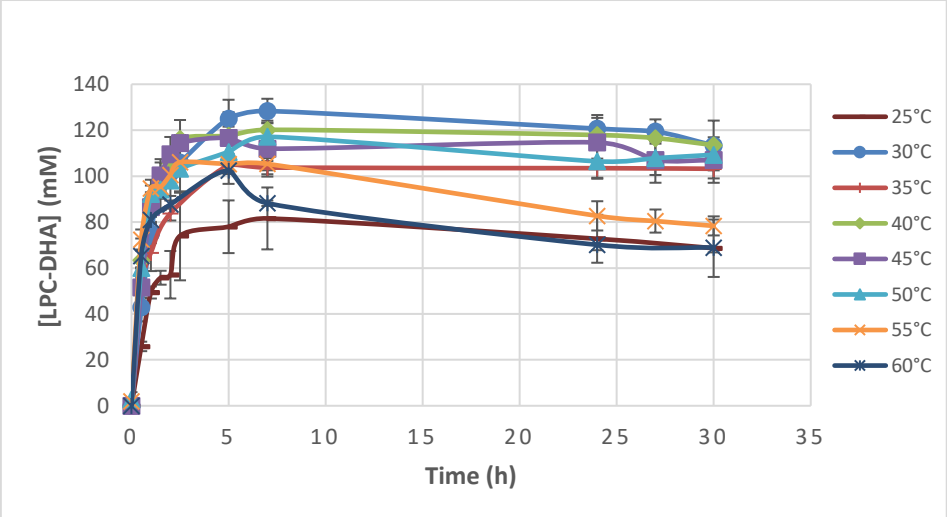

FIGURE 53: ESTERIFICATION KINETICS BETWEEN GPC AND DHA AT TEMPERATURES FROM 25 TO 60°C

Esterification reactions were catalyzed by Novozym 435 and carried under the following reaction conditions: biocatalyst quantity (15%), molar ratio (18), temperature (varying from 25°C to 45°C) and under atmospheric pressure. Data points are shown as mean ± SD of triplicate. Statistical significance was determined using T- test analysis.

For temperatures ranging from 30°C to 50°C, the [LPC-DHA] at 30 hours of reaction, were not significantly different with an average value of 120 mM (p-value > 0.05) (figure 53). For higher temperatures (55°C and 60°C), a decrease in [LPC-DHA] was observed over time, from 5 hours of reaction (p-value < 0.05). At 30 hours of reaction this decrease represents respectively 25 and 30% of the value at 5 hours. This decrease may be explained by a shift in the equilibrium of the reaction towards hydrolysis.

From these results, the reaction rates over the first half-hour ($V_{0.5h}$) were calculated for each temperature (figure 54).

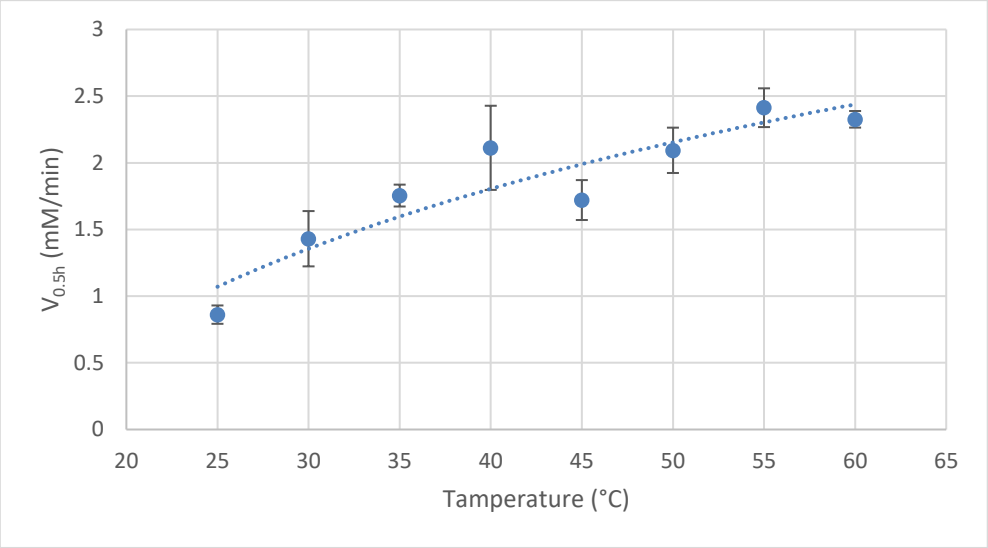

FIGURE 54: INITIAL RATES AFTER 0.5 HOURS AT TEMPERATURES FROM 25 TO 60°C

As observed in figure 54, the calculated $V_{0.5h}$ increased from 0.8 to 2.3 mM/min with the increase of the temperature from 25°C to 60°C. Therefore, no denaturation of the lipase occurs at a temperature as high as 60°C. This observation is consistent with the well-known thermostability of N 435.

The values of Y_{GPC} after 5 and 30 hours of reaction obtained with the various temperature tested, are compiled in the figure 55 below.

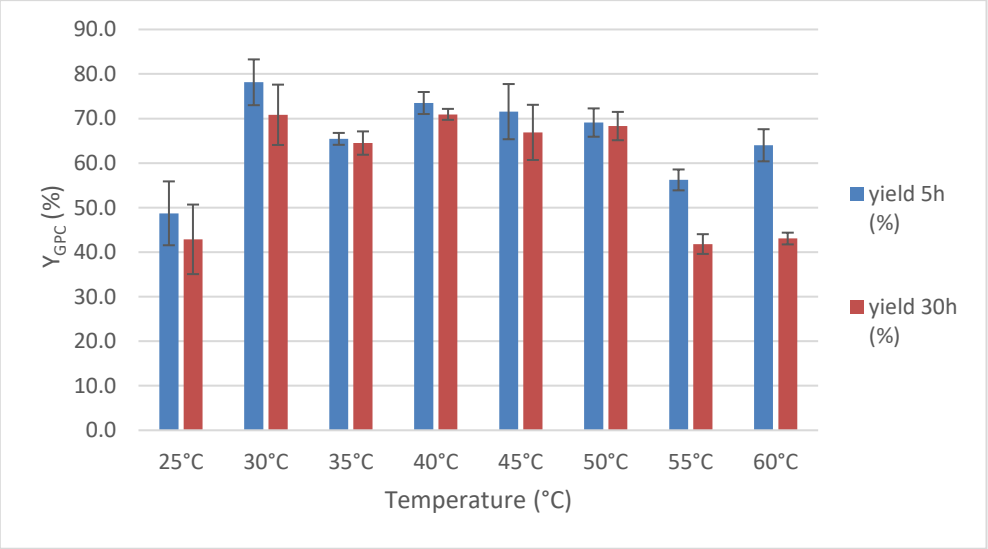

FIGURE 55: YIELD OF GPC CONVERSION OBTAINED AFTER 5 AND 30 HOURS OF REACTION AT TEMPERATURES FROM 25°C TO 60°C

After 30 hours of reaction, the study of the Y_{GPC} (figure 55) highlights that at a temperature between 30 °C and 50 °C, the synthesis seems to reach a maximum, at around 70%. Regarding the Y_{GPC} after 5 hours in this range of temperature, they were not different from those after 30 hours (*p*-value > 0.05).

According to the literature, esterification reactions are most often carried out at temperatures varying between 40 and 70°C with different biocatalysts. Hong *et al.* (2011) and Liu *et al.* (2017) are the only ones who tested a temperature as low as 20°C for the synthesis of LPC-CLA and LPC-PUFAs, respectively. In both cases, a low Y_{GPC} of 10% was obtained. Other studies such as Liu *et al.* (2017) and Wang *et al.* (2020a) tested high temperatures ranging from 50°C to 70°C. In their case temperatures over 55°C resulted in lower $Y_{GPC.}$

Hong *et al.* (2011) tested the effect of temperature on the synthesis of LPC-CLA with N 435. No decrease in Y_{GPC} was observed at high temperature of 60°C. A Y_{GPC} of 40% was obtained after 12 hours of reaction at temperatures ranging from 40 to 60°C. It can be suggested that the decrease is not observed in their study because it is carried out on a time of 12 hours which is shorter than 30h ours.

For the implementation of the design of experiment, the range over which the temperature will be studied will be varied from 25°C to 60°C.

2. Matrix of experiments

As already mentioned, we aimed to optimize the synthesis of LPC-DHA. Different informations can be obtained from the enzymatic kinetics. The initial speed at the beginning of the kinetic ($V_{0.5h}$) and the concentration of the product obtained at the end ([LPC-DHA]) as well as the conversion yield of the initial substrates (Y_{GPC} and Y_{DHA}). In this work we were interested in optimizing the following responses: Y_{GPC} and the [LPC-DHA].

From the preliminary experiments described above, three factors were selected to perform the optimization of these two responses by RSM. These factors are: the biocatalyst quantity (BQ), the molar ratio (MR) and the temperature (T).

In this work, a Box Behnken design (BBD) was performed, using Modde® software. It allows to study three factors by performing twelve experiments to which three central points are added. Thus, the BBD does not include experiments in which all the factors have an extreme value, for example, the combination of low values for all three factors studied (Box and Behnken 1960).

The BBD is widely used in several scientific fields. It has been used in several fields of chemistry (analytical chemistry, spectrophotometry, chromatography, *etc.*) in order to optimize several chemical and physical processes (Ferreira *et al.* 2007).

BBD is applied in studies having 2 to 4 factors and requires 3 levels of each factor (-1, 0, 1). The number of experiments required to realize a BBD is defined as:

$$N = 2\,K\,(K\text{-}1) + C_0$$

With,

N: number of experiments.

K: number of factors.

C_0: number of central points.

The processing combinations in this design are in the middle of the edges of the processing space and in the center (figure 56).

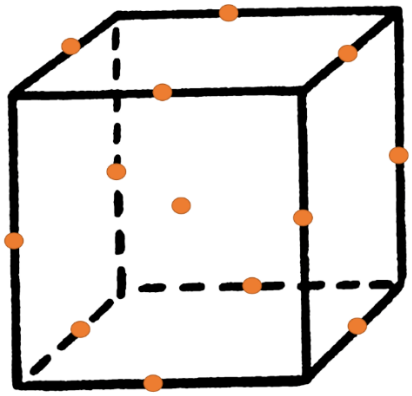

FIGURE 56: GEOMETRIC LOCUS OF EXPERIMENTAL POINTS IN A THREE-FACTOR BOX-BEHNKEN DESIGN

The BBD has the advantage to be less expensive in terms of time (reduced number of experiments) and resources to invest in experimentation. As already mentioned, BBD does not include experiments for which all factors are simultaneously placed at their high or low level. The BBD matrix therefore minimizes the combinations located in the extremities of the factor variation domain where an unsatisfactory response is generally observed (high or low response). This may be advantageous when the points on the edges of the cube represent combinations of factor levels that are expensive or impossible to test due to the technical restrictions of the process (Box and Behnken 1960, Ferreira *et al.* 2007).

Thus, three levels are assigned to each factor: higher level (+1), low level (-1) and central point level (0) as illustrated in table 16. The high and low levels were determined from the previous experiments and the central level is the middle level between the high and the low levels.

TABLE 16: STUDIED FACTORS AND THEIR ASSIGNED LEVELS

Factors	Low level (-1)	Central point (0)	High level (+1)
Biocatalyst amount (%)	5	10	15
Molar ratio (DHA/GPC)	4	11	18
Temperature (°C)	26	43	60

The BB experimental matrix for three factors contains 15 experiments, including 3 repetitions of the center point of the experimentation area (table 17). These experiments have been performed in a random order to avoid bias results.

For each experiment, kinetics over 30 hours of reaction were performed. As expected, it was observed that in some cases (for instance, MR: 4, T: 26°C and BQ: 10%; figure 57) the equilibrium was not reached after 5 hours of reaction, as it was the case in all the previous experiments. In the case of figure 57, the equilibrium is not reached even after 30 hours of reaction. Therefore, the values of the two responses ([LPC-DHA] and Y_{GPC}) were those obtained at a reaction time of 30 hours.

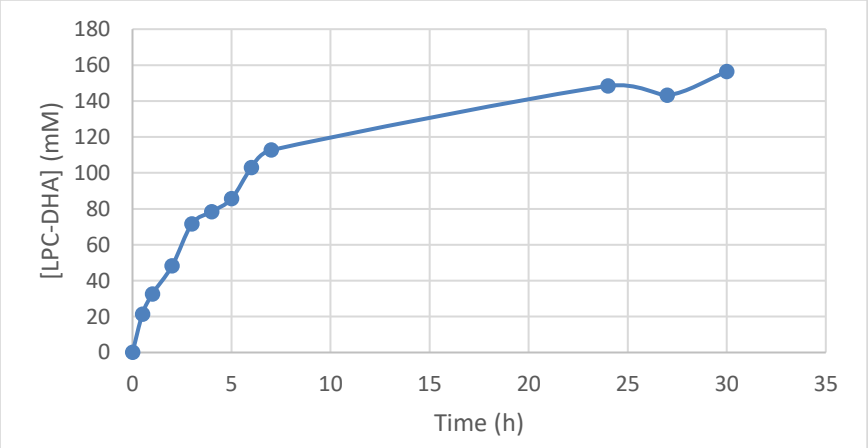

FIGURE 57: ESTERIFICATION KINETICS BETWEEN GPC AND DHA AT 26°C, MOLAR RATIO OF 4 AND 10% BIOCATALYST

Esterification reactions were catalyzed by Novozym 435 and carried under the following reaction conditions: biocatalyst quantity (10%), molar ratio (4), temperature (26°C) and under atmospheric pressure.

Table 17 summarizes the combination of the three factors as well as the experimental results for all experiments.

TABLE 17: EXPERIMENTAL MATRIX AND VALUES OF THE RESPONSES

Exp. No	Run order	Molar Ratio (DHA/GPC)	Biocatalyst quantity (%)	Temperature (°C)	[LPC-DHA] (mM)	Y_{GPC} (%)
1	1	4	5	43	98.5	14
2	2	18	5	43	83.2	52
3	3	4	15	43	239.8	33
4	7	18	15	43	122.8	77
5	8	4	10	26	156.3	22
6	11	18	10	26	101.8	64
7	12	4	10	60	121.6	17
8	14	18	10	60	84	53
9	9	11	5	26	87.3	33
10	10	11	15	26	198.6	76
11	15	11	5	60	67.8	26
12	4	11	15	60	133.6	51
13	13	11	10	43	136.3	52
14	5	11	10	43	146.5	56
15	6	11	10	43	154.4	59

The experiments n° 13, 14 and 15 (MR: 11, T: 43, BQ: 10%) correspond to the center of the experimental area and were realized in triplicate to measure the pure error. The figure 58 represents the average of these 3 independent experiments, performed on different days. Thus, obviously the good reproducibility of the experiments could be seen, in which low standard deviations were obtained.

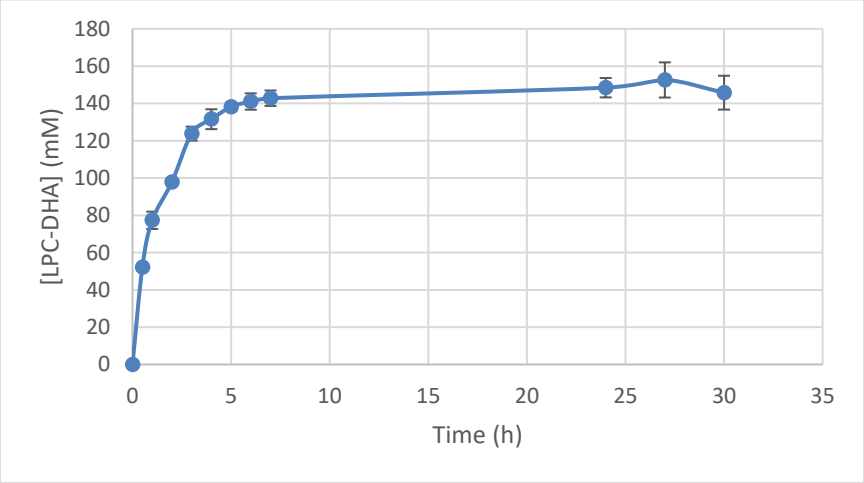

FIGURE 58: ESTERIFICATION KINETICS FOR THE CENTRAL POINTS

Esterification reactions were catalyzed by Novozym 435 and carried under the following reaction conditions: biocatalyst quantity (10%), molar ratio (11), temperature (43°C) and under atmospheric pressure. Data points are shown as mean ± SD of triplicate.

3. Design analysis for the concentration of LPC-DHA

Once the experiments of the matrix have been performed, a statistical treatment of the results has been realized in order to obtain, optimize and validate the mathematical model.

The calculation of the coefficients was provided by the Modde® version 10 software (table 18). This software allows statistical processing, and includes a large number of features. It supports analysis of variance calculations and gives many types of graphics.

To construct the statistically significant mathematical model, the factors that have a significant effect on the response are first selected. The factors exhibiting a significant effect are those with a significant coefficient.

Modde® software allows to find the significant regression coefficients (RC) in two different graphic representation ways. The first one is a list of the coefficients with associated *p*-values (table 18). The *p*-value is used as a statistical indicator to evaluate the most significant model terms. A *p*-value lower than 0.05 indicates that the corresponding term is statistically significant.

TABLE 18: ESTIMATED COEFFICIENTS FOR THE AMOUNT OF LPC-DHA

	[LPC-DHA] (mM)		
Factor	**Coefficient**	**Standard Error**	***p*-value***
Constant	145.8	5.7	1.8e-006
Molar Ratio	-28.04	3.5	0.0005
Biocatalyst quantity	44.8	3.5	5.40e-05
Temperature	-17.1	3.5	0.005
MR*MR	-7.8	5.2	**0.19**
BQ*BQ	-1.9	5.2	**0.73**
T*T	-22.04	5.2	0.008
MR*BQ	-25.4	5	0.004
MR*T	4.2	5	**0.44**
BQ*T	-11.4	5	**0.07**

***p*-values > 0.05 are shown in bold type**

The results can also be presented in the form of a diagram (the coefficient diagram) as shown in figure 59.

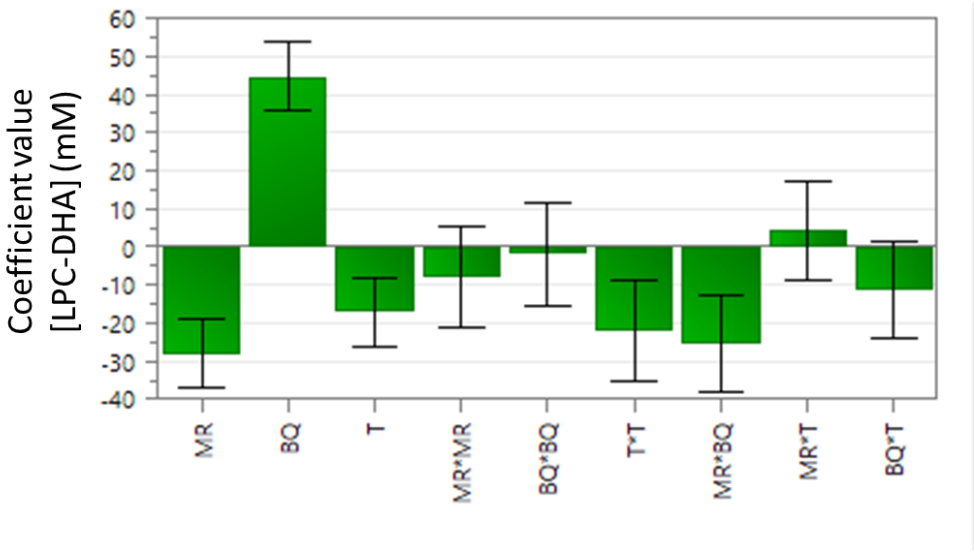

FIGURE 59: COEFFICIENT DIAGRAM FOR THE CONCENTRATION OF SYNTHESIZED LPC-DHA

The coefficient diagram represents the value of each coefficient of the model as well as error bars corresponding to 95% confidence intervals.

The value of a coefficient can be either positive, indicating that the factor positively influences the response, or negative when the factor negatively influences the response. Moreover, the higher the absolute value of a coefficient, the more the corresponding factor influences the response.

In addition, when the error bar on the coefficient diagram includes the value 0, this means that the effect of the factor is not significant. Thus, according to table 18 and figure 59, there is no significant effect of the MR*T and BQ*T interactions and of the MR*MR and BQ*BQ quadratic terms of the model, as they exhibit *p*-values > 0.05 (table 18) and their coefficients were close to 0 (figure 59).

Thus, these four terms of the model (quadratic coefficients MR*MR, BQ*BQ and the interaction coefficients MR*T and BQ*T) have been removed and a new model with a new coefficient diagram is obtained (table 19 and figure 60).

TABLE 19: ESTIMATED COEFFICIENTS FOR THE AMOUNT OF LPC-DHA AFTER ELIMINATION OF THE NON-SIGNIFICANT COEFFICIENTS

	[LPC-DHA] (mM)		
Factor	**Coefficient**	**Standard Error**	***p*-value***
Constant	140.2	5.7	1.8e-006
Molar Ratio	-28	3.5	0.0005
Biocatalyst quantity	44.8	3.5	5.40e-05
Temperature	-17.1	3.5	0.005
T*T	-21.4	5.2	0.008
MR*BQ	-25.4	5	0.004

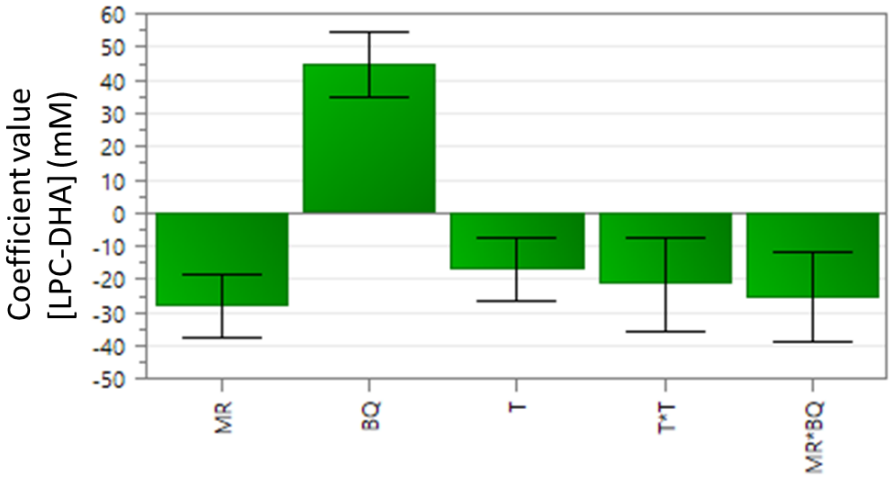

FIGURE 60: COEFFICIENT DIAGRAM FOR THE CONCENTRATION OF LPC-DHA AFTER ELIMINATION OF THE NON-SIGNIFICANT COEFFICIENTS

Therefore, the optimal polynomial regression equation for the obtained model is as follows:

$$[\text{LPC-DHA}] = 140.2 - 28\ MR + 44.8\ BQ - 17.1\ T - 21.4\ T*T - 25.4\ MR*BQ$$

Analyzing this model, it was shown that [LPC-DHA] was positively related to the BQ while the corresponding quadratic term (BQ*BQ) was found to be non-significant (table 19 and figure 60). This means that a linear increase of [LPC-DHA] occurs with an increase of BQ. Moreover, [LPC-DHA] was negatively related to the factor MR and its quadratic term (MR*MR) was not found significant (table 19) resulting in a linear decrease in [LPC-DHA] with MR. These findings were those expected from the preliminary experiments carried out for the selection of the factors.

Concerning the factor T (temperature), both its linear and quadratic effects were significant giving an overall curvilinear effect on [LPC-DHA]. This is in accordance with our previous findings in which [LPC-DHA] increased with the increase of T from 25°C to 45°C and decreased at higher T resulting in a curvilinear relation between T and [LPC-DHA].

Interestingly, it can be seen that an interaction effect occurs between MR and BQ on [LPC-DHA]. This interaction was antagonistic, which means that the effects of these two factors are opposite. In other words, an increase in BQ increases the [LPC-DHA] while an increase in MR decreases the [LPC-DHA]. The validity of the model was investigated by an ANOVA approach, which results are summarized in table 20.

TABLE 20: ANOVA FOR THE LPC-DHA CONCENTRATION RESPONSE

Source	**FD**	**SS**	**MS**	**F**	***p***
Regression model	5	28958	5792	40	< 0.001
Residual variation	9	1319	147		
Lack of fit	7	1155	165	2	0.373
Pure error	2	165	82		
Total	15	279258	18617		
$Q^2 = 0.869$ $R^2 = 0.956$ $R^2_{adjusted} = 0.932$					
FD: degree of freedom ***SS: Sum of Squares*** ***MS: variance (Mean Square)*** ***F: Fisher test*** ***p: probability of lack of fit***					

The goodness of fit can be seen in the high value of the coefficient of determination $R^2 = 0.956$, and a very small *p*-value < 0.001. This indicates the model adequacy to explain 95% of variability in the [LPC-DHA]. This is supported by the closely agreeing value of adjusted coefficient of determination $R^2_{adjusted} = 0.932$ to that of the R^2. Moreover, the ANOVA of variables revealed that the F-value for the lack of fit is 2 which was indicative of a well-fitted model. Indeed, the probability of a lack of fit is non-significant ($p = 0.373 > 0.05$) (table 19). Therefore, it is concluded that the model is statistically validated.

4. Design analysis for the GPC conversion yield

To study the effect of the various factors on Y_{GPC}, the same analytical method was performed. The obtained coefficient diagram is shown in figure 61.

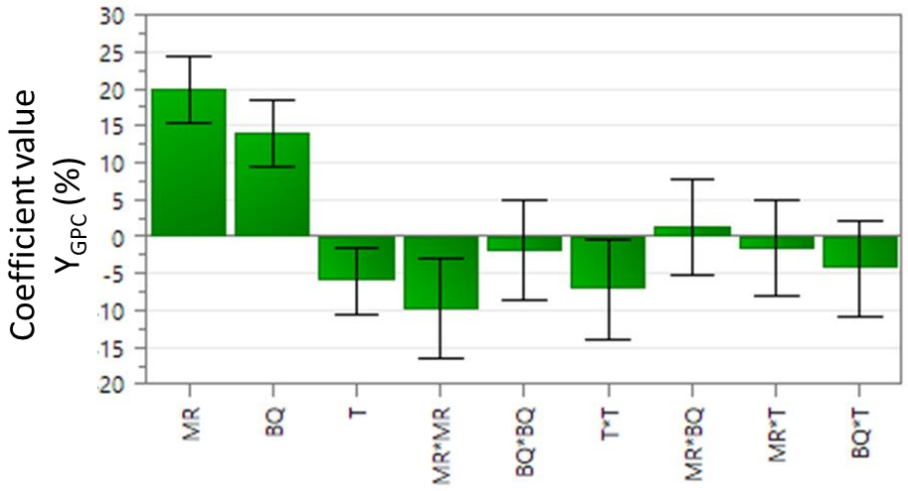

FIGURE 61: COEFFICIENT DIAGRAM FOR THE GPC CONVERSION YIELD

After eliminating the non-significant coefficients, the coefficient diagram presented in figure 62 was obtained, and the predicted model was as following:

$$Y_{GPC} = 54.4 + 19.9\ MR + 14\ BQ - 6\ T - 9.6\ MR*MR - 7\ T*T$$

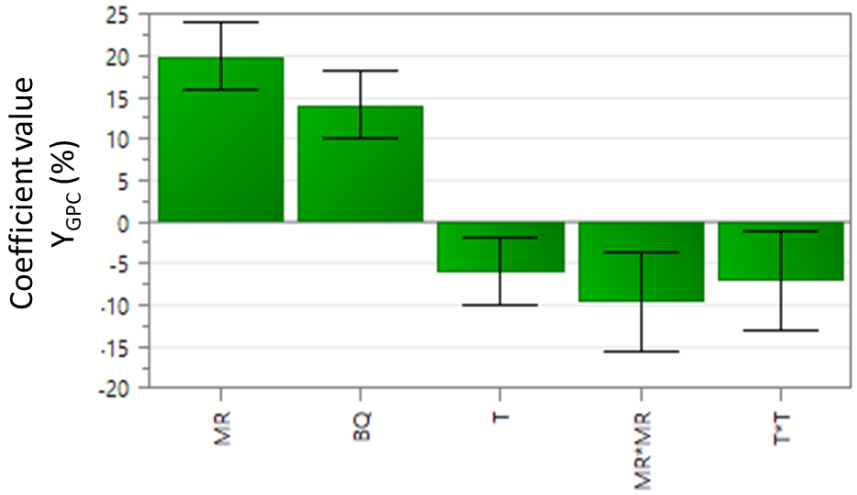

FIGURE 62: COEFFICIENT DIAGRAM FOR THE GPC CONVERSION YIELD AFTER ELIMINATION OF THE NON-SIGNIFICANT COEFFICIENTS

According to these results, the MR and the BQ were found to be the two most influencing factors on the Y_{GPC}.

Y_{GPC} was positively related to the BQ and the quadratic term was found to be non-significant (figures 61 and 62), which resulted in a linear increase in Y_{GPC} with BQ. Regarding the effect of the factor T, Y_{GPC}

depends on T in a curvilinear manner, as it was the case for [LPC-DHA], as both the linear and quadratic coefficients were significant.

Regarding the effect of MR, the positive linear and the negative quadratic effects shown in figure 62, indicated that the overall effect of MR was curvilinear. This indicates that as MR increases, so does the Y_{GPC}, but only up to a certain value of MR, after which, the Y_{GPC} decreases.

The validity of the model was investigated by an ANOVA approach, which results are summarized in table 21.

TABLE 21: ANOVA FOR GPC CONVERSION YIELD RESPONSE

Source	FD	SS	MS	F	*p*
Regression model	5	5534	1107	43	< 0.001
Residual variation	9	233	26		
Lack of fit	6	209	30	2	0.316
Pure error	2	24	12		
Total	15	36905	2460		
$Q^2 = 0.877$ $R^2 = 0.96$ $R^2_{adjusted} = 0.937$					
FD: degree of freedom ***SS: Sum of Squares*** ***MS: variance (Mean Square)*** ***F: Fisher test*** ***p: probability of lack of fit***					

The lack-of-fit test and the ANOVA test showed that the model obtained for Y_{CPG} is a good model with a very small *p*-value (< 0.001) and a suitable coefficient of determination value $R^2 = 0.960$, supported by the closely agreeing value of adjusted R^2 value (0.937). Moreover, the probability of a lack of fit is non-significant ($p = 0.316$, F-value = 2.49). Therefore, as for the [LPC-DHA], the model for the response Y_{GPC} is statistically validated.

5. Analysis of the response surfaces

Modde® software allows to obtain a representation in the form of response surfaces (figures 63 and 64). Each of the 3 contour plots shows the studied response, regarding the values of the 2 factors BQ and T, the MR was fixed at 4 (level -1), at 11 (level 0) or 18 (level +1).

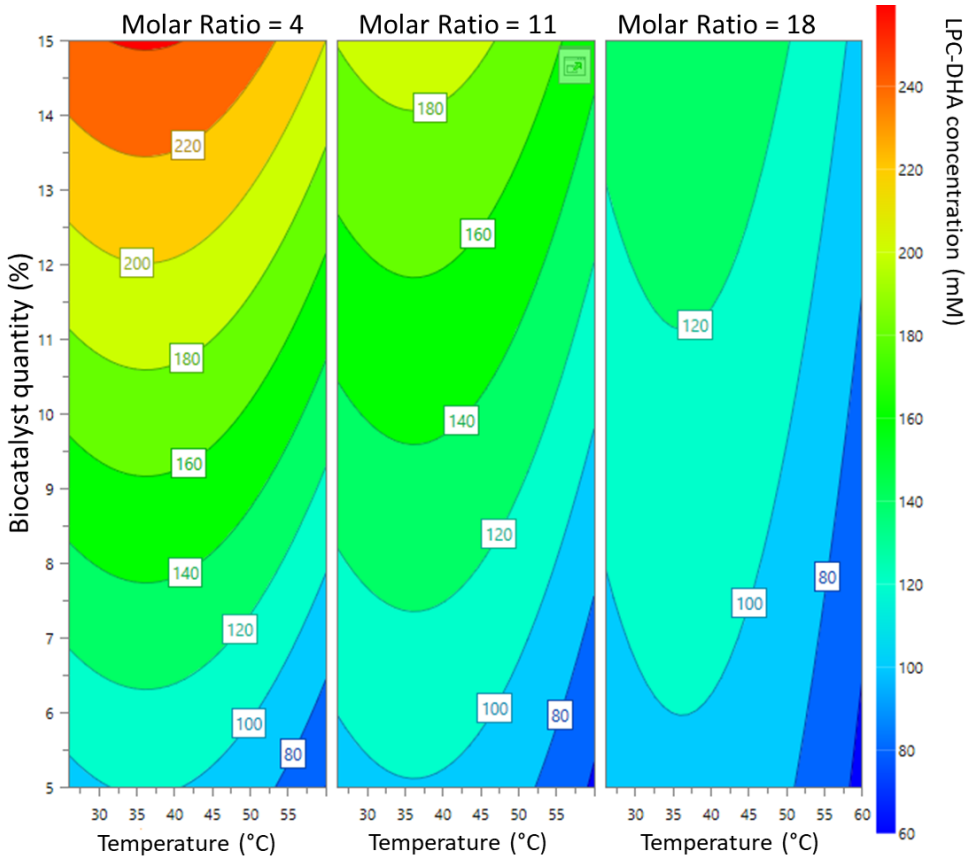

FIGURE 63: CONTOUR PLOT SHOWING THE INTERACTION BETWEEN TWO FACTORS, BIOCATALYST QUANTITY AND TEMPERATURE, AT DIFFERENT MOLAR RATIOS ON THE SYNTHESIS OF LPC-DHA

According to figure 63, we noticed that there is a direct relation between the [LPC-DHA] and the BQ while an inversely proportional relation exists between this concentration and the MR. In other words, an increase in the MR (low [GPC]i) decreases the amount of synthesized LPC-DHA while an increase in the BQ increases this amount.

To achieve maximum amount of synthesized LPC-DHA, T should be maintained in the range of 30°C-45˚C (red color) at a MR equal to 4 and with 15% of biocatalyst.

Similarly to the [LPC-DHA], a high BQ and a T in the range between 30°C and 45˚C gave a maximum Y_{GPC} (figure 64). However, this maximum value was reached for a high MR equal to 18 which confirms the inversely proportional relationship between [LPC-DHA] and Y_{GPC}.

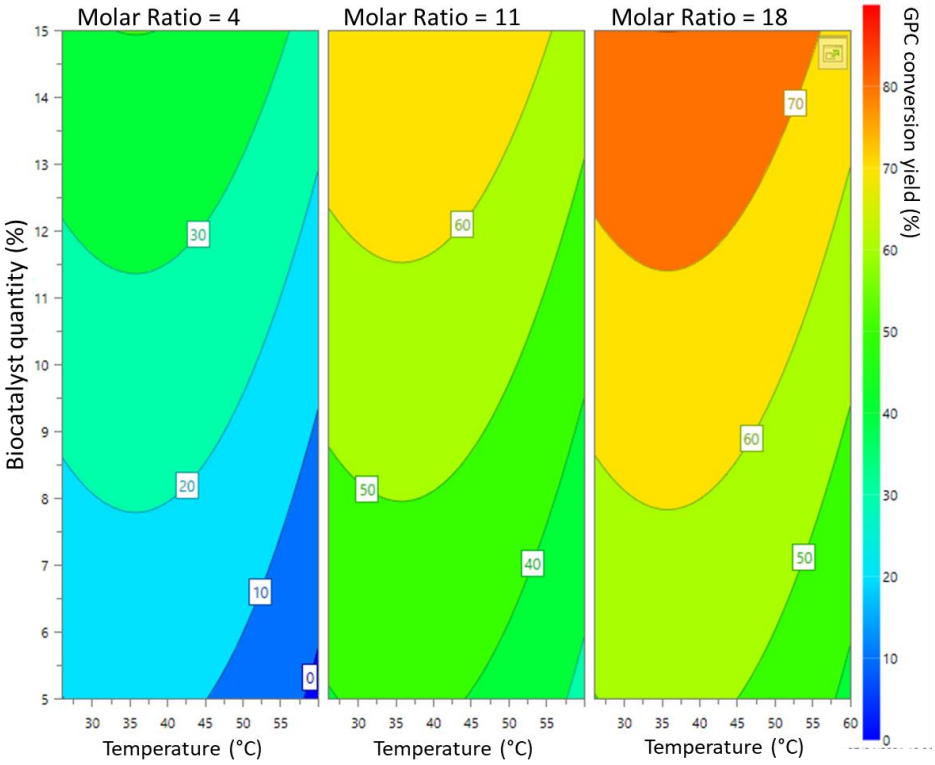

FIGURE 64: CONTOUR PLOT SHOWING THE INTERACTION BETWEEN TWO FACTORS, BIOCATALYST QUANTITY AND TEMPERATURE, AT DIFFERENT MOLAR RATIOS ON THE GPC CONVERSION YIELD

Overall, for the two responses, an increase in the BQ increased the response studied. A low T (30°C-45˚C) resulted in maximum [LPC-DHA] and Y_{GPC}. A low MR (MR =4) resulted in high [LPC-DHA], while a high MR (low [GPC]i) was required to maximize the Y_{GPC} response. These findings are in accordance with the results obtained in the preliminary experiments.

Regarding the relationship between the two factors MR and T, it could be expected that an increase in T might increase the Y_{GPC} in a low MR medium (MR = 4) by reducing the viscosity of the reaction mixture. However, as shown in the curves, it was not the case: a maximum Y_{GPC} was reached at a high MR and at a T between 30°C and 45˚C (figure 64).

6. Experimental validation of the models

One of the fundamental steps in experimental design is the experimental validation of the model. It consists in comparing the theoretical result of an experiment predicted by the model, with the actual result of the experiment. The model will be validated if the obtained response is very close to the predicted one.

In this work, the values of the factors that gave the maximal response are used to validate each model. For each response, the experiment was performed in triplicate.

Table 22 shows the value of each factor, determined by Modde® software, which combination maximizes the studied response.

TABLE 22: FACTORS VALUES THAT MAXIMIZE THE RESPONSES

Response	Molar ratio (DHA/GPC)	Biocatalyst quantity (%)	Temperature (°C)
Y_{GPC} (%)	17	15	36
[LPC-DHA] (mM)	4	15	36

Table 23, shows the predicted and measured values for each response. The table present the range of the predicted values by the model and the observed responses corresponding to the experimental obtained values. Each measured value is mentioned with its standard deviation value.

TABLE 23: PREDICTED AND MEASURED VALUES FOR EACH RESPONSE

		Predicted and observed values for each response			
		[LPC-DHA] (mM)		Y_{GPC} (%)	
		Predicted	Observed	Predicted	Observed
Model	Y_{GPC}	[113.4-156.6]	107 ± 9	[72.6-87.6]	66.9 ± 5.6
	[LPC-DHA]	[220.3-263.5]	245.5 ± 2.8	[32.6-47.7]	34.2 ± 0.4

This table allows us to evaluate more precisely the quality of the adjustment made. The comparison between the predicted and observed values confirmed that the model fit was valid. The obtained responses for [LPC-DHA] were very close to the predicted ones, in which the mean of the 3 experiments is within the confidence interval (table 23). For the Y_{GPC} the mean is lower than the minimum value of the range but considering the standard deviation, the obtained value became very close to the predicted one. The fit of the models was thus validated.

B. Purification of LPC-DHA and structural analysis by NMR

After optimization of the synthesis, we aimed to purify the synthesized LPC-DHA in order to characterize it and study its effect on breast cancer cells. The purification and the analysis of the spectra were carried out in the Institute of Molecules and Materials of Le Mans (IMMM- UMR CNRS 6283) by Pr. Arnaud Martel.

In the ^{1}H NMR spectrum signals from the glycerol, choline and docosahexaenoic acid were identified. Figure 65, shows the obtained ^{1}H NMR spectrum and the expected structure of the LPC-DHA obtained after synthesis and submitted to NMR analysis for checking.

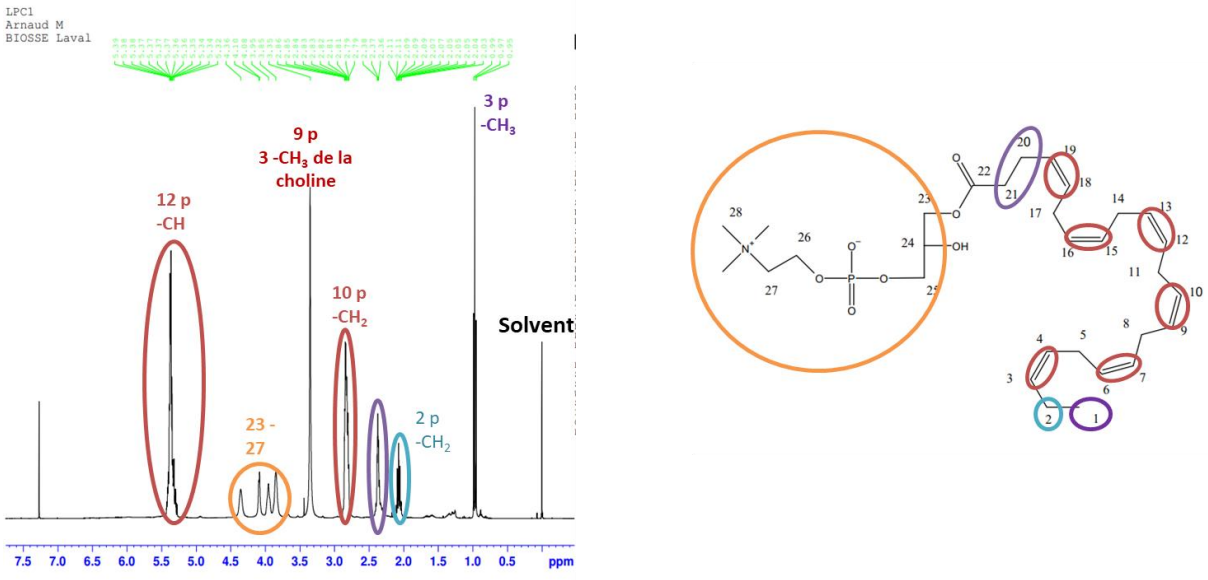

FIGURE 65: ^{1}H NMR SPECTRUM AND EXPECTED STRUCTURE OF LPC-DHA OBTAINED AFTER SYNTHESIS

The ^{1}H NMR analyses showed that all the characteristic shifts that was expected regarding the LPC-DHA structure, namely the number of protons are present.

Table 24, shows the spectrum signals displacements of each proton in the LPC-DHA structure of figure 65.

TABLE 24: SPECTRUM SIGNALS DISPLACEMENTS OF EACH PROTON IN THE LPC-DHA STRUCTURE

Signals (ppm)	Number of protons	Associated proton
0.97	3 H	H-1
2.07	2 H	H-2
2.31 - 2.42	4 H	H-21, H-20
2.77 - 2.89	10 H	H-5, H-8, H-11, H-14, H-17
3.29 – 3.43	9 H	H-28
3.8 – 3.89	3 H	H-27, H-25
3.91 - 4	2 H	H-24, H-25
4.06 – 4.12	2 H	H-23
4.31 – 4.41	2 H	H-26
5.27 – 5.44	12 H	H-3, H-4, H-6, H-7, H-9, H-10, H-12, H-13, H-15, H-16, H-18, H-19
7.3 ppm	1 H	OH

All the signals shown in table 24 were associated to a function in the LPC-DHA structure as seen in figure 65. Among them, the 12 -CH protons of the six double bonds of DHA were detected (table 24).

These results show that DHA has not been oxidized during the reaction or during the purification on silica. Also, the ^{1}H NMR spectrum did not show any parasitic signals which shows that the analyses were performed on a pure product (figure 65).

The proton of the OH group (hydroxyl group) can lead to a particularly wide range of chemical displacement. The cause of this range is essentially due to its greater or lesser mobility, which depends on the structure of the rest of the molecule, the solvent and the concentration. In this case the detected signal at 7.3 ppm is attributed to the proton of the hydroxyl (–OH) group.

In order to characterize the synthesized isomer, a ^{13}C NMR spectra with an Heteronuclear Single Quantum Coherence (HSQC) (figure 66) followed by an Heteronuclear Multiple Bond Correlation (HMBC) (figure 67) were realized to identify the DHA position on the glycerol.

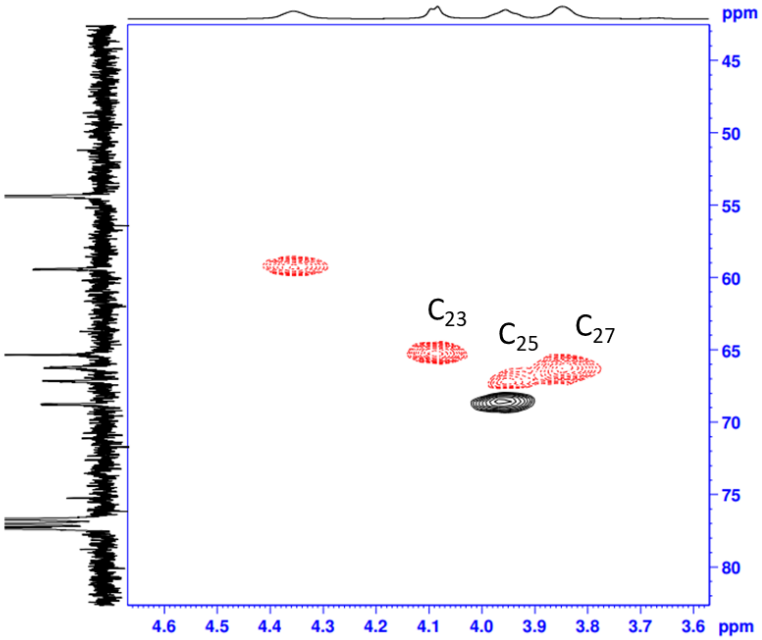

FIGURE 66: HSQC SPECTRUM

The HSQC spectrum allowed to associate the $–CH_2$ protons to their carbons (figure 66). And then the HMBC showed that the $–CH_2$ of C_{23} is associated to the C_{22} as it can be seen in figure 67.

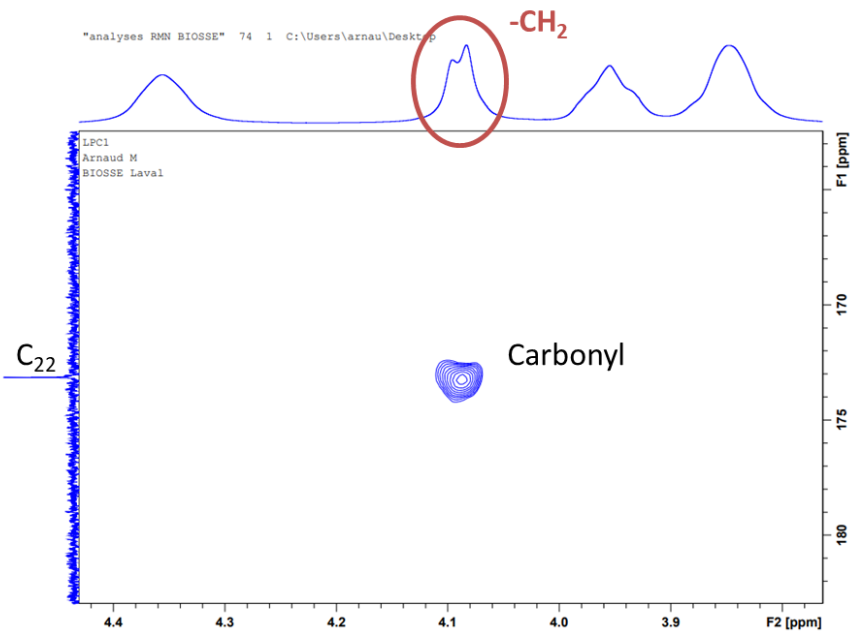

FIGURE 67: HMBC SPECTRUM

These results allowed to confirm that as expected the DHA was esterified on the *sn*-1 position of the GPC during the esterification reaction, as the N 435 is 1,3 regioselective. This result indicates that no migration occurred which justify the absence of the synthesis of PC-DHA.

Summing up the first part, it can be reported that pure, un-oxidized *sn*-1 LPC-DHA synthesis was demonstrated using Novozym® 435, in 5 hours which is a shorter time than that announced in the literature of 24 hours.

Figure 68 shows the Y_{GPC} and [LPC-DHA] obtained for each optimized model in this work and the highest responses obtained in the literature. Under each response the reaction conditions that allowed to obtain these results are also mentioned.

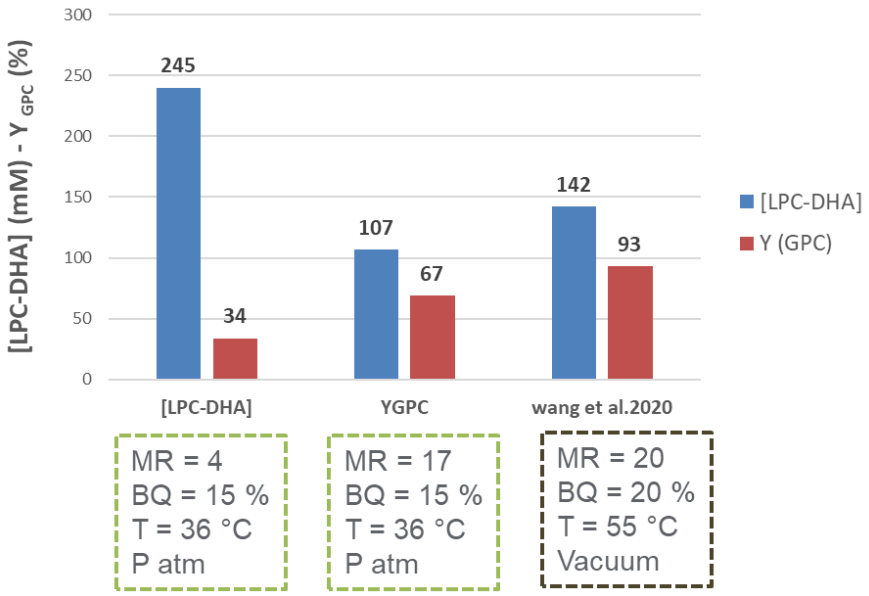

FIGURE 68: Y_{GPC} AND [LPC-DHA] OBTAINED WITH THE TWO OPTIMIZED MODELS AND THE ONES OF WANG *et al.* 2020

This figure allows us to visualize the following points:

1- An [LPC-DHA] of 245 mM is obtained. This indicates that the production of LPC-DHA is increased almost 2-fold compared to the literature, where the highest concentration obtained in the literature is around 140 mM of LPC rich in PUFAs (Wang *et al*. 2020).

2- The production is doubled, with more favorable conditions compared to the literature, lower MR, lower temperature, lower BQ and under atmospheric pressure.

3- The Y_{GPC} was not higher than the one obtained in the literature but nevertheless a good yield of 67% is obtained with more favorable conditions compared to the literature. In which lower temperature, lower BQ and an atmospheric pressure were needed.

II. Effect of LPC-DHA on MDA-MB-231 human breast cancer cells

A. Specificity of the effect of LPC-DHA on cell viability decrease

LPC-DHA is known for increasing the bioavailability of DHA and for exhibiting many biological interests (chapter 1: section II-C). In addition, DHA was found to inhibit the MDA-MB-231 breast cancer cell viability and this cell line is known for being aggressive and resistant to hormone therapy. Thus, we aimed to see if LPC-DHA would inhibit cell viability too.

DHA and GPC, which constitute LPC-DHA, are also tested on their own, in order to determine if the effect comes from either of these molecules or from the LPC-DHA form specifically.

Figure 69 shows the cellular viability of MDA-MB-231 cells when treated with different concentrations of LPC-DHA, GPC and DHA.

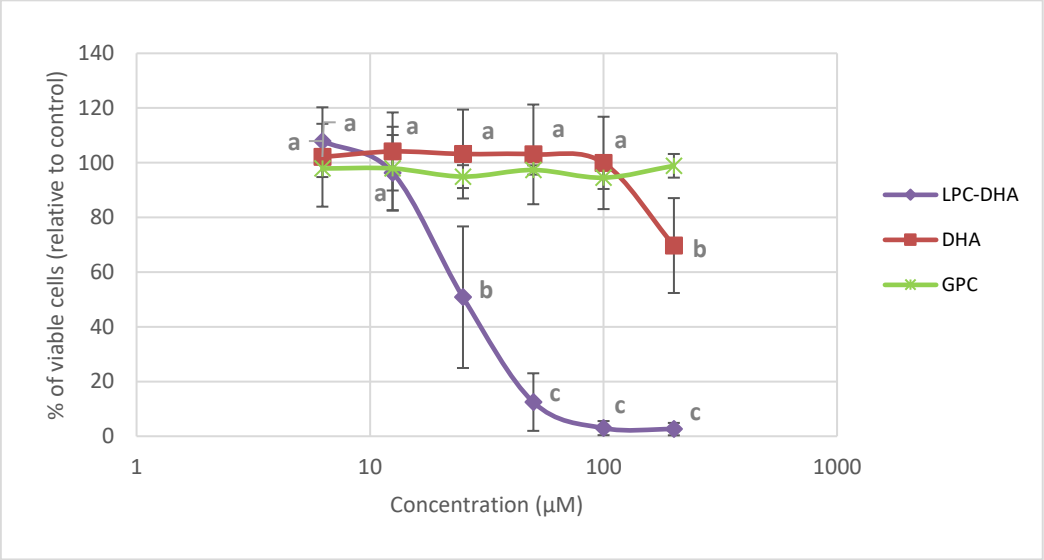

FIGURE 69: DOSE-EFFECT RELATIONSHIP OF LPC-DHA, DHA AND GPC ON MDA-MB-231 CELL VIABILITY

Cells were treated with different concentrations (6.25-200 µM) of LPC-DHA, DHA and GPC for 24 hours. The viability is tested by the neutral red test. Data points are shown as mean ± SD of 3 independent experiments each done in triplicate. Statistical significance was determined using ANOVA with post hoc Fisher's test. Means associated with letters indicate significative difference at $p < 0.05$, with a > b > c.

According to figure 69, no effect on viability was observed in MDA-MB-231 cells treated with LPC-DHA concentration of 6.25 µM. The cell viability decrease tends to start from 12.5 µM. Significant cell viability reduction was observed in MDA-MB-231 cells treated with LPC-DHA at concentrations higher than 25 µM ($p < 0.001$). An IC_{50} value of 25 µM was calculated for LPC-DHA. IC_{50} is a quantitative measure that indicates the concentration of a inhibitory substance (e.g. drug) that inhibit by 50%, *in vitro*, a given biological process or biological component.

LPC-DHA is constituted from a phosphatidic part (GPC) and a FA (DHA). Thus, one of our goals was to study if one of these two parts was responsible on exhibiting the observed effect or it is the entire molecule that exhibits this effect. So, the effect of DHA and GPC on cell viability was also studied.

No decrease in cell viability was observed in cells treated with DHA for concentrations between 6.25 µM and 100 µM. A significant decrease in the viability of MDA-MB-231 cells was observed at the highest concentration of DHA tested, 200 µM, with an estimated IC_{50} of 347 µM. No effect on cell viability was observed in cells treated with GPC, the percentage of cells remained constant, close to 100% (figure 69).

According to the observed results, both LPC-DHA and DHA were shown to exhibit an inhibitory effect on cell viability, noting that the effect of LPC-DHA is higher than that observed with DHA. Based on these results, two hypotheses can be proposed: either LPC-DHA enhances the DHA effect by increasing its incorporation, or LPC-DHA reduces cell viability independently of DHA.

To our knowledge, no information is available in the literature concerning LPC-DHA on cancer cells. The only study carried out on the effect of LPC-DHA on cancer focused, on angiogenesis and showed that 100 µM of LPC-DHA exhibited an effective suppression of angiogenesis on rat main artery and human umbilical cord vein endothelial cell (Tsushima *et al.* 2012).

Considerable data on the effect of free DHA on MDA-MB-231 cells are available. Our results agree with the literature but with a different concentration. Indeed, in previous studies, a concentration of 100 µM of DHA has been reported to have a significant effect (Chénais *et al*. 2020; Javadian *et al.* 2020) while in our work, an effect was observed at a higher concentration of 200 µM. On the other hand, Rizzo *et al.* (2021) reported a decrease in MDA-MB-231 viability from a concentration of 200 µM of DHA, which is consistent with our results. The difference in concentrations at which the effect is observed could be explained by different experimental methodologies in each study.

In order to verify whether the observed effect is specific for LPC-DHA or for the LPC structure, various LPC molecules with various chain lengths (LPC-C8:0, LPC-C14:0, LPC-C18:0 and LPC-C22:0) and various degrees of unsaturation (LPC-C18:0, LPC-C18:1, LPC-C18:2, LPC-C22:0 and LPC-C22:6) were selected.

Figure 70 shows the viability of cells treated with different LPC species.

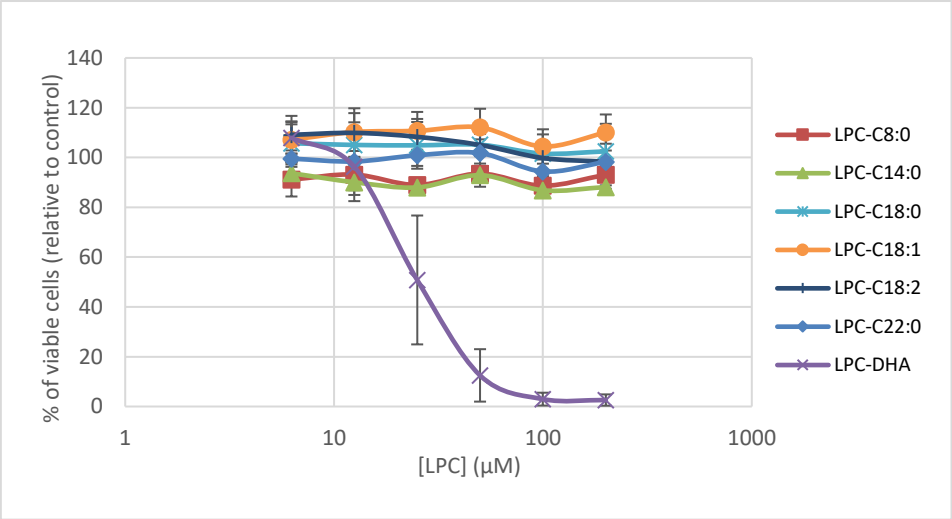

FIGURE 70: DOSE-EFFECT RELATIONSHIP OF VARIOUS LPCS SPECIES ON MDA-MB-231 CELL VIABILITY

Cells were treated with different concentrations (6.25-200 µM) of various LPC species for 24 hours. The viability is tested by the neutral red test. Data points are shown as mean ± SD of 3 independent experiments each done in triplicate. Statistical significance was determined using ANOVA with post hoc Fisher's test.

In figure 70 the results obtained previously with LPC-DHA are also presented in order to be compared with the other LPC species. For LPC species, interestingly no effect was observed, the percentage of cells remained constant, close to 100% (figure 70). These results indicate that the observed effect is specific to the LPC structure carrying a DHA.

To our knowledge, no studies have investigated the effect of various LPCs on breast cancer cells but some studies have shown the effect of LPCs on other types of cancer cells. Kim *et al.* (2007) demonstrated that the cytotoxic effect on leukemia cancer (Jurkat T) cells was specific for LPC among several LPLs (LPA, LPS, LPE and LPG) tested. They also showed that 20 µM of LPC-C16:0 inhibited 90% of cell viability, among 11 various LPCs containing saturated and unsaturated FA with various chain length (C6 to C24). Contrary to our study, they found that 20 µM of LPC-C18:0 and LPC-C18:1, were moderately cytotoxic, reducing cell viability by 60% and 30%, respectively. Moreover, 450 µM of LPC-C18:0 reduced the metastatic spread in murine melanoma B16.F10 cells after 72 hours (Ross *et al.* 2016). The fact that no inhibitory effect was observed with LPC-C18:0 and LPC-C18:1 on MDA-MB-231 could be justified by the different sensitivity of different cell types to a given molecule. It could be hypothesized that leukemia and melanoma cell lines are more sensitive to LPC-C18:0 and LPC-C18:1 than the breast cancer cells. Moreover, the effect reported by Ross *et al.* (2016) was observed at high concentrations of LPC-C18:0 that we did not test.

These results showed that LPC has an important role on cancer cells reduction and that this effect differs depending on the type of cancer cells and the FA attached to the LPC. In our case LPC containing

DHA was specific in reducing viability of MDA-MB-231 cell and the other tested LPCs were not, also LPC-DHA was more effective than DHA in inhibiting viability of MDA-MB-231 breast cancer cells.

B. Specificity of the effect of LPC-DHA compared to other lipids containing DHA

Other lipids containing DHA were reported to reduce cell viability of different cancer types in literature, as mentioned in chapter 1 (section III-B). Thus, in order to see the influence of different DHA transporters on MDA-MB-231 cell viability, the effect of different lipids containing DHA was investigated.

Recent studies have shown that MAG-DHA reduced cell viability of colon cancer cells (HCT116 and HT-29) (Morin *et al.* 2013; González-Fernández *et al.* 2019), lung cancer cells (A549) (Morin *et al.* 2012) and breast cancer cells (SKBR3 and E0771) (Zhang *et al.* 2020b). PC-DHA was also reported to reduce cell viability of lung cancer cells (LLC) (Liu *et al.* 2021), colon cancer cells (HT-29, Caco-2, DLD-1 and CCD-18Co) (Hossain *et al.* 2006 and 2008).

Moreover, González-Fernández *et al.* (2019) showed that MAG-DHA was more effective in reducing cell viability of colon cancer cells than DHA. Same findings were found for PC-DHA in which PC-DHA was more effective in reducing cell viability of colon cancer cells than DHA (Hossain *et al.* 2008).

In this context, we aimed to compare the observed inhibitory effect of LPC-DHA with monodocosahexaenoin (MAG-DHA). Also, it was aimed to understand whether the number of DHA chain of the lipid has an influence on the effect. Therefore, phosphatidylcholine carrying two chains of DHA (PC-DHA), di-, and tri-docosahexaenoin (DAG-DHA and TAG-DHA) were also tested.

Figure 71 shows the viability of cells treated with these lipids containing various DHA chains.

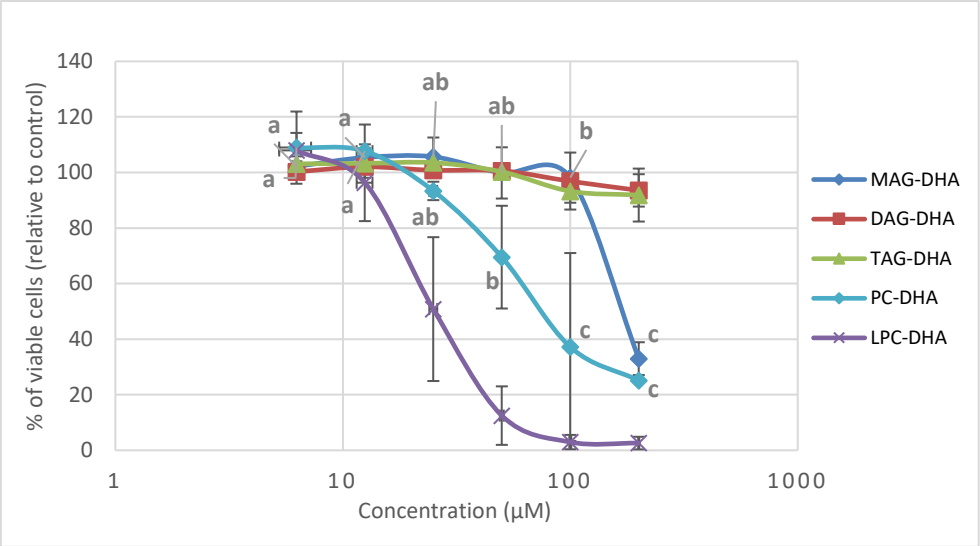

FIGURE 71: DOSE-EFFECT RELATIONSHIP OF VARIOUS LIPID SPECIES CONTAINING VARIOUS DHA MOLECULES ON MDA-MB-231 CELL VIABILITY

Cells were treated with different concentrations (6.25-200 µM) of lipid species containing DHA for 24 hours. The viability is tested by the neutral red test. Data points are shown as mean ± SD of 3 independent experiments each done in triplicate. Statistical significance was determined using ANOVA with post hoc Fisher's test. Means associated with letters indicate significative difference at $p < 0.05$, with a > b > c.

According to figure 71, the cell viability significantly decreased by 70% from a concentration of 200 µM of MAG-DHA ($p = 0.001$), while remaining close to the control at lower concentrations (6.25-100 µM). An estimated IC_{50} value of 170 µM was calculated for MAG-DHA. However, no effect was observed with either DAG-DHA or TAG-DHA, the percentage of viable cells remained constant, close to 100% at all tested concentrations.

In addition, no effect on cell viability was observed in MDA-MB-231 cells treated with PC-DHA concentration of 6.25 µM and 12.5 µM. The cell viability decrease tends to start from 25 µM. Significant cell viability reduction was observed in MDA-MB-231 cells at concentrations greater than 50 µM PC-DHA ($p = 0.001$) (figure 71). An IC_{50} value of 50 µM was calculated for PC-DHA.

According to these results, LPC-DHA, PC-DHA and MAG-DHA shown to have an effect on cell viability with LPC-DHA being the most potent. We also notice that increasing the number of chains of DHA attached to the lipid carrier does not improve the observed effect but even reduces it. As already mentioned, it cannot be concluded whether the observed effect with LPC-DHA, PC-DHA and MAG-DHA were due to the enhancement of the incorporation of DHA or it is a specific effect exhibited by these molecules. If the observed effects are related to the absorption hypothesis, it can be suggested that LPC-DHA was more potent than PC-DHA in inhibiting cell viability due to the fact that LPC-DHA is more

potent in enriching the cell with DHA than PC-DHA, as Sugasini *et al.* (2017) reported that LPC-DHA was more potent in enriching brain and eye in DHA compared to PC-DHA.

To our knowledge, until now, no study has been conducted on the effect of DAG-DHA and TAG-DHA on cancer cells. PC-DHA and MAG-DHA have been reported to show an effect on cancer cells as presented in the literature review of this manuscript (chapter 1: section III-B-4), and these effects have been observed in our work as well.

Concerning MAG-DHA, there is no study that has been conducted on MDA-MB-231 cells but studies were conducted on other types of breast cancer cells. Comparing our results with these previous studies, it can be observed that the effect reported by Zhang *et al.* (2020b) on other breast cancer lines (SKBR3 and E0771) was more effective than our reported effect on MDA-MB-231 cells. They obtained lower IC_{50} of 20 µM and 16 µM, respectively, while our estimated IC_{50} was of 300 µM. The effect of MAG-DHA has also been studied on colon cancer cells (HCT116 and HT-29) by Morin *et al.* (2013) and González-Fernández *et al.* (2019). IC_{50} of 2 µM and 135 µM were reported in these studies. Thus, it can be noticed that the effect of MAG-DHA is higher on colon cancer cell lines than on MDA-MB-231 cell line.

In contrast to MAG-DHA, the effect observed for PC-DHA on MDA-MB-231 cells, with an IC_{50} of 90 µM, is higher than that reported in the literature on lung (LLC) and colon cancer (HT-29 and Caco-2). Indeed, on these cancer cells, the inhibition of cell viability has been observed at higher concentrations of 300 µM (Liu *et al.* 2021) and 100 µM (Hossain *et al.* 2008), respectively.

Plant-derived natural molecules have been reported to have a significant role in inhibiting MDA-MB-231 cell viability. Catechol is a naturally occurring compound present in plants such as onions, apples and in olive oil. It has been shown to decrease MDA-MB-231 cell viability with an IC_{50} of 74 µM after 48 hours of contact (Vazhappilly *et al.* 2021). Moreover, dillapiole which is an organic compound present in fennel flowers and dill weed decreased MDA-MB-231 viability with an IC_{50} of 25 µM after 24 hours of contact (Ferreira *et al.* 2014). Thus, LPC-DHA shows good and equivalent effects to other molecules of natural origin as it reduced cell viability with an IC_{50} of 20 µM after 24 hours.

As an intermediate conclusion, it can be reported that:

1- GPC, LPC species with different chain length and degree of unsaturation, DAG-DHA and TAG-DHA do not exhibit any effect on MDA-MB-231 cell viability.
2- LPC-DHA, PC-DHA, MAG-DHA and DHA decreased cell viability in the following descending order: LPC-DHA > PC-DHA > MAG-DHA > DHA.
3- Increasing the number of chains of DHA attached to the lipid carrier decrease the effect.
4- Phospholipidic vector seems to be more important, as the observed effect were higher with LPC-DHA and PC-DHA.

C. Effect of LPC-DHA on the viability of cancer cells other than MDA-MB-231 cells

DHA, LPC-DHA and PC-DHA compounds were sent to ImPACcell, (Rennes, France) in order to test the effect of these compounds on various cancer cell lines, including MDA-MB-231 cell line, and on non-cancerous cells (fibroblasts). MAG-DHA was not studied on these cells since it was not yet integrated in our study at that time.

Before presenting the obtained results, it is necessary to mention that these experiments were performed at the beginning of the thesis with 20,000 cells/well while after, a concentration of 10,000 cells/well was adopted to realize our experiments as described in the Materials and Methods section. For this reason, a difference in obtained results was observed compared to the results that were presented before.

Table 25 shows the IC_{50} of each compound on the different cell lines.

TABLE 245: THE IC_{50} VALUES FOR EACH PRODUCT AFTER 24 HOURS TREATMENT

		IC_{50} (µM) after 24 hours treatment		
Cell line	**Cancer type**	**LPC-DHA**	**PC-DHA**	**DHA**
Huh7	Liver	24	72	-
Caco2	Colon	30	41	-
MDA-MB-231	Breast	50	83	-
PC3	Prostate	36	35	-
MDA-MB-468	Breast	19	27	-
MCF7	Breast	45	24	-
Fibroblasts	-	-	-	-

Cells were treated with different concentrations (6.25-200 µM) of LPC-DHA, PC-DHA and DHA for 24 hours. No IC_{50} was calculated for DHA (table 25), since the number of viable cells after treatment with DHA was similar to the control, with all tested concentrations. Therefore, DHA does not seem to induce any inhibition of cell viability on any of the cell lines studied. The absence of DHA effect on MDA-MB-

231 viability, contrary to what was mentioned before, could be due to the fact that there were more seeded cells in the well.

Moreover, no IC_{50} was calculated with fibroblasts treated with the three molecules, as no effect was observed on these cells. Based on these results, it can be suggested that the effect observed on cancer cell lines is not a cytotoxic effect but a specific effect that inhibits cancer cell viability. It could also be suggested that fibroblasts may be resistant to the effects of these compounds. It should be noted that none of the previously published studies that have investigated the effect of DHA and PC-DHA on different types of cancer cells have verified the cytotoxic effect of these compounds on non-cancerous cells.

The IC_{50} values of LPC-DHA and PC-DHA show that these two molecules exhibited a negative effect on the viability of the six cancer cell lines studied. The extent of this effect varies slightly depending on the cell line, with IC_{50} ranging from 19 to 50 µM for LPC-DHA and from 24 to 83 µM for PC-DHA (table 24).

Except for MCF7 and PC3 cell lines, LPC-DHA had a higher effect than PC-DHA, in the range of 1.5 and 3 times more effective according to the cell type. For MCF7 cells, PC-DHA (IC_{50} = 24 µM) was twice more effective than LPC-DHA (IC_{50} = 45 µM), and for PC3 cells, both compounds have similar effect (IC_{50} ≈ 35 µM) (table 24).

Regarding the MDA-MB-231 cells the obtained IC_{50} for LPC-DHA and PC-DHA are 50 and 83 µM, respectively (table 25), while the ones that we obtained previously are smaller, namely 25 µM for LPC-DHA and 50 µM for PC-DHA. The difference in these values could be due to the fact that there were more seeded cells in the wells, the higher the number of cells, the higher the concentration of products is needed to observe the same effect.

D. Cell death mechanisms

After having studied and selected the molecules having an inhibitory effect on the MDA-MB-231 cell viability, the main mechanisms of cell death caused by LPC-DHA, MAG-DHA, PC-DHA and DHA were explored, in order to describe the mode of action of these molecules and to see if there is any difference between them. The studied cell death mechanisms were apoptosis and autophagy. In addition, membrane damage, DNA damage and oxidative stress were also studied.

A DAPI test was performed at the same time as the immunolabeling as a control, to verify the presence of the inhibitory effect on viability caused by the tested molecules. The results of the DAPI test confirmed the presence of the effect observed with the neutral red test.

1. Apoptosis

Apoptosis was studied by active caspase-3 immunolabelling. Caspase 3 is an effective caspase that gets activated when the apoptosis procedure has been initiated in the cell (Keane *et al*. 1999).

Figure 68 shows the intensity of active caspase-3 immunolabelling in cells treated with DHA, MAG-DHA, PC-DHA and LPC-DHA. For each tested molecule the dose effect curves (from figures 69 and 71), are added on the figure in order to visualize the possible relation between the inhibitory effect and the parameter studied, which is active caspase 3 for figure 72.

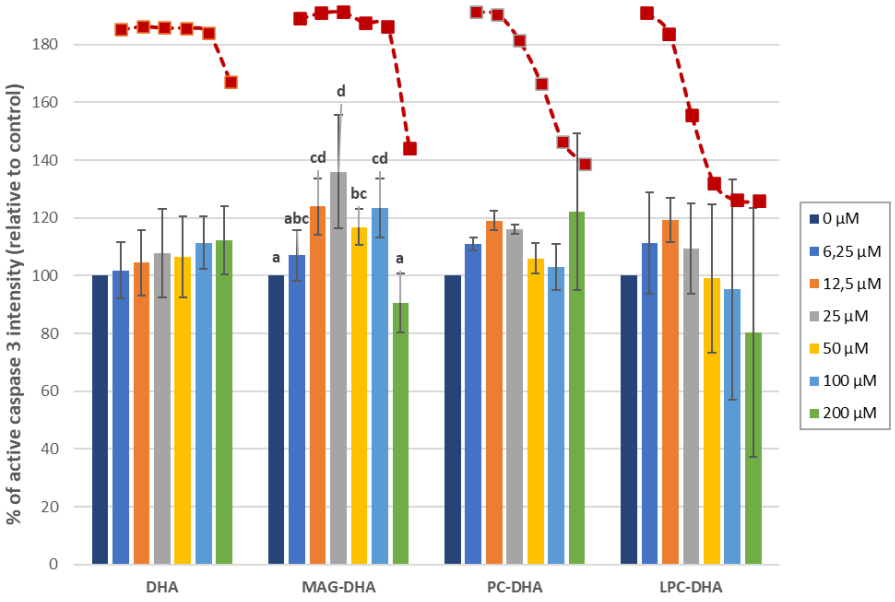

FIGURE 72: THE INTENSITY OF ACTIVATION OF THE APOPTOSIS PATHWAY BY THE CASPASE-3 MARKER

Cells were treated with different concentrations (6.25-200 µM) of lipid species containing DHA for 24 hours. Data points are shown as mean ± SD of 3 independent experiments each done in triplicate. Statistical significance was determined using ANOVA with post hoc Fisher's test. Means associated with letters indicate significative difference at $p < 0.05$, with a < b < c < d.

Treatment with either LPC-DHA, PC-DHA or free DHA did not increase the percentage of active caspase-3 fluorescence intensity, at all tested concentrations (figure 72). Thus, these three molecules do not promote apoptotic cell death.

Active caspase-3 intensity was statistically significantly increased in cells treated with 25 µM of MAG-DHA ($p = 0.0021$) (figure 72). However, the decrease in cell viability in cells treated with MAG-DHA was significantly observed with concentrations higher than 100 µM. Thus, it can be suggested that the active caspase-3 intensity increase was not biologically significant at 25 µM. Moreover, it can also be suggested that this incoherence may be due to the high SD obtained with only 3 experiments. With

these results, as no significant increase in caspase-3 was obtained at 200 µM, concentration that triggered cell viability decrease, it can be suggested that MAG-DHA does not promote apoptosis.

Unlike our results, PC-DHA and DHA have been reported to reduce the viability of LLC lung cancer cell lines (Liu *et al.* 2021) and colorectal cancer cell lines (HT-29, Caco-2 and DLD-1) (Hossain *et al.* 2008) viability by promoting apoptotic cell death. An increase in caspase-3 activity was reported in these studies. Moreover, caspase-3 activity was also increased after treatment of HCT116 colon cancer cell lines (Zhang *et al.* 2020b) and breast cancer cell lines (SKBR3 and E0771) (González-Fernández *et al.* 2019) with MAG-DHA.

2. Autophagy

Autophagy was studied using microtubule associated protein light chain3 B (LC3B) which is a mammalian homolog protein localized on the autophagosome membrane and is a widely used marker of autophagosomes. It is a pivotal protein in the autophagy pathway in which it is involved in autophagy substrate selection and autophagosome biogenesis (Tanida *et al.* 2008).

Figure 73 shows the intensity of LC3B immunolabelling in cells treated with DHA, MAG-DHA, PC-DHA and LPC-DHA.

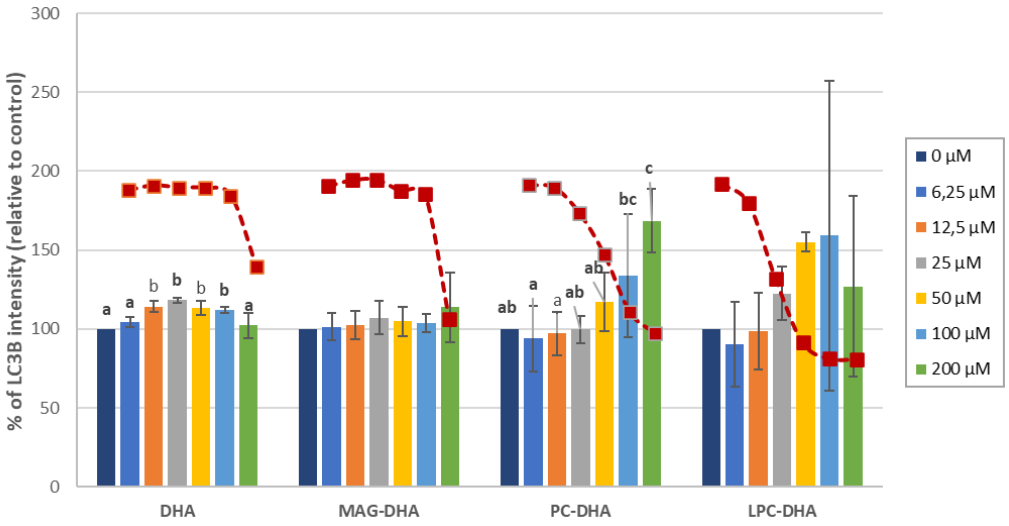

FIGURE 73: THE INTENSITY OF ACTIVATION OF THE AUTOPHAGY PATHWAY BY THE LC3B MARKER

Cells were treated with different concentrations (6.25-200 µM) of lipid species containing DHA for 24 hours. Data points are shown as mean ± SD of 3 independent experiments each done in triplicate. Statistical significance was determined using ANOVA with post hoc Fisher's test. Means associated with letters indicate significative difference at $p < 0.05$, with a < b < c.

A significant increase in LC3B fluorescence intensity is observed with DHA concentrations between 12.5 µM and 100 µM ($p = 0.0003$) (figure 73). However, no reduction in cell viability was observed as these concentrations, thus it can be suggested that this increase is not biologically significant. In

addition, as no increase in LC3B intensity was observed at 200 µM, which the concentration that decreased cell viability, we can suggest that autophagy is not triggered by DHA.

Exposure of MDA-MB-231 cells to either MAG-DHA or LPC-DHA had no effect on the level of LC3B intensity (figure 73).

LC3B fluorescence intensity tends to increase from 100 µM and this increase became significant at 200 µM (*p*-value = 0.005) (figure 73). This indicates that autophagy is involved in the death of MDA-MB-231 cells at a high dose of PC-DHA of 200 µM and is not involved in the cell death induced by PC-DHA at lower concentrations in the range 50 – 100 µM.

Contrary to our results, Zhang *et al.* (2020b) showed that LC3B markers were significantly increased in breast cancer cells (SKBR3 and E0771) treated with MAG-DHA. Moreover, Tsai *et al.* (2021) showed an increase in LC3B expression in MCF-7 breast cancer cells treated with DHA. Thus, it can be suggested that MAG-DHA reduces cell viability in MDA-MB-231 independently of autophagy. In addition, higher concentrations of DHA should be studied in order to better estimate whether treatment with DHA promotes autophagy or not.

3. Membrane damage

A number of methods are commonly used to verify cell leakage and membrane permeability. Among them the activity of lactate dehydrogenase (LDH), which is a cytosolic enzyme present in all mammalian cells, can be detected. Plasma membrane is impermeable to LDH. When the cell lost its integrity, LDH will be released in the supernatant, where its enzymatic activity can be measured (Krysko *et al.* 2008).

Figure 74 shows the percentage of LDH release in cells treated with DHA, MAG-DHA, PC-DHA and LPC-DHA.

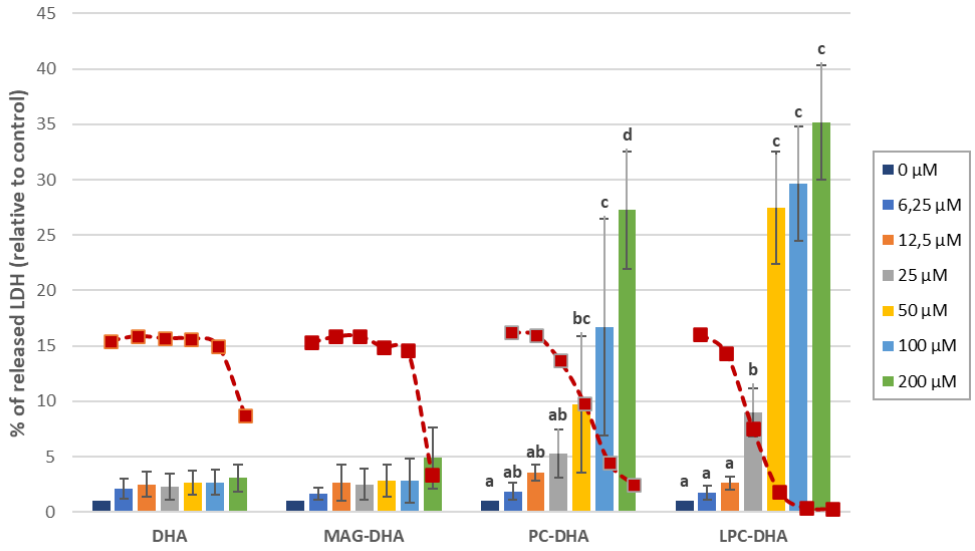

FIGURE 74: EVALUATION OF MEMBRANE DAMAGE

Cells were treated with different concentrations (6.25-200 µM) of lipid species containing DHA for 24 hours. Data points are shown as mean ± SD of 3 independent experiments each done in triplicate. Statistical significance was determined using ANOVA with post hoc Fisher's test. Means associated with letters indicate significative difference at $p < 0.05$, with a < b < c < d.

MAG-DHA and free DHA do not trigger the release of LDH at all studied concentrations (figure 74). The absence of LDH release at concentrations ranging between 6.25 µM and 100 µM was expected as no reduce in cell viability was observed. However, the absence of LDH release at 200 µM of both compounds indicated the absence of membrane damage.

The percentage of released LDH increased significantly ($p<0.0001$) with increasing concentrations of PC-DHA and LPC-DHA up to 27% and 35% respectively (figure 74). The increase in LDH release was correlated with the cell viability curve. LDH release tended to be significant from 50 µM for PC-DHA and 25 µM for LPC-DHA, the concentrations at which the reduction in cell viability became significant.

Thus, these results indicate that LPC-DHA and PC-DHA induced a significant membrane damage in MDA-MB-231 cells at the highest doses (50 - 100 µM) and to a lesser extent at 25 µM.

In the literature, none of the studies have shown that MAG-DHA and PC-DHA caused membrane rupture. However, Pizato *et al.* (2018) showed that 200 µM of DHA inhibited 50% of MDA-MB-231 cell viability by promoting pyroptosis. Pyroptosis is a lytic programmed cell death mediated by caspases and lead to the cell membrane rupture. Thus, contrary to us, DHA caused the rupture of MDA-MB-231 cell membrane in Pizato *et al.* (2018) study. However, the effect at 200 µM was greater than the observed effect in our conditions, thus, we can suggest that, by testing higher concentrations of DHA an LDH release would occur.

4. Oxidative stress

Oxidative stress was studied through the quantification of two enzymes, heme oxygenase-1 (HO-1) which is a stress enzyme, induced in response to a variety of oxidative challenges (Choi and Alam 1996), and the superoxide dismutase 2 (SOD-2) which is known for controlling and limiting the harmful effects of reactive oxygen species (ROS) (Melov *et al*. 1999).

Figures 75 and 76 show the HO-1 and SOD-2 immunolabelling intensities in cells treated with DHA, MAG-DHA, PC-DHA and LPC-DHA.

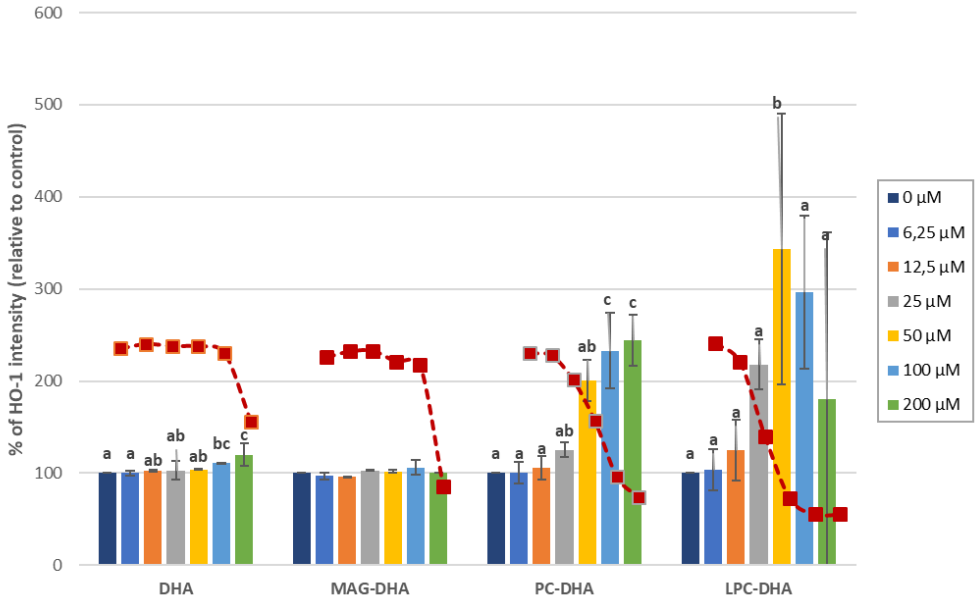

FIGURE 75: THE INTENSITY OF ACTIVATION OF THE OXIDATIVE STRESS PATHWAY BY THE HO-1 MARKER

Cells were treated with different concentrations (6.25-200 µM) of lipid species containing DHA for 24 hours. Data points are shown as mean ± SD of 3 independent experiments each done in triplicate. Statistical significance was determined using ANOVA with post hoc Fisher's test. Means associated with letters indicate significative difference at $p < 0.05$, with a < b < c.

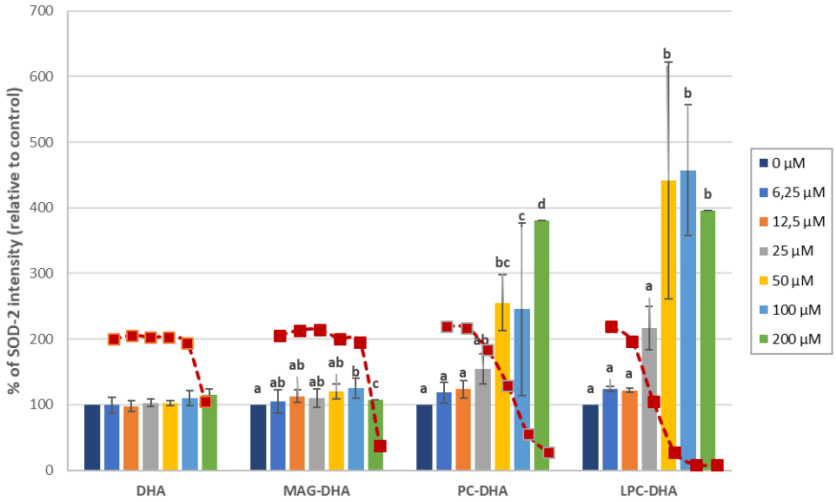

FIGURE 76: THE INTENSITY OF ACTIVATION OF THE OXIDATIVE STRESS PATHWAY BY THE SOD-2 MARKER

Cells were treated with different concentrations (6.25-200 µM) of lipid species containing DHA for 24 hours. Data points are shown as mean ± SD of 3 independent experiments each done in triplicate. Statistical significance was determined using ANOVA with post hoc Fisher's test. Means associated with letters indicate significative difference at $p < 0.05$, with a < b < c < d.

HO-1 intensity was significantly increased after exposure of MDA-MB-231 cells to 200 µM of DHA (p = 0.009) (figure 75). However, no increase in SOD-2 intensity was observed (figure 76). Thus, DHA causes oxidative damage in the MDA-MB-231 cells.

Exposure of MDA-MB-231 cells to MAG-DHA had no effect on the level of HO-1 intensity (figure 75). However, SOD-2 was significantly increased after exposure of MDA-MB-231 cells to 200 µM of MAG-DHA (p = 0.0002) (figure 76). Thus, MAG-DHA causes oxidative damage in the MDA-MB-231 cells.

Fluorescence intensities demonstrated a dose-dependent increase in HO-1 and SOD-2 intensity in the PC-DHA treated cells. Both HO-1 and SOD-2 intensities tend to increase from 25 µM, however this increase was significant, HO-1 (p = 0.0018) and SOD-2 (p = 0.0012), from 100 µM of PC-DHA (figures 75 and 76).

For LPC-DHA, a significant increase in HO-1 fluorescence intensity was observed only in cells treated with 50 µM of LPC-DHA (p = 0.0087) (figure 75). A significant increase in SOD-2 fluorescence intensity was observed with the increase of LPC-DHA concentration from 50 µM to 200 µM (p = 0.0002) (figure 76).

Similar to our results, some research studies have demonstrated that DHA reduces cancer cell viability by inducing oxidative stress in A549 lung cancer cells (Yin *et al.* 2017) and in MCF-7 breast cancer cells (Tsai *et al.* 2021). In addition, HO-1 was significantly increased with 100 µM DHA treatment in human aortic endothelial cells (Sakai *et al.* 2017).

The oxidative stress caused by MAG-DHA, PC-DHA and LPC-DHA was not correlated with the dose-effect curve. The increase in these markers was observed at concentrations corresponding to high cell death percentage (between 60 and 100 %). Thus, we can suggest that the observed oxidative stress is due to the cytotoxicity of the medium caused by the high level of cell death.

5. DNA damage

DNA damage was studied by Ataxia telangiectasia mutated (ATM) and γH2AX immunolabellings. ATM protein is activated following double-strand DNA breaks. It then phosphorylates H2AX, a variant of the histone family, which recruits several proteins to the damaged DNA site that are subsequently phosphorylated by ATM. These ATM substrates will allow the repair of the damaged DNA (Burma *et al.* 2001).

Figures 77 and 78 show the ATM and γH2AX immunolabelling intensities in cells treated with DHA, MAG-DHA, PC-DHA and LPC-DHA.

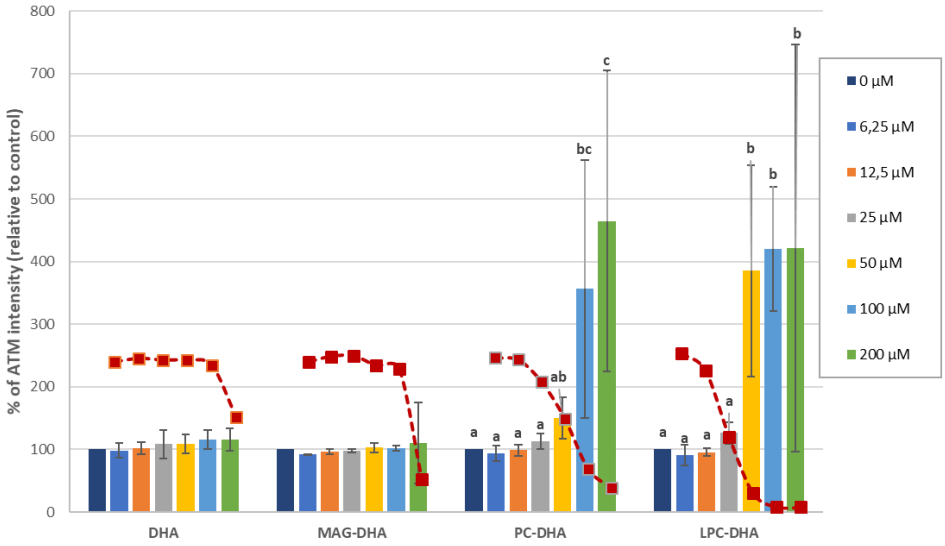

FIGURE 77: THE INTENSITY OF ACTIVATION OF THE DNA DAMAGE RESPONSE PATHWAY BY THE ATM MARKER

Cells were treated with different concentrations (6.25-200 µM) of lipid species containing DHA for 24 hours. Data points are shown as mean ± SD of 3 independent experiments each done in triplicate. Statistical significance was determined using ANOVA with post hoc Fisher's test. Means associated with letters indicate significative difference at $p < 0.05$, with a < b < c.

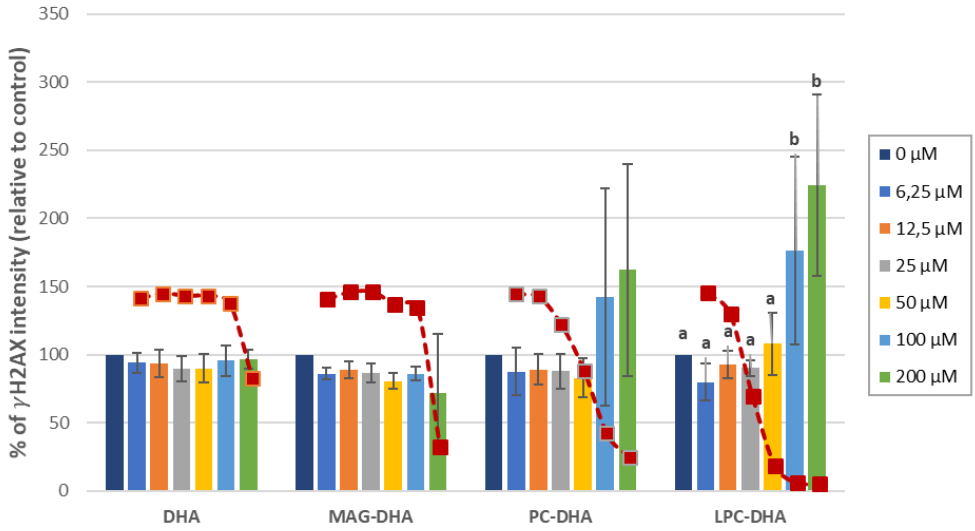

FIGURE 78: THE INTENSITY OF ACTIVATION OF THE DNA DAMAGE RESPONSE PATHWAY BY THE γH2AX MARKER

Cells were treated with different concentrations (6.25-200 µM) of lipid species containing DHA for 24 hours. Data points are shown as mean ± SD of 3 independent experiments each done in triplicate. Statistical significance was determined using ANOVA with post hoc Fisher's test. Means associated with letters indicate significative difference at $p < 0.05$, with a < b.

Exposure of MDA-MB-231 cells to either DHA or MAG-DHA had no effect on the level of ATM and γH2AX fluorescence intensities (figures 77 and 78), indicating that the cell death caused by DHA and MAG-DHA is not associated with DNA double strand breaks.

According to figure 77, an increase in ATM fluorescence intensity was observed with the increase of PC-DHA concentration from 50 µM to 200 µM. However, this increase was statistically significant at 200 µM ($p = 0.0082$). In parallel, no significant increase in the γH2AX intensity was observed following exposure to PC-DHA at all tested concentrations (figure 78).

For LPC-DHA, a significant increase in ATM fluorescence intensity was observed with the increase of LPC-DHA concentration from 50 µM to 200 µM (figure 77). The phosphorylation of H2AX occurred from a concentration of 100 µM, in which a significant increase in γH2AX fluorescence intensity was observed with the increase of LPC-DHA concentration at 100 µM and 200 µM ($p = 0.0024$) (figure 78).

The DNA damage caused by PC-DHA and LPC-DHA was not correlated with the dose-effect curve. The increase in these markers was observed at concentrations corresponding to high cell death percentage (between 60 and 100 %). Thus, we can suggest that the observed DNA damage is due to the cytotoxicity of the medium caused by the high level of cell death.

In the literature, many studies have shown that DHA induced oxidative DNA damage (Song and Kim 2016). Oxidative DNA damage was induced after treatment of MDA-MB-231 cells (Chénais *et al.* 2020),

and vascular endothelial cells (Sakai *et al.* 2017) with 100 µM of DHA. To find out if DHA causes DNA damage, higher concentrations of DHA should be tested.

Table 26 summarizes the concentrations at which significant decrease in cell viability started and at which significant cell death mechanisms were observed.

TABLE 256: TABLE ILLUSTRATING THE CONCENTRATIONS AT WHICH SIGNIFICANT EFFECT WAS OBTAINED WITH THE DIFFERENT STUDIED CELL DEATH MECHANISM AND VIABILITY

	Test or Marker	Molecules			
		DHA	**MAG-DHA**	**PC-DHA**	**LPC-DHA**
Cell viability	Neutral Red	200 µM	200 µM	50 µM	25 µM
Apoptosis	Caspase-3	X	X	X	X
Membrane damage	LDH release	X	X	100 µM	25 µM
Autophagy	LC3B	X	X	200 µM	X
Oxidative stress	HO-1	200 µM	X	100 µM	50 µM
	SOD-2	X	200 µM	100 µM	50 µM
DNA damage	ATM	X	X	200 µM	50 µM
	γH2AX	X	X	X	100 µM

All these results reveal a strong structure-function relationship of DHA-carrying lipids on the viability of MDA-MB-231 cells. To summarize, in this work, DHA and MAG-DHA were shown to inhibit cell viability by promoting oxidative stress at 200 µM (table 26). However higher concentrations should be tested to investigate the cell death mechanism induced by the oxidative stress, as many cell death modes can be triggered by the oxidative stress.

Interestingly, PC-DHA mainly induced membrane damage and oxidative stress at 100 µM (table 26). No mechanism was correlated with the reduction in cell viability at 50 µM. Autophagy and DNA damage were induced at the highest tested concentration of PC-DHA, 200 µM. Based on these findings it can be suggested that PC-DHA induces autophagy and DNA damage by triggering oxidative stress in the cells, as Tsai *et al.* (2021) showed that DHA promoted the formation of autophagosomes in MCF-7 breast cancer cells through oxidative stress. Also, Sakai *et al.* (2017) showed that DHA induced oxidative stress and DNA damage in human vascular endothelial cells.

Regarding LPC-DHA, reduction in cell viability was highly correlated with the LDH release, in which both observed results were significant from 25 µM of LPC-DHA (table 26). Oxidative stress and DNA damage were significantly promoted after treatment with 50 µM of LPC-DHA. As already mentioned, it can be suggested that DNA damage was induced by the oxidative stress.

This results interestingly shows that the mechanism of action of MAG-DHA is very different from that of LPC-DHA and PC-DHA. Thus, further experiments should be realized to also identify the cell death mechanism caused by PC-DHA and LPC-DHA.

It can be suggested that these two molecules reduce the cell viability through necrosis. In order to validate this hypothesis a close observation of the morphological modifications is needed. Necrosis is characterized by the increase in cell volume and organelles swelling at the beginning, before membrane disrupture. Necrotic cells reveal a mitochondrial dysfunction, that causes a significant increase in the production of oxidative free radicals, and DNA damage (DNA fragments of random size) (Panawala 2017).

In addition to the classic death mechanisms, a new mechanism was described in 2012 which is an iron-dependent form of regulated non-apoptotic cell death, called ferroptosis. This form of cell death is caused by the accumulation of lipid-based ROS, and causes a disrupting in membrane integrity (Dixon *et al*. 2012). A study has shown that DHA induced cell death in HCC liver cancer cells through the ferroptosis pathway (Ou *et al*. 2017). Thus, one of the hypotheses that could be suggested is that PC-DHA and LPC-DHA induce ferroptosis in MDA-MB-231 cells, as they induce oxidative stress and membrane damage. To validate this hypothesis, further experiments should be carried out like a cell treatment with ferrostatin, a ferroptosis inhibitor.

As an intermediate conclusion, the study of the cell death mechanism did not give us a definite conclusion. However, we have seen that:

1- Apoptosis is not involved in cells death after treatment with LPC-DHA, PC-DHA, MAG-DHA and DHA.
2- LPC-DHA triggered membrane damage.
3- Oxidative stress is commonly triggered in cells treated with LPC-DHA, PC-DHA, MAG-DHA and DHA.
4- Each compound triggered a different response, which reconfirm that the observed effect is related to the chemical structure of the lipid.

E. Evaluation of the synthesized LPC-DHA effect on cell viability

After synthesizing LPC-DHA the aim was to evaluate its effect on MDA-MB-231 viability. For this a sample was collected from the enzymatic esterification reaction after 30 hours, diluted with methanol and purified by preparative thin layer chromatography (TLC). Purified LPC-DHA was recovered from scrapped silica with ethanol and analyzed by HPLC in order to check for purity and determine the concentration of the purified LPC-DHA solution.

Concentrations varying between 6.25 µM and 200 µM were prepared and tested on MDA-MB-231 cells. Figure 79 shows the cellular viability of MDA-MB-231 cells when treated with different concentrations of purified LPC-DHA.

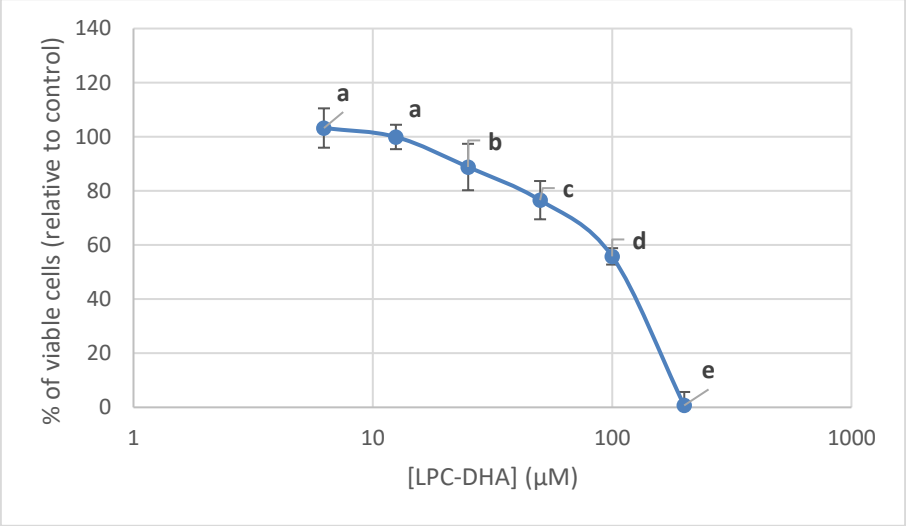

FIGURE 79: DOSE-EFFECT RELATIONSHIP OF PURIFIED LPC-DHA ON MDA-MB-231 CELL VIABILITY

Cells were treated with different concentrations (6.25-200 µM) of LPC-DHA for 24 hours. The viability is tested by the neutral red test. Data points are shown as mean ± SD of 3 independent experiments each done in triplicate. Statistical significance was determined using ANOVA with post hoc Fisher's test. Means associated with letters indicate significative difference at $p < 0.05$, with a < b < c < d < e.

According to figure 79, no effect on cell viability was observed in MDA-MB-231 cells treated with LPC-DHA concentration of 6.25 µM and 12.5 µM. Interestingly, a significant cell viability reduction was observed in MDA-MB-231 cells treated with LPC-DHA at concentrations greater than 25 µM ($p < 0.001$). An IC_{50} value of 118 µM was calculated for LPC-DHA. This IC_{50} (118 µM) is higher than that obtained with the commercialized LPC-DHA (20 µM).

These interesting results indicate that the inhibitory effect observed with the commercialized LPC-DHA is also seen with the synthesized LPC-DHA. The difference in the IC_{50} may be due to the fact that the product after purification by TLC was not pure in our condition. Indeed, a peak corresponding to an

unknown compound was observed on the HPLC chromatogram. However, despite the impurity, the study has been done with the same concentration used with the commercial LPC-DHA.

We could suggest that this peak corresponds to an oxidized product of LPC-DHA, as silica is known for its oxidative capacity. However, two arguments are against this hypothesis. First, the product is not retained by the stationary phase and is eluted early in the dead volume. This suggest that the peak could not correspond to an oxidized product of LPC-DHA which would be retained by the stationary phase. Secondly, after purification on the silica column and subsequent NMR analysis of the purified product, it has been shown that the product is not oxidized, so this hypothesis is eliminated.

At this time, it is not possible to specify which product it could correspond to the peak. However, further experiments will be conducted to identify the eluted impurity. But the evaluation of our synthesized LPC-DHA must be repeated with a totally pure sample.

Conclusion and perspectives

Conclusion and perspectives

In this study, an esterification enzymatic process was developed and optimized, using the Novozym® 435, for the synthesis of LPC rich in DHA. Also, the effect of LPC-DHA on breast cancer cells was evaluated.

This study has been carried out in a favorable context of interest for lysophospholipids enriched with DHA. These molecules can be used as a vector for PUFAs, especially for DHA. The therapeutic properties of LPCs containing a DHA are the subject of numerous studies and their functions are increasingly well known. Moreover, the DHA is highly sensitive to oxidation and LPCs provide a protection against oxidation.

Lipase-catalyzed synthesis of LPC-DHA was performed by esterification of DHA on GPC. The reaction was performed in a free solvent medium, to adapt non-toxic reaction conditions allowing the use of this compound as food supplement or for therapeutic purposes. In a first step, a biocatalyst screening allowed to select the Novozym® 435 biocatalyst (immobilized lipase from *Candida antarctica*, from Novozymes, Denmark) as the most efficient biocatalyst among five commercially available immobilized lipases tested. The reaction conditions were then optimized according to the response surface methodology (RSM) using a Box-Behnken design of experiments. Three factors were studied, namely the molar ratio, the biocatalyst quantity and the temperature. Two responses were measured, namely the GPC conversion yield and the concentration of LPC-DHA in the medium after 30 hours of reaction. Regarding the GPC conversion yield, the maximal value obtained was 67% under the following reaction conditions: a molar ratio DHA/GPC of 17, a reaction temperature of 36°C and an amount of Novozym® 435 of 15% (relative to the mass of substrates). Our study did not lead to an improvement of the yield compared to the few other published results. Nevertheless, interestingly enough, our yield has been achieved with a lower molar ratio and a lower temperature than those described in literature. Moreover, remarkably, this yield has been achieved without the need to carry out the reaction under vacuum, which, in the published studies, was the main parameter for achieving high yields. Regarding the LPC-DHA concentration, the maximal value was 246 mM and it was achieved under the following conditions: a molar ratio DHA/GPC of 4, a temperature of 36°C and a load of Novozym® 435 of 15%. It is interesting to note that in the literature, only the GPC conversion yield is studied and modifications of the reaction conditions aiming to improve this yield have been performed. In this work, it was shown that a high molar ratio is required to achieve a high yield while a low molar ratio is required to achieve a high concentration of LPC-DHA. In order to compare our results with those of the literature, the concentrations of LPC-DHA were calculated from the data provided in the published articles and it turned out that the concentration achieved in our conditions was the highest. Moreover, kinetics of

the synthesis of LPC-DHA revealed that the reaction equilibrium was reached after 5 hours, which is interestingly a shorter reaction time comparing with those reported in literature. Following this synthesis, a column purification followed by NMR analysis was done to characterize the obtained LPC-DHA. The results of NMR showed the synthesis of a fully pure non-oxidized *sn*-1 isomer.

During this study the reuse of Novozym® 435 was studied and it was shown that it was not possible to reuse it. This can be caused either by the desorption of the enzyme by the detergent effect of LPC-DHA or by the limitation of substrates access to the active site by congestion in the enzyme microenvironment caused by DHA or LPC-DHA.

Regarding the obtained two models the question arises on the choice of the most suitable model. From our point of view, regarding the high price of LPC-DHA compared to GPC, it is more advantageous to increase the production of LPC-DHA, therefore the model aiming to optimize [LPC-DHA] will be more advantageous. But we can also optimize the conditions in order to maximize the two responses. The optimization of these two responses, through Modde® software, makes it possible to obtain [LPC-DHA] = 200 mM and Y_{GPC} = 63% under the following conditions: a molar ratio DHA/GPC of 9, a temperature of 36°C and a load of Novozym® 435 of 15%. Thus, carrying out the reaction under the conditions which optimize these two responses is still advantageous as the production is increased comparing to the literature with an acceptable yield. Also these results are obtained with a lower MR of 9, therefore using a lower excess of DHA.

As perspectives for the continuity of this work, it is necessary to find out why the reuse of Novozym® 435 is impossible. Lipase desorption is often considered to be primarily caused by the reaction medium (e.g., agitation, high concentration of organic co-solvents), ignoring the fact that many substrates or products of reactions can behave as a detergent at very high concentrations. As an example, in the hydrolysis of oils, DAG and MAG have tension-active properties that desorbed the enzyme (Murty *et al.* 2002). So, in certain cases, the desorption problems encountered when using lipases physically immobilized on hydrophobic supports can be related to the presence of the reaction products and not only to the conditions of the reaction medium. Thus, for the assessment of desorption of lipase toward LPC-DHA, Novozym® 435 should be incubated with 90 mM LPC-DHA, which is the concentration at which the reaction equilibrium is reached. After incubation, samples from supernatant, should be analyzed by SDS-PAGE. If the electrophoretical analysis showed a large amount of enzyme in the supernatant this indicates that the lipase molecules had been desorbed from the support. If desorption is confirmed it is necessary to move towards the idea of changing the biocatalyst, in order to find a biocatalyst more resistant to the desorption caused by the LPC-DHA. Ortiz *et al.* (2019) have announced several solutions to limit the desorption of Novozym® 435, including cross-linking of the

biocatalyst. In this work three different ways of cross-linking were tried but the reaction was limited which can be suggested that these cross-linkings limited the access of the substrate to the active site. Another solution was announced which is to cover Novozym® 435 with silicone. Indeed, it was found to reduce enzyme leaching from the support, if the biocatalyst is fully closed in a silicone matrix. Thus, it would be interesting to test this solution to see if it would reduce the enzyme leaching in our conditions.

If desorption is not confirmed, we should pass to the second hypothesis which is the limitation of access to the active site by the LPC-DHA or DHA. Our objective from the beginning was to synthesize LPC-DHA in a solvent-free medium in order to avoid the use of toxic solvents, but for several reasons (problem of solubility and reuse of biocatalysts) it may not be the most adequate process for this type of synthesis. So, one of the perspectives is to try to develop a synthesis method using a green solvent. It can be considered to carry out the reaction with non-toxic solvents which could increase the solubilization between the substrates as well as the partition coefficient between the liquid phase, containing the substrates and the product, and the solid phase which is the biocatalyst. This could decrease the possibility of inhibition due to an excess of product or substrate around the biocatalyst. Many solvents could be used such as the eco-friendly solvent 2-methyltetrahydrofuran (MeTHF). MeTHF is produced from renewable biomass and is considered as a green solvent. It was applied as a solvent in esterification reactions providing an efficient synthetic route with satisfactory conversion yields >99% and it did not show any inhibition effect on Novozym® 435 (Lăcătuş *et al.* 2018).

Also, the use of a continuous reactor could avoid the limitation of access to the enzyme by removing the product and feeding the medium progressively with the substrate. At the same time, a bubble column reactor could overcome limitations due to the high viscosity in the solvent free esterification.

Regarding the second objective of this work, namely, the evaluation of the effect of LPC-DHA on the viability of MDA-MB-231 breast cancer cells, we first compared the effect of LPC-DHA to that of free DHA in a range of concentration up to 200 µM. No decrease of the cell viability was observed with DHA at concentration less or equal to 100 µM. In contrast, LPC-DHA effect follows a dose-response curve with an IC_{50} of 19 µM. Our results showed the efficiency and the specificity of LPC-DHA in inhibiting MBA-MB-231 cell viability, compared to other LPC carrying a fatty acid chain with various length and unsaturation degrees (namely, C8:0, C14:0, C18:0, C18:1, C18:2 and C22:0) for which no effect was observed. In addition to LPC-DHA, the effect on MBA-MB-231 cells of various lipids carrying one to three DHA chains was studied. These lipids were: monodocosahexaenoin (MAG-DHA), didocosahexaenoin (DAG-DHA), tridocosahexaenoin (TAG-DHA) and didocosahexaenoyl phosphatidylcholine (PC-DHA). It was shown that LPC-DHA was the most effective on cell viability

followed by PC-DHA (IC_{50} = 50 µM), MAG-DHA (IC_{50} = 170 µM), and free DHA (IC_{50} = 347 µM). TAG-DHA and DAG-DHA did not show any effect on the cell viability whatever the tested concentration.

Moreover, LPC-DHA effect on various cancer cell lines and on fibroblasts was studied. It has been shown that LPC-DHA inhibited the cell viability of all studied cancer cell lines while it did not exhibit any effect against fibroblast cells.

Finally, the mechanisms of cell death triggered by the compounds were also investigated. Cell death caused by LPC-DHA and PC-DHA did not promote apoptosis. In contrast, it was mainly related to oxidative stress and membrane damage. These findings suggest that the death of cells treated with LPC-DHA and PC-DHA could occur *via* a non-apoptic cell death mechanism. Concerning DHA and MAG-DHA, which showed an effect on the cell viability only at the highest concentration tested (200 µM), only an oxidative stress was detected. This suggests that the mechanism of action of MAG-DHA is different from that of LPC-DHA and PC-DHA. All these results reveal an interesting and strong structure-function relationship of DHA-carrying lipids on the viability of MDA-MB-231 cells.

In the future, it would be interesting to test the effect of these molecules on epithelial non-cancerous breast cells to calculate the cytotoxic selectivity ratio, as a representation of drug selectivity between normal and cancer cell lines. If the observed effect caused by LPC-DHA is membranous, as the membrane damage was highly correlated with the observed inhibitory effect of LPC-DHA, it could give us an idea on the selectivity of LPC-DHA effect towards cancerous cell membranes.

The study of the effect of *sn*-2 LPC-DHA will be also interesting to evaluate, as the DHA position have been shown to influence the biological effect. For example, Hung *et al*. (2011) reported that the metabolic effect of *sn*-1 LPC-DHA are different from those of *sn*-2 LPC-DHA. In which the *sn*-2 LPC-DHA was reported to be more efficient in reducing inflammation in mice compared to the *sn*-1 isomer as it is better absorbed than the *sn*-1 isomer. However, Sugasini *et al.* (2020) showed that both *sn*-1 and *sn*-2 LPC-DHA increased retinal and brain DHA content similarly. Thus, comparing these two isomers will allow to verify if the position of DHA plays a role on the inhibitory effect of LPC-DHA on MDA-MB-231 cells.

In addition, it is important to extract and analyze the total lipids of treated MDA-MB-231 and identify the FAs to know whether LPC-DHA increases the effect of DHA by increasing its incorporation in the cell or whether this observed effect is specific to the LPC-DHA molecule. If these molecules play the role of a vector, we will be able to evaluate their capacity to integrate DHA into the cells and see if the DHA cell enrichment with LPC is more important, followed by PC-DHA and MAG-DHA. This will allow to verify the importance of the effect between these molecules.

Further experiments should be conducted to better identify the cell death mechanism triggered by MAG-DHA, PC-DHA and LPC-DHA. We can suggest that cell death is due to the lipidic peroxidation due to the increase of ROS by the vulnerization of the membrane and the loss of its rigidity by the presence of a high quantity of DHA. Thus, it would be interesting to incubate the cells with ROS scavengers as the 2',7'-dichlorodihydrofluorescein diacetate (H2DCF-DA) in order to verify the presence of ROS after treatment. Moreover, the level of lipid peroxidation marker malondialdehyde (MDA) should be measured in cultured MDA-MB-231 cells after treatment using a quantitation kit. MDA level is commonly known as a marker of oxidative stress and the antioxidant status in cancerous cells. The measurement of MDA should be taken into consideration as MDA is one of the final products of PUFAs peroxidation in the cells. An increase in free radicals causes overproduction of MDA.

In summary, this work has contributed to the synthesis of LPC-DHA, a molecule of interest, with industrially favorable conditions and at higher concentrations compared to the literature. This work also studied and demonstrated the effect of LPC-DHA in reducing the viability of MDA-MB-231 breast cancer cells.

References

References

AbuMweis, S.; Jew, S.; Tayyem, R.; Agraib, L. 2018. Eicosapentaenoic acid and docosahexaenoic acid containing supplements modulate risk factors for cardiovascular disease: a meta-analysis of randomised placebo-control human clinical trials. *Journal of Human Nutrition and Dietetics* 31: 67–84.

Adlercreutz, D.; Wehtje, E. 2001. A simple HPLC method for the simultaneous analysis of phosphatidylcholine and its partial hydrolysis products 1- and 2-acyl lysophosphatidylcholine. *Journal of the American Oil Chemists' Society* 78: 1007–1011.

Adlercreutz, P. 2013. Immobilisation and application of lipases in organic media. *Chemical Society Reviews* 42: 6406–6436.

Adlercreutz, P.; Gitlesen, T.; Ncube, I.; Read, J.S. 1997. [12] Vernonia lipase: A plant lipase with strong fatty acid selectivity. In: *Methods in Enzymology*, Vol. 284, Academic Press, p.220–232.

Ahmmed, M.K.; Ahmmed, F.; Tian, H. (Sabrina); Carne, A.; Bekhit, A.E.D. 2020. Marine omega-3 (n-3) phospholipids: A comprehensive review of their properties, sources, bioavailability, and relation to brain health. *Comprehensive Reviews in Food Science and Food Safety* 19: 64–123.

Ailte, I.; Lingelem, A.B.D.; Kvalvaag, A.S.; Kavaliauskiene, S.; Brech, A.; Koster, G.; Dommersnes, P.G.; Bergan, J.; Skotland, T.; Sandvig, K. 2017. Exogenous lysophospholipids with large head groups perturb clathrin-mediated endocytosis. *Traffic* 18: 176–191.

Anderson, E.M.; Larsson, K.M.; Kirk, O. 1998. One Biocatalyst–Many Applications: The Use of *Candida antarctic*a B-lipase in organic synthesis. *Biocatalysis and Biotransformation* 16: 181–204.

Anderson, R.E.; Benolken, R.M.; Dudley, P.A.; Landis, D.J.; Wheeler, T.G. 1974. Polyunsaturated fatty acids of photoreceptor membranes. *Experimental Eye Research* 18: 205–213.

Arshad, A.; Isherwood, J.; Mann, C.; Cooke, J.; Pollard, C.; Runau, F.; Morgan, B.; Steward, W.; Metcalfe, M.; Dennison, A. 2017. Intravenous ω-3 fatty acids plus gemcitabine. *Journal of Parenteral and Enteral Nutrition* 41: 398–403.

Baba, T.; Downs, D.; Jackson, K.W.; Tang, J.; Wang, C.S. 1991. Structure of human milk bile salt activated lipase. *Biochemistry* 30: 500–510.

Badve, S.; Dabbs, D.J.; Schnitt, S.J.; Baehner, F.L.; Decker, T.; Eusebi, V.; Fox, S.B.; Ichihara, S.; Jacquemier, J.; Lakhani, S.R.; Palacios, J.; Rakha, E.A.; Richardson, A.L.; Schmitt, F.C.; Tan, P.-H.; Tse, G.M.; Weigelt, B.; Ellis, I.O.; Reis-Filho, J.S. 2011. Basal-like and triple-negative breast cancers: a critical review with an emphasis on the implications for pathologists and oncologists. *Modern Pathology* 24: 157–167.

Bakir, N.; Ilyasoglu, H.; Yucetepe, A.; Kasapoglu, K.N.; Demircan, E.; Ozcelik, B. 2018. Production of structured lipids from hazelnut oil with conjugated linoleic acid by lipase-catalyzed esterification: Optimization by response surface methodology. *Acta Alimentaria* 47: 1–9.

Balcão, V.M.; Paiva, A.L.; Xavier Malcata, F. 1996. Bioreactors with immobilized lipases: State of the art. *Enzyme and Microbial Technology* 18: 392–416.

Banno, F.; Doisaki, S.; Shimizu, N.; Fujimoto, K. 2002. Lymphatic absorption of docosahexaenoic acid given as monoglyceride, diglyceride, triglyceride, and ethyl ester in rats. *Journal of Nutritional Science and Vitaminology* 48: 30–35.

Barbosa, O.; Torres, R.; Ortiz, C.; Fernandez-Lafuente, R. 2012. The slow-down of the CALB immobilization rate permits to control the inter and intra molecular modification produced by glutaraldehyde. *Process Biochemistry* 47: 766–774.

Bazinet, R.P.; Layé, S. 2014. Polyunsaturated fatty acids and their metabolites in brain function and disease. *Nature Reviews Neuroscience* 15: 771–785.

Beckermann, B.; Beneke, M.; Seitz, I. 1990. Comparative bioavailability of eicosapentaenoic acid and docasahexaenoic acid from triglycerides, free fatty acids and ethyl esters in volunteers. *Arzneimittel-Forschung* 40: 700–704.

Beisson, F.; Ferté, N.; Bruley, S.; Voultoury, R.; Verger, R.; Arondel, V. 2001. Oil-bodies as substrates for lipolytic enzymes. *Biochimica et Biophysica Acta (BBA) - Molecular and Cell Biology of Lipids* 1531: 47–58.

Belafriekh, A. 2017. Enantioselective enzymatic resolution of racemic alcohols by lipases in green organic solvents. *Chemistry, Medicinal plants, Badji Mokhtar* - Annaba University.

Benolken, R.M.; Anderson, R.E.; Wheeler, T.G. 1973. Membrane fatty acids associated with the electrical response in visual excitation. *Science* 182: 1253–1254.

Béréziat, G.; Chambaz, J.; Colard, O.; Wolf, C. 1988. Les multiples fonctions des phospholipides cellulaires. *Médecine sciences 4, N° 1; p.8-15*.

Berquin, I.M.; Edwards, I.J.; Chen, Y.Q. 2008. Multi-targeted therapy of cancer by omega-3 fatty acids. *Cancer Letters* 269: 363–377.

Berquin, I.M.; Min, Y.; Wu, R.; Wu, J.; Perry, D.; Cline, J.M.; Thomas, M.J.; Thornburg, T.; Kulik, G.; Smith, A.; Edwards, I.J.; D'Agostino, R.; Zhang, H.; Wu, H.; Kang, J.X.; Chen, Y.Q. 2007. Modulation of prostate cancer genetic risk by omega-3 and omega-6 fatty acids. *The Journal of Clinical Investigation* 117: 1866–1875.

Bilyk, O.; Hamedi, B.; Dutta, I.; Newell, M.; Bukhari, A.B.; Gamper, A.M.; McVea, R.C.; Liu, J.; Schueler, J.; Siegers, G.M.; Field, C.J.; Postovit, L.-M. 2021. Docosahexaenoic acid in the inhibition of tumor cell growth in preclinical models of ovarian cancer. *Nutrition and Cancer* 0: 1–15.

Birgbauer, E.; Chun, J. 2006. New developments in the biological functions of lysophospholipids. *Cellular and Molecular Life Sciences CMLS* 63: 2695–2701.

Blanckaert, V.; Ulmann, L.; Mimouni, V.; Antol, J.; Brancquart, L.; Chénais, B. 2010. Docosahexaenoic acid intake decreases proliferation, increases apoptosis and decreases the invasive potential of the human breast carcinoma cell line MDA-MB-231. *International Journal of Oncology* 36: 737–742.

Blasi, F.; Cossignani, L.; Maurizi, A.; Simonetti, M.; Damiani, P. 2008. Enzymatic synthesis of structured 1,2-diacyl-*sn*-glycero-3-phosphocholines from glycerol-*sn*-3-phosphocholine. *Italian Journal of Food Science* 20: 39-47.

Box, G.E.P.; Behnken, D.W. 1960. Some New Three Level Designs for the Study of Quantitative Variables. *Technometrics* 2: 455–475.

Box, G.E.P.; Hunter, W.G.; Hunter, J.S. 1978. *Statistics for experimenters: an introduction to design, data analysis, and model building*. *New york: Wiley*.

Bozzuto, G.; Molinari, A. 2015. Liposomes as nanomedical devices. *International Journal of Nanomedicine* 10: 975-999.

Breitsamer, M.; Winter, G. 2019. Vesicular phospholipid gels as drug delivery systems for small molecular weight drugs, peptides and proteins: State of the art review. *International Journal of Pharmaceutics* 557: 1–8.

Brown, I.; Lee, J.; Sneddon, A.A.; Cascio, M.G.; Pertwee, R.G.; Wahle, K.W.J.; Rotondo, D.; Heys, S.D. 2020. Anticancer effects of n-3 EPA and DHA and their endocannabinoid derivatives on breast cancer cell growth and invasion. *Prostaglandins, Leukotrienes and Essential Fatty Acids* 156: 102024.

Burdge, G.C.; Calder, P.C. 2005. Conversion of α-linolenic acid to longer-chain polyunsaturated fatty acids in human adults. *World Review of Nutrition and Dietetics*: 112: 1-16.

Burma, S.; Chen, B.P.; Murphy, M.; Kurimasa, A.; Chen, D.J. 2001. ATM phosphorylates histone H2AX in response to DNA double-strand breaks. *Journal of Biological Chemistry* 276: 42462–42467.

Cadario, F.; Pozzi, E.; Rizzollo, S.; Stracuzzi, M.; Beux, S.; Giorgis, A.; Carrera, D.; Fullin, F.; Riso, S.; Rizzo, A.M.; Montorfano, G.; Bagnati, M.; Dianzani, U.; Caimmi, P.; Bona, G.; Ricordi, C. 2019. Vitamin D and ω-3 supplementations in mediterranean diet during the 1st year of overt type 1 diabetes: A cohort study. *Nutrients* 11: 2-158.

Calder, P.C. 2016. Docosahexaenoic acid. *Annals of Nutrition & Metabolism* 69 Suppl 1: 7–21.

Carlson, S.E.; Colombo, J.; Gajewski, B.J.; Gustafson, K.M.; Mundy, D.; Yeast, J.; Georgieff, M.K.; Markley, L.A.; Kerling, E.H.; Shaddy, D.J. 2013. DHA supplementation and pregnancy outcomes. *The American Journal of Clinical Nutrition* 97: 808–815.

Carroll, K.K.; Braden, L.M. 1984. Dietary fat and mammary carcinogenesis. *Nutrition and Cancer* 6: 254–259.

Casas-Godoy, L.; Duquesne, S.; Bordes, F.; Sandoval, G.; Marty, A. 2012. Lipases: An Overview. In: Sandoval, G. (Ed.), *Lipases and Phospholipases: Methods and Protocols*, Humana Press, Totowa, NJ, p.3–30.

Chandra, P.; Enespa, N.; Singh, R.; Arora, P.K. 2020. Microbial lipases and their industrial applications: a comprehensive review. *Microbial Cell Factories* 19: 169.

Chappell, J.E.; Clandinin, M.T.; Kearney-Volpe, C. 1985. Trans fatty acids in human milk lipids: influence of maternal diet and weight loss. *The American Journal of Clinical Nutrition* 42: 49–56.

Chénais, B.; Cornec, M.; Dumont, S.; Marchand, J.; Blanckaert, V. 2020. Transcriptomic response of breast cancer cells MDA-MB-231 to docosahexaenoic acid: downregulation of lipid and cholesterol metabolism genes and upregulation of genes of the pro-apoptotic ER-stress pathway. *International Journal of Environmental Research and Public Health* 17: 37-46.

Choi, A.M.; Alam, J. 1996. Heme oxygenase-1: function, regulation, and implication of a novel stress-inducible protein in oxidant-induced lung injury. *American Journal of Respiratory Cell and Molecular Biology* 15: 9–19.

Chong, B.W.; Othman, R.; Putra Jaya, R.; Mohd Hasan, M.R.; Sandu, A.V.; Nabiałek, M.; Jeż, B.; Pietrusiewicz, P.; Kwiatkowski, D.; Postawa, P.; Abdullah, M.M.A.B. 2021. Design of Experiment on Concrete Mechanical Properties Prediction: A Critical Review. *Materials* 14: 18-66.

Chouinard-Watkins, R.; Vandal, M.; Léveillé, P.; Pinçon, A.; Calon, F.; Plourde, M. 2017. Docosahexaenoic acid prevents cognitive deficits in human apolipoprotein E epsilon 4-targeted replacement mice. *Neurobiology of Aging* 57: 28–35.

Christensen, M.M.; Høy, C.-E. 1997. Early dietary intervention with structured triacylglycerols containing docosahexaenoic acid. Effect on brain, liver, and adipose tissue lipids. *Lipids* 32: 185–191.

Clissold, D.; Thickitt, C. 1994. Recent eicosanoid chemistry. *Natural Product Reports* 11: 621–637.

Cockbain, A.J.; Toogood, G.J.; Hull, M.A. 2012. Omega-3 polyunsaturated fatty acids for the treatment and prevention of colorectal cancer. *Gut* 61: 135–149.

Cook, C.M.; Hallaråker, H.; Sæbø, P.C.; Innis, S.M.; Kelley, K.M.; Sanoshy, K.D.; Berger, A.; Maki, K.C. 2016. Bioavailability of long chain omega-3 polyunsaturated fatty acids from phospholipid-rich herring roe oil in men and women with mildly elevated triacylglycerols. *Prostaglandins, Leukotrienes and Essential Fatty Acids* 111: 17–24.

Corsetto, P.A.; Cremona, A.; Montorfano, G.; Jovenitti, I.E.; Orsini, F.; Arosio, P.; Rizzo, A.M. 2012. Chemical–physical changes in cell membrane microdomains of breast cancer cells after omega-3 PUFA incorporation. *Cell Biochemistry and Biophysics* 64: 45–59.

Cotman, C.; Blank, M.L.; Moehl, A.; Snyder, F. 1969. Lipid composition of synaptic plasma membranes isolated from rat brain by zonal centrifugation. *Biochemistry* 8: 4606–4612.

Crowe, J.H.; Crowe, L.M.; Carpenter, J.F.; Aurell Wistrom, C. 1987. Stabilization of dry phospholipid bilayers and proteins by sugars. *The Biochemical Journal* 242: 1–10.

Cruz-Hernandez, C.; Thakkar, S.K.; Moulin, J.; Oliveira, M.; Masserey-Elmelegy, I.; Dionisi, F.; Destaillats, F. 2012. Benefits of structured and free monoacylglycerols to deliver eicosapentaenoic (EPA) in a model of lipid malabsorption. *Nutrients* 4: 1781–1793.

Cruz-Hernandez, C.; Destaillats, F.; Thakkar, S.K.; Goulet, L.; Wynn, E.; Grathwohl, D.; Roessle, C.; De Giorgi, S.; Tappy, L.; Giuffrida, F.; Giusti, V. 2016. Monoacylglycerol-enriched oil increases EPA/DHA delivery to circulatory system in humans with induced lipid malabsorption conditions1. *Journal of Lipid Research* 57: 2208–2216.

Cullis, P.R.; de Kruijff, B. 1979. Lipid polymorphism and the functional roles of lipids in biological membranes. *Biochimica et Biophysica Acta* 559: 399–420.

Cunnane, S.C.; Chouinard-Watkins, R.; Castellano, C.A.; Barberger-Gateau, P. 2013. Docosahexaenoic acid homeostasis, brain aging and Alzheimer's disease: Can we reconcile the evidence? *Prostaglandins, Leukotrienes, and Essential Fatty Acids* 88: 61–70.

Cygler, M.; Grochulski, P.; Kazlauskas, R.J.; Schrag, J.D.; Bouthillier, F.; Rubin, B.; Serreqi, A.N.; Gupta, A.K. 1994. A structural basis for the chiral preferences of lipases. *Journal of the American Chemical Society* 116: 3180–3186.

Da Costa, T.H.M.; Ito, M.K. 2003. *Phospholipids - an overview | ScienceDirect Topics*. (https://www.sciencedirect.com/topics/neuroscience/phospholipids). Accessed on 30 Apr. 2019.

Daoming, L.; Weifei, W.; Li, Z.; Nan, L.; Muniba, F.; Chin Ping, T.; Bo, Y.; Dongming, L.; Yonghua, W. 2018. Synthesis of CLA-rich lysophosphatidylcholine by immobilized MAS1-H108A-catalyzed esterification: effects of the parameters and monitoring of the reaction process. *European Journal of Lipid Science and Technology - Wiley Online Library* 120: 1700529.

Delgado Naranjo, J.M.; Jiménez Callejón, M.J.; Peñuela Vásquez, M.; Rios, L.A.; Robles Medina, A. 2021. Optimization of the enzymatic synthesis of structured triacylglycerols rich in docosahexaenoic acid at *sn*-2 position by acidolysis of Aurantiochytrium limacinum SR21 oil and caprylic acid using response surface methodology. *Journal of Applied Phycology* 33: 2031–2045.

D'Eliseo, D.; Velotti, F. 2016. Omega-3 fatty acids and cancer cell cytotoxicity: Implications for multi-targeted cancer therapy. *Journal of Clinical Medicine* 5.

Dent, R.; Trudeau, M.; Pritchard, K.I.; Hanna, W.M.; Kahn, H.K.; Sawka, C.A.; Lickley, L.A.; Rawlinson, E.; Sun, P.; Narod, S.A. 2007. Triple-negative breast cancer: Clinical features and patterns of recurrence. *Clinical Cancer Research* 13: 4429–4434.

Destaillats, F.; Oliveira, M.; Bastic Schmid, V.; Masserey-Elmelegy, I.; Giuffrida, F.; Thakkar, S.K.; Dupuis, L.; Gosoniu, M.L.; Cruz-Hernandez, C. 2018. Comparison of the incorporation of DHA in circulatory and neural tissue when provided as Triacylglycerol (TAG), Monoacylglycerol (MAG) or Phospholipids (PL) provides new insight into fatty acid bioavailability. *Nutrients* 10: 620.

Devos, M.; Poisson, L.; Ergan, F.; Pencreac'h, G. 2006. Enzymatic hydrolysis of phospholipids from Isochrysis galbana for docosahexaenoic acid enrichment. *Enzyme and Microbial Technology* 39: 548–554.

Dixon, S.J.; Lemberg, K.M.; Lamprecht, M.R.; Skouta, R.; Zaitsev, E.M.; Gleason, C.E.; Patel, D.N.; Bauer, A.J.; Cantley, A.M.; Yang, W.S.; Morrison, B.; Stockwell, B.R. 2012. Ferroptosis: an iron-dependent form of nonapoptotic cell death. *Cell* 149: 1060–1072.

Djoussé, L.; Gaziano, J.M.; Buring, J.E.; Lee, I.-M. 2011. Dietary omega-3 fatty acids and fish consumption and risk of type 2 diabetes. *The American Journal of Clinical Nutrition* 93: 143–150.

Dossat, V.; Combes, D.; Marty, A. 2002. Efficient lipase catalysed production of a lubricant and surfactant formulation using a continuous solvent-free process. *Journal of Biotechnology* 97: 117–124.

Dyerberg, J.; Bang, H.O.; stoffersen, E.; moncada, S.; Vane, J.R. 1978. Eicosapentaenoic acid and prevention of thrombosis and atherosclerosis. *The Lancet* 312: 119-119.

Echeverría, F.; Valenzuela, R.; Catalina Hernandez-Rodas, M.; Valenzuela, A. 2017. Docosahexaenoic acid (DHA), a fundamental fatty acid for the brain: New dietary sources. *Prostaglandins, Leukotrienes, and Essential Fatty Acids* 124: 1–10.

Elagizi, A.; Lavie, C.J.; O'Keefe, E.; Marshall, K.; O'Keefe, J.H.; Milani, R.V. 2021. An update on omega-3 polyunsaturated fatty acids and cardiovascular health. *Nutrients* 13: 204.

El-Gawad, A. 2014. Oil and grease removal from industrial wastewater using new utility approach. *Advances in Environmental Chemistry* 2014: e916878.

Ericsson, D.J.; Kasrayan, A.; Johansson, P.; Bergfors, T.; Sandström, A.G.; Bäckvall, J.-E.; Mowbray, S.L. 2008. X-ray structure of *Candida antarctica* lipase A shows a novel lid structure and a likely mode of interfacial activation. *Journal of Molecular Biology* 376: 109–119.

Ewaschuk, J.B.; Newell, M.; Field, C.J. 2012. Docosahexanoic acid improves chemotherapy efficacy by inducing CD95 translocation to lipid rafts in ER− breast cancer cells. *Lipids* 47: 1019–1030.

Fabian, C.J.; Kimler, B.F.; Hursting, S.D. 2015. Omega-3 fatty acids for breast cancer prevention and survivorship. *Breast Cancer Research: BCR* 17: 62.

Farnet, A.-M.; Qasemian, L.; Gil, G.; Ferré, E. 2013. The importance of water availability in the reaction equilibrium of hydrolases in forest litters from a mediterranean area: a study on lipases. *European Journal of Soil Science* 64: 661–666.

Feltes, M.M.C.; Villeneuve, P.; Baréa, B.; Barouh, N.; de Oliveira, J.V.; de Oliveira, D.; Ninow, J.L. 2012. Enzymatic production of Monoacylglycerols (MAG) and Diacylglycerols (DAG) from fish oil in a solvent-free system. *Journal of the American Oil Chemists' Society* 89: 1057–1065.

Ferchaud-Roucher, V.; Kramer, A.; Silva, E.; Pantham, P.; Weintraub, S.T.; Jansson, T.; Powell, T.L. 2019. A potential role for lysophosphatidylcholine in the delivery of long chain polyunsaturated fatty acids to the fetal circulation. *Biochimica et Biophysica Acta Molecular and Cell Biology of Lipids* 1864: 394–402.

Fernandez-Lopez, L.; Virgen-ORTÍz, J.J.; Pedrero, S.G.; Lopez-Carrobles, N.; Gorines, B.C.; Otero, C.; Fernandez-Lafuente, R. 2018. Optimization of the coating of octyl-CALB with ionic polymers to improve stability and decrease enzyme leakage. *Biocatalysis and Biotransformation* 36: 47–56.

Ferreira, A.K.; de-Sá-Júnior, P.L.; Pasqualoto, K.F.M.; de Azevedo, R.A.; Câmara, D.A.D.; Costa, A.S.; Figueiredo, C.R.; Matsuo, A.L.; Massaoka, M.H.; Auada, A.V.V.; Lebrun, I.; Damião, M.C.F.C.B.; Tavares, M.T.; Magri, F.M.M.; Kerkis, I.; Parise Filho, R. 2014. Cytotoxic effects of dillapiole on MDA-MB-231 cells involve the induction of apoptosis through the mitochondrial pathway by inducing an oxidative stress while altering the cytoskeleton network. *Biochimie* 99: 195–207.

Ferreira, S.L.C.; Bruns, R.E.; Ferreira, H.S.; Matos, G.D.; David, J.M.; Brandão, G.C.; da Silva, E.G.P.; Portugal, L.A.; dos Reis, P.S.; Souza, A.S.; dos Santos, W.N.L. 2007. Box-Behnken design: An alternative for the optimization of analytical methods. *Analytica Chimica Acta* 597: 179–186.

Fhaner, M.; Hwang, H.-S.; Winkler-Moser, J.K.; Bakota, E.L.; Liu, S.X. 2016. Protection of fish oil from oxidation with sesamol. *European Journal of Lipid Science and Technology* 118: 885–897.

Foresti, M.L.; Pedernera, M.; Bucalá, V.; Ferreira, M.L. 2007. Multiple effects of water on solvent-free enzymatic esterifications. *Enzyme and Microbial Technology* 41: 62–70.

Gendaszewska-Darmach, E.; Drzazga, A. 2014. Biological Relevance of Lysophospholipids and Green Solutions for Their Synthesis. *Current Organic Chemistry* 18: 2928–2949.

Gerber, M. 2012. Omega-3 fatty acids and cancers: a systematic update review of epidemiological studies. *The British Journal of Nutrition* 107 Suppl 2: S228-239.

Ghasemifard, S.; Turchini, G.M.; Sinclair, A.J. 2014. Omega-3 long chain fatty acid "bioavailability": A review of evidence and methodological considerations. *Progress in Lipid Research* 56: 92–108.

González-Fernández, M.J.; Fabrikov, D.; Ramos-Bueno, R.P.; Guil-Guerrero, J.L.; Ortea, I. 2019. SWATH Differential Abundance Proteomics and Cellular Assays Show In Vitro Anticancer Activity of Arachidonic Acid- and Docosahexaenoic Acid-Based Monoacylglycerols in HT-29 Colorectal Cancer Cells. *Nutrients* 11: 2984.

Govardhan, C.P. 1999. Crosslinking of enzymes for improved stability and performance. *Current Opinion in Biotechnology* 10: 331–335.

Grimsgaard, S.; Bønaa, K.H.; Hansen, J.B.; Myhre, E.S. 1998. Effects of highly purified eicosapentaenoic acid and docosahexaenoic acid on hemodynamics in humans. *The American Journal of Clinical Nutrition* 68: 52–59.

Gupta, C.; Prakash, D.; Gupta, S. 2015. A Biotechnological Approach to Microbial Based Perfumes and Flavours. *Journal of Microbiology & Experimentation* 2:11-18.

Han, J.J.; Rhee, J.S. 1995. Lipase-catalyzed synthesis of lysophosphatidic acid in a solvent free system. *Biotechnology Letters* 17: 531–536.

Han, J.J.; Rhee, J.S. 1998. Effect of salt hydrate pairs for water activity control on lipase-catalyzed synthesis of lysophospholipids in a solvent-free system. *Enzyme and Microbial Technology* 22: 158–164.

Hara, F.; Nakashima, T.; Fukuda, H. 1997. Comparative study of commercially available lipases in hydrolysis reaction of phosphatidylcholine. *Journal of the American Oil Chemists' Society* 74: 1129–1132.

Hasan, F.; Shah, A.A.; Hameed, A. 2006. Industrial applications of microbial lipases. *Enzyme and Microbial Technology* 39: 235–251.

Heras-Sandoval, D.; Pedraza-Chaverri, J.; Pérez-Rojas, J.M. 2016. Role of docosahexaenoic acid in the modulation of glial cells in Alzheimer's disease. *Journal of Neuroinflammation* 13: 61.

Herbst, D.; Peper, S.; Niemeyer, B. 2012. Enzyme catalysis in organic solvents: influence of water content, solvent composition and temperature on Candida rugosa lipase catalyzed transesterification. *Journal of Biotechnology* 162: 398–403.

Herries, D.G. 1985. Enzyme structure and mechanism (second edition), by Alan Fersht. *Biochemical Education* 13: 146–146.

Hidayat, K.; Yang, J.; Zhang, Z.; Chen, G.-C.; Qin, L.-Q.; Eggersdorfer, M.; Zhang, W. 2018. Effect of omega-3 long-chain polyunsaturated fatty acid supplementation on heart rate: a meta-analysis of randomized controlled trials. *European Journal of Clinical Nutrition* 72: 805–817.

Holland, B.; Bernhardt, R.; Sajic, B. 2020. Cold-water laundry detergents. *United States Patent*. US 10,570,352 B2.

Hong, S.I.; Kim, Y.; Kim, C.-T.; Kim, I.-H. 2011. Enzymatic synthesis of lysophosphatidylcholine containing CLA from sn-glycero-3-phosphatidylcholine (GPC) under vacuum. *Food Chemistry* 129: 1–6.

Hosokawa, M.; Ono, M.; Takahashi, K.; Inoue, Y. 1998. Increase in deformability of human erythrocytes through the action of β-lysophospholipid rich in n-3 polyunsaturated fatty acid content. *Journal of Japan Oil Chemists' Society* 47 (12): 1313–1318.

Hosomi, R.; Fukunaga, K.; Nagao, T.; Shiba, S.; Miyauchi, K.; Yoshida, M.; Takahashi, K. 2019. Effect of dietary oil rich in docosahexaenoic acid-bound lysophosphatidylcholine prepared from fishery

by-products on lipid and fatty acid composition in rat liver and brain. *Journal of Oleo Science* 68: 781–792.

Hossain, Z.; Hosokawa, M.; Takahashi, K. 2008. Growth inhibition and induction of apoptosis of colon cancer cell lines by applying marine phospholipid. *Nutrition and Cancer* 61: 123–130.

Hossain, Z.; Konishi, M.; Hosokawa, M.; Takahashi, K. 2006. Effect of polyunsaturated fatty acid-enriched phosphatidylcholine and phosphatidylserine on butyrate-induced growth inhibition, differentiation and apoptosis in Caco-2 cells. *Cell Biochemistry and Function* 24: 159–165.

Huang, L.S.; Hung, N.D.; Sok, D.-E.; Kim, M.R. 2010. Lysophosphatidylcholine containing docosahexaenoic acid at the *sn*-1 position is anti-inflammatory. *Lipids* 45: 225–236.

Hubert, F. 2018. Synthèse enzymatique de phospholipides structurés riches en DHA. Thesis, Université du Maine, (https://tel.archives-ouvertes.fr/tel-01887172).

Hung, N.D.; Kim, M.R.; Sok, D.-E. 2011a. Oral administration of 2-docosahexaenoyl lysophosphatidylcholine displayed anti-inflammatory effects on zymosan a-induced peritonitis. *Inflammation* 34: 147–160.

Hung, N.D.; Kim, M.R.; Sok, D.-E. 2011b. Mechanisms for anti-inflammatory effects of 1-[15(S)-hydroxyeicosapentaenoyl] lysophosphatidylcholine, administered intraperitoneally, in zymosan A-induced peritonitis. *British Journal of Pharmacology* 162: 1119–1135.

Hvidsten, I.B.; Marchetti, J.M. 2021. Novozym® 435 as bio-catalyst in the synthesis of methyl laurate. *Energy Conversion and Management: X* 10: 100061.

Innes, J.K.; Calder, P.C. 2020. Marine omega-3 (n-3) fatty acids for cardiovascular health: An update for 2020. *International Journal of Molecular Sciences* 21: E1362.

Islam, M.A.; Amin, M.N.; Siddiqui, S.A.; Hossain, M.P.; Sultana, F.; Kabir, M.R. 2019. Trans fatty acids and lipid profile: A serious risk factor to cardiovascular disease, cancer and diabetes. *Diabetes & Metabolic Syndrome* 13: 1643–1647.

Jaeger, K.-E.; Reetz, M.T. 1998. Microbial lipases form versatile tools for biotechnology. *Trends in Biotechnology* 16: 396–403.

Jaeger, K.-E.; Eggert, T. 2002. Lipases for biotechnology. *Current Opinion in Biotechnology* 13: 390–397.

Jaeger, K.-E.; Dijkstra, B.W.; Reetz, M.T. 1999. Bacterial biocatalysts: molecular biology, three-dimensional structures, and biotechnological applications of lipases. *Annual Review of Microbiology* 53: 315–351.

Jala, R.C.R.; Hu, P.; Yang, T.; Jiang, Y.; Zheng, Y.; Xu, X. 2012. Lipases as biocatalysts for the synthesis of structured lipids. *Lipases and Phospholipases: Methods and Protocols*, Humana Press, Totowa, NJ, p.403–433.

Javadian, M.; Shekari, N.; Zangbar, M.S.S.-; Mohammadi, A.; Mansoori, B.; Maralbashi, S.; Shanehbandi, D.; Baradaran, B.; Darabi, M.; Kazemi, T. 2020. Docosahexaenoic acid suppresses

migration of triple-negative breast cancer cell through targeting metastasis-related genes and microRNA under normoxic and hypoxic conditions. *Journal of Cellular Biochemistry* 121: 2416–2427.

Jensen, R.G.; deJong, F.A.; Clark, R.M. 1983. Determination of lipase specificity. *Lipids* 18: 239–252.

Ji, X.-W.; Wang, J.; Shen, Q.-M.; Li, Z.-Y.; Jiang, Y.-F.; Liu, D.-K.; Tan, Y.-T.; Li, H.-L.; Xiang, Y.-B. 2021. Dietary fat intake and liver cancer incidence: A population-based cohort study in Chinese men. *International Journal of Cancer* 148: 2982–2996.

Jin, M.C.; Hung, N.D.; Yoo, J.M.; Kim, M.R.; Sok, D.-E. 2012. Suppressive effect of docosahexaenoyl-lysophosphatidylcholine and 17-hydroxydocosahexaenoyl-lysophosphatidylcholine on levels of cytokines in spleen of mice treated with lipopolysaccharide. *European Journal of Lipid Science and Technology* 114: 114–122.

Jolly, J.F. 2015. Enzymatic methods of flavor modification. *United States Patent*.

Judge, M.P.; Harel, O.; Lammi-Keefe, C.J. 2007. A docosahexaenoic acid-functional food during pregnancy benefits infant visual acuity at four but not six months of age. *Lipids* 42: 117–122.

Juhan, K.; Byung-Gee, K. 1998. Lipase-catalyzed synthesis of lysophosphatidylcholine. *Annals of the New York Academy of Sciences* 864:341-344.

Juhan, K.; Byung-Gee, K. 2000. Lipase-catalyzed synthesis of lysophosphatidylcholine using organic cosolvent for in situ water activity control. *Journal of the American Oil Chemists' Society* 77: 151-742.

Han, J.; Rhee, J. 1998. Effect of salt hydrate pairs for water activity control on lipase-catalyzed synthesis of lysophospholipids in a solvent-free system. *Enzyme and Microbial Technology* 22: 158-164.

Kapoor, M.; Gupta, M.N. 2012. Lipase promiscuity and its biochemical applications. *Process Biochemistry* 47: 555–569.

Keane, M.M.; Ettenberg, S.A.; Nau, M.M.; Russell, E.K.; Lipkowitz, S. 1999. Chemotherapy augments tRAIL-induced apoptosis in breast cell lines. *Cancer Research* 59: 734–741.

Keskin Gündoğdu, T.; Deniz, İ.; Çalışkan, G.; Şahin, E.S.; Azbar, N. 2016. Experimental design methods for bioengineering applications. *Critical Reviews in Biotechnology* 36: 368–388.

Khaddaj-Mallat, R.; Morin, C.; Rousseau, É. 2016. Novel n-3 PUFA monoacylglycerides of pharmacological and medicinal interest: Anti-inflammatory and anti-proliferative effects. *European Journal of Pharmacology* 792: 70–77.

Kim, J.; Kim, B.-G. 2000. Lipase-catalyzed synthesis of lysophosphatidylcholine using organic cosolvent for in situ water activity control. *Journal of the American Oil Chemists' Society* 77: 791–797.

Kim, N.; Jeong, S.; Jing, K.; Shin, S.; Kim, S.; Heo, J.-Y.; Kweon, G.-R.; Park, S.-K.; Wu, T.; Park, J.-I.; Lim, K. 2015. Docosahexaenoic acid induces cell death in human non-small cell lung cancer cells by

repressing mTOR via AMPK activation and PI3K/Akt inhibition. *BioMed Research International* 2015: e239764.

Kim, S.; Jing, K.; Shin, S.; Jeong, S.; Han, S.-H.; Oh, H.; Yoo, Y.-S.; Han, J.; Jeon, Y.-J.; Heo, J.-Y.; Kweon, G.-R.; Park, S.-K.; Park, J.-I.; Wu, T.; Lim, K. 2018. ω3-polyunsaturated fatty acids induce cell death through apoptosis and autophagy in glioblastoma cells: In vitro and in vivo. *Oncology Reports* 39: 239–246.

Kim, Y.-L.; Im, Y.-J.; Ha, N.-C.; Im, D.-S. 2007. Albumin inhibits cytotoxic activity of lysophosphatidylcholine by direct binding. *Prostaglandins & Other Lipid Mediators* 83: 130–138.

Kirk, R. 2002. Experimental Design. *Handbook of Psychology* 2: 3–32.

Klibanov, A.M. 2001. Improving enzymes by using them in organic solvents. *Nature* 409: 241–246.

Kobata, K.; Kawaguchi, M.; Watanabe, T. 2002. Enzymatic synthesis of a capsinoid by the acylation of vanillyl alcohol with fatty acid derivatives catalyzed by lipases. *Bioscience, Biotechnology, and Biochemistry* 66: 319–327.

Köhler, A.; Sarkkinen, E.; Tapola, N.; Niskanen, T.; Bruheim, I. 2015. Bioavailability of fatty acids from krill oil, krill meal and fish oil in healthy subjects–a randomized, single-dose, cross-over trial. *Lipids in Health and Disease* 14: 19.

Kontogianni, A.; Skouridou, V.; Sereti, V.; Stamatis, H.; Kolisis, F.N. 2003. Lipase-catalyzed esterification of rutin and naringin with fatty acids of medium carbon chain. *Journal of Molecular Catalysis B: Enzymatic* 21: 59–62.

Krysko, D.V.; Vanden Berghe, T.; D'Herde, K.; Vandenabeele, P. 2008. Apoptosis and necrosis: detection, discrimination and phagocytosis. *Methods* 44: 205–221.

Lăcătuş, M.A. ; Bencze, L.C. ; Toşa, M.I. ; Paizs, C. ; Irimie, F-D. 2018. Eco-friendly enzymatic production of 2,5-Bis(hydroxymethyl)furan fatty acid diesters, potential biodiesel additives. *ACS Sustainable Chemistry & Engineering* 6 : 11353-11359.

Lacombe, R.J.S.; Chouinard-Watkins, R.; Bazinet, R.P. 2018. Brain docosahexaenoic acid uptake and metabolism. *Molecular Aspects of Medicine* 64: 109–134.

Lauritzen, L.; Brambilla, P.; Mazzocchi, A.; Harsløf, L.B.S.; Ciappolino, V.; Agostoni, C. 2016. DHA effects in brain development and function. *Nutrients* 8: E6.

Lee, S.A.; Whenham, N.; Bedford, M.R. 2019. Review on docosahexaenoic acid in poultry and swine nutrition: Consequence of enriched animal products on performance and health characteristics. *Animal Nutrition* 5: 11–21.

Lee, S.-M.; Asaduzzaman, A.K.M.; Chun, B.-S. 2012. Characterization of lecithin isolated from anchovy (Engraulis japonica) residues deoiled by supercritical carbon dioxide and organic solvent extraction. *Journal of Food Science* 77: C773–C778.

Li, B.; Wang, F.; Li, K.; Sun, S. 2021a. Biodiesel preparation from high acid value phoenix seed oil using Eversa transform 2.0 as a novel catalyst. *Biomass Conversion and Biorefinery*. https://doi.org/10.1007/s13399-021-01814-1

Li, D.; Wang, W.; Zhang, L.; Liu, N.; Faiza, M.; Tan, C.P.; Yang, B.; Lan, D.; Wang, Y. 2018a. Synthesis of CLA-Rich lysophosphatidylcholine by immobilized MAS1-H108A-catalyzed esterification: Effects of the parameters and monitoring of the reaction process. *European Journal of Lipid Science and Technology* 120: 1700529.

Li, J.; Pora, B.L.R.; Dong, K.; Hasjim, J. 2021b. Health benefits of docosahexaenoic acid and its bioavailability: A review. *Food Science & Nutrition* 9: 5229–5243.

Li, W.; Du, W.; Li, Q.; Sun, T.; Liu, D. 2010. Study on acyl migration kinetics of partial glycerides: Dependence on temperature and water activity. *Journal of Molecular Catalysis B: Enzymatic* 63: 17–22.

Li, X.-F.; Zong, M.-H.; Wu, H.; Lou, W.-Y. 2006. Markedly improving Novozym 435-mediated regioselective acylation of 1-β-d-arabinofuranosylcytosine by using co-solvent mixtures as the reaction media. *Journal of Biotechnology* 124: 552–560.

Liedtke, C.; Mazouni, C.; Hess, K.R.; André, F.; Tordai, A.; Mejia, J.A.; Symmans, W.F.; Gonzalez-Angulo, A.M.; Hennessy, B.; Green, M.; Cristofanilli, M.; Hortobagyi, G.N.; Pusztai, L. 2008. Response to neoadjuvant therapy and long-term survival in patients with triple-negative breast cancer. *Journal of Clinical Oncology* 26: 1275–1281.

Liu, Y.; Levine, B. 2015. Autosis and autophagic cell death: the dark side of autophagy. *Cell Death & Differentiation* 22: 367–376.

Liu, Y.; Tian, Y.; Cai, W.; Guo, Y.; Xue, C.; Wang, J. 2021. DHA/EPA-enriched phosphatidylcholine suppresses tumor growth and metastasis via activating peroxisome proliferator-activated receptor γ in lewis lung cancer mice. *Journal of Agricultural and Food Chemistry* 69: 676–685.

Liu, Y.; Zhang, Q.; Guo, Y.; Liu, J.; Xu, J.; Li, Z.; Wang, J.; Wang, Y.; Xue, C. 2017. Enzymatic synthesis of lysophosphatidylcholine with n−3 polyunsaturated fatty acid from sn-glycero-3-phosphatidylcholine in a solvent-free system. *Food Chemistry* 226: 165–170.

Lundstedt, T.; Seifert, E.; Abramo, L.; Thelin, B.; Nyström, Å.; Pettersen, J.; Bergman, R. 1998. Experimental design and optimization. *Chemometrics and Intelligent Laboratory Systems* 42: 3–40.

Lux, G.; Mansfeld, J.; Ulbrich-Hofmann, R. 2014. Phospholipase A2-catalyzed acylation of lysophospholipids analyzed by experimental design. *Enzyme and Microbial Technology* 64–65: 60–66.

Lyberg, A.-M.; Fasoli, E.; Adlercreutz, P. 2005. Monitoring the oxidation of docosahexaenoic acid in lipids. *Lipids* 40: 969.

Lykidis, A. 2007. Comparative genomics and evolution of eukaryotic phospholipid biosynthesis. *Progress in Lipid Research* 46: 171–199.

Madani, S.; Hichami, A.; Charkaoui-Malki, M.; Khan, N.A. 2004. Diacylglycerols containing omega 3 and omega 6 fatty acids bind to RasGRP and modulate MAP Kinase activation. *Journal of Biological Chemistry* 279: 1176–1183.

Majno, G.; Joris, I. 1995. Apoptosis, oncosis, and necrosis. An overview of cell death. *The American Journal of Pathology* 146: 3–15.

Malipeddi, H.; Das, P.; Karigar, A. 2011. Green technique-solvent free synthesis and its advantages. *International Journal of Research and Pharmacy* 2: 1079–1086.

Mallick, R.; Basak, S.; Duttaroy, A.K. 2019. Docosahexaenoic acid,22:6n-3: Its roles in the structure and function of the brain. *International Journal of Developmental Neuroscience* 79: 21–31.

Manan, F.M.A.; Attan, N.; Zakaria, Z.; Keyon, A.S.A.; Wahab, R.A. 2018. Enzymatic esterification of eugenol and benzoic acid by a novel chitosan-chitin nanowhiskers supported Rhizomucor miehei lipase: Process optimization and kinetic assessments. *Enzyme and Microbial Technology* 108: 42–52.

Mandal, C.C.; Ghosh-Choudhury, T.; Yoneda, T.; Choudhury, G.G.; Ghosh-Choudhury, N. 2010. Fish oil prevents breast cancer cell metastasis to bone. *Biochemical and Biophysical Research Communications* 402: 602–607.

Manual Kollareth, D.J.; Deckelbaum, R.J.; Liu, Z.; Ramakrishnan, R.; Jouvene, C.; Serhan, C.N.; Ten, V.S.; Zirpoli, H. 2020. Acute injection of a DHA triglyceride emulsion after hypoxic-ischemic brain injury in mice increases both DHA and EPA levels in blood and brain. *Prostaglandins, Leukotrienes and Essential Fatty Acids* 162: 102176.

Mason, R.P.; Libby, P.; Bhatt, D.L. 2020. Emerging mechanisms of cardiovascular protection for the omega-3 fatty acid eicosapentaenoic acid. *Arteriosclerosis, Thrombosis, and Vascular Biology* 40: 1135–1147.

Mayurasakorn, K.; Niatsetskaya, Z.V.; Sosunov, S.A.; Williams, J.J.; Zirpoli, H.; Vlasakov, I.; Deckelbaum, R.J.; Ten, V.S. 2016. DHA but not EPA emulsions preserve neurological and mitochondrial function after brain hypoxia-ischemia in neonatal mice. *PLOS ONE* 11: e0160870.

Van Meer, G.; Voelker, D.R.; Feigenson, G.W. 2008. Membrane lipids: where they are and how they behave. *Nature Reviews. Molecular Cell Biology* 9: 112–124.

Melov, S.; Coskun, P.; Patel, M.; Tuinstra, R.; Cottrell, B.; Jun, A.S.; Zastawny, T.H.; Dizdaroglu, M.; Goodman, S.I.; Huang, T.-T.; Miziorko, H.; Epstein, C.J.; Wallace, D.C. 1999. Mitochondrial disease in superoxide dismutase 2 mutant mice. *Proceedings of the National Academy of Sciences* 96: 846–851.

Mitchell, P. 2012. Autophagy. *Nexcelom Bioscience*.

Mizushima, N.; Komatsu, M. 2011. Autophagy: renovation of cells and tissues. *Cell* 147: 728–741.

Mnasri, T.; Ergan, F.; Herault, J.; Pencreac'h, G. 2017a. Lipase-catalyzed Synthesis of oleoyl-lysophosphatidylcholine by direct esterification in solvent-free medium without water removal. *Journal of Oleo Science* advpub.

Mnasri, T.; Hérault, J.; Gauvry, L.; Loiseau, C.; Poisson, L.; Ergan, F.; Pencréac'h, G. 2017b. Lipase-catalyzed production of lysophospholipids. *OCL* 24: D405.

Moghadasian, M.H. 2008. Advances in dietary enrichment with n-3 fatty acids. *Critical Reviews in Food Science and Nutrition* 48: 402–410.

Morin, C.; Fortin, S.; Rousseau, E. 2012. Docosahexaenoic acid monoacylglyceride decreases endothelin-1 induced Ca2+ sensitivity and proliferation in human pulmonary arteries. *American Journal of Hypertension* 25: 756–763.

Morin, C.; Rousseau, É.; Fortin, S. 2013. Anti-proliferative effects of a new docosapentaenoic acid monoacylglyceride in colorectal carcinoma cells. *Prostaglandins, Leukotrienes and Essential Fatty Acids* 89: 203–213.

Morin, C.; Rousseau, E.; Blier, P.U.; Fortin, S. 2015. Effect of docosahexaenoic acid monoacylglyceride on systemic hypertension and cardiovascular dysfunction. *American Journal of Physiology-Heart and Circulatory Physiology* 309: H93–H102.

Morland, S.L.; Martins, K.J.B.; Mazurak, V.C. 2016. N-3 polyunsaturated fatty acid supplementation during cancer chemotherapy. *Journal of Nutrition & Intermediary Metabolism* 5: 107–116.

Mortimore, G.E.; Miotto, G.; Venerando, R.; Kadowaki, M. 1996. Autophagy. In: Lloyd, J.B.; Mason, R.W. (Eds.), *Biology of the Lysosome*, Springer US, Boston, MA, p.93–135. https://doi.org/10.1007/978-1-4615-5833-0_4

Mun, J.G.; Legette, L.L.; Ikonte, C.J.; Mitmesser, S.H. 2019. Choline and DHA in maternal and infant nutrition: Synergistic implications in brain and eye health. *Nutrients* 11: E1125.

Nakajima, N.; Ishihara, K.; Hamada, H.; Kawabe, S.-I.; Furuya, T. 2000. Regioselective acylation of flavonoid glucoside with aromatic acid by an enzymatic reaction system from cultured cells of Ipomoea batatas. *Journal of Bioscience and Bioengineering* 90: 347–349.

Newell, M.; Baker, K.; Postovit, L.M.; Field, C.J. 2017. A critical review on the effect of docosahexaenoic acid (DHA) on cancer cell cycle progression. *International Journal of Molecular Sciences* 18: 1784.

Newell, M.; Patel, D.; Goruk, S.; Field, C.J. 2020. Docosahexaenoic acid incorporation is not affected by doxorubicin chemotherapy in either whole cell or lipid raft phospholipids of breast cancer cells in vitro and tumor phospholipids in vivo. *Lipids*.

Nguyen, H.H.; Kim, M. 2017. An overview of techniques in enzyme immobilization. *Applied Science and Convergence Technology* 26: 157–163.

Niyonzima, F.N.; More, S.S. 2015. Coproduction of detergent compatible bacterial enzymes and stain removal evaluation. *Journal of Basic Microbiology* 55: 1149–1158.

Okuro, P.K.; Gomes, A.; Costa, A.L.R.; Adame, M.A.; Cunha, R.L. 2019. Formation and stability of W/O-high internal phase emulsions (HIPEs) and derived O/W emulsions stabilized by PGPR and lecithin. *Food Research International* 122: 252–262.

Ono, M.; Hosokawa, M.; Inoue, Y.; Takahashi, K. 1997. Water activity-adjusted enzymatic partial hydrolysis of phospholipids to concentrate polyunsaturated fatty acids. *Journal of the American Oil Chemists' Society* 74: 1415–1417.

Ortiz, C.; Luján Ferreira, M.; Barbosa, O.; Santos, J.C.S. dos; C. Rodrigues, R.; Berenguer-Murcia, Á.; E. Briand, L.; Fernandez-Lafuente, R. 2019. Novozym 435: the "perfect" lipase immobilized biocatalyst? *Catalysis Science & Technology* 9: 2380–2420.

Osborn, H.T.; Akoh, C.C. 2002. Structured lipids-novel fats with medical, nutraceutical, and food applications. *Comprehensive Reviews in Food Science and Food Safety* 1: 110–120.

Osborne, C.K. 1998. Tamoxifen in the treatment of breast cancer. *New England Journal of Medicine* 339: 1609–1618.

Ou, W.; Mulik, R.S.; Anwar, A.; McDonald, J.G.; He, X.; Corbin, I.R. 2017. Low-density lipoprotein docosahexaenoic acid nanoparticles induce ferroptotic cell death in hepatocellular carcinoma. *Free Radical Biology and Medicine* 112: 597–607.

Panawala, L. 2017. Difference between apoptosis and necrosis. *PEDIAA*.

Pando, M.E.; Rodríguez, A.; Valenzuela, M.A.; Berríos, M.M.; Rivera, M.; Romero, N.; Barriga, A.; Aubourg, S.P. 2021. Acylglycerol synthesis including EPA and DHA from rainbow trout (Oncorhynchus mykiss) belly flap oil and caprylic acid catalyzed by Thermomyces lanuginosus lipase under supercritical carbon dioxide. *European Food Research and Technology* 247: 499–511.

Park, J.; Choi, J.; Kim, D.-D.; Lee, S.; Lee, B.; Lee, Y.; Kim, S.; Kwon, S.; Noh, M.; Lee, M.-O.; Le, Q.-V.; Oh, Y.-K. 2021. Bioactive lipids and their derivatives in biomedical applications. *Biomolecules & Therapeutics* 29: 465–482.

Peng, B.; Chen, F.; Liu, X.; Hu, J.-N.; Zheng, L.-F.; Li, J.; Deng, Z.-Y. 2020. Trace water activity could improve the formation of 1,3-oleic-2-medium chain-rich triacylglycerols by promoting acyl migration in the lipase RM IM catalyzed interesterification. *Food Chemistry* 313: 126130.

Pereira, L.M.S.; Milan, T.M.; Tapia-Blácido, D.R. 2021. Using Response Surface Methodology (RSM) to optimize 2G bioethanol production: A review. *Biomass and Bioenergy* 151: 106166.

Peters, G.H.; Toxvaerd, S.; Olsen, O.H.; Svendsen, A. 1997. Computational studies of the activation of lipases and the effect of a hydrophobic environment. *Protein Engineering, Design and Selection* 10: 137–147.

Petersson, A.E.V.; Adlercreutz, P.; Mattiasson, B. 2007. A water activity control system for enzymatic reactions in organic media. *Biotechnology and Bioengineering* 97: 235–241.

Pfleeger, S.L. 1995. Experimental design and analysis in software engineering: Types of experimental design. *ACM SIGSOFT Software Engineering Notes* 20: 14–16.

Pizato, N.; Luzete, B.C.; Kiffer, L.F.M.V.; Corrêa, L.H.; de Oliveira Santos, I.; Assumpção, J.A.F.; Ito, M.K.; Magalhães, K.G. 2018. Omega-3 docosahexaenoic acid induces pyroptosis cell death in triple-negative breast cancer cells. *Scientific Reports* 8: 1952.

Plourde, M.; Cunnane, S.C. 2007. Extremely limited synthesis of long chain polyunsaturates in adults: implications for their dietary essentiality and use as supplements. *Applied Physiology, Nutrition, and Metabolism* 32: 619–634.

Poisson, L.; Devos, M.; Godet, S.; Ergan, F.; Pencreac'h, G. 2009. Acyl migration during deacylation of phospholipids rich in docosahexaenoic acid (DHA): an enzymatic approach for evidence and study. *Biotechnology Letters* 31: 743–749.

Pollak, A.; Blumenfeld, H.; Wax, M.; Baughn, R.L.; Whitesides, G.M. 1980. Enzyme immobilization by condensation copolymerization into crosslinked polyacrylamide gels. *Journal of the American Chemical Society* 102: 6324–6336.

Radmacher, M.D.; Simon, R. 2000. Estimation of tamoxifen's efficacy for preventing the formation and growth of breast tumors. *JNCI: Journal of the National Cancer Institute* 92: 48–53.

Rahman, M.M.; Veigas, J.M.; Williams, P.J.; Fernandes, G. 2013. DHA is a more potent inhibitor of breast cancer metastasis to bone and related osteolysis than EPA. *Breast Cancer Research and Treatment* 141: 341–352.

Reis, P.; Holmberg, K.; Watzke, H.; Leser, M.E.; Miller, R. 2009. Lipases at interfaces: A review. *Advances in Colloid and Interface Science* 147–148: 237–250.

Rizzo, A.M.; Colombo, I.; Montorfano, G.; Zava, S.; Corsetto, P.A. 2021. Exogenous fatty acids modulate ER lipid composition and metabolism in breast cancer cells. *Cells* 10: 175.

Rosen, C.L.; Lisanti, M.P.; Salzer, J.L. 1992. Expression of unique sets of GPI-linked proteins by different primary neurons *in vitro*. *The Journal of Cell Biology* 117: 617–627.

Ross, T.; Jakubzig, B.; Grundmann, M.; Massing, U.; Kostenis, E.; Schlesinger, M.; Bendas, G. 2016. The molecular mechanism by which saturated lysophosphatidylcholine attenuates the metastatic capacity of melanoma cells. *FEBS Open Bio* 6: 1297–1309.

Rosu, R.; Yasui, M.; Iwasaki, Y.; Yamane, T. 1999. Enzymatic synthesis of symmetrical 1,3-diacylglycerols by direct esterification of glycerol in solvent-free system. *Journal of the American Oil Chemists' Society* 76: 839.

Rosu, R.; Iwasaki, Y.; Shimidzu, N.; Doisaki, N.; Yamane, T. 1998. Enzymatic synthesis of glycerides from DHA-enriched PUFA ethyl ester by glycerolysis under vacuum. *Journal of Molecular Catalysis B: Enzymatic* 4: 191–198.

Rueda, N.; Santos, J.C.S. dos; Torres, R.; Ortiz, C.; Barbosa, O.; Fernandez-Lafuente, R. 2015. Improved performance of lipases immobilized on heterofunctional octyl-glyoxyl agarose beads. *RSC Advances* 5: 11212–11222.

Ryan, A.S.; Keske, M.A.; Hoffman, J.P.; Nelson, E.B. 2009. Clinical overview of algal-docosahexaenoic acid: Effects on triglyceride levels and other cardiovascular risk factors. *American Journal of Therapeutics* 16: 183–192.

Rychlicka, M.; Niezgoda, N.; Gliszczyńska, A. 2020. Development and optimization of lipase-catalyzed synthesis of phospholipids containing 3,4-dimethoxycinnamic acid by Response Surface Methodology. *Catalysts* 10: 588.

Sá, A.G.A.; Meneses, A.C. de; Araújo, P.H.H. de; Oliveira, D. de. 2017. A review on enzymatic synthesis of aromatic esters used as flavor ingredients for food, cosmetics and pharmaceuticals industries. *Trends in Food Science & Technology* 69: 95–105.

Sakai, C.; Ishida, M.; Ohba, H.; Yamashita, H.; Uchida, H.; Yoshizumi, M.; Ishida, T. 2017. Fish oil omega-3 polyunsaturated fatty acids attenuate oxidative stress-induced DNA damage in vascular endothelial cells. *PLOS ONE* 12: e0187934.

Salem, N.; Vandal, M.; Calon, F. 2015. The benefit of docosahexaenoic acid for the adult brain in aging and dementia. *Prostaglandins, Leukotrienes, and Essential Fatty Acids* 92: 15–22.

Sarney, D.B.; Fregapane, G.; Vulfson, E.N. 1994. Lipase-catalyzed synthesis of lysophospholipids in a continuous bioreactor. *Journal of the American Oil Chemists' Society* 71: 93–96.

Saunders, P.; Brask, J. 2021. Improved immobilization supports for *Candida antarctica* lipase B. *Biocatalysis in Polymer Chemistry*, John Wiley & Sons, Ltd, p.65–82.

Schmid, R.D.; Verger, R. 1998. Lipases: Interfacial enzymes with attractive applications. *Angewandte Chemie International Edition* 37: 1608–1633.

Schneider, M. 2001. Phospholipids for functional food. *European Journal of Lipid Science and Technology* 103: 98–101.

Schuchardt, J.P.; Hahn, A. 2013. Bioavailability of long-chain omega-3 fatty acids. *Prostaglandins, Leukotrienes and Essential Fatty Acids* 89: 1–8.

Shahidi, F.; Ambigaipalan, P. 2018. Omega-3 polyunsaturated fatty acids and their health benefits. a*nnual review of food science and technology* 9: 345–381.

Shan, C.; Wang, R.; Wang, S.; Zhang, Z.; Xing, C.; Feng, W.; Zhao, Z.; Zhou, S.; Zhao, A.Z.; Mu, Y.; Li, F. 2021. Endogenous production of n−3 polyunsaturated fatty acids protects mice from carbon tetrachloride-induced liver fibrosis by regulating mTOR and Bcl-2/Bax signalling pathways. *Experimental Physiology* 106: 983–993.

Shanab, S.M.M.; Hafez, R.M.; Fouad, A.S. 2018. A review on algae and plants as potential source of arachidonic acid. *Journal of Advanced Research* 11: 3–13.

Sharma, R.; Sharma, N. 2018. Microbial lipase mediated by health beneficial modification of cholesterol and flavors in food products: A Review. *Recent Patents on Biotechnology* 12: 81–91.

Sharma, S.; Kanwar, S.S. 2014. Organic solvent tolerant lipases and applications. *The Scientific World Journal* 2014: e625258.

Sharma, T.; Sharma, A.; Maheshwari, R.; Pachori, G.; Kumari, P.; Mandal, C.C. 2020. Docosahexaenoic acid (DHA) inhibits Bone Morphogenetic Protein-2 (BMP-2) elevated osteoblast potential of metastatic breast cancer (MDA-MB-231) cells in mammary microcalcification. *Nutrition and Cancer* 72: 873–883.

Sheldon, R.; Pelt, S. van. 2013. Enzyme immobilisation in biocatalysis: why, what and how. *Chemical Society Reviews* 42: 6223–6235.

Shi, H.; Zou, J.; Zhang, T.; Che, H.; Gao, X.; Wang, C.; Wang, Y.; Xue, C. 2018. Protective effects of DHA-PC against vancomycin-induced nephrotoxicity through the inhibition of oxidative stress and apoptosis in BALB/c Mice. *Journal of Agricultural and Food Chemistry* 66: 475–484.

Siddiqui, R.A.; Harvey, K.A.; Xu, Z.; Bammerlin, E.M.; Walker, C.; Altenburg, J.D. 2011. Docosahexaenoic acid: A natural powerful adjuvant that improves efficacy for anticancer treatment with no adverse effects. *BioFactors* 37: 399–412.

Silva, T.J.; Barrera-Arellano, D.; Ribeiro, A.P.B. 2021. Margarines: Historical approach, technological aspects, nutritional profile, and global trends. *Food Research International (Ottawa, Ont.)* 147: 110486.

Sommerfeld, M. 1983. Trans unsaturated fatty acids in natural products and processed foods. *Progress in Lipid Research* 22: 221–233.

Song, E.A.; Kim, H. 2016. Docosahexaenoic acid induces oxidative DNA damage and apoptosis, and enhances the chemosensitivity of cancer cells. *International Journal of Molecular Sciences* 17: 1257.

Sousa, R.R.; Silva, A.S.; Fernandez-Lafuente, R.; Ferreira-Leitão, V.S. 2021. Solvent-free esterifications mediated by immobilized lipases: a review from thermodynamic and kinetic perspectives. *Catalysis Science & Technology* 11: 5696–5711.

Stauch, B.; Fisher, S.J.; Cianci, M. 2015. Open and closed states of *Candida antarctica* lipase B: protonation and the mechanism of interfacial activation. *Journal of Lipid Research* 56: 2348–2358.

Stead, D. 1986. Microbial lipases: their characteristics, role in food spoilage and industrial uses. *The Journal of Dairy Research* 53: 481–505.

Stillwell, W.; Wassall, S.R. 2003. Docosahexaenoic acid: membrane properties of a unique fatty acid. *Chemistry and Physics of Lipids* 126: 1–27.

Straarup, E.M.; Høy;, C.-E. 2000. Structured lipids improve fat absorption in normal and malabsorbing rats. *The Journal of Nutrition* 130: 2802–2808.

Sugasini, D.; Subbaiah, P.V. 2017. Rate of acyl migration in lysophosphatidylcholine (LPC) is dependent upon the nature of the acyl group. Greater stability of *sn*-2 docosahexaenoyl LPC compared to the more saturated LPC species. *PloS One* 12: e0187826.

Sugasini, D.; Yalagala, P.C.R.; Subbaiah, P.V. 2020. Efficient enrichment of retinal DHA with dietary lysophosphatidylcholine-DHA: Potential application for retinopathies. *Nutrients* 12: 3114.

Sugasini, D.; Thomas, R.; Yalagala, P.C.R.; Tai, L.M.; Subbaiah, P.V. 2017. Dietary docosahexaenoic acid (DHA) as lysophosphatidylcholine, but not as free acid, enriches brain DHA and improves memory in adult mice. *Scientific Reports* 7: 1–11.

Sugasini, D.; Yalagala, P.C.R.; Goggin, A.; Tai, L.M.; Subbaiah, P.V. 2019. Enrichment of brain docosahexaenoic acid (DHA) is highly dependent upon the molecular carrier of dietary DHA: lysophosphatidylcholine is more efficient than either phosphatidylcholine or triacylglycerol. *The Journal of Nutritional Biochemistry* 74: 108231.

Tamarindo, G.H.; Góes, R.M. 2020. Docosahexaenoic acid differentially modulates the cell cycle and metabolism- related genes in tumor and pre-malignant prostate cells. *Biochimica et Biophysica Acta (BBA) - Molecular and Cell Biology of Lipids* 1865: 158766.

Tan, S.T.; Ramesh, T.; Toh, X.R.; Nguyen, L.N. 2020. Emerging roles of lysophospholipids in health and disease. *Progress in Lipid Research* 80: 101068.

Tanida, I.; Ueno, T.; Kominami, E. 2008. LC3 and Autophagy. *Methods in Molecular Biology (Clifton, N.J.)* 445: 77–88.

Thornberry, N.A. 1998. Caspases: key mediators of apoptosis. *Chemistry & Biology* 5: R97-103.

Tokumura, A.; Sinomiya, J.; Kishimoto, S.; Tanaka, T.; Kogure, K.; SUGIURA, T.; SATOUCHI, K.; WAKU, K.; FUKUZAWA, K. 2002. Human platelets respond differentially to lysophosphatidic acids having a highly unsaturated fatty acyl group and alkyl ether-linked lysophosphatidic acids. *Biochemical Journal* 365: 617–628.

Trevan, M.D. 1988. Enzyme immobilization by adsorption. In: Walker, J.M. (Ed.), *New Protein Techniques*, Humana Press, Totowa, NJ, p.481–489.

Troesch, B.; Eggersdorfer, M.; Laviano, A.; Rolland, Y.; Smith, A.D.; Warnke, I.; Weimann, A.; Calder, P.C. 2020. Expert opinion on benefits of long-chain omega-3 fatty acids (DHA and EPA) in aging and clinical nutrition. *Nutrients* 12: E2555.

Tsai, C.-H.; Lii, C.-K.; Wang, T.-S.; Liu, K.-L.; Chen, H.-W.; Huang, C.-S.; Li, C.-C. 2021. Docosahexaenoic acid promotes the formation of autophagosomes in MCF-7 breast cancer cells through oxidative stress-induced growth inhibitor 1 mediated activation of AMPK/mTOR pathway. *Food and Chemical Toxicology* 154: 112318.

Tsushima, T.; Matsubara, K.; Ohkubo, T.; Inoue, Y.; Takahashi, K. 2012. Docosahexaenoic- and Eicosapentaenoic Acid-bound Lysophospholipids are More Effective in Suppressing Angiogenesis than Conjugated Docosahexaenoic Acid. *Journal of Oleo Science* 61: 427–432.

Ulbrich-Hofmann, R. 2000. Phospholipases used in lipid transformations. *Enzymes in Lipid Modification*, John Wiley & Sons, Ltd, p.217–262.

Uppenberg, J.; Patkar, S.; Bergfors, T.; Jones, T.A. 1994. Crystallization and Preliminary X-ray Studies of Lipase B from Candida antarctica. *Journal of Molecular Biology* 235: 790–792.

Uribe, S.; Sampedro, J.G. 2003. Measuring solution viscosity and its effect on enzyme activity. *Biological Procedures Online* 5: 108–115.

Valenzuela, A.; Morgado, N. 1999. Trans fatty acid isomers in human health and in the food industry. *Biological Research* 32: 273–287.

Valenzuela Bonomo, C.; Nieto, S.; Sanhueza, J.; Morgado, N.; Rojas, I.; Zañartu, P. 2010. Supplementing female rats with DHA-lysophosphatidylcholine increases docosahexaenoic acid and acetylcholine contents in the brain and improves the memory and learning capabilities of the pups. 61: 16–23.

Van Meer, G.; Voelker, D.R.; Feigenson, G.W. 2008. Membrane lipids: where they are and how they behave. *Nature Reviews. Molecular Cell Biology* 9: 112–124.

Vazhappilly, C.G.; Hodeify, R.; Siddiqui, S.S.; Laham, A.J.; Menon, V.; El-Awady, R.; Matar, R.; Merheb, M.; Marton, J.; Al Zouabi, H.A.K.; Radhakrishnan, R. 2021. Natural compound catechol induces DNA damage, apoptosis, and G1 cell cycle arrest in breast cancer cells. *Phytotherapy Research* 35: 2185–2199.

Verdasco-Martín, C.M.; Villalba, M.; dos Santos, J.C.S.; Tobajas, M.; Fernandez-Lafuente, R.; Otero, C. 2016. Effect of chemical modification of Novozym 435 on its performance in the alcoholysis of camelina oil. *Biochemical Engineering Journal* 111: 75–86.

Verger, R.; de Haas, G.H. 1976. Interfacial enzyme kinetics of lipolysis. *Annual Review of Biophysics and Bioengineering* 5: 77–117.

Vikbjerg, A.F. 2006. Enzyme catalysed production of phospholipids with modified fatty acid profile. *PhD. BioCentrum-DTU. Technical University of Denmark.*

Virto, C.; Adlercreutz, P. 2000. Lysophosphatidylcholine synthesis with Candida antarctica lipase B (Novozym 435). *Enzyme and Microbial Technology* 26: 630–635.

Virto, C.; Svensson, I.; Adlercreutz, P. 1999. Enzymatic synthesis of lysophosphatidic acid and phosphatidic acid. *Enzyme and Microbial Technology* 24: 651–658.

Wang, C.; Wang, D.; Xu, J.; Yanagita, T.; Xue, C.; Zhang, T.; Wang, Y. 2018. DHA enriched phospholipids with different polar groups (PC and PS) had different improvements on MPTP-induced mice with Parkinson's disease. *Journal of Functional Foods* 45: 417–426.

Wang, L.; Folson, A.; Zheng, Z.; Pankow, J.; Eckfeldt, J. 2003. Plasma fatty acid composition and incidence of diabetes in middle-aged adults: the Atherosclerosis Risk in Communities (ARIC) Study. *The American Journal of Clinical Nutrition* 78: 91–98.

Wang, X.; Devaiah, S.P.; Zhang, W.; Welti, R. 2006. Signaling functions of phosphatidic acid. *Progress in Lipid Research* 45: 250–278.

Wang, X.; Zhao, X.; Yang, Z.; Wang, X.; Wang, T. 2020a. Effect of solvent on acyl migration of 2-monoacylglycerols in enzymatic ethanolysis. *Journal of Agricultural and Food Chemistry* 68: 12358–12364.

Wang, X.; Qin, X.; Li, X.; Zhao, Z.; Yang, B.; Wang, Y. 2020b. An efficient synthesis of lysophosphatidylcholine enriched with n-3 polyunsaturated fatty acids by immobilized MAS1 Lipase. *Journal of Agricultural and Food Chemistry* 68: 242–249.

Warden, C.; Davis, R.; Yoon, M.; Hui, D.; Svenson, K.; Xia, Y.; Diep, A.; He, K.; Lusis, A. 1993. Chromosomal localization of lipolytic enzymes in the mouse: pancreatic lipase, colipase, hormone-sensitive lipase, hepatic lipase, and carboxyl ester lipase. *Journal of Lipid Research* 34: 1451–1455.

Wilczynska, A.; Modrzewski, A.F. 2019. Chapter 15 - Fatty acids in human diet and their impact on cognitive and emotional functioning. Singh, R.B.; Watson, R.R.; Takahashi, T. (Eds.), *The Role of Functional Food Security in Global Health*, Academic Press, p.261–270.

Williams, J.J.; Mayurasakorn, K.; Vannucci, S.J.; Mastropietro, C.; Bazan, N.G.; Ten, V.S.; Deckelbaum, R.J. 2013. N-3fatty acid rich triglyceride emulsions are neuroprotective after Cerebral Hypoxic-Ischemic Injury in neonatal mice. *PLOS ONE* 8: e56233.

Wong, B.H.; Silver, D.L. 2020. Mfsd2a: A physiologically important lysolipid transporter in the brain and eye. *Advances in Experimental Medicine and Biology* 1276: 223–234.

Xu, X. 2000. Enzymatic production of structured lipids: process reactions and acyl migration. *Inform* 11: 1121–1131.

Xu, X.; Balchen, S.; Høy, C.E.; Adler-Nissen, J. 1998. Production of specific-structured lipids by enzymatic interesterification in a pilot continuous enzyme bed reactor. *Journal of the American Oil Chemists' Society* 75: 1573–1579.

Yalagala, P.C.R.; Sugasini, D.; Dasarathi, S.; Pahan, K.; Subbaiah, P.V. 2019. Dietary lysophosphatidylcholine-EPA enriches both EPA and DHA in the brain: potential treatment for depression. *Journal of Lipid Research* 60: 566–578.

Yamagami, T.; Porada, C.D.; Pardini, R.; Zanjani, E.D.; Almeida-Porada, G.D. 2009. Docosahexanoic acid induces dose dependent cell death in an early undifferentiated subtype of acute myeloid leukemia cell line. *Cancer Biology & Therapy* 8: 331–337.

Yan, G.; Elbadawi, M.; Efferth, T. 2020. Multiple cell death modalities and their key features (Review). *World Academy of Sciences Journal* 2: 39–48.

Yang, G.; Yang, R.; Hu, J. 2015. Lysophosphatidylcholine synthesis by lipasecatalyzed ethanolysis. *Journal of Oleo Science*.

Yanjun, L.; Qin, Z.; Yongli, G.; Junyi, L.; Jie, X.; Zhaojie, L.; Jingfeng, W.; Yuming, W.; Changhu, X. 2017. Enzymatic synthesis of lysophosphatidylcholine with n−3 polyunsaturated fatty acid from *sn*-glycero-3-phosphatidylcholine in a solvent-free system. *Food chemistry* 226: 165-170.

Yin, Y.; Sui, C.; Meng, F.; Ma, P.; Jiang, Y. 2017. The omega-3 polyunsaturated fatty acid docosahexaenoic acid inhibits proliferation and progression of non-small cell lung cancer cells through the reactive oxygen species-mediated inactivation of the PI3K /Akt pathway. *Lipids in Health and Disease* 16: 87.

Zaak, H.; Fernandez-Lopez, L.; Otero, C.; Sassi, M.; Fernandez-Lafuente, R. 2017. Improved stability of immobilized lipases via modification with polyethylenimine and glutaraldehyde. *Enzyme and Microbial Technology* 106: 67–74.

Zeisel, S.H. 1993. Choline phospholipids: signal transduction and carcinogenesis. *FASEB journal: official publication of the Federation of American Societies for Experimental Biology* 7: 551–557.

Zhang, J.; Yang, Y.; Wang, F.; Yang, W.; zou, Z. 2020a. MAG-DHA induces apoptosis and autophagy in breast cancer cells via lipid peroxidation-mediated endoplasmic reticulum stress. *Journal of Food Science*. https://doi.org/10.21203/rs.3.rs-35529/v1

Zhang, L.; Ding, L.; Shi, H.; Wang, C.; Xue, C.; Zhang, T.; Wang, Y. 2021. The different protective effects of phospholipids against obesity-induced renal injury mainly associate with fatty acid composition. *European Journal of Lipid Science and Technology* 123: 2100011.

Zhang, L.-Y.; Ding, L.; Shi, H.-H.; Xu, J.; Xue, C.-H.; Zhang, T.-T.; Wang, Y.-M. 2019a. Eicosapentaenoic acid in the form of phospholipids exerts superior anti-atherosclerosis effects to its triglyceride form in ApoE−/− mice. *Food & Function* 10: 4177–4188.

Zhang, T.-T.; Xu, J.; Wang, Y.-M.; Xue, C.-H. 2019b. Health benefits of dietary marine DHA/EPA-enriched glycerophospholipids. *Progress in Lipid Research* 75: 100997.

Zhang, Y.; Wu, G.; Zhang, Y.; Wang, X.; Jin, Q.; Zhang, H. 2020b. Advances in exogenous docosahexaenoic acid-containing phospholipids: Sources, positional isomerism, biological

activities, and advantages. *Comprehensive Reviews in Food Science and Food Safety* 19: 1420–1448.

Zhou, H.; Zhang, Z.; Lee, W.J.; Xie, X.; Li, A.; Wang, Y. 2021. Acyl migration occurrence of palm olein during interesterification catalyzed by sn-1,3 specific lipase. *LWT* 142: 111023.

Zhou, M.; Che, H.; Huang, J.; Zhang, T.; Xu, J.; Xue, C.; Wang, Y. 2018. Comparative Study of Different Polar Groups of EPA-Enriched Phospholipids on Ameliorating Memory Loss and Cognitive Deficiency in Aged SAMP8 Mice. *Molecular Nutrition & Food Research* 62: 1700637.

Titre : Synthèse enzymatique de la DHA-lysophosphatidylcholine et évaluation de son effet sur la lignée cellulaire de cancer du sein humain MDA-MB 231

Mots clés : DHA-lysophosphatidylcholine, estérification, plan d'expérience (RSM), lignée cellulaire MDA-MB-231, cancer du sein

Résumé : Ce travail étudie la synthèse de DHA-lysophosphatidylcholine (LPC-DHA) par estérification enzymatique sans solvant ainsi que la capacité de la LPC-DHA à réduire la viabilité cellulaire de la lignée cancéreuse humaine MDA-MB-231. Une optimisation des paramètres de l'estérification entre la glycerophosphatidylcholine (GPC) et l'acide docosahexaénoïque (DHA, C22 :6 ω-3) a été réalisée selon la méthodologie des surfaces de réponse (RSM). Deux réponses ont été mesurées : le rendement de conversion de la GPC et la concentration en LPC-DHA dans le milieu. Un rendement de conversion de la GPC de 67% est obtenu dans les conditions réactionnelles suivantes : rapport molaire DHA/GPC de 17, température de réaction de 36°C et quantité de Novozym® 435 de 15%. La concentration maximale de LPC-DHA obtenue est de 245 mM dans les conditions suivantes : rapport molaire DHA/GPC de 4, température de 36°C et quantité de Novozym® 435 de 15%. Une caractérisation par RMN a permis de confirmer que le composé synthétisé correspond à l'isomère *sn*-1 de la LPC-DHA, qu'il est pur et non oxydé. L'étude *in vitro* de l'effet de différentes LPC et différents vecteurs lipidiques du DHA sur les cellules MDA-MB-231 a montré que la LPC-DHA est la plus efficace pour réduire la viabilité cellulaire, les IC_{50} de la LPC-DHA, PC-DHA, du MAG-DHA, et du DHA libre étant de 19 µM, 50 µM, 170 µM et 347 µM, respectivement. La LPC-DHA et la PC-DHA réduisent la viabilité cellulaire principalement en induisant un stress oxydatif et une altération de la membrane plasmique. Le DHA et le MAG-DHA induisent également un stress oxydatif. En conclusion, ce travail a abouti à la synthèse de LPC-DHA dans des conditions de réaction favorables et a montré un effet inhibiteur significatif de la viabilité de cellules de cancer du sein, *in vitro*.

Title : Enzymatic synthesis of DHA-lysophosphatidylcholine and evaluation of its effect on the MDA-MB-231 human breast cancer cell line

Keywords : DHA-lysophosphatidylcholine, esterification, immobilized lipase, design of experiments (RSM), MDA-MB-231 cell line, breast cancer

Abstract : This work studies the synthesis of DHA-lysophosphatidylcholine (LPC-DHA) by solvent-free enzymatic esterification and the ability of LPC-DHA to reduce cell viability of the human cancer cell line MDA-MB-231. Optimization of esterification parameters between glycerophosphatidylcholine (GPC) and docosahexaenoic acid (DHA) was performed using response surface methodology (RSM). Two responses were measured: the conversion yield of GPC and the concentration of LPC-DHA in the medium. A GPC conversion yield of 67% is obtained under the following reaction conditions: a DHA/GPC molar ratio of 17, a reaction temperature of 36°C and a Novozym® 435 load of 15%. The maximum concentration of LPC-DHA obtained is 245 mM under the following conditions: a DHA/GPC molar ratio of 4, temperature of 36°C and a Novozym® 435 load of 15%. NMR characterization confirmed that the synthesized compound is pure and unoxidized *sn*-1 LPC-DHA. *In vitro* study of the effect of different LPCs and different lipid vectors of DHA on MDA-MB-231 showed that LPC-DHA was the most effective in reducing cell viability, with IC50 for LPC-DHA, PC-DHA, MAG-DHA, and free DHA of 19 µM, 50 µM, 170 µM, and 347 µM, respectively. LPC-DHA and PC-DHA reduce cell viability primarily by inducing oxidative stress and plasma membrane damage. DHA and MAG-DHA also induced oxidative stress. In conclusion, this work led to the synthesis of LPC-DHA under favorable conditions and showed a significant effect in reducing breast cancer cell viability *in vitro*.